

ELECTROPHYSIOLOGY AND TRANSMITTER SENSITIVITIES
OF ISOLATED RAT PETROSAL NEURONS:
SYNAPSE FORMATION AND HYPOXIC SIGNALING
IN CO-CULTURE WITH CAROTID BODY CHEMORECEPTORS

By

HUIJUN ZHONG, M.D.

A Thesis
Submitted to the School of Graduate Studies
in Partial Fulfilment of the Requirements
for the Degree
Doctor of Philosophy

McMaster University
(c) Copyright by Huijun ZHONG, May, 1997

SYNAPTIC PHYSIOLOGY OF CULTURED O₂-CHEMOSENSORY NEURONS

DOCTOR OF PHILOSOPHY (1997)
(Biology)

McMASTER UNIVERSITY
Hamilton, Ontario

TITLE: Electrophysiology and Transmitter Sensitivities of Isolated Rat Petrosal Neurons:
Synapse Formation and Hypoxic Signaling in Co-culture with Carotid Body
Chemoreceptors

AUTHOR: Huijun Zhong, M.D.
(Shandong Medical University)

SUPERVISOR: Professor Colin A. Nurse

NUMBER OF PAGES: xv, 256

ABSTRACT

The mammalian carotid body (CB), located at the carotid bifurcation, is a peripheral chemosensory organ which senses arterial P_{O_2} , P_{CO_2} and pH, and controls breathing via reflex responses. Chemoreceptor (glomus) cells in the CB contain various neurotransmitters which are released in response to chemosensory stimuli onto petrosal sensory nerve endings, but the underlying synaptic mechanisms are unclear. In this study, a combination of electrophysiological and pharmacological techniques were used to characterize membrane currents and sensitivity of cultured rat petrosal neurons (PN) to putative CB neurotransmitters. Further, co-cultures of PN and glomus cells were used to test for *de novo* functional synapse formation, and to elucidate the neurotransmitter mechanisms that mediate hypoxic signaling.

Conventional whole-cell and perforated patch recordings revealed that many PN contained, in addition to previously-characterized voltage-gated Na^+ , K^+ , and Ca^{2+} currents, a cation non-selective inward rectifier (I_h) which was activated at hyperpolarized membrane potentials, and appears to regulate spike frequency during chemosensory signaling. A subpopulation of PN contained a fast inactivating outward current (I_A), which also regulates spike frequency in neurons. The membrane properties of PN were largely unaffected by the natural CB stimulus, hypoxia ($P_{O_2} = \sim 25$ mm Hg). Acetylcholine (ACh), a putative CB neurotransmitter, was excitatory and depolarized $\sim 68\%$ of petrosal neurons ($n=109$) via hexamethonium-sensitive, nicotinic ACh receptors (nAChR). 5-HT, another putative CB

neurotransmitter, was also excitatory and depolarized ~ 43% of PN (n = 123), in association with a conductance *increase*; this response was mediated by MDL72222-sensitive 5-HT₃ receptors. More than one-half of CB glomus cells (n = 20) were also excited by 5-HT, but in contrast, this response was associated with a conductance *decrease*, and mediated by 5-HT₂ receptors. Dopamine depolarized approximately 30% PN (n = 69), but inhibited spike activity triggered by depolarizing stimuli (n = 4). Similarly, GABA also caused depolarization in ~ 84% of PN (n = 90), but inhibited spike activity via GABA_A receptors.

In co-cultures of dissociated rat PN and CB cells, synaptic-like activity was recorded from some neurons that were juxtaposed to glomus cell clusters. This activity, absent in PN cultured alone (n = 104), was observed in 77 out of 170 co-cultured neurons, and comprised spikes and subthreshold potentials (SSP) that resembled postsynaptic potentials seen at chemical synapses. Moreover, and especially in HCO₃⁻/CO₂-buffered medium, many chemosensory complexes were functional, since a hypoxic stimulus (Po₂ = ~ 25 mm Hg) was transduced and relayed (as a depolarization and/or increased spike discharge) to ~ 30% 'juxtaposed' neurons (n = 140). These spike discharges and SSP were reversibly inhibited by 200 μM hexamethonium (n = 12), suggesting that functional chemical synapses can develop *de novo* in co-culture and that ACh is likely an important excitatory neurotransmitter in CB chemoreception. Substance P (SP) increased spontaneous spike activity in co-cultured PN (21/ 36) via SP NK-1 receptors, and this may be related to its ability to modulate the transient I_A current in these neurons. Thus, these co-cultures have provided new insights into the synaptic and neurotransmitter mechanisms underlying CB chemoreception during hypoxia.

ACKNOWLEDGEMENTS

I wish to express my appreciation to all the people who contributed to the completion of this thesis. Firstly, I would like to thank Dr. Colin A. Nurse for being my supervisor, and his criticisms during my Ph. D. studies. I am grateful to the remaining members of my supervisory committee, Dr. Christopher M. Wood, Dr. Michael J. O'Donnell, and Dr. Carlos Barajas-Lopez for their guidance and help. In addition, I appreciate the help and cooperation of the other members of the laboratory, past and present, including Anthony J. Stea, Steve Alexander, Lynn Macintyre, Adele Jackson, Roger Thompson, Min Zhang, Erik Dreifelds, Mark Paciga. I thank Cathy Vollmer for expert technical assistance in preparing co-cultures and immunofluorescence (Chapter 6. Fig. 1).

I express my appreciation to the Biology department personnel and graduate students for their friendliness and aid during my years in the program. The years I have spent at McMaster have been of enjoyment due in large part to my friends, Tyler Linton, C.K. Wang, Ping Wang, Hongjie Yang, Daneal Yang, Yutian Wang, Heather Peter, Ben Hartford.

Finally, I would like to thank my Parents and family for all their love and support through my life. I am thankful to my beloved wife, Rong, for her patience and contribution to my "success". I express my love to my son, Yi, for his making everything worthwhile.

TABLE OF CONTENTS

	Page
Title Page	i
Descriptive Note	ii
Abstract	iii
Acknowledgement	v
Table of Contents	vi
List of Figures	ix
Abbreviations	xiii
Contributions	xiv
CHAPTER 1 General Introduction	1
1. Introduction	1
2. Structure of the carotid body (CB)	3
3. Physiological studies on the carotid body	7
4. Chemotransduction theories of the carotid body	8
4.1 Identification of chemoreceptor elements: glomus cells or nerve endings?	8
4.2 O ₂ -chemotransduction in glomus cells: The plasma membrane model	10
4.3 Alternative model for O ₂ sensing by glomus cells	13
5. Neurotransmitters of the carotid body	14
5.1 Catecholamines (CA)	14
5.2 Acetylcholine (ACh)	16
5.3 5-Hydroxytryptamine (5-HT) or serotonin	18
5.4 Substance P (SP)	19
5.5 Other putative neurotransmitters/neuromodulators	20
6. Structure of the petrosal ganglion	22

7. Electrophysiology of the petrosal ganglion	24
8. Studying synaptic transmission in the carotid body: problems and solutions	26
9. Patch-clamp techniques for electrophysiological studies	28
10. Goals and organization of thesis	30
CHAPTER 2 Characterization of a Hyperpolarization-activated Inward Current in Rat Chemosensory Petrosal Neurons <i>in vitro</i>	34
CHAPTER 3 Nicotinic Acetylcholine Sensitivity of Rat Petrosal Sensory Neurons in Dissociated Cell Culture	62
CHAPTER 4 Comparison of 5-HT Receptors on Isolated Rat Petrosal Neurons and O ₂ -chemoreceptor Target Cells <i>in vitro</i>	88
CHAPTER 5 GABA Sensitivity of Isolated Rat Petrosal Neurons <i>in vitro</i>	120
CHAPTER 6 Synapse Formation and Hypoxic Signaling in Co-cultures of Rat Chemosensory Neurons and Carotid Body Type I cells	145
CHAPTER 7 Discussion of the Mechanisms of Transduction and Chemosensory Transmission in the Carotid Body	185
1. Mechanisms of hypoxic transduction	185
1.1 Roles of ion channels, and intracellular Ca ²⁺ in hypoxic chemotransduction	185
1.2 Effects of HCO ₃ ⁻ /CO ₂ buffered media and pH _i on hypoxic chemotransduction	190
1.3 Model of oxygen-sensing mechanisms	192
2. I _h and the electrophysiology of afferent petrosal sensory neurons	196

3. Chemosensory transmission between CB chemoreceptors and afferent nerve endings	198
3.1 The coding of sensory information and hypoxia threshold	198
3.2 Receptor potential and generator potential	199
3.3 The initiation of sensory nerve impulses	200
4. Acetylcholine (ACh) and its receptors	202
4.1 Excitatory effects of ACh in the carotid body	203
4.2 Involvement of nAChR in hypoxic chemosensory signaling	204
4.3 Are AChRs on glomus cells mediators of positive feedback?	205
5. Putative excitatory neurotransmitters/neuromodulators	208
5.1 The effects of 5-HT in the carotid body	208
5.2 Substance P and NK-1 receptors	210
6. Putative inhibitory neurotransmitters/neuromodulators	213
6.1 GABA _A receptors on petrosal neurons	213
6.2 Dopamine and D ₂ receptors	214
7. Future directions	221
References	224
Appendices	250

LIST OF FIGURES

Chapter 1

- Fig. 1.1 Schematic diagram of the rat carotid body 5

Chapter 2

- Fig. 1 Current- and voltage-clamp recordings from cultured petrosal neurons 43
Fig. 2 Reversal potential of I_h 46
Fig. 3 Effects of high potassium and low sodium on I_h 48
Fig. 4 Voltage dependence of I_h activation 51
Fig. 5 Kinetics of I_h activation and deactivation 54
Fig. 6 Effects of chloride substitution, barium and cesium on I_h 56

Chapter 3

- Fig. 1 Responses of cultured rat petrosal neurons (PN) to ACh 72
Fig. 2 Effects of ACh on membrane potential and whole-cell current
in cultured petrosal neurons 74
Fig. 3 Evidence for nicotinic ACh receptors on petrosal neurons 76
Fig. 4 Reversal potential and inward rectification of nAChRs in
petrosal neurons 78
Fig. 5 Dose-response curve for ACh concentration vs I_{ACh}
in a petrosal neuron 79
Fig. 6 The activation and desensitization phases of I_{ACh} 82
Fig. 7 Estimation of the nAChR single-channel conductance from fluctuation
analysis of the ACh-induced whole-cell current in a petrosal neuron 83

Chapter 4

Fig. 1 Effects of 5-HT on petrosal sensory neurons <i>in vitro</i>	98
Fig. 2 Evidence for 5-HT ₃ receptor on petrosal neurons	100
Fig. 3 The reversal potential of 5-HT responses in petrosal neurons	101
Fig. 4 Dose-response curve of 5-HT effects on petrosal neurons	103
Fig. 5 The activation and desensitization of I _{5-HT}	105
Fig. 6 Estimation of the 5-HT ₃ receptor single-channel conductance from fluctuation analysis of the 5-HT-induced whole-cell current in a petrosal neuron	107
Fig. 7 Effects of 5-HT on the membrane potential of cultured glomus cells	109
Fig. 8 The reversal potential of 5-HT response in a glomus cell	110
Fig. 9 Effects of 5-HT on the membrane currents of cultured glomus cells	112
Fig. 10 Effects of hypoxia on whole-cell currents and membrane potential in cultured glomus cells	113

Chapter 5

Fig. 1 Effects of GABA on petrosal sensory neurons <i>in vitro</i>	129
Fig. 2 GABA _A receptors mediate depolarization in cultured petrosal neurons	130
Fig. 3 The reversal potential of GABA _A receptor channels in a petrosal neuron	132
Fig. 4 Dose-response relationship of GABA-evoked responses in petrosal neurons	135
Fig. 5 Estimation of the GABA _A receptor single-channel conductance from fluctuation analysis of the GABA-induced whole-cell current in a petrosal neuron	136
Fig. 6 Power spectral density analysis of GABA-induced current noise in a petrosal neuron	138
Fig. 7 GABA reduces excitability of petrosal neurons	140

Chapter 6

Fig. 1 Immunofluorescent staining of a co-culture of dissociated rat petrosal neurons and carotid body type 1 cells	155
Fig. 2 Comparison of the effects of hypoxia on carotid body type 1 cells and petrosal neurons cultured separately	158
Fig. 3 Effects of co-culture on spontaneous membrane activity recorded with the perforated-patch technique from petrosal neurons	160
Fig. 4 Effect of low calcium/ high magnesium on the spontaneous activity recorded in a co-cultured petrosal neuron	163
Fig. 5 Amplitude and interval distribution of spontaneous subthreshold potentials (SSP) in a co-cultured petrosal neuron	165
Fig. 6 Chemotransduction and afferent signaling of a hypoxic stimulus in co-culture	168
Fig. 7 Effect of hypoxia on frequency of action potentials and postsynaptic potentials (PSP) in co-cultured PN	170
Fig. 8 Evidence for involvement of nicotinic acetylcholine receptors (nAChR) in hypoxic signaling in co-culture	172
Fig. 9 Effect of hypoxia and hexamethonium on frequency of postsynaptic potentials in a co-cultured PN	173
Fig. 10 Contrasting effects of CO ₂ -HCO ₃ ⁻ vs HEPES- buffered media on spontaneous activity and hypoxic signaling in co-cultured PN	175

Chapter 7

Fig. 7.1 Possible mechanisms for hypoxic chemotransduction in glomus cells	187
Fig. 7.2 Mechanisms of detection of the hypoxic stimulus	194
Fig. 7.3 Schematic diagram of proposed hypoxia transduction, neurosecretion and ACh function	206
Fig. 7.4 Flow diagram summarizing the effects of some carotid body transmitters	219

Appendices

Appendix 1 Effects of hydrogen peroxide and hypercapnia on whole-cell currents from cultured glomus cells	250
Appendix 2 Effects of 5-HT ₃ receptor antagonist on chemosensory signaling in co-culture	252
Appendix 3 Effects of substance P (SP) on the membrane activity of co-cultured petrosal neurons	253
Appendix 4 Effects of SP on spike activity and membrane currents of dissociated petrosal neurons	254
Appendix 5 Effects of dopamine on spike activity and membrane potential of dissociated petrosal neurons	256

ABBREVIATIONS

5-HT	- 5-hydroxytryptamine or serotonin
ACh	- acetylcholine
AChE	- acetylcholinesterase
AChR	- ACh receptors
ANP	- atrial natriuretic peptide
BBM	- bicarbonate buffered media
cAMP	- adenosine 3',5'-cyclic monophosphate
CA	- catecholamines
CB	- carotid body
CPG	- central pattern generator
CSN	- carotid sinus nerve
D ₂ R	- Dopamine D ₂ receptors
DA	- dopamine
EGTA	- ethylene glycol-bis(β-aminoethyl ether)-N,N,N',N'-tetraacetic acid
EPSP	- excitatory post-synaptic potentials
GABA	- γ-aminobutyric acid
HBM	- HEPES-buffered media
HEPES	- N-2-hydroxyethylpiperazine-N'-2-ethanesulonic acid
I _A	- fast transient K ⁺ current
I _{ACh}	- ACh induced current
I _h	- hyperpolarization activated inward rectifier current
mAChR	- muscarinic ACh receptors
nAChR	- nicotinic ACh receptors
pH _i	- intracellular pH
PKC	- protein kinase C
PLC	- phospholipase C
PN	- petrosal (ganglion) neurons
P _{co₂}	- partial pressure of carbon dioxide
P _{o₂}	- partial pressure of oxygen
PSP	- postsynaptic potentials (including SSP and spikes)
SDP	- spontaneous depolarizing potentials
SOD	- superoxide dismutase
SP	- substance P
SSP	- spontaneous subthreshold potentials
TH	- tyrosine hydroxylase
TTX	- tetrodotoxin
Type I cell	- chemosensor/glomus cells
[Ca ²⁺] _i	- intracellular free calcium
[Ca ²⁺] _o	- extracellular free calcium

CONTRIBUTIONS TO THE THESIS

Chapter 1. Introduction

Chapter 2: Manuscript by H. Zhong and C. A. Nurse; (in press) Journal: '*Primary Sensory Neuron*'.

1. I prepared and maintained cell cultures.
2. I performed all electrophysiological recordings.
3. I performed all data analysis and generated all figures in text.

Chapter 3: Manuscript by H. Zhong and C. A. Nurse; (in press) Journal: '*Brain Research*'.

1. I maintained cell cultures; Cathy Vollmer prepared most (~95%) of the cultures.
2. I performed all electrophysiological recordings. Dr. Min Zhang assisted in the later stages of experiments with design of the fast perfusion system for applying ACh.
3. I performed all data analysis and generated all figures in text.

Chapter 4: Manuscript in preparation. Order of authors will be: H. Zhong, M. Zhang and C. A. Nurse.

1. I maintained cell cultures; Cathy Vollmer prepared most (~95%) of the cultures.
2. I performed most (~80%) of electrophysiological experiments and data collection in this study. Dr. M. Zhang assisted me in data collection in the remaining (20%), mainly on recordings from glomus cells.
3. I performed all data analysis and generated all figures in text.

Chapter 5: Manuscript in preparation. Order of authors will be: H. Zhong, M. Zhang and C. A. Nurse.

1. I maintained cell cultures; Cathy Vollmer prepared most (~95%) of the cultures.
2. For this study electrophysiological experiments and data collection were done jointly with Dr. M. Zhang. My contribution was ~ 50%.
3. I performed all data analysis and generated all figures in text.

Chapter 6: Manuscript has been submitted for publication. Order of authors is:

H. Zhong, M. Zhang and C. A. Nurse.

1. I maintained cell cultures and prepared about 5 % of co-cultures; Cathy Vollmer prepared about 95% of co-cultures and carried out double-label immunofluorescence in Figure 1.
2. I performed about 90% of the electrophysiological experiments. The main observations that *de novo* chemical synapses form between petrosal neurons and glomus cells in co-culture and that acetylcholine mediates hypoxic signaling were made by me (see Zhong and Nurse, 1994). Dr. M. Zhang assisted in the design of the fast perfusion system for applying hypoxic solutions. He collaborated in the later stages, particularly in data collection that validated my initial observation that ACh was secreted in co-culture.
3. I performed all data analysis and generated all figures in text except figure 1.

CHAPTER 1

General Introduction

1. Introduction

Respiration, a process by which oxygen (O₂) and carbon dioxide (CO₂) are exchanged between an organism and its environment, is crucial for survival since most cells die if deprived of O₂ or if CO₂ removal is prevented. Respiration in mammals relies on a neuronal network, known as respiratory control system, which includes a central respiratory control center, sensors and effectors. One of the most important functions of this control system is to adjust ventilation to meet changes in O₂ consumption and CO₂ production, thereby maintaining homeostasis in the organism. In mammals breathing is a rhythmic, unconscious process which includes two basic phases, inspiration and expiration. This rhythm is thought to be generated by a central pattern generator (CPG), located in the medullary region of the brain stem (Rhoades and Pflanzner, 1992; Bianchi et al., 1995). Although the CPG contains an intrinsic rhythm, sensory inputs from peripheral, and central chemoreceptors, as well as pulmonary afferents can modulate the respiratory rhythm and adapt breathing patterns to meet different conditions (Demsey and Forster, 1982; Bianchi et al., 1995).

Ventilation in mammals is regulated mainly by central and peripheral chemoreceptors which sense the chemical composition of arterial blood and signal the respiratory control center via reflex responses (Demsey and Forster, 1982; Gonzalez et al., 1994). These chemoreceptors are strategically located in the body to detect changes in blood gases and pH

levels, and trigger ventilatory responses that result in the protection of vital organs such as the brain. For instance, the central chemoreceptors located in the medulla of the brain stem mainly sense CO₂ levels, probably via changes in pH of cerebrospinal fluid (see Demsey and Forster, 1982), while the peripheral chemoreceptors located primarily in the carotid and aortic bodies are O₂ sensitive, though at least the carotid body (CB) can also sense CO₂ and pH (Demsey and Forster, 1982; Rhoades and Pflanzner, 1992). When the partial pressure of arterial oxygen (Po₂) is reduced, for example during lung disease or breathing at high altitude, the CB chemoreceptors are stimulated and transmit nervous signals to the nucleus tractus solitarius (NTS) resulting in hyperventilation, following increased impulse activity in phrenic motor neurons (Demsey and Forster, 1982; Rhoades and Pflanzner, 1992). The focus of this thesis is to understand the peripheral mechanisms that operate in the CB during chemical stimulation, e.g. by reduced Po₂ in arterial blood.

The cellular and molecular mechanisms that underlie the transduction of the chemosensory stimuli in CB chemoreceptors are controversial. However, the popular view is that the arterial chemoreceptors or O₂-sensors are specialized chromaffin-like cells, known as glomus or type I cells (Gonzalez et al., 1994; Lopez-Barneo, 1996; see however, Sun and Reis, 1994). These cells detect chemical stimuli in arterial blood, and transduce them into a change in membrane potential or action potential frequency, followed by an increase in intracellular calcium and neurosecretion (Peers and Buckler, 1995; Lopez-Barneo, 1996). The release of neurotransmitter(s) from glomus cells is then thought to activate the closely-apposed sensory terminals of the carotid sinus nerve (CSN), and convey information on the strength and duration of the stimulus by a frequency code, which signals the central

respiratory rhythm generator in the brain stem (Gonzalez et al., 1994).

2. Structure of the carotid body (CB)

The carotid bodies are paired organs located between the internal and external carotid arteries near the bifurcation of the common carotid arteries (McDonald, 1981). In mammals, the organ is adjacent to the superior cervical sympathetic ganglion (SCG) and nodose ganglion and receives its sensory innervation from the CSN, a branch of the glossopharyngeal nerve (IXth cranial nerve) (McDonald, 1981). The CB is also innervated by sympathetic and parasympathetic fibers and its gross anatomical location and main innervation is shown in Figure 1.1A (from McDonald and Mitchell, 1975). Although the dimensions of the CB varies with the size of animal, it is roughly egg-shaped and measures 0.6 x 0.6 x 1.5 mm in the rat (McDonald and Mitchell, 1975). In mammalian embryos the CB develops in the third branchial arch next to the third arch artery (Boyd, 1937), and its primordium can be distinguished at 14 days of gestation in the rat (Kondo, 1975) and 6 weeks of gestation in the human embryo (McDonald, 1981). The parenchymal cells of the organ are grouped together into cell clusters, separated by interstitial connective tissue containing nerve fiber bundles and blood vessels. The clusters are composed of mainly two cell types, the glomus or type I cells and glial-like sustentacular or type II cells. Chemoreceptive type I cells originate from the neural crest (Pearse et al., 1973) and in most species are about five times more numerous than type II cells (McDonald, 1981). The CB is also reported to be the most richly vascularized organ in the body, and morphometric measurements indicate that one-quarter to one-third of its volume is occupied by capillaries and venules (De Castro and Rubio, 1968; McDonald,

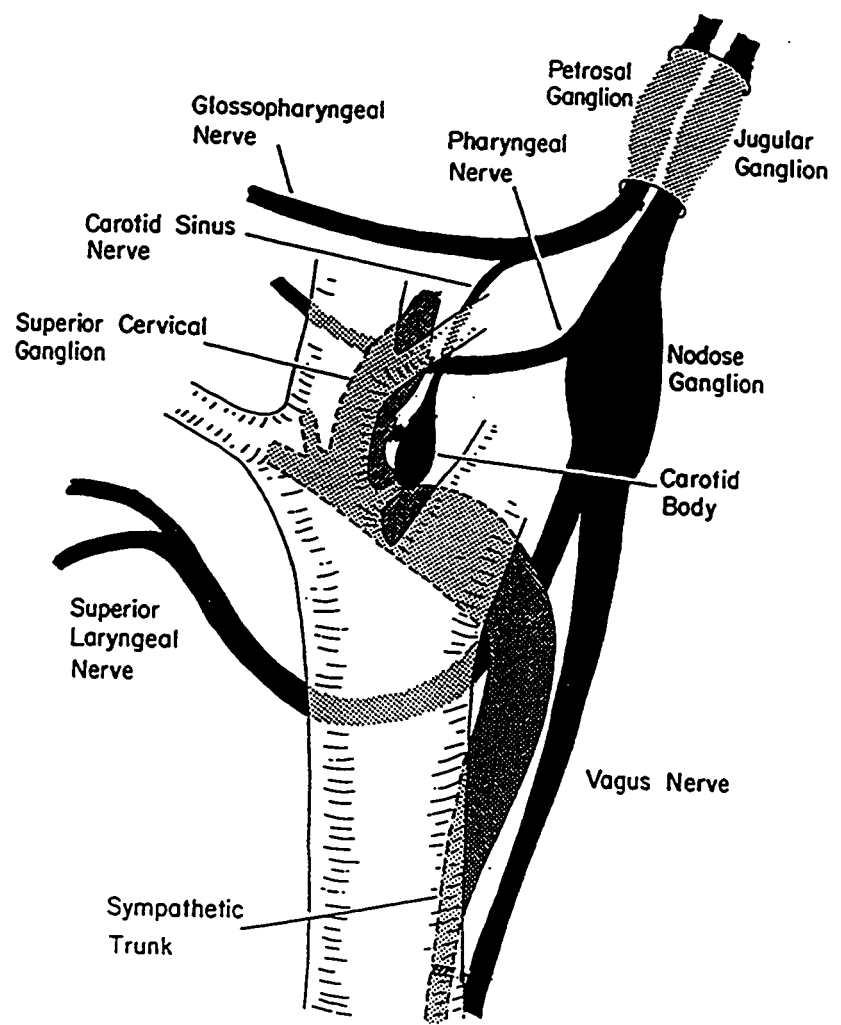
1981).

Glomus or type I cells are readily distinguished from type II cells, and appear round or ovoid in shape with an average diameter of 8-15 μm . Glomus cells have the morphological characteristics of cells that actively synthesize and package substances for secretion. The presence of large numbers of cytoplasmic dense core vesicles, clear core vesicles and staining for the chromaffin reaction is evidence for a link with adrenal medullary chromaffin cells (Lever and Boyd, 1957; Kobayashi, 1971). These vesicles in the glomus cell appear to contain multiple putative neurotransmitters, including biogenic amines, acetylcholine and neuropeptides (Eyzaguirre and Zapata, 1984; Fidone et al., 1988; Gonzalez et al., 1994). The possible physiological role of these substances will be discussed later.

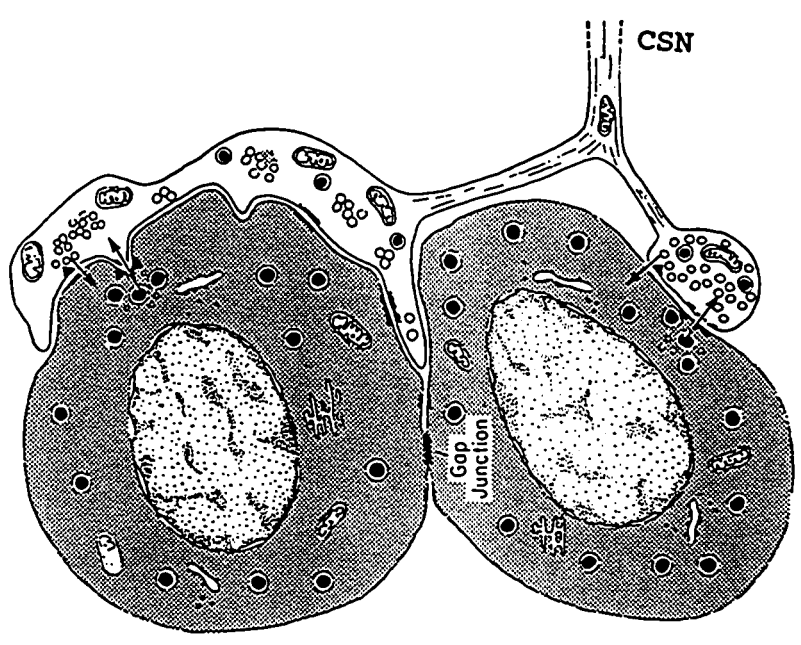
Glomus cells are joined by gap junctions which are proposed to be important for electrical coupling and intracellular communication (McDonald and Mitchell, 1975; Monti-Bloch and Eyzaguirre, 1990). In the electron microscope, reciprocal synapses have been described between neighbouring glomus cells and between glomus cells and sensory nerve endings of the CSN (McDonald and Mitchell, 1975; McDonald, 1981). The sensory fibers of CSN include both myelinated and unmyelinated afferent fibers whose parent cell bodies lie in the petrosal ganglia (Fidone and Sato, 1969). Each fiber undergoes multiple branching and innervates numerous glomus cells, which in turn may be innervated by multiple contacts from the same or different fibers (McDonald, 1981). Approximately 95% of the sensory afferent nerve endings form synaptic contact with glomus cells and these synapses are polarized from glomus cell to nerve terminal, from nerve terminal to glomus cell, or are reciprocally polarized (Fig. 1.1B from McDonald, 1981).

Figure 1.1 Schematic diagram of the rat carotid body. **A.** Schematic diagram of the relationship of the rat carotid body to adjacent nerve, ganglia, and arteries. It shows the egg-shaped carotid body (CB) located in the bifurcation of the common carotid arteries, adjacent to the superior cervical sympathetic ganglion and nodose ganglion. The CB is innervated by carotid sinus nerve (CSN), a branch of the glossopharyngeal nerve (IXth cranial nerve), as well as by sympathetic nerves. Another branch of the glossopharyngeal nerve innervates the tongue and pharyngeal structures. The blood supply of the CB arises from the external carotid artery (from McDonald and Mitchell, 1975). **B.** Schematic representation of the synaptic connections between sensory nerve endings and glomus cells. Arrows indicate the presumed direction of synaptic transmission. In this diagram each sensory nerve terminal is presynaptic and postsynaptic, and both of the endings contain synaptic vesicles (clear-cored) and large dense-cored vesicles. Dense-cored vesicles are predominant in the glomus cells and tend to be clustered. The presence of gap junctions suggests some glomus cells are electrically coupled (from McDonald, 1981).

A



B



The type II cells lack specialized contact with sensory nerve fibers and surround the glomus cell clusters. They are considered to be "glial-like" cells and are presumed to serve a supportive function in chemoreception (McDonald, 1981; Gonzalez, et al., 1994). They lack dense-cored vesicles and this feature distinguishes them from glomus cells. Their number ranges from 21% - 43% of the total CB cell population (McDonald, 1981).

3. Physiological studies on the carotid body

Although the first anatomical description of the carotid body was in the early 1700's, the physiological studies of the CB were not performed until 1930's (see Biscoe, 1971). Heymans obtained the Nobel prize in Physiology and Medicine for his contributions to the study of CB physiology (Eyzaguirre and Zapata, 1984). In the early studies, extracellular recordings were obtained from the carotid sinus nerve (CSN) and changes in activity in response to different stimuli were recorded. The results have demonstrated a hyperbolic relationship between blood P_{O_2} and CSN discharge frequency, while a linear relationship was obtained for P_{CO_2} and pH stimuli (Eyzaguirre and Koyano, 1965a; Eyzaguirre and Zapata, 1984; Gonzalez et al., 1994). It therefore appears that different mechanisms underlie responses to these chemosensory stimuli. Since results from *in vivo* preparations could be affected by circulatory factors, several groups have employed *in vitro* preparations, in which the carotid body and sinus nerve are isolated from the animal (Eyzaguirre et al, 1989; Kholwadwala and Donnelly, 1992; Pepper et al., 1995; Iturriaga et al., 1996). Using this *in vitro* preparation, hypoxia (low P_{O_2}) or hypercapnia (high P_{CO_2}) induced an increase in discharge recorded from the attached sinus nerve fibers in both rat (Kholwadwala and

Donnelly, 1992; Pepper et al., 1995) and cat (Iturriaga et al., 1996). More recently, nerve recordings from the *in vitro* preparation have been combined with carbon fiber monitoring of tissue catecholamine, the predominant amine stored in the dense cored vesicles of type I cells. Donnelly (1996) found that catecholamine secretion was not causal to the hypoxia-induced increase in nerve activity of rat CB, since pretreatment with reserpine (24 h) nearly abolished catecholamine release, but the nerve response was unaffected. A similar conclusion was reached by Iturriaga et al. (1996) from studies on the superfused *in vitro* CB-sinus nerve preparation from cats.

4. Chemotransduction theories of the carotid body

4.1 Identification of chemoreceptor elements: glomus cells or nerve endings?

To study the physiology of the CB at the receptor level, it is essential to know which element within the sensory organ is the primary sensing element. There are at least two candidates for the role of chemosensors, the sensory nerve endings and the glomus cells. As the chemical stimuli increase the sensory nerve discharge in a dose-dependent fashion, it is possible that the stimulus acts directly on the nerve terminals and that the glomus cells play some other role (Biscoe, 1971). Biscoe (1971) found that the nerve endings that were in synaptic apposition to glomus cells were efferent. These observations led to the hypothesis that in CB chemoreception the free nerve endings are the transducing elements which directly sense low P_{O_2} , high P_{CO_2} , and low pH and encode the information in the discharge pattern along the CSN; glomus cells were presumed to act as interneurons which modulate the responses to the various chemostimuli (see McDonald, 1981). This hypothesis has been

criticized because the free nerve endings are poorly defined and have not been observed in other laboratories (Gonzalez et al., 1992). Another objection is that although hypoxia tends to depolarize the membrane potential of some nerve fibers, hypercapnia and acidity have membrane stabilizing effects. It appeared inconceivable that a membrane stabilizer would increase the sensory discharge similar to a depolarizing agent (Eyzaguirre, 1993). In a recent study Sun and Reis (1994), using *in vivo* recording from rat CSN combined with pharmacological tools, investigated whether several putative CB neurotransmitters could be the mediators exciting the sensory afferents after systemic hypoxia or histotoxic hypoxia, where was used as a stimulus. They concluded that transmitter release from rat carotid body may not be essential for hypoxic chemoreception and the afferent nerves themselves might function as oxygen sensors.

The second hypothesis was initially proposed by De Castro in 1928. He postulated that the glomus cells are the primary chemosensors which sense chemical stimuli and release neurotransmitter(s) to activate the nerve endings (reviewed by Gonzalez et al., 1992). Consequently chemosensory information is transduced into electrical signals which are then conveyed to the respiratory control center (Gonzalez et al., 1994). This view was reinforced by ultrastructural and biochemical findings which identified a synaptic relationship between glomus cells and sensory nerve endings, and the presence of synaptic vesicles and putative neurotransmitters in glomus cells (McDonald and Mitchell, 1975; McDonald, 1981; Gonzalez et al., 1994). Most of the available evidence to date favours this hypothesis. First, electrophysiological studies on isolated glomus cells indicate their membrane properties can be modulated by O₂ sensitive K⁺ channels and chemical stimuli induce depolarization. Second,

natural chemical stimuli for the CB induce neurotransmitter release from glomus cells. Third, hypoxia-induced increase in intracellular calcium in glomus cells is coupled to neurotransmitter release. Fourth, hypoxia-induced increase of CSN discharge can be mimicked by putative CB neurotransmitters and in some experiments appropriate receptor antagonists were found to block (at least partially) the discharge induced by natural stimuli (reviewed by Gonzalez et al., 1994; Eyzaguirre and Zapata, 1984).

4.2 O₂-chemotransduction in glomus cells: The plasma membrane model

The majority of experimental evidence currently favours a plasma membrane model for the mechanism of hypoxic chemotransduction. This model proposes that low Po₂ modulates the electrical properties of glomus cells resulting in membrane depolarization and/or increase in action potential frequency. This in turn promotes Ca²⁺ influx through voltage-dependent L-type calcium channels, increasing intracellular Ca²⁺ and neurosecretion (Gonzalez et al., 1992; Peers and Buckler, 1995 Lopez-Barneo, 1996). Evidence for this scheme has come from electrophysiological studies on glomus cells isolated from two species, rabbit and rat. In whole-cell voltage clamp experiments it was found that dissociated glomus cells from the CB of adult rabbit possess voltage-dependent sodium, potassium and calcium channels (Urena et al., 1989). A transient Ca²⁺-independent component of outward K⁺ current was reversibly inhibited by lowering Po₂ while the inwardly directed Na⁺ and Ca²⁺ currents were unaffected in initial studies (Lopez-Barneo et al., 1988; Hescheler et al., 1989; Delpiano and Hescheler, 1989; Ganformina and Lopez-Barneo, 1991). In more recent studies on the same preparation, low Po₂ caused a voltage-dependent inhibition of L-type Ca²⁺ channels

(Montoro et al., 1996; Lopez-Barneo, 1996). In other studies on glomus cells isolated from neonatal rats, low P_{O_2} inhibited a Ca^{2+} -dependent component of outward K^+ current (Peers, 1990; Stea and Nurse, 1991a; Wyatt and Peers, 1995). Interestingly, O_2 -sensitive K^+ channels have more recently been identified in other cell types including pulmonary neuroepithelial bodies (NEB; Youngson et al., 1993; Wang et al., 1996) and pulmonary artery smooth muscle (Yuan et al., 1993; Archer et al., 1996). Although there are discrepancies in the K^+ channel subtype which is inhibited by hypoxia (see Buckler, 1997), the basic observation that O_2 -sensitive K^+ channels exist in glomus cells favours a mechanism where hypoxia leads to closure of K^+ channels, cell depolarization, influx of extracellular Ca^{2+} and neurotransmitter release. In current-clamp recordings, acute hypoxia has been shown to depolarize and increase action potential frequency in glomus cells of rabbit (Lopez-Lopez et al., 1989; Delpiano and Hescheler, 1989) and rat (Buckler and Vaughan-Jones, 1994). Further, acute hypoxia stimulates catecholamine secretion via influx of extracellular calcium from isolated glomus cells in both species (Fishman et al., 1985; Montoro et al., 1996; Jackson and Nurse, 1997 in press).

The major initial criticism of this membrane model was that the relationship between P_{O_2} and K^+ channel inhibition did not parallel the hyperbolic curve relating P_{O_2} to impulse activity in the intact CB (Gonzalez et al., 1992). Therefore direct regulation of this K^+ channel activity by P_{O_2} alone could not account for the oxygen-sensing properties of the intact CB. However, there may be additional pathways through which P_{O_2} can regulate channel activity in glomus cells. For example cyclic AMP (cAMP), which rises in glomus cells during acute hypoxia (Wang et al., 1991), has been demonstrated to inhibit O_2 -sensitive K^+ currents in

rabbit glomus cells (Lopez-Lopez et al., 1993). Thus, dual regulation of these channels through the membrane-delineated mechanism and intracellular cAMP could give rise to a more physiologically-relevant relationship between P_{O_2} and K^+ channel activity. Alternatively, simultaneous regulation of different types of ion channels by low P_{O_2} may contribute to the overall response. For example, Montoro et al. (1996) have recently shown that in single-isolated rabbit glomus cells, catecholamine secretion due to low P_{O_2} parallels the hyperbolic (physiological) dose-response relation when the voltage-dependent inhibition of L-type Ca^{2+} channels by hypoxia is also taken into account. Recent studies on isolated rat glomus cells suggest the situation is even more complex. Buckler (1997) revealed a novel O_2 -sensitive leak K^+ channel in rat glomus cells that was open at the resting membrane potential but showed little voltage sensitivity, and was insensitive to charybdotoxin, TEA, and 4-AP. This channel was proposed to be the main cause of the receptor potential in rat glomus cells, since the O_2 (charybdotoxin-sensitive) Ca^{2+} -dependent K^+ channels were presumed to be closed at the resting potential. However, recent studies on isolated clusters of rat glomus cells indicate that a more specific blocker of the Ca^{2+} -dependent K^+ channels, iberiotoxin (200 μ M), markedly stimulates dopamine secretion, suggesting that these channels are active even at relatively high P_{O_2} (160 mm Hg; Jackson and Nurse, 1997).

Acker and colleagues (1992) proposed a redox mechanism by which K^+ channels may be directly regulated by P_{O_2} . They suggested that the O_2 sensor is a cytochrome-b protein which may be linked to a NADPH-oxidase, similar to the one that generates the respiratory burst in neutrophils. Under normoxic conditions the oxidase synthesizes superoxide (O_2^-) which is then converted to hydrogen peroxide (H_2O_2) by superoxide dismutase. This H_2O_2 is

then further reduced to H_2O with consequent oxidation of glutathione. Under hypoxic conditions H_2O_2 production falls, with a consequent increase in the reduced form of glutathione. This reduced glutathione, or the fall in H_2O_2 levels may inhibit K^+ channels in glomus cells, as has been shown for certain types of K^+ channels on isolated membrane patches (Ruppersberg et al., 1991; Park et al., 1995). Consistent with this model, it has been reported that H_2O_2 selectively inhibits the inactivation of voltage-dependent K^+ channels expressed in oocytes (Vega-Saenz de Miera and Rudy, 1992) and increases the amplitude of a similar K^+ current in pulmonary NEB cells of rabbit (Wang et al., 1996), as well as a K^+ current in non-excitabile cells (Kuo et al., 1993). H_2O_2 was able to abolish the hypoxia-induced discharge recorded from rat CSN (Acker et al., 1992). In addition, a NADPH oxidase inhibitor, diphenylene iodonium (DPI), blocks the hypoxia-induced increase in CSN discharge in isolated perfused CB preparation (Cross, et al., 1990) and caused a reduction of a hypoxia-sensitive K^+ current in NEB cells (Youngson et al., 1993).

4.3 Alternative model for O_2 sensing by glomus cells

Early studies suggested that the stimulus-induced rise in intracellular Ca^{2+} is the signal for neurosecretion and critical to glomus cell chemotransduction (reviewed by Gonzalez et al., 1992). Two models have evolved to explain the low PO_2 -dependent neurosecretion from glomus cells, one of which (and the most popular) was discussed above. In an alternative model, Duchon and Biscoe (1992) propose that hypoxia would slow electron transfer and decrease the proton electrochemical gradient across mitochondria of chemoreceptor cells. Consequently, the hypoxic stimulus would cause a release of calcium from intracellular stores

rather than an influx from an extracellular source. In support of this model, Duchen and Biscoe (1992) demonstrated that the mitochondrial metabolism in the glomus cell is unusually sensitive to changes in P_{O_2} , and that hypoxia depolarized the mitochondrial membrane potential and caused an elevation in NADPH. These correlated with changes in intracellular Ca^{2+} and led to the proposal that the rise of intracellular Ca^{2+} resulted primarily from Ca^{2+} release from intracellular stores. The latter model is a variation of the "metabolic hypothesis" which proposes that hypoxia decreases ATP level via a metabolic mechanism and consequently stimulates the CB chemoreceptors. The experimental data from Lahiri et al. (1993), using perfused cat CB-CSN preparations, showed that carbon monoxide (CO) at high partial pressure (~ 500 mm Hg) excited the CB in a light-sensitive manner. The suggested explanation for these results is that in the dark CO at high partial pressure stops O_2 consumption and the synthesis of ATP. Lack of ATP would affect the pumping of Na^+ out of cell and the electrophysiological properties of the chemosensor thereby produces the activation of CSN discharge. Since the binding of CO to mitochondrial cytochrome oxidase is strongly dissociated by visible light of certain intensity, the effects of CO is photolabile. In general, these alternative models propose that O_2 -sensing in the CB occurs primarily in the mitochondria of glomus cells.

5. Neurotransmitters of the carotid body

5.1 Catecholamines (CA)

It is well established that multiple neurotransmitters co-exist within the chemoreceptor cells of the carotid body including catecholamines (CA), acetylcholine (ACh), 5-

hydroxytryptamine (5-HT or serotonin) and neuropeptides (Eyzaguirre and Zapata, 1984; Fidone et al., 1990; Gonzalez et al., 1994). The predominant catecholamine in the CB is dopamine (~ 70%), whereas norepinephrine is found in smaller amounts (~ 30%; Hanbauer and Hellstrom, 1978; Gonzalez et al., 1994). Consistent with its high catecholamine levels, the CB contains high levels of tyrosine-hydroxylase (TH) the rate-limiting enzyme for CA synthesis. Therefore, most glomus cells appear capable of synthesizing dopamine (DA) and some of them may synthesize norepinephrine as well. In agreement with the studies on isolated cells (discussed above), during acute hypoxia the intact CB releases dopamine in a calcium-dependent manner (Fidone et al., 1982; Donnelly, 1993). In addition, there is evidence that other chemosensory stimuli, e.g. low pH (acidosis) and elevated CO₂ (hypercapnia), stimulate CA release as well (Fitzgerald et al., 1983; Rigual et al., 1991; Gonzalez et al., 1994). These results suggest that DA could be an important neurotransmitter involved in the relay of chemosensory information from glomus cells to the apposed sensory nerve endings. However, electrophysiological and pharmacological studies of DA in the CB have produced variable and inconsistent results. Exogenous dopamine has mostly been found to have an inhibitory role in the human, cat, dog, and rat CB (Docherty and McQueen, 1978; Welsh et al., 1978; Bisgard et al., 1979; Cardenas and Zapata, 1981). However, at high doses DA appears excitatory in the cat CB (Okajima and Nishi, 1981). The D₂-subtype of dopamine receptors has been shown to be present in both the chemoreceptor cells (presynaptic structures) and in the CSN sensory nerve endings (postsynaptic structures) of several species (Gonzalez et al., 1994). It was proposed that the presynaptic D₂ receptors have a higher affinity for dopamine than the postsynaptic D₂ receptors; thus, a low exogenous dose of DA

would preferentially act at the presynaptic receptors to decrease the release of DA resulting in an inhibitory action. On the other hand, at higher doses, injected DA would reach effective concentrations in the synaptic cleft to override the presynaptic inhibition resulting in excitation (Gonzalez et al., 1994). Whether DA is an excitatory transmitter mediating chemosensory information or an inhibitory neuromodulator is still unclear. However, recent studies have shown a clear dissociation between DA release and the hypoxia-evoked neuronal discharge, suggesting that DA is not necessary for hypoxic signaling in the CB (Donnelly, 1996; Iturriaga et al., 1996).

5.2 Acetylcholine (ACh)

Several studies have demonstrated the presence of ACh in the CB of different species (Eyzaguirre and Koyano, 1965b; Fidone et al., 1977; Eyzaguirre and Zapata, 1984). In addition, glomus cells have a high affinity uptake mechanism for choline, and choline acetyltransferase, the ACh synthesizing enzyme, has been detected in the CB of rat, cat and rabbit (Gonzalez et al., 1994). Furthermore, ACh persists in CB after chronic section of the CSN suggesting that ACh is probably located in glomus tissue (Fidone et al., 1977). Acetylcholinesterase (AChE), the ACh-degrading enzyme, has also been detected in the organ (Jones, 1975; Gonzalez et al., 1994), and has been localized intracellularly in glomus cells, as well as extracellularly, between contiguous glomus cells in dissociated rat CB cultures (Nurse, 1987). The first indication that glomus cells might release an ACh-like substance was obtained by Schweitzer and Wright (1938). They found that prostigmine, an inhibitor of AChE, enhanced ventilation similar to the application of exogenous ACh. This

observation was confirmed by other laboratories and the cholinergic hypothesis of CB neurotransmission was developed later (Eyzaguirre et al., 1965). In a perfusion experiment with the *in vitro* cat CB preparation, Eyzaguirre and Zapata (1968) demonstrated that an ACh-like substance released from an upstream CB could excite a downstream one. Stimulation of the upstream CB electrically or by asphyxia produced an increased CSN discharge from the downstream organ. The latter discharge could be augmented by eserine (an inhibitor of AChE) and blocked by mecamylamine (a blocker of nicotinic ACh receptors) (Eyzaguirre and Zapata, 1968). These experiments suggested that an acetylcholinesterase-sensitive, ACh-like substance, is released from CB chemoreceptor cells during chemical or electrical stimulation.

Other experimental results support the cholinergic hypothesis. For example, evidence for release of ACh from dog and cat CB has been obtained in perfusion experiments with bioassay techniques (Metz, 1969; Fitzgerald and Shirahata, 1996). In addition, eserine often increased the frequency of the basal CSN discharge from the CB and the excitatory effects of ACh on the CB are blocked by the cholinergic blockers, mecamylamine, hexamethonium, and curare (Eyzaguirre and Koyano, 1965b). Recently, an *in vivo* perfusion experiment combined with extracellular recording from CSN of cat demonstrated that cholinergic blockers reduced the CB response to hypoxia (Fitzgerald and Shirahata, 1994). However, there are some objections against the "cholinergic hypothesis". The incomplete block by cholinergic antagonists of the CSN discharge to natural stimuli did not favour this idea (Biscoe, 1971; Eyzaguirre and Zapata, 1984). In fact, the activity of ACh also showed species differences and there were reports of excitatory effects in cat, but inhibitory effects in rabbit

(Monti-Bloch and Eyzaguirre, 1980). Some of these discrepancies may be due to the different kinds of ACh receptors (AChR) present in the CB of different species. For instance, nicotinic AChR are more prevalent in the cat (Hirano et al., 1992), while muscarinic receptors predominate in the rabbit CB. In rat, both nicotinic and muscarinic AChR are present in glomus cells (Wyatt and Peers, 1993; Dasso et al., 1997).

5.3 5-Hydroxytryptamine (5-HT) or serotonin

5-Hydroxytryptamine has been identified in the chemoreceptor cells of the carotid body of many species, including mouse (Oomori et al., 1994), rat (Gronblad et al., 1983), cat (Abramovici et al., 1991) and humans (Perrin et al., 1986). An *in vitro* study reported that 5-HT was found in and released from cultured rat glomus cells (Fishman et al., 1985), though the release of endogenous 5-HT by natural chemostimuli, e.g. hypoxia, *in vivo* has not been reported to date. The CB of adult rat contains about 3.8 pmol of 5-HT, representing ~ 14% of the total amine content compared to 19% for human CB (Hellstrom and Koslow, 1975; Steele and Hinterberger, 1972). 5-HT has many effects on respiration and CB chemoreception. For instance, application of exogenous 5-HT to the CB produces hyperventilation that is abolished by carotid sinus nerve (CSN) section in rat (Sapru and Krieger, 1977). Intracarotid injection of 5-HT in the cat produces a transient increase followed by a decrease in CSN discharge (Nishi, 1975). The 5-HT induced increase of CSN discharge was quite similar to that induced by hypoxia, but 5-HT₃ receptor-specific antagonists selectively blocked the 5-HT induced-chemoexcitation, but failed to affect the hypoxia-induced CSN activity in the cat (Kirby and McQueen, 1984). Similar results were

reported for the rat carotid body (Yoshioka, 1989) suggesting that hypoxic signaling was not mediated by 5-HT. However, a later study showed that application of selective 5-HT₃ receptor antagonists in high doses reduced both the basal- and hypoxia-induced CSN discharge, contradicting previous reports. Thus, the possibility that 5-HT₃ receptors may still mediate synaptic transmission between chemoreceptors and the afferent nerve ending remains viable (McQueen and Evrard, 1990). Clearly, 5-HT has not been studied as extensively as catecholamines and ACh in relation to their role in the CB function.

5.4 Substance P (SP)

The neuropeptide, substance P, has been found in nerve fibers and glomus cells of the CB in many species and its levels have been measured in cat (Prabhakar et al., 1989), rabbit (Hanson et al., 1986) and human (Smith et al., 1990). However, SP and SP receptor mRNAs were detectable in the petrosal ganglion, but not in glomus cells of adult rat (Gauda and Gerfen, 1996). It has been reported that acute hypoxic stimulation increases the SP levels in the cat CB (Prabhakar et al., 1989), but reduces the peptide level in rabbit (Hanson et al., 1986). Pharmacological studies of SP actions in the CB indicate that this peptide is primarily excitatory. Exogenous SP produced an increase in basal CSN discharge and augmentation of the response to cyanide in cat (McQueen, 1980). SP stimulates the CB in rat and rabbit and studies described thus far suggest that SP is uniformly excitatory on CB across species (see however, Bisgard et al., 1994). Prabhakar and co-workers (1993) demonstrated that certain SP antagonists abolished or reduced the natural chemoreceptor response to hypoxia in cat and rat (Cragg et al., 1994). However, earlier pharmacological studies did not support these

results (Shirahata, 1989; McQueen and Evrard, 1990). In a recent review, Prabhakar (1994) described the actions of exogenous SP on mitochondrial metabolism and the increase in intracellular calcium in rat glomus cells; he proposed that the effect of SP on the CB is complex, and that it may not be viewed as a classical neurotransmitter, acting only on afferent nerve endings. Indeed, at present, the site(s) of action of SP in the CB is still controversial and information on second messenger systems coupled to the SP receptor would be of great interest in understanding the mechanism(s) of its action.

5.5 Other putative neurotransmitters/neuromodulators

There are several other putative neurotransmitters/neuromodulators localized to the CB. Some of these agents have pharmacological effects on the CSN discharge. Adenosine triphosphate (ATP) co-exists with CA in dense-cored vesicles of the CB (Bock, 1980), and consequently should be released with CA during exocytosis. ATP is also known to be present in cholinergic vesicles of nerve terminals (Burnstock, 1990) and exogenous ATP can reciprocally interact with ACh at the postsynaptic level in rat sympathetic neurons (Nakazawa, 1994). Pharmacological studies show that adenosine, a degraded product of ATP, increases CSN discharge recorded from the CB of rat and cat (McQueen and Ribeiro, 1983; Runold et al., 1990). In rat CB, adenosine A₂ receptor mRNA expression has been detected with *in situ* hybridization (Weaver, 1993) and electrophysiological studies revealed that purinergic P_{2x} receptors are ligand-gated cation channels which mediate excitation in nodose sensory neurons (Khakh et al., 1995). The nodose neurons are developmentally related to afferent chemosensory neurons in the petrosal ganglia (LeDouarin et al., 1981).

Taken together, these observations suggest that ATP and/or adenosine may act as excitatory transmitters in the CB via activation of presynaptic A_2 receptors and/or the postsynaptic P_{2x} receptors (see however, Spergel and Lahiri, 1993; Sun and Reis, 1994).

The glomus cells of the CB contain opioid peptides that are co-stored with CA in dense-core granules and released upon stimulation (Hanson et al., 1986). Pharmacological studies on the effects of opioid peptides on CSN discharge indicate primarily an inhibitory action for these putative neuromodulators. The δ -opioid receptors located on the chemoreceptor cells mediated the inhibition, though it is not known whether δ -opioid receptors are also located on afferent sensory nerve endings (Gonzalez-Guerrero et al., 1993).

From the above studies the most popular view is that the primary chemosensory element of the CB is the glomus cell, which augments the neural discharge in the apposed sensory terminals through the release of excitatory transmitter(s). Within this context it is assumed that sensory inhibition is also produced via a synaptic mechanism, by release of inhibitory agents from the glomus cell (Eyzaguirre et al., 1983). Thus, the final output that modulates CSN discharge is thought to represent a balance between excitatory and inhibitory influences. Two modulatory substances, GABA and atrial natriuretic peptide (ANP), have been considered as inhibitory candidates in the CB. GABA is a potent inhibitor in both the central and peripheral nervous system (Hille, 1992), and interestingly, a recent study has localized GABA-like immunoreactivity in the glomus cells of mouse CB (Oomori et al., 1994). Atrial natriuretic peptide (ANP) was revealed by immunocytochemistry in the glomus cells of cat CB and found to inhibit chemosensory discharge in response to hypoxia (Wang

et al., 1991). The effects of ANP are associated with increased levels of cyclic GMP (cGMP), suggesting that in the CB, ANP receptors are coupled to membrane bound guanylate cyclase. The physiological roles of these neuromodulators during the chemosensory responses of the CB still need further investigation (Wang et al., 1991). A briefly summary of the main putative carotid body neurotransmitters is given in Table 1.

6. Structure of petrosal ganglion

The sensory petrosal ganglion is located near the carotid bifurcation in mammals at the rostral end of the nodose ganglion. It contains many chemosensory neurons whose axons run in the glossopharyngeal (IX) nerve. The latter has two main branches: the carotid sinus nerve (CSN) which innervates the carotid body and sinus, and the remaining branch that leads to the tongue and pharynx (McDonald, 1983; Katz and Black, 1986). In the adult rat each CSN contains ~ 600 axons, of which 86% are unmyelinated (mean diameter of 0.78 μm) and the rest myelinated (mean diameter of 2.49 μm ; see McDonald, 1983). In the cat, the CSN contains ~ 2000 axons, of which 68% are unmyelinated. Among the unmyelinated axons, approximate 17% are chemoreceptor afferents; the others include baroreceptor afferents and sympathetic efferents. While, two-thirds of the myelinated axons are chemoreceptor afferents and the remainder baroreceptor afferents (Fidone and Sato, 1969; McDonald, 1983).

Neurons of the petrosal ganglion (PG) are derived from the embryonic ectodermal placode, unlike their target glomus cells which derive from the neural crest (reviewed by LeDouarin et al., 1981). The peripheral processes of PG neurons innervate the chemosensory

Table 1. Putative Carotid Body Neurotransmitters

Transmitters	Species	Effects	Receptors	Reference
Dopamine	rat, cat, rabbit, dog, mouse, pig	inhibitory excitatory	D ₂	McDonald, 1981 Gonzalez et al, 1994
Norepinephrine	rat, cat, rabbit, pig, human	inhibitory excitatory	α_2 β	McDonald, 1981 Prabhakar, 1994
Acetylcholine	rat, cat, rabbit, dog, pig	excitatory	nicotinic muscarinic	Eyzaguirre and Zapata, 1984 Dinger et al., 1991; Dasso et al., 1997
Serotonin (5-HT)	cat, rat, human, pig, mouse	excitatory	5-HT ₁ 5-HT ₂	Kirby and McQueen, 1984 Nishi, 1975
Substance P	cat, rabbit, human	excitatory	NK-1	Prabhakar, 1994
GABA	mouse	inhibitory	GABA _A	Oomori et al., 1994; Chapter 5
Opioid peptides	rabbit, cat, dog, monkey	inhibitory	δ -opioid	Prabhakar, 1994 Gonzalez et al., 1994
Adenosine (ATP)	rat, cat	excitatory	A ₂ (P _{2x} ?)	Sebastiao and Ribiero, 1996 McQueen and Ribiero, 1983 Bock, 1980
ANP	cat	inhibitory		Wang et al., 1993
Nitric oxide	cat, rat	inhibitory		Wang et al., 1995; Trzebski et al., 1995
CO	cat	inhibitory		Lahiri et al., 1993; Prabhakar, 1994

CB, whereas their central processes project to the respiratory control neurons in the nucleus tractus solitarius or NTS (Finley et al., 1992). Axonal degeneration studies in the rat carotid body have shown that 95% of the nerve endings are from the PG (McDonald and Mitchell, 1975). Retrograde-labeling and immunocytochemical staining techniques have revealed that the CB is innervated by distinct subsets of sensory neurons that are topographically segregated within the PG. Some neurons, located in the distal one-third of the ganglion, express tyrosine hydroxylase (TH), and account for approximately 41% of all CB afferent neurons (Finley et al., 1992; see however, Ichikawa et al., 1993). The majority of TH-positive neurons are small- or medium-size (mean diameter 15-20 μm), whereas only 7% of all CB afferent neurons express substance P or SP (Finley et al., 1992). Further evidence from immuno-electronmicroscopy showed that the peripheral terminals of TH-positive PG neurons contacted glomus cells in the CB. Further, morphometric analysis revealed that 84% of all TH-positive neurons in the PG were retrogradely labeled by a fluorescent dye infused into CB. In contrast, less than 3% of petrosal TH-positive neurons projected into other glossopharyngeal nerve branches (Katz and Black, 1986). Taken together, these data suggest that in the rat TH-positive neurons in the PG project almost exclusively to the CB and that it is a useful phenotypic marker for identifying CB chemoafferent neurons (Finley et al., 1992).

7. Electrophysiology of petrosal neurons

In addition to the morphological and neurochemical diversity in PG neurons (see above), there are electrophysiological differences identified mainly from studies in cat (Fidone

and Sato, 1969; Belmonte and Gallego, 1983; Gallego, 1983). Intracellular recordings from PG neurons during chemical or mechanical stimulation of the CB or arterial wall respectively, revealed that chemoreceptor neurons showed irregular spontaneous activity, the frequency of which was increased by chemical stimuli, e.g. acidosis or hypoxia (Belmonte and Gallego, 1983). In addition, all chemoreceptor neurons showed a time-dependent rectification in response to hyperpolarizing current pulses (I_h) and had a hump on the falling phase of the action potential. The majority (93%) of these chemoreceptor neurons produced only one spike during a long depolarizing current pulse. These properties may not reliably identify chemoreceptor neurons, since they were also found in some baroreceptor neurons (Belmonte and Gallego, 1983).

Recently, Stea and Nurse (1992) characterized the electrophysiological properties of dissociated petrosal neurons (PN) from neonatal rat using patch-clamp whole-cell recording. They reported that approximately 50% of rat PN had Na^+ currents that were TTX-resistant and the majority of the remaining were TTX-sensitive. A few cells have both TTX-resistant and TTX-sensitive Na^+ currents. All PN had similar voltage-activated Ca^{2+} and K^+ currents, and inward Ca^{2+} current was due mainly to L-type Ca^{2+} channels. The outward currents consisted largely of a delayed rectifying K^+ current and a Ca^{2+} -activated K^+ current. Exposure of cultured rat PN to a chemosensory stimulus, hypoxia, had no effect on voltage-activated currents, though as discussed earlier, hypoxia suppresses an outward K^+ current, in chemoreceptor glomus cells. Consistent with Gallego's (1983) observations on cat PN, Stea and Nurse (1992) found that some rat PN gave single spike during current-clamp recordings, while others gave multiple spikes in response to long-depolarizing stimuli. These studies

provided preliminary information that isolated rat PN were not themselves O₂-sensors, and that the property was confined to glomus cells (see however, Sun and Reis, 1994).

8. Studying synaptic transmission in the carotid body: problems and solutions

In the carotid body each CSN chemosensory fiber innervates approximately 10~20 glomus cells and the complex has been referred to as a 'sensory unit' (Eyzaguirre et al., 1983). The study of generator potentials and synaptic mechanisms in the CB proved difficult for several reasons. First, the terminals of the CSN are buried in the CB and difficult to visualize. Second, the space constant of the sensory fibers is very short due to their small diameter, implying that successful recording of synaptic events requires that the microelectrode impale the terminal portion of the fiber. This problem is further compounded by the small size of the terminals and poor visibility (Eyzaguirre et al., 1983). However, by impaling the whole CB *in vitro* with microelectrodes filled with dye, Hayashida et al. (1980) attempted to record from chemoafferent terminals in the cat. After recording, the impaled structures were stained by injecting dye from the electrode and it allowed subsequent identification of the recorded structure. With this approach recordings from impaled nerve terminals demonstrated the presence of numerous spontaneous depolarizing potentials (SDP's) with the features of postsynaptic events (Hayashida et al., 1980). They had a relatively rapid onset and a much slower decay, and their amplitudes varied from 1-20 mV. In some cases action potentials were seen and though the SDP's resembled postsynaptic events, the possibility that they were simply 'spontaneous' depolarizations of the nerve terminals could not be ruled out (Eyzaguirre et al., 1983). In general, these experiments were tedious and produced a relatively low yield

of successful impalements.

Other strategies for understanding the synaptic relationship between chemosensory nerves and glomus cells involved attempts at re-construction of synapses between glomus cells and a variety of sensory nerves *in vivo* and more recently *in vitro*. For instance, Zapata et al. (1969) reinnervated the carotid body with the superior laryngeal nerve (SLN), which, was supposed to contain only mechanosensory afferents and motor fibers. The newly-established pathway responded to anoxia with an increased sensory discharge. Thus, the SLN fibers, which normally respond only to mechanical stimulation, now responded to chemical stimulation of the CB in addition to mechanical stimulation. At that time, it was assumed that the new pathway became chemosensitive because of the release of acetylcholine (ACh) from glomus cells. In another study, Monti-Bloch et al. (1983) demonstrated that mechanosensory fibers "acquired" chemoreceptive properties after the CB was transplanted to the tenuissimus muscle in the cat. The successful mechanosensory fibers now responded to natural stimuli (hypoxia or hypercapnia) that would normally only increase firing in chemosensory axons of the CSN. Electron microscopic examination revealed that the transplants had some healthy glomus cells and axons appeared to form synaptic contacts with them. These experiments suggest an inductive influence of chemosensory elements (glomus cells) on the function of sensory axons; it may well be that glomus cells may change the properties of sensory fibers by releasing unknown chemicals (Katz and Black, 1986).

Other attempts to study synaptic mechanisms during CB chemosensory signaling utilized co-cultures of glomus cells and dissociated nodose sensory neurons from rat (Alcayaga and Eyzaguirre, 1990). Intracellular recordings of membrane potentials from

nodose neurons situated near to glomus cell clusters revealed spontaneous activity that was seldom seen in nodose neurons cultured alone. Application of an acid stimulus frequently had no effect on pure nodose neurons, but in co-culture it induced depolarization and spike activity (Alcayaga and Eyzaguirre, 1990). However, these co-cultures did not respond to hypoxic stimuli. These results suggest that the co-culture method, combined with electrophysiological and pharmacological tools may provide a useful approach to study synaptic transmission in the CB. This method combined with patch-clamp recording techniques, described below, was successfully used in this thesis.

9. Patch-clamp techniques for electrophysiological studies

Patch-clamp recording methods evolved with the need to record and study directly the behaviour of single ion channel proteins in biological membranes. An important spin-off, exploited in this thesis, was that it became a powerful tool for studying the electrophysiological properties of small cells (Hamill et al., 1981). In 1952, the studies of Hodgkin and Huxley on the squid axon revealed that analysis of the mechanisms underlying electrical activity in excitable cells can be most easily studied with "voltage-clamp", where the potential across the cell membrane is controlled. The voltage-clamp apparatus uses a feedback circuit to maintain a constant membrane potential by injecting a current equal and opposite to that generated by the membrane. The recorded membrane current at any given potential can usually be separated into capacitive and ionic components, where the latter is a direct measure of the currents flowing through open ion channel proteins in the membrane. With this approach, Hodgkin and Huxley (1952) established the model where movement of sodium and

potassium ions across the membrane were responsible for the action potential in the squid axon.

Although the methods of Hodgkin and Huxley, and later variations, made important contributions to electrophysiology (Jones, 1990; Hille, 1992), they were limited to few cell types that were large enough for manipulation with the available electrodes. However, in 1976 the novel patch-clamp technique was invented by Neher and Sakmann, and this allowed voltage-clamp recordings from small, fragile cells. Before then, fine glass microelectrodes were used for impaling cells, but the damage introduced by the electrode made recording from small cells ($<15\ \mu\text{m}$) unreliable. The patch clamp technique uses a single electrode to pass current and record voltage simultaneously, but most important, the shunt between electrode and cell membrane is drastically reduced. Following application of slight suction within a fresh pipette ($\sim 1\ \mu\text{m}$ in diameter at the tip), a high resistance "gigaseal" can be formed between the glass and membrane (Hamill et al., 1981), resulting in the ability to resolve tiny currents (through single ion channel proteins) above background noise. Furthermore, gigaseals are mechanically stable, so that the patches can be withdrawn from the cell and studied in isolation. Various configurations allow the study of single channel activity, including cell-attached configuration, inside-out patch, outside-out patch (Hamill et al., 1981; Jones, 1990). In the whole-cell configuration, which was used frequently during the course of this thesis, the patch is broken and pipette solution has free access to the cell interior.

The whole-cell configuration of the patch clamp technique is quite similar to conventional intracellular recording methods that preceded it. Since ion channels can be regulated by second messengers, regulatory proteins and by phosphorylation, a disadvantage

of the whole-cell method is that these regulatory molecules may be lost through dialysis when the patch is ruptured (Sakmann and Neher, 1983). This is partially offset by the ability to control the intracellular media, where the ionic composition is known. To avoid the loss of important cytoplasmic factors through dialysis during whole-cell recording, variations of the technique aimed at achieving electrical continuity between pipette and cytoplasm (while minimizing dialysis), were explored. It was found that certain pore-forming antibiotics could be used to permeabilize patches and allow selective exchange of small ions without perturbing the intracellular biochemistry. These techniques, known as perforated-patch recording, were developed by Horn and Marty (1988) and were also used extensively in this thesis.

10. Goals and organization of thesis

As is evident from the above discussion, there is a large void in our understanding of the mechanisms underlying the processing of chemosensory information in the mammalian carotid body. Particularly, the neurotransmitter mechanisms by which the output from chemoreceptor cells is translated into a frequency code carried by impulse activity in the carotid sinus nerve (CSN) are poorly understood. The presence of multiple neurotransmitters or neuromodulators in chemoreceptor cells, as summarized in Table 1, undoubtedly has contributed to the complexity of the system. Also, electrophysiological methods used to date have largely been limited to the monitoring of the spike discharge in the afferent CSN at distances located far away from the transduction and synaptic sites. This has seriously hampered the understanding of synaptic events because of the overriding influences of the action potential mechanism (Katz, 1969). A major goal of this thesis was to bridge this void

in our knowledge and hopefully provide new mechanistic insight into the role of synaptic and neurotransmitter mechanisms in the encoding of chemosensory stimuli in the carotid body. As discussed below, the thesis is organized in Chapters, prepared as manuscripts for publication in various refereed journals.

To achieve the above goals several new strategies were employed. Since many laboratories (including our own) were studying the properties of isolated chemoreceptor (glomus) cells *in vitro*, I focussed primarily on the petrosal neurons which supply the afferent innervation of glomus cells. I began by characterizing the electrophysiological properties of isolated rat petrosal neurons, and extended the studies initiated by Stea and Nurse (1992). Since chemosensory information in the carotid body is carried by a frequency code in petrosal afferents, a complete knowledge of the types of ionic currents expressed by petrosal neurons was considered necessary. I therefore paid special attention to those ionic currents that were not previously characterized, but are generally known to regulate spike frequency in neurons, either directly, or following modulation by various neurotransmitters (Rudy, 1988; Hille, 1992). During the course of the study two such types of K^+ currents were uncovered, i.e. a hyperpolarization-activated, inward rectifier current, I_h , and an A-type current, I_A . Chapter 2 of the thesis provides a detailed characterization of this I_h in petrosal neurons, and the paper is now in press in the journal, *Primary Sensory Neuron*. Interestingly, during the course of this thesis, the presence of an inward rectifier current in rat petrosal afferents was inferred indirectly, from the change in hypoxic response of the carotid body-sinus nerve preparation *in vitro* to the blocker, cesium (Doyle and Donnelly, 1994). The I_A current, which was not observed in the initial studies of Stea and Nurse (1992), was not investigated in the same

detail as I_h , though some interesting properties, particularly its apparent modulation by a carotid body peptide neurotransmitter, substance P, is briefly discussed in the Appendix.

A major portion of the thesis is devoted to a characterization of the response of petrosal neurons to several excitatory and inhibitory neurotransmitters, known to be present in carotid body chemoreceptor cells (Table 1). Since the neurotransmitter sensitivity of the chemosensory afferent (petrosal) fibers was largely unknown, I began a systematic characterization using electrophysiological and pharmacological tools. Since in these experiments the neurotransmitter or an agonist was applied to petrosal cell bodies, the assumption was made that receptors expressed on the cell body were likely to be expressed at the terminals, where the synapses are made with chemoreceptor cells. Though there may be exceptions to this and the receptor densities at synaptic or extrasynaptic region may be dramatically different (Nusser et al., 1995), it seemed a reasonable first assumption. Chapter 3 and 4 focus on the excitatory neurotransmitters acetylcholine (ACh) and 5-HT or serotonin respectively. The results of Chapter 3 are now in press in the journal, *Brain Research*, and those of Chapter 4 are almost ready for submission. In Chapter 4, the direct effects of 5-HT on chemoreceptor cells are also investigated, since they are relevant to understanding the role of 5-HT in the carotid body and (unlike the case for ACh) have not been previously studied. Chapter 5 focuses on the inhibitory neurotransmitter, GABA. Chapter 6 deals with successful efforts to reconstruct a functioning chemoreceptor complex *in vitro* using co-cultures of rat petrosal neurons and glomus cells. In this chapter, evidence for the *de novo* formation of chemical synapses between some neurons and glomus cells is presented, as well as for hypoxia-induced depolarization and/or increased afferent firing in co-cultured neurons

juxtaposed to glomus cell cultures. In these co-cultures at least one of the neurotransmitters (i.e. ACh) mediating hypoxic signaling is identified. Finally, Chapter 7 presents an overview, with a discussion of the physiological relevance of the above findings to the mechanisms of chemoreception in the carotid body. Other relevant data, not investigated in the same detail (including effects of other major CB neurotransmitters, e.g. dopamine and substance P), are presented in the Appendix.

CHAPTER 2

Characterization of A Hyperpolarization-Activated Inward Current in Rat Chemosensory Petrosal Neurons *in Vitro*

Manuscript by H. Zhong and C. A. Nurse; (in press) Journal: '*Primary
Sensory Neuron*'.

1. I prepared and maintained cell cultures.
2. I performed all electrophysiological recordings.
3. I performed all data analysis and generated all figures in text.

ABSTRACT

Regulation of carotid body (CB) chemoafferent discharge in mammals plays an important role in the reflex control of ventilation. A non-selective blocker (cesium) of the inward rectifier is known to inhibit CB afferent discharge during hypoxia, but the underlying current in corresponding neurons of the petrosal ganglia has not been characterized. In this study we provide a detailed description of a voltage-dependent, inwardly rectifying, cation non-selective current, I_h , that was present in $\sim 78\%$ of cultured rat petrosal neurons. Activation of this current appeared to be the basis of the slowly-developing depolarizing sag that was recorded under current clamp during application of hyperpolarizing current pulses. Under voltage clamp, I_h was activated at voltages negative to -60 mV and had an estimated reversal potential (E_h) of $\sim -33.1 \pm 3.4$ mV ($n=20$). Raising extracellular $[K^+]_o$ caused a progressive increase in I_h and a positive shift in E_h , whereas reducing extracellular $[Na^+]_o$ caused a small reduction in I_h and an opposite shift in E_h . Reducing extracellular $[Cl^-]_o$ had no significant effect on E_h , though the amplitude of I_h decreased. Tail current analysis revealed that the activation curve for I_h was well fitted by the Boltzmann distribution, with $V_{1/2} = -90.6 \pm 2.2$ mV (mean \pm S.E.M.; $n=17$) and slope factor $k = 10.8 \pm 0.5$. I_h activated more rapidly at larger hyperpolarizations; elevated $[K^+]_o$ or lowered $[Na^+]_o$ increased the time constant (τ) of I_h activation. The time constant of deactivation of I_h at -60 mV was 317.1 ± 31.9 ms ($n=7$). Extracellular cesium (10 mM) almost completely blocked I_h , whereas barium suppressed I_h by $\sim 50\%$, at a similar concentration. These results, combined with the known sensitivity of

the hypoxic afferent discharge to extracellular cesium, suggest that I_h likely plays an important physiological role during CB chemosensory signalling.

INTRODUCTION

Since the first description by Katz (1949), anomalous or inward rectification has been identified in a variety of cell types including muscle cells, endothelial cells and neurons (Hille 1992). The classic anomalous rectifier (I_{kir}) is K^+ selective, blocked by barium and cesium and activates rapidly at potentials negative to the potassium equilibrium potential (E_K) (Constanti and Galvan 1983; Gay and Stanfield 1977; Hagiwara and Takahashi 1974). Another type, the hyperpolarization-activated inward current (I_h) is cation non-selective (permeable to both Na^+ and K^+ ions), blocked by cesium but not or only partially by barium, and activates more slowly upon hyperpolarization (Crepel and Penit-Soria 1986; DiFrancesco 1981; Kamondi and Reiner 1991; Wollmuth and Hille 1992). I_h has also been described as I_f in pacemaker cells of the heart (Brown and DiFrancesco 1980; Irisawa *et al.* 1993) and as I_Q in hippocampal pyramidal cells (Halliwell and Adams 1982). Though the significance of I_h is unclear it is thought to regulate pacemaker activity in spontaneously-spiking cells (Irisawa *et al.* 1993), or to prevent the over-hyperpolarization of the cell membrane in sensory neurons and thus keep the membrane potential in a range suitable for the discharge and release of neurotransmitters (Fain and Lisman 1981; Mayer and Westbrook 1983).

Our long-range goal is to understand how petrosal sensory afferents receive and process

information from peripheral chemoreceptors in the mammalian carotid body. These visceral afferents project to the respiratory control center in the brainstem and signal changes in arterial Po_2 by regulating spike frequency, apparently in response to neurotransmitters secreted by O_2 -chemoreceptors (Gonzalez *et al.* 1994). Previous studies in our laboratory have characterized a variety of voltage-dependent currents in cultured rat petrosal neurons (Stea and Nurse 1992). These include both tetrodotoxin (TTX)-sensitive and TTX-resistant sodium currents, delayed rectifier and calcium-dependent potassium currents, and L-type calcium currents. In contrast to somatic sensory neurons (Mayer and Westbrook 1983; Scoggs *et al.* 1994), little is known about I_h in visceral sensory neurons, though the presence of inward rectification has been noted in neurons of the nodose and petrosal ganglia in cat (Gallego and Eyzaguirre 1978; Gallego 1983). In the present study we frequently encountered I_h during voltage clamp recordings from cultured rat petrosal neurons, and provide a detailed characterization of its properties. In view of a recent report that extracellular cesium, a non-specific blocker of I_h , inhibits carotid sinus nerve discharges during hypoxia (Doyle and Donnelly 1994), it is likely that this current plays an important role in regulating spike frequency during chemosensory signalling.

METHODS

Cell culture

Dissociated cells from petrosal ganglia were obtained from 2-14-day-old rat pups (Wistar, Charles River, Quebec) as previously described (Stea and Nurse 1992). Briefly, excised

ganglia were incubated for 1 h at 37° C in an enzymatic solution containing 0.1% collagenase/0.1% trypsin (Gibco, Grand Island, NY). The enzyme was then replaced by growth medium consisting of F-12 nutrient medium (Gibco, Grand Island, NY) supplemented with 10% fetal bovine serum (Gibco), 80U/l insulin (Sigma Chemical Co., St. Louis, MO), 0.6% glucose, 2 mM glutamine and 1% penicillin-streptomycin (Gibco). The tissues were mechanically dissociated with forceps, triturated to yield a cell suspension, and plated onto a thin layer of Matrigel (Collaborative Research, Bedford, MA) that was previously applied to the central wells of 35-mm tissue-culture dishes. In some experiments petrosal neurons were grown in co-culture with their normal targets, i.e. glomus cells of the carotid body. The co-cultures were obtained by first preparing cultures of dissociated rat carotid body as previously described (Nurse 1990), and then adding an overlay of dissociated petrosal neurons 3-5 days later. Cultures were grown at 37° C in a humidified atmosphere of 95% air-5% CO₂ for 4 h to 14 days before they were used in the patch-clamp/whole-cell experiments. The growth medium was changed every 4-6 days and in a few experiments was supplemented with the neurotrophic factors BDNF and NT-4 (10 ng/ml; Alomone Laboratories, Jerusalem); data from these experiments were pooled since similar results were obtained under the different growth conditions.

Solutions and drugs

Most experiments were performed using extracellular fluid (ECF) of the following composition (mM): NaCl, 135; KCl, 5; CaCl₂, 2; MgCl₂, 1; glucose, 10; N-2-hydroxyethylpiperazine-N'-2-ethane sulphonic acid (HEPES), 10 at pH 7.4. The stock pipette

solution for conventional whole-cell recording contained (mM) either : (i) KCl, 135; NaCl, 5; CaCl₂, 1; ethylene glycol-bis(β-aminoethyl ether)-N,N,N',N'-tetraacetic acid (EGTA),11; HEPES,10; ATP-Na 2 mM at pH 7.2; or (ii) potassium glutamate or gluconate, 105; KCl, 35; CaCl₂,1; EGTA,11; HEPES,10; ATP-Na 2 mM at pH 7.2. For perforated-patch recordings the pipette contained (mM): potassium glutamate or gluconate, 105; KCl, 35; CaCl₂,1; HEPES, 10 and nystatin 300 μg/ml, at pH 7.2. All solutions were filtered through a 0.45 μm millipore filter before use.

Drugs or reagents used to study the pharmacology of I_n include: tetrodotoxin (TTX; 1 μM), tetraethylammonium (TEA; 5-10 mM) , 4-aminopyridine (4-AP; 5-10 mM), cesium chloride (CsCl; 5-10 mM), barium chloride (BaCl₂ ; 5-10 mM) and cobalt chloride (CoCl₂ ; 2-5 mM); these were obtained from Sigma. All solutions were added to the recording chamber by perfusion under gravity and withdrawn by vacuum suction.

Whole- cell recording

Procedures for whole-cell recording were similar to those described in detail elsewhere (Stea and Nurse 1991a, 1992). Patch pipettes were fabricated from Corning 7052 glass (1.5 mm O.D.) pulled in a Flaming/Brown horizontal puller (Sutter Instrument Co., Novato, CA). The pipettes were fire-polished and their resistance varied between 2-10 MΩ. In some experiments, nystatin perforated-patch recording was used as described elsewhere (Stea and Nurse 1991a). Since in general, results were similar to those obtained with conventional whole-cell recording, data from both methods were pooled. Approximately 75 % of the series resistance, typically in the range 10-20 MΩ, was compensated in most experiments. The seal

resistance between pipette and cell varied between 2 and 10 G Ω . Junction potentials, in the range 2-10 mV, were cancelled at the beginning of the experiment. Most recordings were performed at room temperature; a few, using co-cultures, were done at 35°C.

Whole-cell currents or membrane potential were recorded with an Axopatch 1D patch clamp amplifier and a Labmaster TL-1 A-D converter (Axon Instruments Inc., Foster City, CA), and stored on a 486 Personal Computer. Current and voltage clamp protocols, data acquisition and analysis were performed using pCLAMP software (version 5.5., and 6.0.2, Axon Instruments Inc.).

Data analysis

Exponential fits of the time course of I_h activation and deactivation were obtained using CLAMPFIT (6.0.2, Axon Instruments Inc.). Fits of the voltage dependence of I_h activation to the Boltzmann distribution were obtained using Sigmaplot. The variables $V_{1/2}$ (pre-pulse potential where I_h was half maximal) and $S_{1/2}$ (slope factor at $V_{1/2}$) were adjusted for best fit of the curve to the observed data. Most of the results are represented in the text as mean \pm standard error (S.E.M). Data were compared using a Student's t-test with the level of significance set at $p < 0.01$.

Immunofluorescence

After whole-cell recording, a few cultures were processed for tyrosine hydroxylase (TH) immunoreactivity, to test whether the recorded neuron that expressed I_h was also positive for TH, a biochemical marker for carotid body chemoafferents (Katz and Black 1986; Finley *et al.* 1992). Immunofluorescent staining was visualized using a fluorescein-conjugated

secondary antibody, as described previously (Nurse 1990).

RESULTS

The results of this study are based on observations from 153 rat petrosal neurons grown in dissociated cell culture for 4 h to 14 days. As regards the passive membrane properties, the mean input resistance was $567.2 \pm 102.6 \text{ M}\Omega$ (n=89) and mean input capacitance, determined by integration of the capacity transient, was $22.1 \pm 3.2 \text{ pF}$ (n=89); the membrane time constant determined from the exponential time course of the voltage response to small rectangular current pulses was $11.3 \pm 2.5 \text{ ms}$ (n=40). Of the neurons sampled ~ 78 % showed inward rectification or I_h at voltages negative to resting membrane potential. I_h was present at similar frequencies whether the neurons were cultured alone (~74 %; n= 66), or co-cultured with target cells from the carotid body (~82 %; n= 87). Since in the rat, carotid body chemoafferent neurons in the petrosal ganglion selectively express tyrosine hydroxylase (TH) and a dopaminergic phenotype (Finley *et al.* 1992), we tested in a few cases whether neurons that displayed I_h also expressed TH, as revealed by immunofluorescence. Interestingly, we found that eight neurons with I_h were also TH- positive, whereas two neurons without I_h were TH- negative.

Current-clamp recordings

In current clamp mode, inward rectification was routinely observed in petrosal neurons during the application of long-duration (up to 800 ms) hyperpolarizing current pulses. As

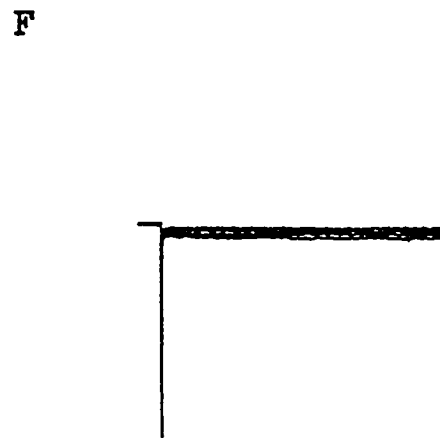
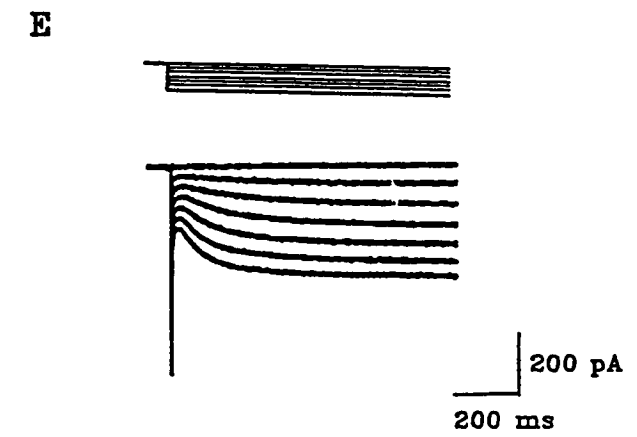
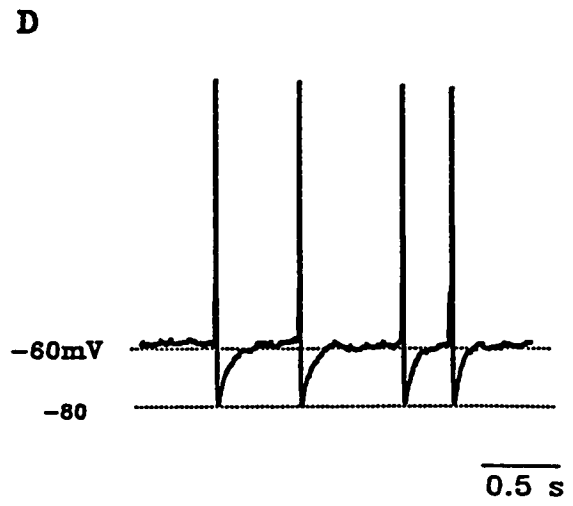
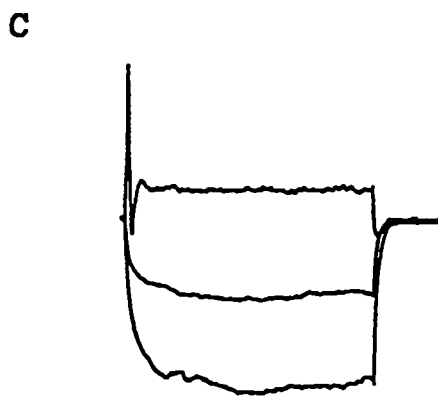
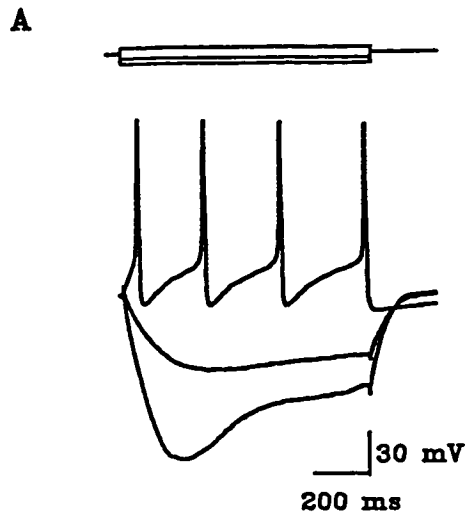
shown in Fig. 1A,B, this inward rectification, evidenced by a slowly developing depolarization sag at more negative membrane potentials, was present in neurons which displayed different firing patterns, e.g. multiple spikes (Fig. 1A) or a single spike (Fig. 1B), when depolarized. A smaller proportion (~ 22%) of neurons showed no evidence of inward rectification (e.g. Fig. 1C). A depolarization sag, similar to Fig. 1A,B, has been reported in cat petrosal neurons (Gallego 1983) and other sensory neurons (Gallego and Eyzaguirre 1978; Mayer and Westbrook, 1983; Scoggs *et al.* 1994) at comparable negative potentials.

The ability of some neurons in co-culture to fire spontaneously afforded the opportunity to test whether the membrane potential might normally reach values sufficiently negative to activate I_h . Generally, this appeared to be the case as shown for the same spontaneously active neuron studied under both current (Fig. 1D) and voltage (Fig. 1E) clamp. In this cell, which had a resting potential of ~ -60 mV, the undershoot reached negative potentials of -80 mV, that is sufficient to activate I_h as seen in voltage clamp records (Fig. 1E; see below).

General characteristics of I_h under voltage clamp

To investigate the ionic basis of the depolarization sag, we began by carrying out voltage-clamp experiments as in Fig. 1E. Hyperpolarizing voltage steps up to -140 mV were applied, in 10 mV increments, to neurons held initially at -60 mV; in many cases a slowly-activating inward current, whose amplitude and rate of activation increased at more negative membrane potentials, developed (Fig. 1E). We refer to this current as I_h because, as detailed below, it has voltage- and time-dependent characteristics, as well as pharmacological properties, similar

Figure. 1. Current- and voltage-clamp recordings from cultured petrosal neurons. A: Hyperpolarizing currents (-50 and -100 pA; top traces), elicited a slowly developing depolarization sag in the membrane potential (lower traces); a depolarizing current pulse triggered multiple spiking in this neuron. B: A different neuron showing a similar depolarization sag in response to hyperpolarizing currents; however, this cell fired only a single spike with depolarizing currents. C: An example of a neuron that showed no depolarization sag or inward rectification with hyperpolarizing currents. D: Spontaneous overshooting action potentials in a petrosal sensory neuron recorded under current clamp; resting potential was ~ -60 mV. Note the undershoot crosses a voltage range sufficiently negative for I_h to become activated (see Fig. E). E: Current records (lower traces) elicited during voltage-clamp steps from a holding potential of -60 to -120 mV, in 10 mV increments. Note the slowly developing inward current at more negative potentials, due to activation of I_h ; the amplitude of I_h increased as the magnitude of the (hyperpolarized) voltage step increased. F. The absence of an inward current at negative test potentials in a typical cell that lacked an I_h ; holding potential -60 mV.



to those described for I_h in other cell preparations (e.g. Bayliss *et al.* 1994; Mayer and Westbrook 1983;). Since in general, cells that did not show the depolarization sag under current clamp (e.g. Fig. 1C) also did not show I_h under voltage clamp (e.g. Fig. 1F), it is likely that I_h underlies the depolarization sag or inward rectification.

Reversal potential of I_h

Since determination of the reversal potential of I_h (E_h) by tail-current analysis proved impractical, due to the occasional presence of a transient outward current (not shown) and a TTX-resistant inward current (Stea and Nurse 1991a), an extrapolation procedure which avoided other voltage-gated currents was used (Mayer and Westbrook, 1983). In Fig. 2A, currents (top traces) were activated by a family of voltage steps (bottom traces) from a holding potential -60 mV; instantaneous current (I_{ins}) was measured immediately following the capacitive transient and plotted against membrane potential (Fig. 2C; closed circles). This relationship was well-fitted with linear regression, indicating only leak currents (but no inward rectification) were present. In contrast to I_{ins} , the steady-state current (I_{ss}), measured at the end of the voltage step, showed strong inward rectification at voltages negative to -60 mV as illustrated in Fig. 2C (open circles). Finally, a second set of I_{ins} measurements was recorded from a holding potential -120 mV (Fig. 2B), where I_h is almost fully activated, and plotted in Fig. 2C (open triangles). The mean reversal potential (\pm S.E.M.) of I_h (E_h), estimated from the intersection of the two extrapolated I_{ins} I-V curves, was -33.1 ± 3.4 mV (n=20).

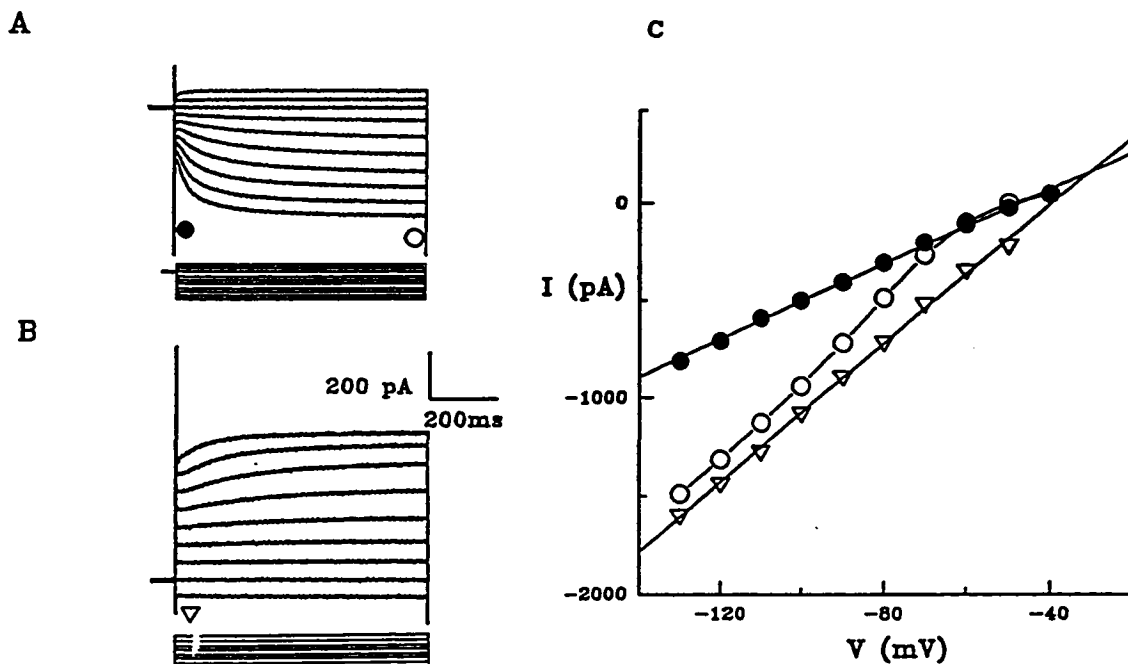


Figure. 2. Reversal potential of I_h . A: Typical current records (top traces) elicited mainly by hyperpolarizing voltage steps (bottom traces) from a holding potential of -60 mV; upper two traces elicited by depolarizing voltage steps to -50 and -40 mV. Instantaneous currents (I_{ms}) were measured soon after the capacitive transient (●) at the beginning of the voltage step; steady-state currents (I_{ss}) were measured at the end of the hyperpolarizing voltage step (○). B: Current records (top traces) elicited mainly by depolarizing voltage steps (bottom traces) from a holding potential of -120 mV; lowest trace elicited by a hyperpolarizing step to -130 mV. C: The plot of steady-state current in A (○) vs membrane potential (V) indicates the activation of I_h occurred at potentials negative to -60 mV. Plots of instantaneous currents, elicited during steps from -60 mV in A (●) and from -120 mV in B (▽), vs membrane potential were well fitted with linear regression. The extrapolated intersection of the two regression lines occurred at ~ -30 mV and represents the estimated reversal potential of I_h .

Ionic basis of I_h

The value of the estimated reversal potential E_h (~ -33 mV; Fig. 2) suggested that I_h was due to a mixed cationic current. In ion substitution experiments, raising $[K^+]_o$ increased the amplitude of I_h (Fig.3A), whereas lowering $[Na^+]_o$ produced a small reduction (Fig.3B). The effects of these ion substitutions on the magnitude of I_h at different voltages are shown in Fig. 3C. In 6 experiments the reversal potential E_h (estimated by the extrapolation method as in Fig. 2) shifted to more positive values in high (10 mM) $[K^+]_o$ (mean = -14 ± 5.4 mV), and more negative values (mean = -65.8 ± 5.3 mV) in low $[Na^+]_o$ (10 mM); examples of these shifts are shown in Fig. 3 D and E respectively. These data suggest that Na^+ and K^+ are the main charge carriers of I_h in petrosal neurons, as occurs in other preparations (Kamondi and Reiner 1991; Mayer and Westbrook 1983).

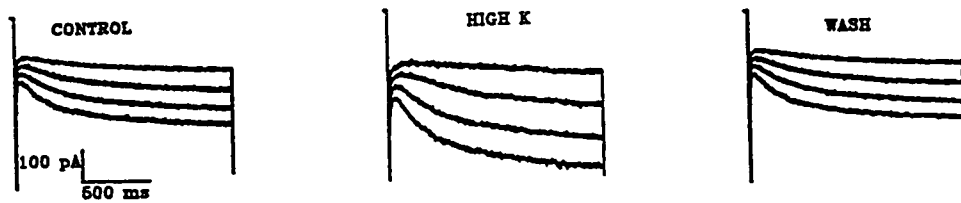
We ruled out possible contributions of an inward chloride current to I_h in experiments where Cl^- was substituted by the large impermeant anion, nitrate (NO_3^-). Reducing extracellular Cl^- from 140 mM to 10 mM, thereby causing ~ 70 mV positive shift in E_{Cl^-} , resulted in no detectable change in the reversal potential of I_h (in 10 mM Cl^- , $E_h = -30.5 \pm 6.4$; $n=5$); current amplitudes, however, were reduced at all negative test potentials (see Fig. 6A). Possible explanations for this reduction are discussed later.

Voltage dependence of I_h activation

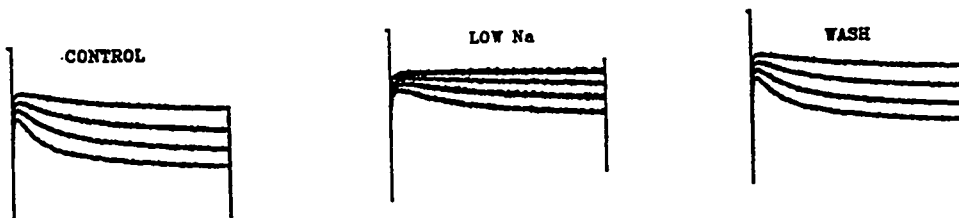
Using a two-step voltage-clamp protocol (Fig. 4A, top traces), which increases the sensitivity of the current measurements, the voltage dependence of I_h activation was determined.

Figure. 3. Effects of high potassium and low sodium on I_h . A: Current traces evoked by voltage steps (omitted for clarity) from a holding potential of -60 mV to -120, -110, -100, and -90 mV in control solution containing normal potassium (5 mM; left), in high potassium (10 mM; middle), and after wash in control solution (right). B: Currents recorded in control solution containing normal sodium (135 mM; left), low sodium (5 mM; middle), and after wash in control solution (right). C: Current - voltage or I-V relation comparing the effects of high potassium (open triangles), low sodium (closed triangles) on I_h relative to control (closed circles). D: Instantaneous I-V relation in high potassium solution is illustrated for steps from a holding potential of -60 mV (closed circles) and -120 mV (open triangles); intersection of the extrapolated linear plots represents the estimated reversal potential E_h (see Fig. 2 and text). High potassium causes a positive shift in E_h from ~ -30 mV (Fig. 2) to -10 mV. E: Instantaneous I-V relation, similar to D, but in low sodium solution which causes a negative shift in E_h from ~ -30 mV to -70 mV.

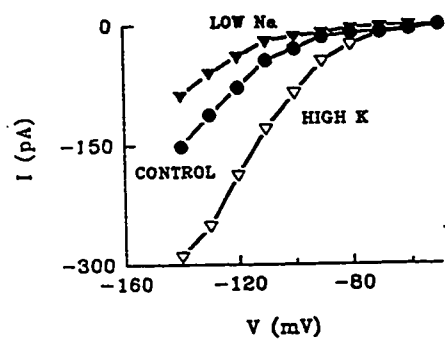
A



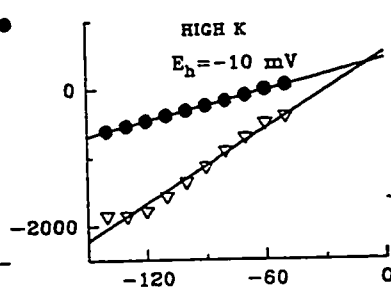
B



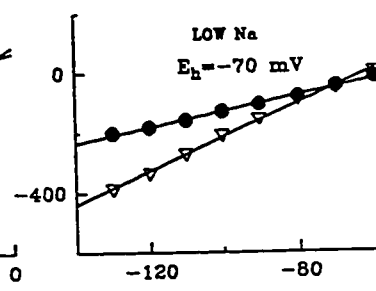
C



D



E



Following 1 sec conditioning steps to various potentials (which partially activated I_h) a test pulse was applied by stepping the membrane potential to -130 mV, where I_h appeared to be fully activated. Tail currents, measured soon after the beginning of the test pulse (at ~20 ms) provided a measure of the proportion of I_h that was activated during the conditioning pulse. The tail current amplitudes were normalized according to the following relationship:

$$I_{\text{norm}} = (I_v - I_{\text{min}}) / (I_{\text{max}} - I_{\text{min}}) \quad (1)$$

where I_{max} is the maximal inward tail current (following steps to -130 mV); I_{min} is the minimal inward tail current (following steps to -40 mV); and I_v is the tail current elicited during a step to -130 mV after a conditioning pulse to various membrane potentials (V). The activation curve of I_h was generated by plotting the normalized current (I_{norm}) against the membrane potential (V) during the conditioning pulse (Fig. 4B). The data points were well fit by a Boltzmann function of the form:

$$I_{\text{norm}} = 1 / \{ 1 + \exp[(V - V_{1/2})/k] \} \quad (2)$$

where $V_{1/2}$ is the potential at which the current is half-maximally activated; and k is the slope factor. Mean values (\pm S.E.M.) of $V_{1/2} = -90.6 \pm 2.2$ mV and $k = 10.8 \pm 0.5$ (n=17) were obtained from best fits of the data points to equation 2. In low extracellular Na^+ (10 mM), there was no obvious change in the voltage dependence of I_h activation (not shown). These results are similar to previous reports from other preparations (Bayliss *et al.* 1994; Kamondi and Reiner 1991; Mayer and Westbrook 1983).

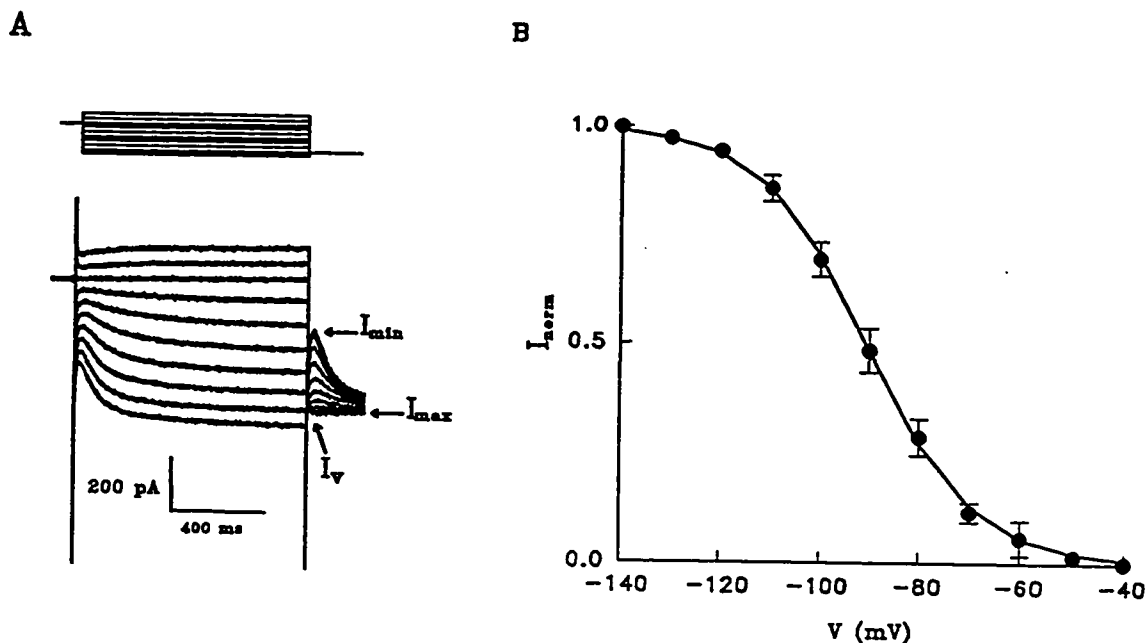


Figure 4. Voltage dependence of I_h activation. A: Conditioning steps from -60 mV to a series of membrane potentials V were applied for 1 sec before a final test pulse to -130 mV (top traces). Current responses (bottom traces) revealed voltage-dependent activation of I_h during the initial conditioning step, followed by tail current relaxations of various amplitudes I_v during the final step to -130 mV. The maximum (I_{max}) and minimum (I_{min}) tail currents elicited during the test pulse are indicated in the figure. B: The normalized current I_{norm} (as defined in text) is plotted against membrane potential during the conditioning step. The data points on graph represent mean \pm S.E.M. from a total of 17 cells. The data were fitted with a smooth curve generated according to the Boltzmann equation (see text) with $V_{1/2} = -90.6$ mV and $k = 10.8$.

Kinetics of I_h

The time course of I_h activation was determined from current records elicited during steps from -60 mV to more hyperpolarized potentials (up to -130 mV). As shown in Fig. 5A,B the activation kinetics of I_h were best fit by a single exponential function of the form :

$$I_t = I_{ss} - I_h * \exp(-t/\tau) \quad (3)$$

where I_t is the current at time t , I_{ss} is the steady-state current at the end of the voltage step, I_h is the difference between I_{ss} and I_{ins} , and τ is the time constant of activation. In high (10 mM) K^+ or low Na^+ (10 mM), τ measured at -100 mV was significantly longer than in normal ionic medium, as shown in Fig. 5A and B respectively. The mean τ (\pm S.E.M.) in control extracellular medium was 335.6 ± 17.4 ms ($n=14$), compared to 577.7 ± 24.2 ms ($n=9$) in low Na^+ , and 390.5 ± 34.6 ms ($n=5$) in high K^+ . The time constant of I_h activation also showed strong voltage sensitivity (Fig. 5C); it was faster at more hyperpolarized membrane potentials, as reported in other cell types (Bayliss et al. 1994; Kamondi and Reiner 1991; Yanagihara and Irisawa 1980).

To study the deactivation kinetics of I_h , the experimental protocol shown in Fig. 5D was used. I_h was first fully activated during a 0.8 s conditioning step from -60 to -130 mV. Subsequently, the membrane potential was returned to -60 mV for varying periods of time 't', before a final (100-ms) hyperpolarizing step to -120 mV was applied. The instantaneous current I_t , initiated by the final hyperpolarizing step, was measured and plotted against 't'. The data were best fit (e.g. Fig. 5E) by a single exponential function of the form :

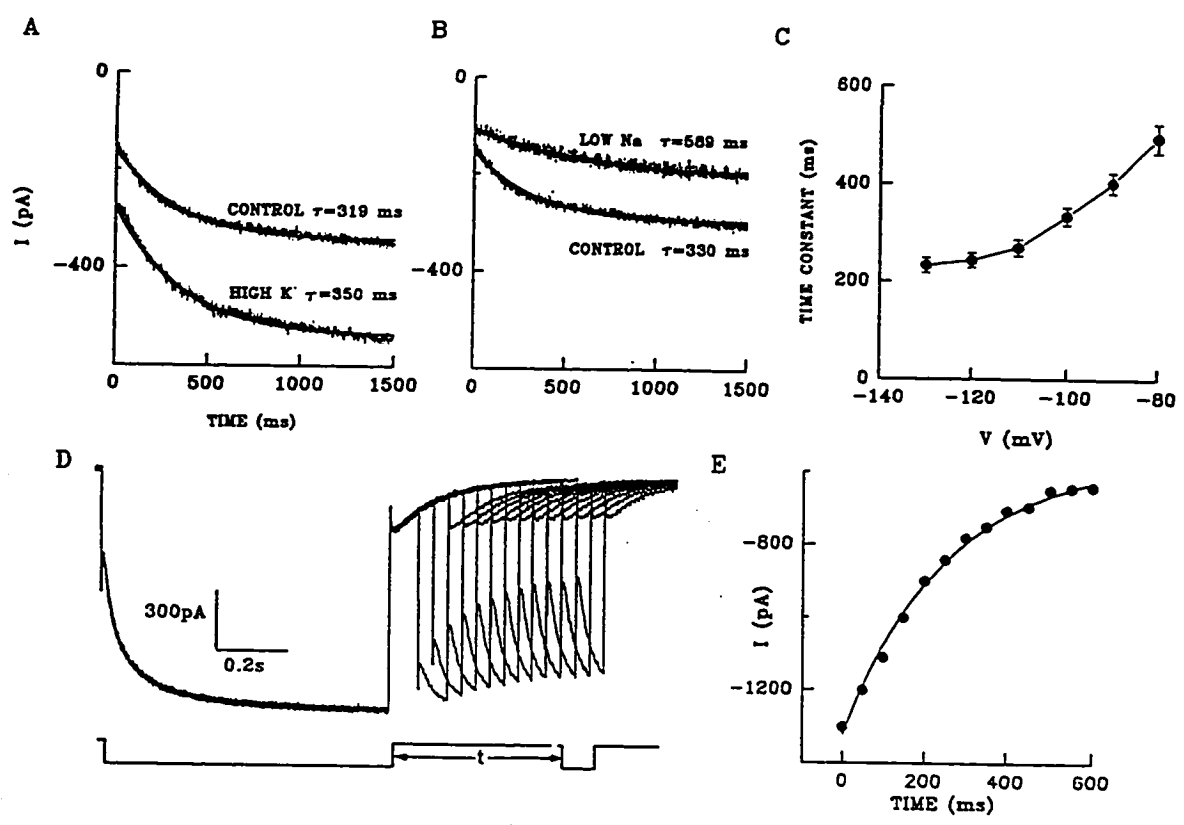
$$I_t = I_{ins} + I_h * \exp(-t/\tau) \quad (4)$$

where I_{ins} is the instantaneous current recorded soon after the start of the conditioning step, and I_h is the difference between the steady state current (at the end of the conditioning step) and I_{ins} . The mean time constant of deactivation at -60 mV was 317.1 ± 31.9 ms ($n=7$), a result similar to previous reports in other cell types (Kamondi and Reiner 1991; Mayer and Westbrook 1983).

Ionic blockade of I_h

As discussed above, during determination of the ionic basis of I_h , it was found that in low chloride extracellular solution the reversal potential E_h was unchanged. However, as shown in Fig. 6A, the current amplitudes were reduced at all negative test potentials. This could be attributed to current blockade by the impermeable anion (nitrate) used for chloride substitution. In other experiments, substitution of chloride with large organic anions, e.g. gluconate or glutamate, completely abolished I_h (not shown). Anion blockade of I_h has been reported in other preparations (Kamondi and Reiner 1991; Mayer and Westbrook 1983). More conventional cationic blockers, barium and cesium (5-10 mM), also reversibly reduced or abolished I_h in petrosal neurons as shown in Fig. 6B,C. Blockade of I_h by both barium and cesium exhibited voltage dependence, becoming more effective at more hyperpolarized potentials (not shown). Barium (10mM) and cesium (10 mM) decreased I_h by ~50% and ~90% respectively at -120 mV. Further, in 5 experiments, barium slowed the activation curve for I_h resulting in an approximate doubling of the time constant of activation (not shown). Tetraethylammonium (TEA; 5-10 mM), 4-aminopyridine (4-AP; 5-10 mM), cobalt (2-5 mM)

Figure. 5. Kinetics of I_h activation and deactivation. A: The time course of I_h (stippled trace), elicited by a hyperpolarizing voltage step (omitted) from -60 to -100 mV, is illustrated for control and high potassium (10 mM) solutions; solid curve represents a single exponential fit to the experimental trace (see text); note the time constant of activation τ is increased in high potassium. B: The same procedure as in A reveals that τ is increased in low sodium (10 mM). C: Relation between time constant (τ) of activation, estimated from single exponential fits as in A,B, and the hyperpolarizing step potential; note τ shows strong voltage dependence over the range -80 to -130 mV (holding potential = -60 mV). Data points represent mean \pm S.E.M.; $n = 14$. D: Experimental protocol for determination of the time course of I_h deactivation. Initial voltage step from -60 to -120 mV (lower trace) for 0.8 s produced full activation of I_h . At the end of this step the membrane potential was returned to -60 mV, for various times 't', before a final 100 ms step to -120 mV. This final step revealed the extent to which I_h decayed during the interval 't'. E: Instantaneous currents, measured at the beginning of the final 100 ms step in D (just after the capacitative transient), are plotted against 't'. Data points were fitted with a single exponential (see text) which described the time course of deactivation. For this cell the deactivation time constant was ~ 280 ms at -60 mV.



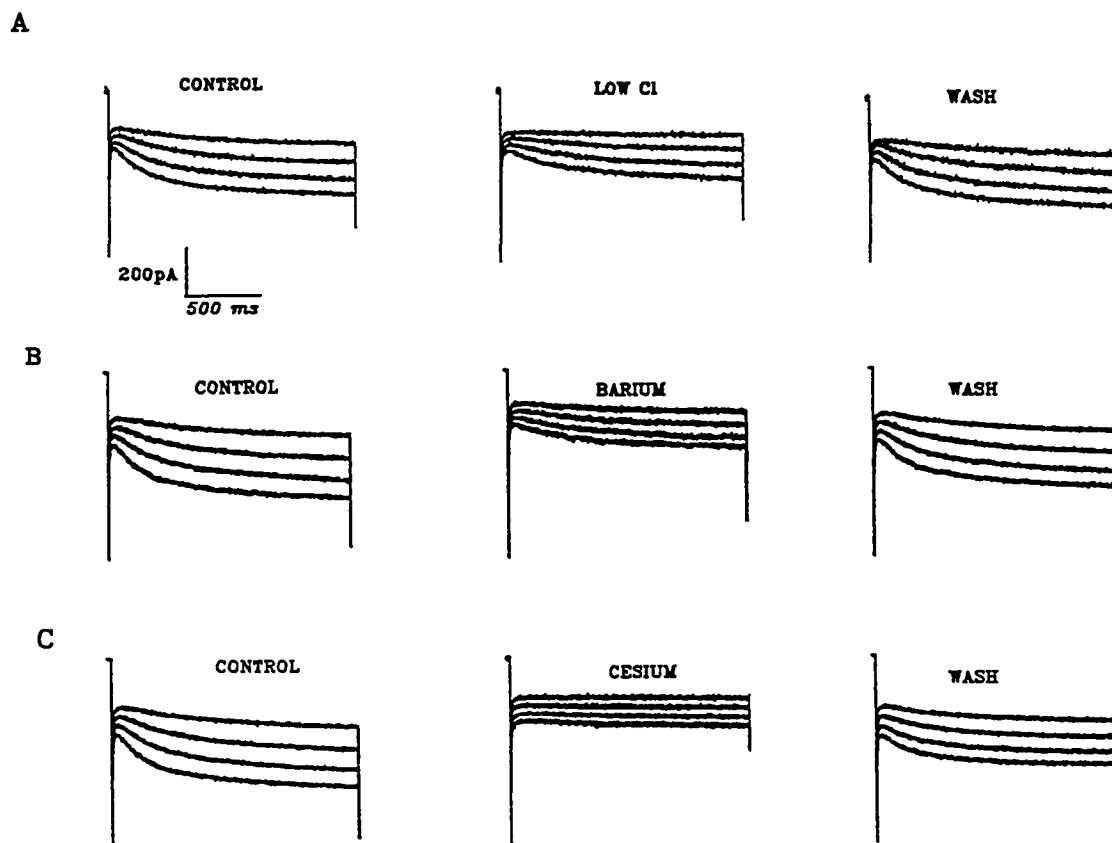


Figure 6. Effects of chloride substitution, barium and cesium on I_h . Current traces elicited by voltage steps (omitted for clarity) from a holding potential -60 mV to -120 , -110 , -100 , and -90 mV are shown in control solution (left panel), in modified extracellular solution (middle panel), and following wash in control solution (right panel). A: Effect of low chloride (10 mM) solution, where nitrate was the substituted anion. B: Effect of 10 mM barium. C: Effect of 10 mM cesium. Currents were reversibly reduced or abolished by these treatments.

and tetrodotoxin (TTX; 1 μ M) had no detectable effects on I_h (not shown). In cat petrosal neurons a portion of the time-dependent rectification, induced by hyperpolarizing current pulses, appeared to be TTX-sensitive (Gallego 1983).

DISCUSSION

Our results indicate that the majority of rat petrosal sensory neurons (~ 78%; n=153) respond to membrane hyperpolarization with a time- and voltage-dependent, non-inactivating inward current I_h , similar to that reported in other neurons (Gallego 1983; Gallego and Eyzaguirre 1978; Kamondi and Reiner 1991; Mayer and Westbrook 1983; Scoggs *et al.* 1994; Spain *et al.* 1987; Travagli and Gillis 1994). I_h was due to a mixed cationic (Na^+ and K^+) current that was blocked or inhibited by extracellular cesium or barium, and it activated with single exponential kinetics as occurs in some (e.g. Crepel and Penit-Soria 1986; Kamondi and Reiner 1991), but not all (e.g. Spain *et al.* 1987) cell types. In rat petrosal neurons the time constant of I_h activation increased in low sodium or high potassium medium, though similar manipulations have led to variable results in other studies (Benham *et al.* 1987; Crepel and Penit-Soria 1986; Kamondi and Reiner 1991; McCormick and Pape 1990a). Based on immunocytochemical and electrophysiological studies the petrosal ganglion is expected to contain several neuronal subtypes, though the majority project to the chemosensory carotid body (Gallego 1983; Gonzalez *et al.* 1994; Katz and Black 1986; Stea and Nurse 1992). Since our procedures for dissecting the petrosal ganglion favoured the distal portion, adjacent to the entry point of the glossopharyngeal nerve (see Stea and Nurse 1992), we expected an

enrichment for tyrosine-hydroxylase (TH)- positive neurons known to be located in this region (Katz and Black 1986). Indeed, immunostaining of cultures prepared in a similar way revealed that >65% of the neurons were TH- positive (Nurse, Vollmer, Zhong and Macintyre, unpublished observations). Further, in a few cases (n=8), we demonstrated that neurons exhibiting I_h were also TH- positive, as determined by immunofluorescent identification after whole-cell recording. Interestingly, in two cases, neurons that lacked I_h were TH- negative, but the significance of these findings are uncertain due to the limited sampling. Nevertheless, since the majority of TH- positive neurons in the distal region of the ganglion directly innervate chemoreceptor cells (Finley *et al.* 1992), it is likely that I_h is present in many, if not all, carotid body chemoafferent neurons in the petrosal ganglion. The possibility that this current is also present in the terminals of these neurons is discussed below.

Possible physiological role of I_h in petrosal neurons

A frequently proposed role for I_h is in the regulation of pacemaker currents and hence interspike intervals, for example in cardiac muscle cells (Brown and DiFrancesco 1980; Irisawa *et al.* 1993). Many petrosal neurons relay chemosensory information from the carotid body and display steep changes in spike frequency in response to arterial P_{O_2} between 10 and 75 torr (Gonzalez *et al.* 1994). Since petrosal afferents discharge spontaneously *in vivo* (and spontaneous action potentials were seen in some neurons in co-culture), it is plausible that I_h might help regulate spike frequency during chemosensory signalling. Indeed, in a recent study

using an in vitro sinus nerve-carotid body preparation from the rat, extracellular cesium did not affect the basal spontaneous discharge recorded from the nerve, but markedly inhibited the increase in discharge during acute hypoxia (Doyle and Donnelly 1994). These authors speculated that an inwardly rectifying K^+ current in petrosal nerve terminals may play an important role in regulating the increase in chemosensory discharge during hypoxia. In the present study we show directly that a cesium-sensitive, inwardly rectifying current is present in rat petrosal cell bodies, but it is cation non-selective, rather than K^+ selective. Though alternative explanations are possible, the simplest interpretation of these data is that an inward rectifier, with the properties of I_h , is present in both the cell bodies and terminals of carotid body chemoafferent neurons. This current, with a reversal potential of ~ -33 mV, could contribute to the shortening of the interspike interval if it were activated during spike afterhyperpolarization (AHP). Another current present in these cells that is likely to contribute to the regulation of spike frequency is the Ca-dependent K^+ current (Stea and Nurse 1992), which together with I_h , have been implicated in the ionic mechanisms underlying the AHP and control of interspike interval in other cells (Spain *et al.* 1987; Schwindt *et al.* 1988; Lorenzon and Foehring 1992). The threshold for I_h activation was near -60 mV and the current was fully activated at about -120 mV. This voltage range partially overlaps that seen during the AHP of spontaneous firing petrosal neurons encountered in the present study, suggesting that I_h could exert a strong depolarizing influence during the interspike interval. Unfortunately, the unavailability of specific I_h blockers precluded a direct test of a possible contribution of I_h to the resting potential, though the activation threshold of I_h is close to the resting potential

in these neurons (~ -60 mV). For example, in current clamp recordings, extracellular cesium or barium caused a small depolarization (4–8 mV) associated with a conductance decrease (our unpublished observations). This depolarization was likely due to a predominant block of other K^+ channels that were open at the resting potential, thereby masking any effect of I_h . A selective blockade of I_h would be expected to cause membrane hyperpolarization if the underlying channels were open at the resting potential. However, our observations (unpublished) that substitution of chloride by large anions (e.g. gluconate), which appear to block I_h , caused membrane hyperpolarization with a conductance decrease, is consistent with a contribution of I_h to the resting potential of petrosal neurons.

Possible regulation of I_h by carotid body neurotransmitters

There is evidence that I_h in neurons of the central nervous system, can be regulated by a variety of neurotransmitters including serotonin (5-HT) (Boker and William 1989; Kinhn and Harris-Warrick 1992; Li *et al.* 1993; McCormick and Pape 1990b; Takahashi and Berger 1990), noradrenaline (McCormick and Pape 1990b), and dopamine (Harris-Warrick *et al.* 1995). Further, in myocytes of the sino-atrial node, acetylcholine (ACh) and adrenaline also regulate I_h (DiFrancesco *et al.* 1986; DiFrancesco and Tromba 1988). These neurotransmitters may act via intracellular second messengers by shifting the voltage dependence of activation or altering the rate of activation (Ingram and Williams 1994; Tokimasa and Akasu 1990). Since these monoamines, as well as ACh, are all putative neurotransmitters in chemoreceptor cells of the carotid body (Gonzalez *et al.* 1994), they are potential candidates for modulation

of I_h in petrosal terminals, following their release by chemosensory stimuli. In this regard it is noteworthy that in the isolated nerve-carotid body preparation, the effect of the I_h blocker, cesium, on afferent chemosensory discharge was most pronounced during hypoxia (Doyle and Donnelly 1994), a stimulus thought to act via release of neurotransmitters from apposed chemoreceptor cells (Gonzalez *et al.* 1994). It remains to be determined whether carotid body neurotransmitters can directly control firing patterns in petrosal chemoafferents, through regulation of I_h .

CHAPTER 3

Nicotinic Acetylcholine Sensitivity of Rat Petrosal Sensory Neurons in Dissociated Cell Culture

Manuscript by H. Zhong and C. A. Nurse; (in press) Journal: '*Brain Research*'.

1. I maintained cell cultures; Cathy Vollmer prepared most (~95%) of the cultures.
2. I performed all electrophysiological recordings. Dr. Min Zhang assisted in the later stages of experiments with design of the fast perfusion system for applying ACh.
3. I performed all data analysis and generated all figures in text.

ABSTRACT

Using whole-cell, patch-clamp techniques we investigated acetylcholine (ACh) sensitivity of dissociated sensory neurons from rat petrosal ganglia after 4 hr to 14 days *in vitro*. In ~68% of petrosal neurons (PN; n = 109) ACh, applied by fast-perfusion or pressure ejection from a 'puffer' pipette, caused a rapid depolarization associated with a conductance increase. Under voltage clamp near the resting potential (~ -60 mV), ACh induced a hexamethonium-sensitive, inward current (I_{ACh}), mimicked by nicotine application, suggesting the presence of neuronal nicotinic acetylcholine receptors (nAChR). The reversal potential of I_{ACh} occurred near 0 mV (n = 4), a region where the I-V curve displayed a prominent rectification. The dose-response relation for I_{ACh} versus ACh concentration was fitted by the Hill equation with $EC_{50} = \sim 33.9 \mu\text{M}$ and Hill coefficient = ~ 1.6 . The activation phase of I_{ACh} was well fitted by a single exponential with mean (\pm S.E.M.) time constant of 102 ± 82 ms (n = 6); the desensitization phase of I_{ACh} was best fitted by the sum of two exponentials, with time constant of 870 ± 210 ms (n = 6) and $8,576 \pm 1,435$ ms (at -70 mV). Fluctuation analysis yielded an apparent single-channel conductance of 21.6 ± 10 pS (mean \pm S.E.M.; n = 4). These data indicate a major subpopulation of sensory neurons in visceral petrosal ganglia of the rat express nAChR. Thus, if similar receptors are present on corresponding nerve terminals, they could mediate fast afferent excitation in response to ACh released at peripheral targets, e.g. the chemosensory carotid body.

1. Introduction

Neuronal nicotinic acetylcholine receptors (nAChR) play a key role in synaptic transmission in both the peripheral (PNS) and central nervous system (CNS) of vertebrates, where they show broad physiological diversity (Sargent, 1993; McGehee and Role, 1995). In the PNS, nicotinic AChR have been best characterized in the autonomic nervous system where they are highly concentrated (Cooper et al., 1991; Sargent, 1993; McGehee and Role, 1995), though subpopulations of somatic sensory neurons in dorsal root and trigeminal ganglia express nAChR (Swanson et al., 1987; McGehee and Role, 1995). In visceral sensory neurons, the distribution of nAChR appears quite variable. For example, in nodose ganglia few neurons are sensitive to acetylcholine (ACh) *in vivo* (Higashi et al., 1982), though AChR expression can be upregulated *in vitro* by eliminating non-neuronal cells, or by adding nerve growth factor (Cooper and Lau, 1986; Mandelzys and Cooper, 1992). On the other hand, visceral nerve endings of the glossopharyngeal complex, that terminate as pressure receptors in the carotid sinus, have long been known to be sensitive to ACh and nicotine, though the physiological significance remains uncertain (Diamond, 1955). Adjacent to these pressure receptors are afferent fibers of the carotid sinus nerve (CSN), which innervate carotid body (CB) chemoreceptors (Eyzaguirre and Zapata, 1984) and are also thought to be sensitive to ACh (Diamond, 1955).

Interestingly, ACh is a putative neurotransmitter thought to be synthesized by CB receptor cells (Fidone et al., 1977), and released during stimulation by natural chemoexcitants, e.g. hypoxia (Eyzaguirre and Zapata, 1968, 1984; Fitzgerald and Shirahata, 1994). The resulting increase in afferent discharge is carried by CSN fibers whose cell bodies reside in the petrosal ganglion. The latter derives embryologically from the ectodermal placode and the distal one-third of the ganglion supplies the major innervation to CB chemoreceptors (Finley et al., 1992). This same embryological region gives rise to nodose neurons, which as described above, are mostly insensitive to ACh *in vivo*. The distribution of ACh sensitivity and the nature of AChR in petrosal neurons have, however, received little attention.

In the present study we isolated neurons from 2-14 day-old rat petrosal ganglia and characterized their sensitivity to ACh after a few hours to several days in culture, using patch-clamp, whole-cell techniques. We found that, in contrast to cultured nodose neurons, a substantial fraction of petrosal neurons was sensitive to ACh, even though no attempts were made to limit proliferation of background non-neuronal cells (Cooper and Lau, 1986; Mandelzys and Cooper, 1992). The responses to ACh were consistently mediated via nicotinic AChR. An abstract on some of these findings has previously been reported (Zhong and Nurse, 1996).

2. Materials and methods

2.1. Cell culture

Dissociated cells from petrosal ganglia were obtained from 2-14-day-old rat pups (Wistar,

Charles River, Quebec) as previously described (Stea and Nurse, 1992). During isolation of the ganglia, the region adjacent to the exit of the glossopharyngeal nerve was always removed, as this was likely to enrich for CB chemoafferent neurons (Katz and Black, 1986; Finley et al., 1992). Briefly, excised ganglia were incubated for 1 hr at 37° C in an enzymatic solution containing 0.1% collagenase/ 0.1% trypsin (Gibco, Grand Island, NY). The tissues were mechanically dissociated with forceps, triturated to yield a cell suspension, and plated onto a thin layer of Matrigel (Collaborative Research, Bedford, MA) that was previously applied to the central wells of 35-mm tissue-culture dishes. In a few experiments petrosal neurons were grown in co-culture with their normal targets, i.e. glomus cells of the carotid body. The co-cultures were obtained by first preparing cultures of dissociated rat carotid body as previously described (Nurse, 1990), and then adding an overlay of dissociated petrosal neurons 3-5 days later. Cultures were grown at 37° C in a humidified atmosphere of 95% air-5% CO₂ for 4 hr to 14 days before they were used in the patch-clamp/whole-cell experiments. The growth medium was changed every 4-6 days and contained F-12 nutrient medium (Gibco, Grand Island, NY) supplemented with 10% fetal calf serum (Gibco), 80 U/l insulin (Sigma Chemical Co., St. Louis, MO), 0.6 % glucose, 2 mM glutamine and 1 % penicillin-streptomycin (Gibco).

2.2. Solutions and drugs

Most experiments were performed using extracellular fluid (ECF) of the following composition (mM): NaCl, 135; KCl, 5; CaCl₂, 2; MgCl₂, 1; glucose, 10; N-2-

hydroxyethylpiperazine-N'-2-ethane sulphonic acid (HEPES), 10 at pH 7.4. In some experiments HEPES was replaced by a bicarbonate-based buffer and the composition of the ECF was (mM): NaCl, 111; KCl, 5; CaCl₂, 2; MgCl₂, 1; glucose, 10; NaHCO₃, 24; a pH of 7.4 was maintained by bubbling with 5% CO₂. The stock pipette solution for conventional whole-cell recording contained (mM) either: (i) KCl, 135; NaCl, 5; CaCl₂, 1; ethylene glycol-bis(β-aminoethyl ether)-N,N,N',N'-tetraacetic acid (EGTA), 11; HEPES, 10; ATP-Na 2 mM at pH 7.2; or (ii) potassium glutamate or gluconate, 105; KCl, 35; CaCl₂, 1; EGTA, 11; HEPES, 10; ATP-Na 2 mM at pH 7.2. For perforated-patch recordings the pipette contained (mM): potassium glutamate or gluconate, 105; KCl, 35; CaCl₂, 1; HEPES, 10 and nystatin 300 μg/ml, at pH 7.2. All solutions were filtered through a 0.45 μm millipore filter before use. During recordings from petrosal neurons the culture was continuously perfused with ECF by gravity flow; removal of excess fluid by suction ensured that the fluid level in the recording chamber remained relatively constant.

The following drugs or reagents used in this study were obtained from Sigma Chemical Co. (St. Louis, MO): acetylcholine (ACh), nicotine, tetrodotoxin (TTX), tetraethylammonium (TEA) and cobalt chloride (CoCl₂). Hexamethonium and atropine were obtained from Research Biochemicals Inc. (RBI; Natick, MA).

2.3. Application of ACh agonists and antagonists

ACh was freshly prepared as a 10 mM stock solution in distilled water or in ECF (see above). Just before use it was diluted to the desired final concentration and then applied to

the cells in one of three ways. In some experiments, ACh or nicotine (0.1-1 mM) was delivered by pressure ejection from a nearby 'puffer' pipette (diameter $\sim 30 \mu\text{m}$) positioned 20 - 40 μm from the neuronal surface. This procedure permitted very rapid application of the agonist over a time interval of 50 - 200 ms, and at a low pressure (4-8 p.s.i.) under control of a solenoid valve (General Valve Corp., NJ). In other experiments, including those designed to vary ACh doses, a fast-perfusion technique was used. In this procedure each barrel of a double-barreled pipette was filled with a different perfusate, and the pipette tip was positioned $\sim 100 \mu\text{m}$ from the neuronal cell body. One barrel contained extracellular fluid (ECF) and the other ECF plus a selected ACh concentration. An electromechanical device permitted a fast switch between the pipettes, thereby allowing the cell to be exposed to control solution or the agonist. The speed of solution change within the vicinity of the neuron was ~ 100 ms. In studies of the dose-response relationship, multiple ACh concentrations were used and the peak current amplitude elicited by the test concentration was compared with that elicited by a saturating concentration (300 μM) of ACh. Thus, the dose-response generated by this method displays normalized values relative to the maximal response (unity) measured with 300 μM ACh.

In studies of the elementary event by fluctuation analysis, a low concentration of ACh (10 μM) was applied by conventional bath perfusion under gravity flow to permit slow activation of the response with minimal desensitization. All antagonists were applied by bath perfusion under gravity.

2.4. Whole-cell recording

Procedures for whole-cell recording were similar to those described in detail elsewhere (Stea and Nurse, 1991a, 1992; Zhong and Nurse, 1995). As there were no obvious differences between results obtained with conventional whole-cell versus perforated-patch recordings in this study, the combined data were pooled. Patch pipettes were fabricated from Corning 7052 glass (1.5 mm O.D.) pulled in a Flaming/Brown horizontal puller (Sutter Instrument Co., Novato, CA). The pipettes were fire-polished and their resistance varied between 2-10 M Ω . In some experiments, nystatin perforated-patch recording was used as described elsewhere (Stea and Nurse, 1991a). In most voltage clamp experiments >80% of the series resistance was compensated. Junction potentials (2 -10 mV) were cancelled at the beginning of the experiment. The ECF was warmed before entering the recording chamber, where the mean temperature was $34 \pm 2^{\circ}$ C over the time course of the experiments.

Whole-cell currents or membrane potential were recorded with the aid of an Axopatch 1D patch clamp amplifier and a Labmaster TL-1 A-D converter (Axon Instruments Inc., Foster City, CA), and stored on a 486 Personal Computer. Current and voltage clamp protocols, data acquisition and analysis were performed using pCLAMP software (version 5.5., and 6.0.2: Axon Instruments Inc.) and Axotape (version 2.02. Axon Instruments Inc.).

2.5. Data analysis

Current fluctuations induced by ACh under whole-cell clamp were analyzed as described elsewhere (Neher and Stevens, 1977). ACh-induced currents were sampled at 0.5 ~ 1 kHz

and stored in a 486 computer for analysis. Exponential fits of the time course of I_{ACh} activation or desensitization were obtained using CLAMPFIT (6.0.2, Axon Instruments Inc.). Fits of the dose-response to Hill equation were obtained using Sigma Plot. The Hill coefficient (n) and half-maximal activation (EC_{50}) were adjusted for best fit of the curve to the observed data; a non-linear fitting routine that minimizes the least-squares difference was used to obtain the best fit. The apparent single-channel conductance was estimated from the relation between the variance of the current noise and mean current (Neher and Stevens, 1977). Most of the results are represented in the text as mean \pm standard error of the mean (S.E.M.).

3. Results

Dissociated rat petrosal neurons were investigated with whole-cell recording techniques after 4 hr to 14 days in culture. Neurons were oval shaped, with diameters in the range 15-30 μm , and were easily distinguished from background non-neuronal cells (Stea and Nurse, 1992). The fact that they appeared to survive better when grown in co-culture with carotid body target cells allowed them to be studied after longer times *in vitro*. The resting membrane potential of petrosal neurons ranged from -40 to -80 mV (mean = -58.5 ± 3 mV; $n=81$), and the majority of experiments was performed on those with resting membrane potentials more negative than -50 mV.

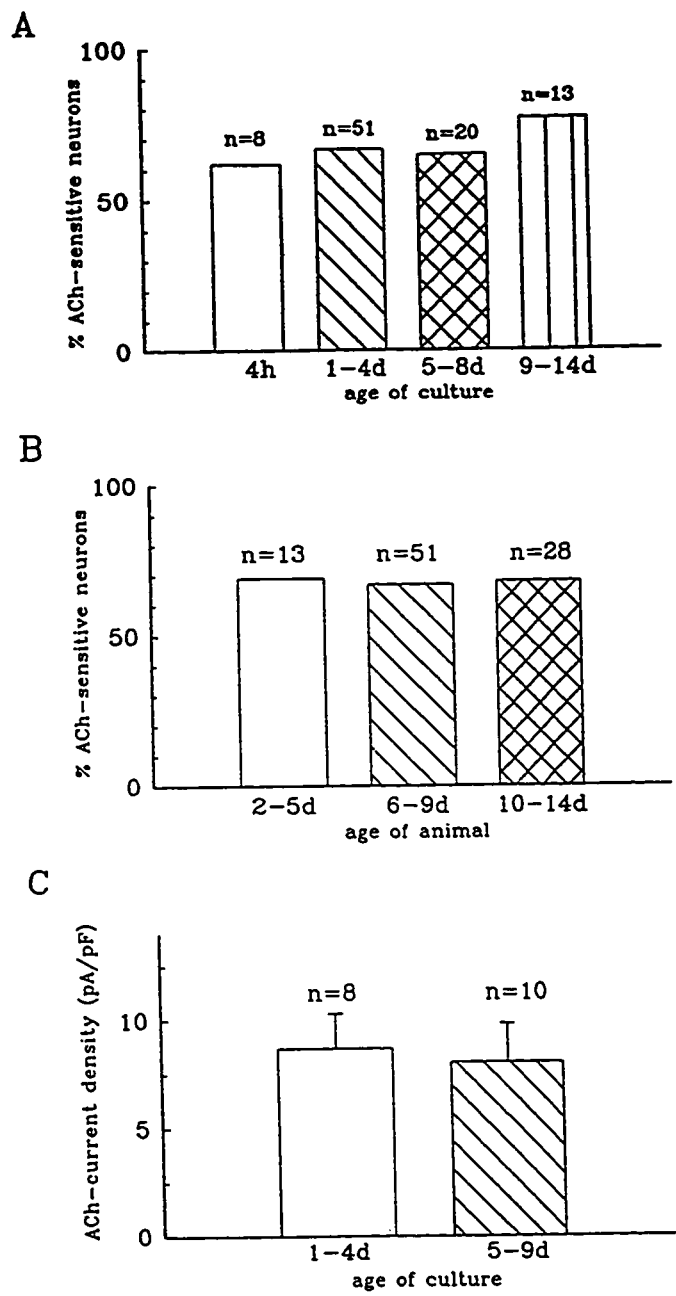
3.1 ACh sensitivity of isolated neurons

Responses to ACh were detected at the earliest sampling time, i.e. after 4 hr *in vitro*,

suggesting that the observed ACh sensitivity was not the result of induction by the foreign culture conditions (Mandelzys and Cooper, 1992). As shown in Fig. 1A, the frequency of encountering ACh-sensitive neurons during random sampling was quite high at all ages in culture (4 hr -14 days), varying from 60 - 85 % of the neurons tested. Also, this frequency was similar among cultures derived from pups of various postnatal ages between 2 and 14 days (Fig. 1B). In these studies, neurons were considered 'sensitive' if they elicited a depolarization (current clamp) or an inward current (voltage clamp at -60 mV) during application of ACh by fast perfusion (20-100 μ M), or by pressure ejection from a 'puffer' pipette (see, Materials and methods). Comparison of the ACh-current density (pA/pF), obtained on dividing peak I_{ACh} (at -60 mV) by whole-cell capacitance, indicated that it remained relatively constant with culture duration, for neurons isolated from animals of different ages (Fig. 1C). The presence of target cells from the carotid body in co-culture had no significant effect on size of petrosal cell bodies or on ACh-current density over 12 days in culture. For example, the mean (\pm SEM) whole-cell capacitance and ACh-current density of neurons cultured alone was 20.4 ± 2.3 pF and 8.6 ± 1.8 pA/pF ($n = 14$) respectively, compared to 22.3 ± 3.2 pF and 8.1 ± 2.1 pA/pF ($n = 6$) for neurons in co-culture.

In many neurons ($\sim 68\%$; $n = 109$) studied under current clamp, the ACh-induced depolarization was accompanied by action potentials (e.g. Fig. 2A). The mean (\pm S.E.M.) ACh-induced depolarization was 20.3 ± 4.1 mV ($n=21$), and reached values up to 35 mV. The depolarization was accompanied by ~ 3 fold increase in input conductance, consistent with the opening of ion channels that were closed at rest (Fig. 2B). Under voltage clamp near

Figure. 1. Responses of cultured rat petrosal neurons (PN) to ACh. A, B show the frequency of ACh-sensitive PN vs age of culture and age of animal, respectively. Note in A that ACh sensitivity was detected in PN cultured for only 4 hr (open bin), suggesting that positive responses were not a result of prolonged culture; for these experiments data were pooled from cultures derived from pups of different postnatal ages between 2 and 14 days. In B, PN were obtained from animals of different ages (indicated), and cultured for varying periods over 2 weeks. In both A and B, the number of responsive neurons to ACh, applied by either 'puffer' or fast perfusion method, is expressed as a percentage of the total sampled (n); note the frequency of ACh responsive neurons was relatively high (> 60%) under these conditions. In C, ACh current density (pA/pF), obtained by dividing peak current by whole-cell capacitance, is plotted vs age of culture; note current density remained relatively constant with age in culture. ACh was applied by the fast perfusion method.



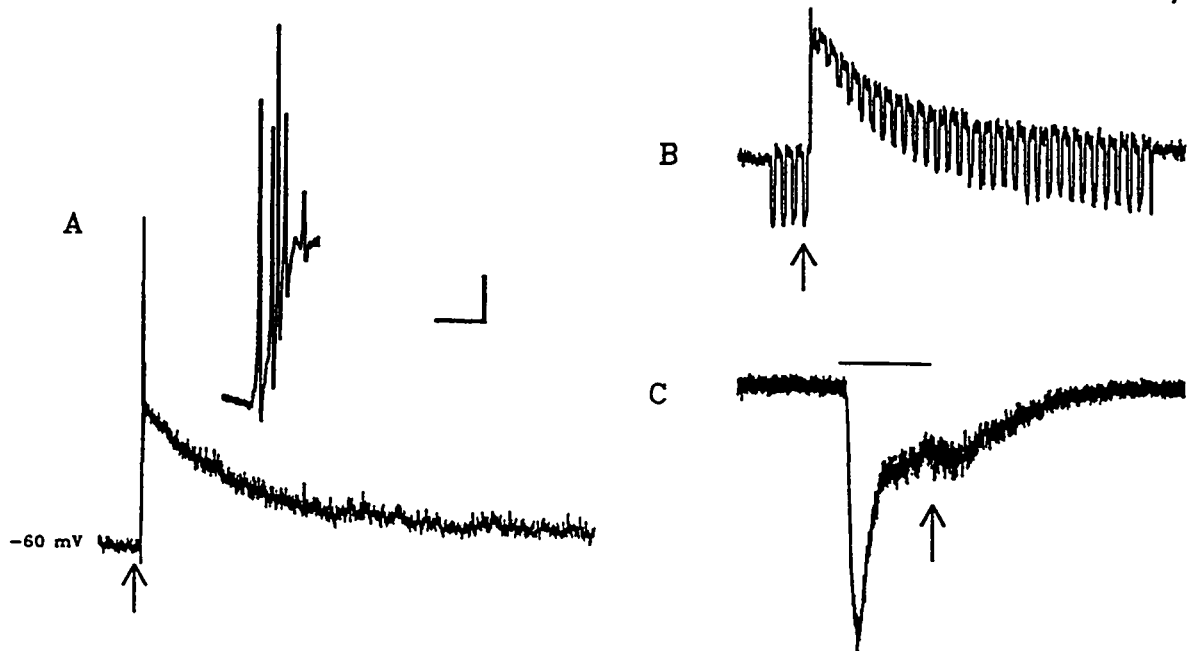


Figure 2. Effects of ACh on membrane potential and whole-cell current in cultured petrosal neurons. A. A puff of ACh (at arrow) delivered by pressure ejection from a 'puffer' pipette, containing 1 mM ACh, evoked membrane depolarization with superimposed action potentials; inset shows the action potentials on a faster sweep. B. A puff of ACh applied to a neuron (at arrow) in the presence of 1 μ M TTX to block action potentials; note the resulting membrane depolarization was accompanied by a conductance increase, indicated by application of constant brief hyperpolarizing current pulses (during downward deflections). The pipette ACh concentration in A and B was 1 mM. C. Under voltage clamp, application of ACh (100 μ M) by the fast-perfusion method produced a rapid inward current followed by a fast and slow phase of desensitization. Arrow indicates rebound of inward current at the end of ACh application (upper horizontal bar). Vertical scale represents 10 mV, 8 mV and 40 pA in A, B, and C respectively, whereas horizontal scale represents 5, 6 and 4 sec.

the resting potential, application of ACh (100 μ M) by the fast perfusion method induced a fast transient inward current (I_{ACh}), followed by desensitization of the response (Fig. 2C). The mean (+ S.E.M.) peak amplitude of I_{ACh} was 173 ± 40 pA ($n = 24$; range 50 - 580 pA). The rate of desensitization was very fast in some cells but slow in others. This desensitization was concentration dependent and will be discussed later.

3.2. Neuronal nicotinic ACh receptors (nAChR) mediate ACh sensitivity

Evidence that nicotinic ACh receptors (nAChR) mediated ACh-induced responses in petrosal neurons was obtained from results of direct nicotine application. As was the case for ACh (Fig. 2B), application of nicotine (1mM; 'puffer' pipette) produced a transient depolarization associated with an increase in membrane conductance (not shown). Under voltage clamp, nicotine activated a rapid, transient inward current (I_{NIC} ; Fig. 3B), similar to that of puffer-applied ACh (1mM; Fig. 3A). The mean amplitude (\pm S.E.M.) of I_{NIC} was 141 ± 26 pA ($n = 15$; range 54 to 416 pA). Further, the response to ACh was reversibly suppressed or abolished by the presence of the nicotinic antagonist, hexamethonium (100 μ M; $n = 12$), as illustrated in Fig. 3C,D. The ACh response was unaffected by the muscarinic antagonist atropine ($n = 6$), at concentrations (1 μ M) known to block muscarinic responses in other preparations (Bowman and Rand, 1980). However, at higher concentrations (50 μ M) atropine partially suppressed the ACh-induced responses in petrosal neurons (not shown). Taken together, these results suggest that nicotinic AChR are the main cholinergic receptor subtype present in petrosal neurons.

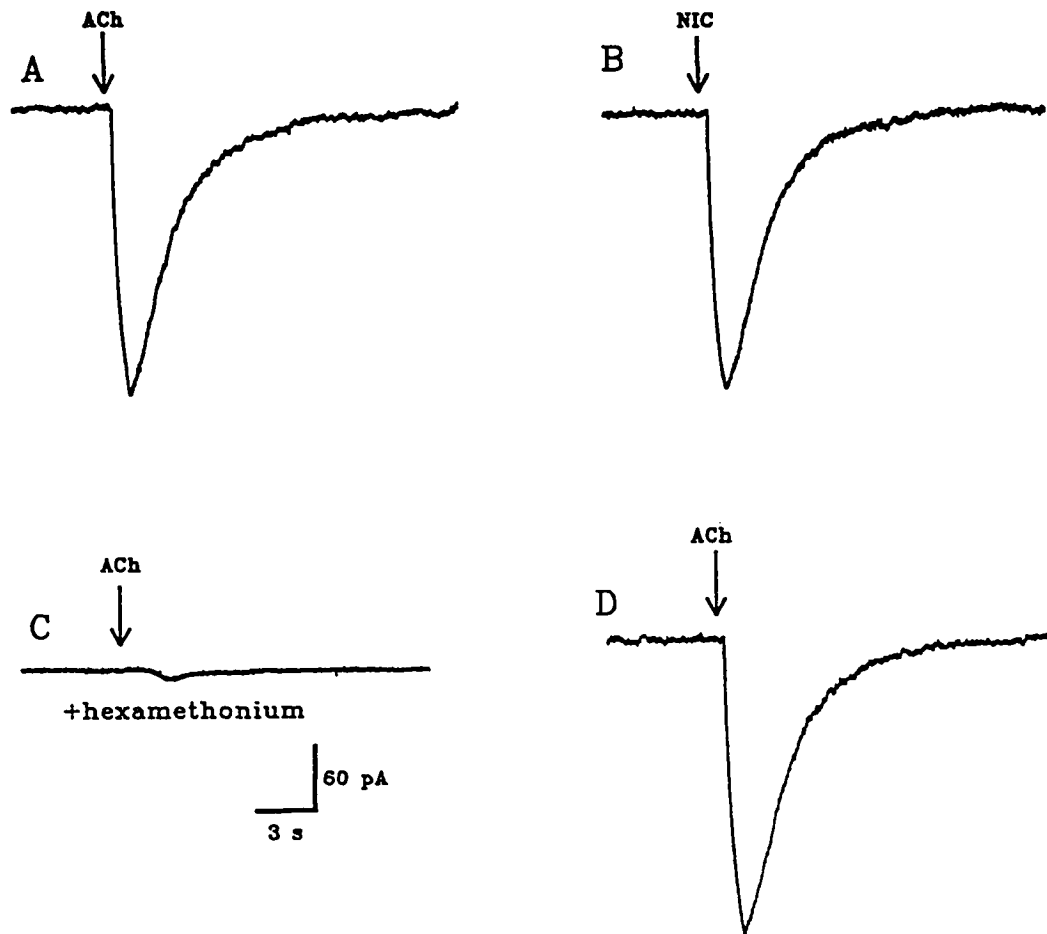


Figure 3. Evidence for nicotinic ACh receptors on petrosal neurons.

A. Under voltage-clamp at -60 mV, a puff of ACh (at arrow; pipette concentration = 1 mM) caused a fast inward current followed by a slower decay. B. Application of a puff of nicotine (at arrow; 1 mM NIC) mimicked the ACh response in the same neuron. C. A puff of ACh as in (A), during continuous perfusion of the nicotinic blocker, hexamethonium (100 μ M), resulted in a diminished response. D. After washing out the blocker, the response to a puff of ACh recovered.

3.3. Reversal potential of the ACh response

The reversal potential (E_{rev}) of the ACh-induced current was estimated from the current-voltage or I-V relationship, following blockade of most of the voltage-dependent Na^+ and K^+ currents with tetrodotoxin (TTX; 1 μM) and tetraethylammonium (TEA; 5 mM) respectively. Inward currents were induced by ACh delivered by a 'puffer' pipette containing 1 mM ACh (see Fig. 4A). As shown in Figure 4B, the I-V curve for ACh-induced currents displayed prominent rectification at more depolarized positive potentials, as observed in other studies (Mathie et al., 1990; Sargent, 1993; Lester and Dani, 1995). The mean reversal potential was 0 ± 5.3 mV ($n = 4$; range -8 to +11 mV), suggesting that the ion channels activated by ACh were cation non-selective (likely permeable to Na^+ , Ca^{2+} and K^+). The accuracy of these estimates, however, may be limited by receptor desensitization, which tends to underestimate the true value of peak currents.

3.4. ACh dose-response relation

Using the fast perfusion technique with the aid of a double-barrel pipette (see Materials and methods), ACh elicited maximal response in petrosal neurons when applied at ~ 300 μM (pipette concentration). At higher concentrations (1 mM) the current activated faster, but the peak response was not significantly different from that at 300 μM (not shown). To obtain the dose-response relation, the mean peak current at each ACh concentration was normalized to that elicited by 300 μM ACh (Figs. 5A,B). The complete dose-response curve was described

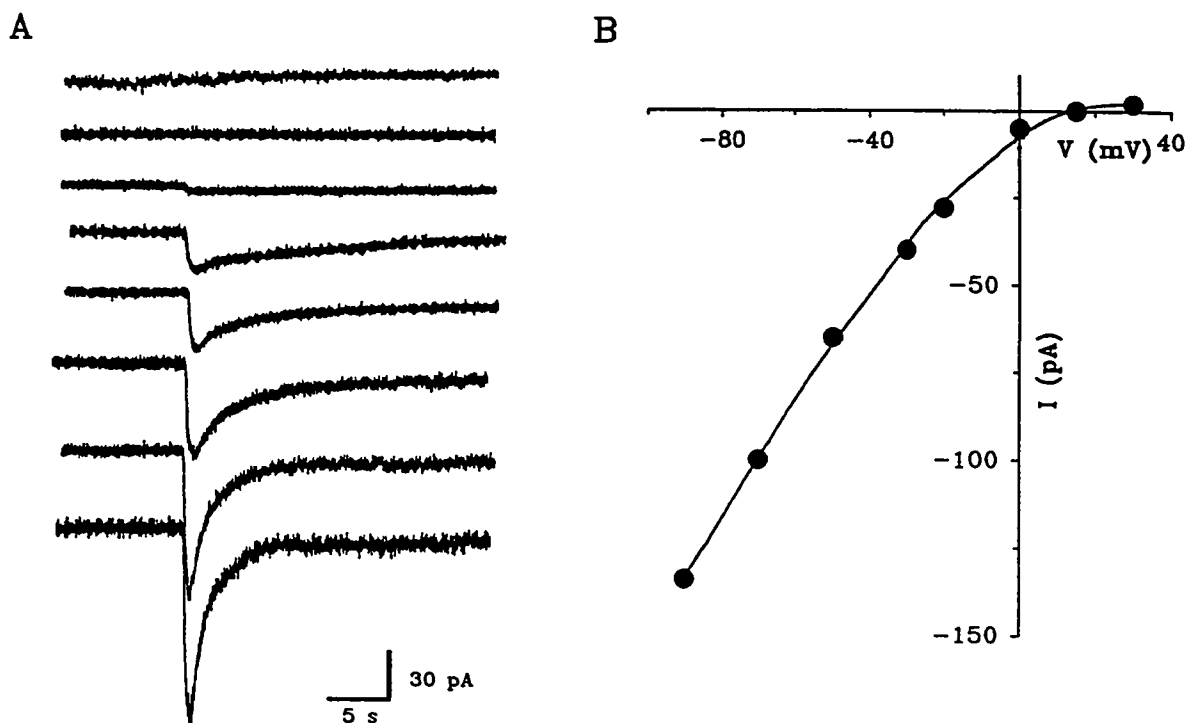


Figure 4. Reversal potential and inward rectification of nAChRs in petrosal neurons. **A.** An example of ACh-evoked inward currents, elicited by the 'puffer' method, at different membrane potentials (+30, +15, 0, -20, -30, -50, -70 and -90 mV, from top to bottom) under voltage-clamp. ACh concentration was 1 mM, and the perfusion fluid contained 1 μ M TTX and 5 mM TEA to block voltage-dependent Na^+ and K^+ currents respectively. **B.** An example illustrating the I-V relationship for the peak current amplitude evoked by ACh as shown in A. The reversal (zero current) potential in this cell is $\sim +10$ mV. Note prominent inward rectification of I_{ACh} near the reversal potential.

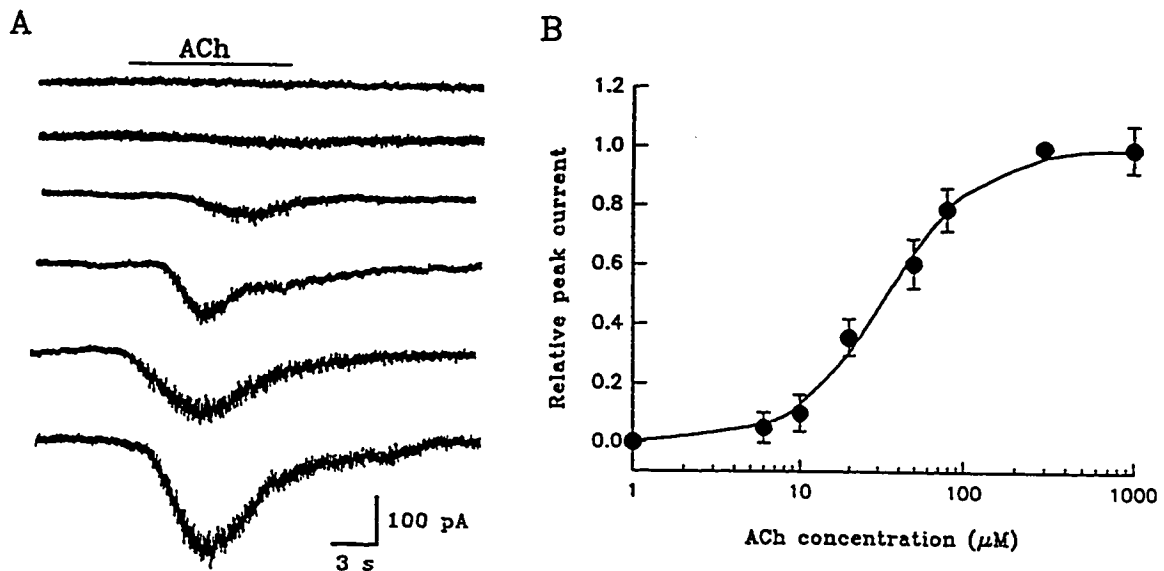


Figure 5. Dose-response curve for ACh concentration vs I_{ACh} in a petrosal neuron. A. An example of whole-cell currents evoked by application of various ACh concentrations with the fast-perfusion method; holding potential = -60 mV. The current traces in the sequence top to bottom were due to ACh concentrations of 1, 6, 10, 20, 50 and 80 μ M. B. The peak current evoked at each concentration is expressed relative to the maximum peak current (at 300 μ M ACh) and plotted against the log [ACh]. Each point is the mean of 5 measurements (from different cells), and the data are fitted by the Hill equation with a slope of 1.61 and $EC_{50} = 33.9 \mu$ M.

by Hill equation:

$$I/I_{\max} = 1/(1+(EC_{50}/[ACh])^n)$$

where I is the measured peak current, I_{\max} is the maximal response, n is the Hill coefficient, and EC_{50} is the concentration of ACh required for half-maximal activation. As shown in Fig. 5B, the EC_{50} for receptor activation was $\sim 33.9 \mu\text{M}$ and the Hill coefficient was 1.6, suggesting two (or more) agonist binding sites per receptor. Errors in these estimates arise from several sources. First, although the double-barrel pipette allowed fast switch, solution exchange was not instantaneous. Second, the presence of receptor desensitization and/or ACh-induced channel block (Colquhoun and Ogden, 1988) may have underestimated the true value of peak currents, especially at high concentrations. The brief "rebound" of inward current that occurred on the removal of ACh (0.1 mM), applied via a double-barrel pipette in Fig. 2C, suggests that the channels are partially blocked by high ACh concentrations. The rebound current is presumed to result from the rapid unblocking of channels as the ACh concentration falls (Dilger and Lui, 1992).

3.5. Kinetics of activation and desensitization of the ACh-induced current

In this study the ACh-induced currents activated more rapidly at higher concentrations. Figure 6A shows a typical example of the activation and desensitization phases of an inward current elicited by bath perfusion 100 μM ACh at -70 mV. The ACh-induced current reached its peak amplitude in ~ 300 ms (e.g. Fig 6B). The activation phase was described by a single exponential with mean (\pm S.E.M.) activation time constant (τ_{on}) of 102 ± 18 ms ($n=12$), a

value somewhat larger ($\sim 10\times$) than that reported for nicotinic AChR in rat sympathetic neurons (Mathie, et al., 1990), but comparable to that for nicotinic AChR in rat spinal neurons (Borday et al., 1996). However, consistent with observations on nicotinic receptors in other preparations (Dilger and Lui, 1992; Lester and Dani, 1995), continuous exposure of petrosal neurons to nicotinic agonists resulted in reversible receptor desensitization. At low ACh concentrations ($< 10 \mu\text{M}$) I_{ACh} desensitized slowly and at higher concentrations ($> 30 \mu\text{M}$) there appeared to be an additional rapid component (Fig. 5A, 6C). In fact, at $100 \mu\text{M}$ ACh, desensitization was well described by the sum of two exponentials (Fig. 6C). The mean time constant (\pm S.E.M) of the fast (τ_f) and slow (τ_s) components were 876 ± 210 ms and 8560 ± 1435 ms respectively ($n = 6$). The fast component comprised $\sim 80\%$ of the desensitizing phase of the current, a result comparable to other studies (Andreev et al., 1984; Lester and Dani, 1995). A wide range of time constants (tens of ms to tens of min) for receptor desensitization has been reported, and the variability appears to be influenced by how rapidly the agonist is applied, as well as by temperature (Edmonds et al., 1995).

3.6. Estimate of single channel conductance by fluctuation analysis of ACh-induced current

The apparent single channel conductance of the nAChR channel was estimated using fluctuation analysis (Neher and Stevens, 1977). First, a low concentration ($10 \mu\text{M}$) of ACh was applied by bath perfusion to produce a steady, non-desensitizing response. Figure 7 (inset) shows a typical segment of a current record used for analysis, where it is evident that the fluctuation in current noise increased as the mean current increased. The plot of the

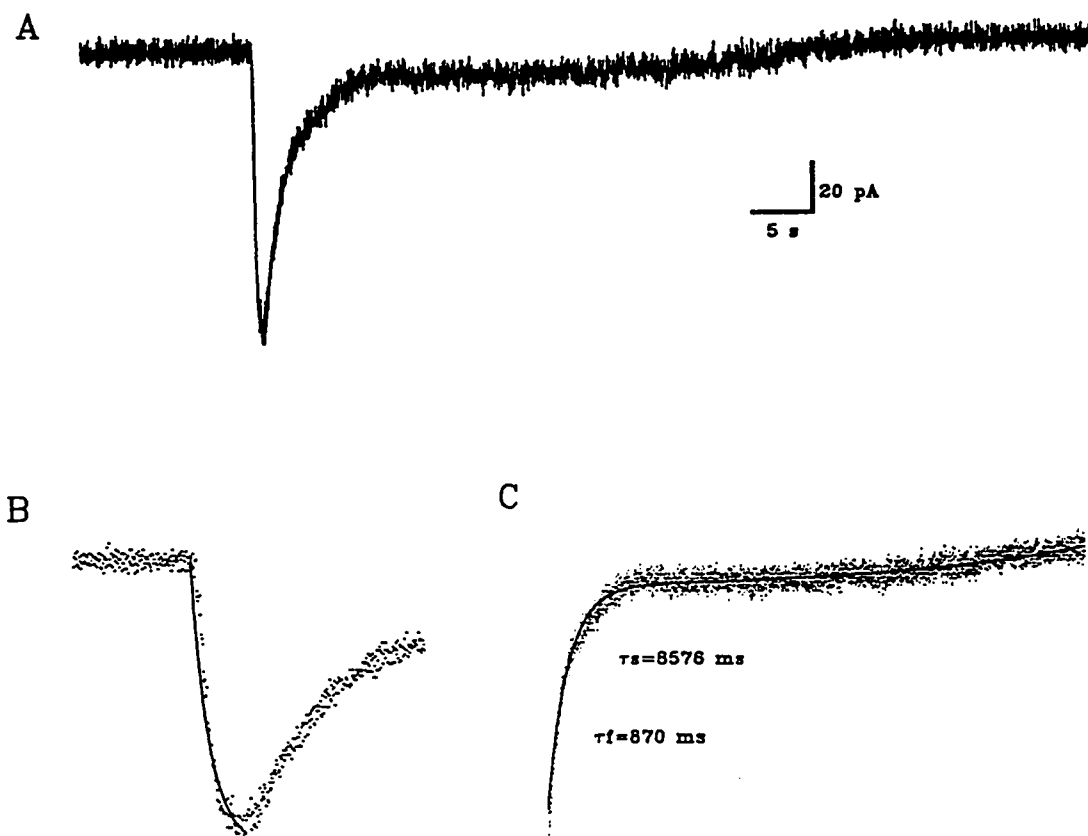


Figure. 6. The activation and desensitization phases of I_{ACh} . A. Whole-cell current (at -70 mV) in a petrosal neuron induced by applying ACh (100 μ M) with the fast-perfusion method. In B, the onset of I_{ACh} (dotted line) is shown in more detail at a faster sweep speed. The onset of I_{ACh} was fitted with a single exponential (solid line) and the activation time constant (τ_{act}) was 127 ms in this cell. C. Desensitization of the AChR is represented by the decay phase of I_{ACh} (dotted line) recorded while ACh was still being perfused; the decay was fitted with the sum of two exponentials (solid line), where the fast (τ_f) and slow (τ_s) time constant was 870 ms and 8576 ms respectively.

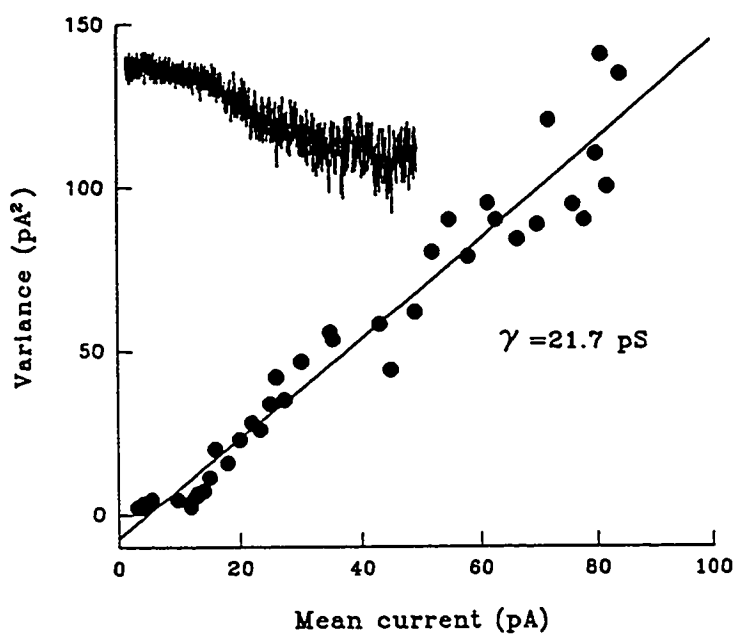


Figure. 7. Estimation of the nAChR single-channel conductance from fluctuation analysis of the ACh-induced whole-cell current in a petrosal neuron. The variance of current noise was plotted vs mean current and the single channel conductance, estimated from the slope of the least-squares linear fit, was 21.7 pS. The inset shows a section of the current record used for fluctuation analysis; note membrane noise increased during the rising phase of the current.

current variance versus the mean current was linear as shown in Fig. 7, and the average single channel conductance, γ , was estimated from the relationship:

$$\gamma = \delta^2 / \Delta I (V_h - V_{eq})$$

where δ^2 is the ACh-induced variance, ΔI is the ACh-induced mean membrane current change, V_h is the holding potential, and V_{eq} is the reversal or zero current potential of ACh response, estimated as ~ 0 mV (see Fig. 5B). The mean single channel conductance (\pm S.E.M) obtained from the above relationship was 21.6 ± 10 pS ($n=4$), a value within the range for nicotinic AChR in peripheral neurons (McGehee and Role, 1995).

4. Discussion

In this study we demonstrate that a substantial proportion (>65%) of petrosal neurons, isolated from neonatal rats are sensitive to ACh and that the responses are mediated by neuronal nicotinic AChR. Under current clamp, application of ACh from a 'puffer' pipette depolarized responsive neurons, often producing bursts of action potentials, and the response was inhibited by the nicotinic ganglionic blocker, hexamethonium (50 - 100 μ M). Under voltage clamp near the resting potential (~ -60 mV) ACh produced an inward current I_{ACh} , which had a reversal potential near 0 mV, suggesting it was carried by a mixture of cations. The I-V relation for this current showed a prominent inward rectification, as previously described for nAChR in other preparations, including rat sympathetic neurons (Mathie et al., 1990; Sargent, 1993); the origin is uncertain but may be due to an intracellular Mg^{2+} block (Mathie et al., 1990), or to the presence of fewer open channels at positive potentials

(Sargent, 1993). Though neurons were studied at various times between 4 hr and 14 days in culture, the frequency of encountering ACh- responsive neurons was quite high (> 60%) regardless of the age of the culture or of the animal (postnatal 2 - 14 days). The fact that ACh responses could be detected as early as 4 hr after isolation, and that ~70% of the neurons were sensitive during the first 48 hr *in vitro*, suggests that nAChR were already present at the time the neurons were brought into culture, and were not induced *de novo* by the foreign culture conditions, or by axotomy (Jacob and Berg, 1987).

It is of interest to compare these results on petrosal neurons with those on neurons from the adjacent and much larger nodose ganglion, which derives from a similar embryonic region, i.e. the ectodermal placode, and depends on similar neurotrophins for survival during fetal development (Conover et al., 1995). It appears that only a few nodose neurons are sensitive to ACh *in vivo* (Higashi et al., 1982), and *in vitro*, if grown with ganglionic non-neuronal cells (Cooper and Lau, 1986). However, nicotinic AChR can be induced in cultured rat nodose neurons if ganglionic non-neuronal cells are eliminated (Cooper and Lau, 1986), or if nerve growth factor (NGF) is present over 1-2 weeks in culture (Mandelzys and Cooper, 1992). In contrast, in the present study, ganglionic non-neuronal cells were allowed to proliferate, and even though their numbers increased with age of the culture, there was a high incidence (>60) of ACh- responsive (petrosal) neurons regardless of the culture age. Perhaps the ACh-sensitive neurons in petrosal ganglia represent a major, separate subpopulation that is either absent, or present in small numbers, in the nodose ganglion. At least one group of sensory neurons, which supply afferent innervation to peripheral arterial chemoreceptors, fits this

category. In particular, the O₂-chemoreceptor or glomus cells of the carotid body (CB) are major targets for a subpopulation of petrosal neurons, the majority of which are immunopositive for tyrosine hydroxylase (TH) and are located in the distal one-third of the ganglion (Katz and Black, 1986; Finley et al., 1992). Similar receptor cells occur in the much smaller aortic bodies, which appear to receive their afferent innervation from the nodose ganglion (Eyzaguirre and Zapata, 1984; Gonzalez et al., 1994). Since our petrosal cultures routinely include the most distal region of the ganglion, adjacent to the exit of the glossopharyngeal nerve (see Materials and methods), there is expected to be an enrichment of CB chemoafferent neurons. Indeed, in preliminary experiments >60 % of cultured petrosal neurons are TH-positive and 30 - 40% of the neurons are immunopositive for both TH and nAChR (Nurse, Vollmer and Zhong, unpublished observations). Thus, it is possible that a substantial fraction of ACh-sensitive neurons correspond to the CB chemoafferent population.

Is there a physiological significance to the high incidence of ACh-responsive neurons in the petrosal ganglion? Acetylcholine has long been implicated in the initiation of CB chemoreceptor reflexes (Hollinshead and Sawyer, 1945; Eyzaguirre and Zapata, 1968, 1984; Fitzgerald and Shirahata, 1994), where its release during natural stimulation was presumed to occur from chemoreceptor (glomus) cells onto petrosal afferent terminals. There is evidence that glomus cells synthesize ACh (Fidone et al., 1977), and contain the degradative enzyme, acetylcholinesterase (Nurse, 1987; Gonzalez et al., 1994). Thus if nAChR, with properties similar to those we have found on cell bodies, are also expressed on petrosal terminals (see Zhong and Nurse, 1996), then they would be strategically placed to provide

fast excitation in response to ACh released from glomus cells. Indeed, we have recent evidence for hypoxia-evoked ACh release from glomus cells onto co-cultured petrosal neurons *in vitro* (Zhong, Zhang and Nurse, submitted).

The nicotinic AChR we found on petrosal neurons showed several properties expected of neuronal nicotinic AChR (Sargent, 1993; McGehee and Role, 1995). They produced rapid excitation in the presence of ACh, and the response was blocked by the classical ganglionic blocker, hexamethonium. The receptors also displayed both fast and slow desensitization in the presence of high ACh concentrations and the observed Hill coefficient (~ 1.6) is consistent with two ACh binding sites per receptor. Noise analysis yielded an apparent mean single channel conductance of ~ 22 pS, a value similar for at least some neuronal AChR *in situ* (McGehee and Role, 1995). Given the limitations of noise analysis, however, this value requires validation using single channel recording methods. Nevertheless, since nAChR have a pentameric structure consisting of various (α and β) subunits, which can co-assemble in different combinations to form functional receptors (Sargent, 1993; McGehee and Role, 1995), it will be of interest to see whether the ones expressed in visceral (e.g. petrosal) ganglia are unique at the molecular level.

CHAPTER 4

Comparison of 5-HT receptors on isolated rat petrosal neurons and O₂-chemoreceptor target cells *in vitro*

Manuscript in preparation. Order of authors will be: H. Zhong, M. Zhang and

C. A. Nurse.

1. I maintained cell cultures; Cathy Vollmer prepared most (~95%) of the cultures.
2. I performed most (~80%) of electrophysiological experiments and data collection in this study. Dr. M. Zhang assisted me in data collection in the remaining (20%), mainly recordings from glomus cells.
3. I performed all data analysis and generated all figures in text.

ABSTRACT

The petrosal ganglion supplies chemoafferent pathways via the glossopharyngeal nerve to visceral organs including the main arterial Po_2 sensor, the carotid body (CB). Serotonin (5-HT) is a putative neurotransmitter identified in CB chemoreceptors, i.e. type 1 cells, and exogenous 5-HT is known to increase chemoreceptor discharge. To characterize the underlying receptor subtypes and their location, we used whole cell, patch-clamp techniques to investigate 5-HT sensitivity of isolated rat petrosal neurons (PN) and CB type 1 cells. The dominant response of PN to 5-HT, applied by fast perfusion or from a 'puffer' pipette, was a rapid depolarization associated with a conductance *increase* in ~43% of the neurons (53/123). Under voltage-clamp near the resting potential (~-60 mV), 5-HT induced a transient inward current ($I_{5\text{-HT}}$), mimicked by 5-HT₃ receptor-specific agonist 2-methyl-5-HT, suggesting it was mediated by 5-HT₃ receptors. Further, $I_{5\text{-HT}}$ was selectively inhibited by the 5-HT₃ receptor-specific antagonist MDL72222 (1-10 μM), but unaffected by either 5-HT₁/5-HT₂ receptor antagonist, spiperone, or by 5-HT₂ receptor-specific antagonist, ketanserin (10 μM). The mean reversal potential (\pm S.E.M.) of $I_{5\text{-HT}}$ was -5.5 ± 5.8 mV (n=5). Application of 5-HT (dose range: 0.1~100 μM) onto PN produced a dose-response curve that was fitted by the Hill equation with $\text{EC}_{50} = \sim 3.4$ μM and Hill coefficient = ~ 1.6 (n =8). The activation phase of $I_{5\text{-HT}}$ (5-HT 10 μM at -60 mV) was well fitted by a single exponential with mean (\pm S.E.M.) time constant of 45 ± 30 ms (n =6). The desensitization phase of $I_{5\text{-HT}}$ was best fitted by a single exponential with mean (\pm S.E.M.) time constant of 660 ± 167 ms (n

=6). Fluctuation analysis of I_{5-HT} yielded an apparent single-channel conductance of 2.7 ± 1.5 pS (mean \pm S.E.M.; $n=4$) at -60 mV. In contrast, the majority (~ 70 %) of type 1 cells (14/20), as well as a minority (~ 7 %) population of PN (8/123), responded to 5-HT with a depolarization associated with a conductance *decrease*. In some cases the depolarization in type 1 cells triggered action potentials, and was blocked by the 5-HT₂ receptor antagonist, ketanserin (50 μ M). Whereas in these chemoreceptive cells, acute hypoxia suppresses a Ca²⁺-dependent K⁺ current, 5-HT suppressed a Ca²⁺-independent outward K⁺ current and the effect was mimicked by the PKC activator, 1-oleoyl-2-acetyl glycerol (OAG; 50 μ M). Taken together, these results allow for the possibility that 5-HT, released from type 1 cells during chemosensory signaling, may regulate PN firing directly, via 5-HT₃ receptors on petrosal terminals and/or indirectly, via autocrine or paracrine activation of 5-HT₂ receptors.

1. INTRODUCTION

Serotonin (5-hydroxytryptamine; 5-HT) is considered an important neuromodulator or neurotransmitter in the mammalian nervous system where it may have both excitatory and inhibitory actions (Hoyer et al., 1994). 5-HT regulates pharmacologically and structurally distinct subclasses of 5-HT receptors, including the cation permeable channels or 5-HT₃ receptors, and the 5-HT₂ receptors, which are coupled to K⁺ channels via G proteins and the phosphatidylinositol pathway (Hoyer et al., 1994; Baxter et al., 1995). The 5-HT₃ ligand-gated channels occur in both the central and peripheral nervous system, where autonomic and sensory neurons have been best studied (reviewed by Jackson & Yakel, 1995). Though there

is evidence that 5-HT₃ receptors mediate depolarization and excitation of sensory neurons (Wallis et al., 1982; Higashi and Nishi, 1982), and can regulate calcium fluxes, the precise function of 5-HT₃ receptor has proved difficult to characterize (Jackson and Yakel, 1995).

We are interested in neurotransmitter mechanisms in a peripheral chemosensory pathway, i.e. carotid body - sinus nerve, which is involved in the reflex control of respiration in mammals (Gonzalez et al., 1994). *In situ*, 5-HT has been identified in the chemoreceptor (glomus) cells of the carotid body (CB) in many species, including rat (Gronblad et al., 1983) and cat (Abramovici et al., 1991), and is released from isolated rat chemoreceptor cells *in vitro* (Fishman et al., 1985). However, the role of 5-HT in the CB chemoreceptor response to natural stimuli, e.g. hypoxia, has proved difficult to evaluate *in vivo*, in part because different subtypes of 5-HT receptors appear to be present, and their relative distribution on chemoreceptor cells versus afferent nerve terminals is unclear. For example, intracarotid injection of 5-HT produces a transient increase followed by a decrease in discharge from the carotid sinus nerve (CSN) in the cat (Nishi, 1975). Further in this species, though the 5-HT-induced increase in CSN discharge appeared similar to that elicited by hypoxia, 5-HT₃ receptor antagonists selectively blocked the 5-HT-induced chemoexcitation, but failed to affect the hypoxia-induced discharge (Kirby and McQueen, 1984). Similar results were reported for the rat CB (Yoshioko, 1989), where in addition, application of exogenous 5-HT to the CB produced a hyperventilation that was abolished by transection of the CSN (Sapru and Krieger, 1977). Though these studies argue that 5-HT may not be the principal mediator of hypoxic chemoexcitation in the CB, in a more recent study high doses of a selective 5-HT₃

receptor antagonist, reduced both basal- and hypoxia-induced CSN discharge (McQueen and Evrard, 1990), indicating the role of 5-HT in CB chemosensory signaling is equivocal.

It is evident from the above discussion that 5-HT action in the carotid body is complex, and there has been no clear dissociation of pre- from post-synaptic effects. Besides these complex neurogenic responses, 5-HT can also have circulatory effects. Kirby and McQueen (1984) suggested that 5-HT₃ receptors on sensory nerve endings could mediate transient excitation, whereas 5-HT₂ receptors, located on blood vessels or chemoreceptor type 1 cells, were associated with delayed chemoexcitation in the cat. In the present study, we isolated separately both pre- and post-synaptic elements *in vitro* and compared the distribution of 5-HT receptors using whole-cell recording. To ensure second messenger systems remained intact, especially important for 5-HT₂ receptors (Hoyer et al., 1994), most experiments were done with the nystatin perforated-patch whole cell technique to limit intracellular dialysis (see Horn and Marty, 1988). We found that whereas 5-HT₃ receptor was the predominant one on petrosal neurons, 5-HT₂ receptor was dominant on type 1 cells.

2. MATERIALS AND METHODS

Cell culture

The procedures for the isolation and culture of petrosal sensory neurons by combined enzymatic and mechanical dissociation of the rat petrosal ganglia were similar to those previously described (Stea & Nurse 1992; Zhong & Nurse 1994). Briefly, the region of the petrosal ganglion adjacent to the exit of the glossopharyngeal (IXth) nerve was excised from

2-14-day-old rat pups (Wistar, Charles River, Quebec). Excised ganglia were then incubated for 1 h at 37° C in an enzymatic solution containing 0.1% collagenase/ 0.1% trypsin (Gibco, Grand Island, NY). The tissues were mechanically dissociated with forceps, triturated to yield a cell suspension, and plated onto a thin layer of Matrigel (Collaborative Research, Bedford, MA) that was previously applied to the central wells of 35-mm tissue culture dishes. In other experiments, carotid body (CB) type 1 cells were grown in dispersed cell culture as previously described (Stea and Nurse, 1991a). Cultures were grown at 37° C in a humidified atmosphere of 95% air-5% CO₂ for 4 h to 14 days before they were used in the patch-clamp/whole-cell experiments. The growth medium was changed every 4-6 days.

Solutions and drugs

Most experiments were performed using extracellular fluid (ECF) of the following composition (mM): NaCl, 111; KCl, 5; CaCl₂, 2; MgCl₂, 1; glucose, 10; NaHCO₃, 24; a pH of 7.4 was maintained by bubbling with 5% CO₂. The stock pipette solution for conventional whole-cell recording contained (mM) either : (i) KCl, 135; NaCl, 5; CaCl₂, 1; ethylene glycol-bis(β-aminoethyl ether)-N,N,N',N'-tetraacetic acid (EGTA), 11; HEPES, 10; ATP-Na 2 mM at pH 7.2; or (ii) potassium glutamate or gluconate, 105; KCl, 35; CaCl₂, 1; EGTA, 11; HEPES, 10; ATP-Na 2 mM at pH 7.2. For nystatin perforated-patch recordings (see Stea and Nurse, 1991a), the pipette contained (mM): potassium glutamate or gluconate, 105; KCl, 35; CaCl₂, 1; HEPES, 10 and nystatin 300 µg/ml, at pH 7.2. All solutions were filtered through a 0.45 µm millipore filter before use. During recordings the culture was continuously perfused

by gravity flow and removal of excess fluid by suction ensured that the fluid level in the recording chamber remained relatively constant.

The drugs tetrodotoxin (TTX), tetraethylammonium (TEA), and 1-oleoyl-2-acetylgllycerol (OAG) were obtained from Sigma Chemical Co. (St. Louis, MO). Serotonin (5-HT), 2-methyl-serotonin, MDL-72222 (1 α H, 3 α H, 5 α H,-tropan-3-yl-3,5-dichlorobenzoate methanesulphonate), spiperone, ketanserin, and 3-tropany-indole-3-carboxylate (ICS205-930) were obtained from Research Biochemicals Inc. (RBI; Natick, MA).

Application of 5-HT agonists and antagonists

5-HT was freshly prepared as a 10 mM stock solution in distilled water or in ECF (see above). Just before use it was diluted to the desired final concentration and then applied to the cells in one of three ways. In some experiments, 5-HT or 2-methyl-serotonin (0.1-1 mM) was delivered by pressure ejection from a nearby 'puffer' pipette positioned 20 - 40 μ m from the neuronal surface. This procedure permitted very rapid application of the agonist over a time interval of 50 - 200 ms, and at a low pressure (4-8 p.s.i.) under control of a solenoid valve (General Valve Corp., NJ). In other experiments, including those designed to vary 5-HT doses, a fast-perfusion technique was used (Lester et al., 1990; Zhong, Zhang and Nurse 1997). In this procedure an electromechanical device (Piezo Systems Inc. MA) permitted a fast switch between barrels of a double-barreled pipette, thereby allowing the cell to be exposed to control solution (in one barrel) or the agonist (in the other barrel). In studies of

the dose-response relationship, the peak current amplitude elicited by the test concentration was compared with that elicited by a saturating concentration (10 μM) of 5-HT. Thus, the dose-response generated by this method displays normalized values relative to the maximal response (unity) measured with 10 μM 5-HT.

In studies of the elementary event by fluctuation analysis, a low concentration of 5-HT (0.5 μM) was applied by conventional bath perfusion under gravity flow to permit slow activation of the response with minimal desensitization. All antagonists were applied by bath perfusion under gravity.

Whole-cell recording

Both conventional whole-cell and perforated-patch recordings were used in this study, according to procedures described in detail elsewhere (Stea and Nurse, 1991a, 1992). In many cases, especially where 5-HT₃ receptors were studied, results obtained by the two methods were similar. In most experiments >80% of the series resistance was compensated, and junction potentials (2 -10 mV) were cancelled at the beginning of the experiment. The ECF was warmed before entering the recording chamber, where the mean temperature was $34 \pm 2^\circ \text{C}$ over the time course of the experiments.

Whole-cell currents or membrane potential were recorded with the aid of an Axopatch 1D patch clamp amplifier and a Digidata 1200 A-D converter (Axon Instruments Inc., Foster City, CA), and stored on a 486 Personal Computer. Current and voltage clamp protocols, data acquisition and analysis were performed using pCLAMP software (version 5.5., and

6.0.2: Axon Instruments Inc.) and Axotape (version 2.02. Axon Instruments Inc.).

Data analysis

5-HT-induced currents were sampled at 0.5 ~ 1 kHz and stored in a 486 computer for analysis. Exponential fits of the time course of $I_{5\text{-HT}}$ activation or desensitization were obtained using CLAMPFIT (6.0.2, Axon Instruments Inc.). Fits of the dose-response to Hill equation were obtained using Sigma Plot. The Hill coefficient (n) and half-maximal activation (EC_{50}) were adjusted for best fit of the curve to the observed data; a non-linear fitting routine that minimizes the least-squares difference was used to obtain the best fit. Current fluctuations induced by 5-HT under whole-cell voltage clamp were analyzed as described elsewhere (Neher and Stevens, 1977). The apparent single-channel conductance was estimated from the relation between the variance of the current noise and mean current. Most of the results are represented in the text as mean \pm standard error of the mean (S.E.M.).

3.RESULTS

5-HT Sensitivity of Petrosal Neurons

3.1. Effects of 5-HT on membrane potential

Dissociated rat petrosal neurons (PN) were investigated with whole-cell recording techniques after 4 hr to 12 days in culture. Under current-clamp 5-HT, applied by bath perfusion (1-100 μM) or pressure ejection (0.1-1 mM), induced rapid depolarization followed by a slower repolarization in 43% of the neurons sampled (n = 123; e.g. Fig. 1A). A burst

of action potentials was often superimposed on the rapid depolarizing phase. In the presence of tetrodotoxin (TTX; 0.1 μ M), action potentials were completely blocked but the 5-HT-induced depolarization persisted (Fig. 1B). As shown in Fig. 1B, the depolarization in the majority of 5-HT sensitive neurons was accompanied by an approximately 2~3 fold increase in membrane conductance (mean = $2.5 \pm 1.4x$; n = 10), and was mimicked by the 5-HT₃ receptor agonist (2-methyl-serotonin, 10 μ M; n = 12) and reversibly blocked by the 5-HT₃ receptor antagonist (MDL-72222, 10 μ M; n = 6, see later).

The magnitude of 5-HT induced responses varied greatly from cell to cell, probably due to geometric factors that influence the rate of activation and desensitization as well as the magnitude of response (Yakel and Jackson, 1988). 5-HT sensitivity was detected in neurons as early as 4 hr after isolation (4 out of 6 neurons), suggesting that the 5-HT₃ receptors were already expressed on the cells prior to culture. These receptors also persisted on the neurons for at least 12 days *in vitro*.

Many PN (62 out of 123) did not show any detectable response to 5-HT application and these were not investigated further. In a minority population (n = 8), application of 5-HT led to membrane depolarization with conductance *decrease* (Fig. 1C); this effect was blocked by the 5-HT₂ receptor-specific antagonist, ketanserin (10 μ M; n = 2), but not the 5-HT_{1A} and 5-HT_{2A} antagonist, spiperone (10 μ M), nor the 5-HT₃ receptor antagonist, MDL-72222 (10 μ M). Similar receptors were found on the majority of type 1 cells and will be discussed in more detail later.

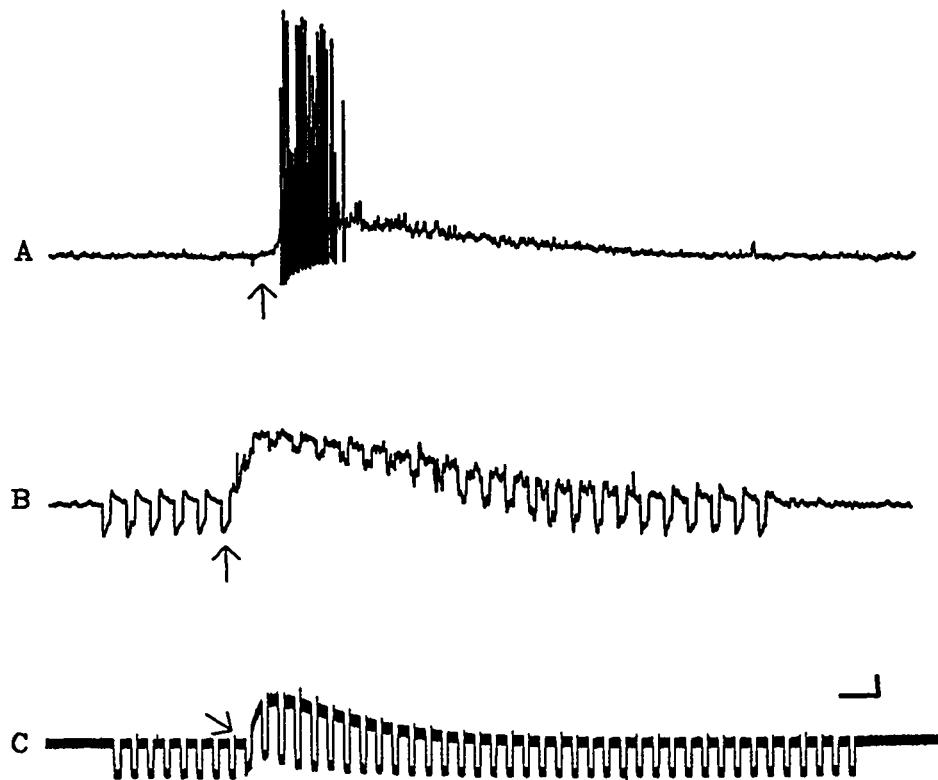


Figure 1. Effects of 5-HT on petrosal sensory neurons *in vitro*.

A. Under current-clamp, pressure ejection of 5-HT (1 mM; applied at arrow) evoked membrane depolarization with superimposed action potentials. B. 5-HT applied on the same neuron (with 1 μ M TTX in the bath to block action potentials) induced membrane depolarization with a conductance *increase*, as indicated by application of brief hyperpolarizing current pulses (downward deflections). C. An example of 5-HT-induced depolarization with conductance *decrease* in a cultured petrosal neuron; this response occurred in a minority population of neurons. Vertical calibration bar (lower right) represents 10 mV in A, B, and 5mV in C; horizontal bar represents 2 s in A, B, and 3 s in C.

3.2. 5-HT induced current (I_{5-HT}) mediated by 5-HT₃ receptors

In order to analyze the 5-HT₃ receptors in more detail, neurons were studied under voltage clamp. In responding neurons, 5-HT (10 μ M) induced a transient inward current (I_{5-HT}) at the holding membrane potential of -60 mV. As shown in Fig. 2A,B, I_{5-HT} was mimicked by 5-HT₃ receptor-specific agonist, 2-methyl-serotonin (10 μ M; n =22) applied by fast perfusion, and was reversibly blocked (Fig. 2C,D) by the 5-HT₃ receptor-specific antagonist, MDL-72222 (10 μ M; n = 16). In most cases, MDL72222 completely abolished I_{5-HT} , though in a few cases only partial blocking was observed. Another selective 5-HT₃ receptor antagonist, 3-tropanyl-indole-3-carboxylate (ICS205-930; 100 nM) was also an effective blocker of I_{5-HT} (n= 6, not shown); this current was unaffected by 5-HT_{1A} and 5-HT_{2A} receptor antagonist, spiperone (10 μ M) and 5-HT₂ receptor antagonist, ketanserin (10 μ M).

3.3. Reversal potential of the 5-HT response

The reversal potential of the 5-HT response (E_{5-HT}) was obtained in current clamp experiments during application of 5-HT (1 mM) from a 'puffer' pipette, and with 0.1 μ M TTX and 5mM TEA present in the bath. An example of these responses (mV) at different membrane potentials between -80 and -10 mV is shown in Figure 3A, where E_{5-HT} shifts from depolarizing to hyperpolarizing between -10 and +10 mV (top 2 traces). For this cell the reversal potential was at \sim -5mV, as determined from the response-voltage relation in Fig. 3B. The mean (\pm S.E.M.) reversal potential E_{5-HT} was -5.5 ± 5.8 mV (n =5), which is in good agreement with that for 5-HT₃ receptors in other studies on sensory neurons from nodose

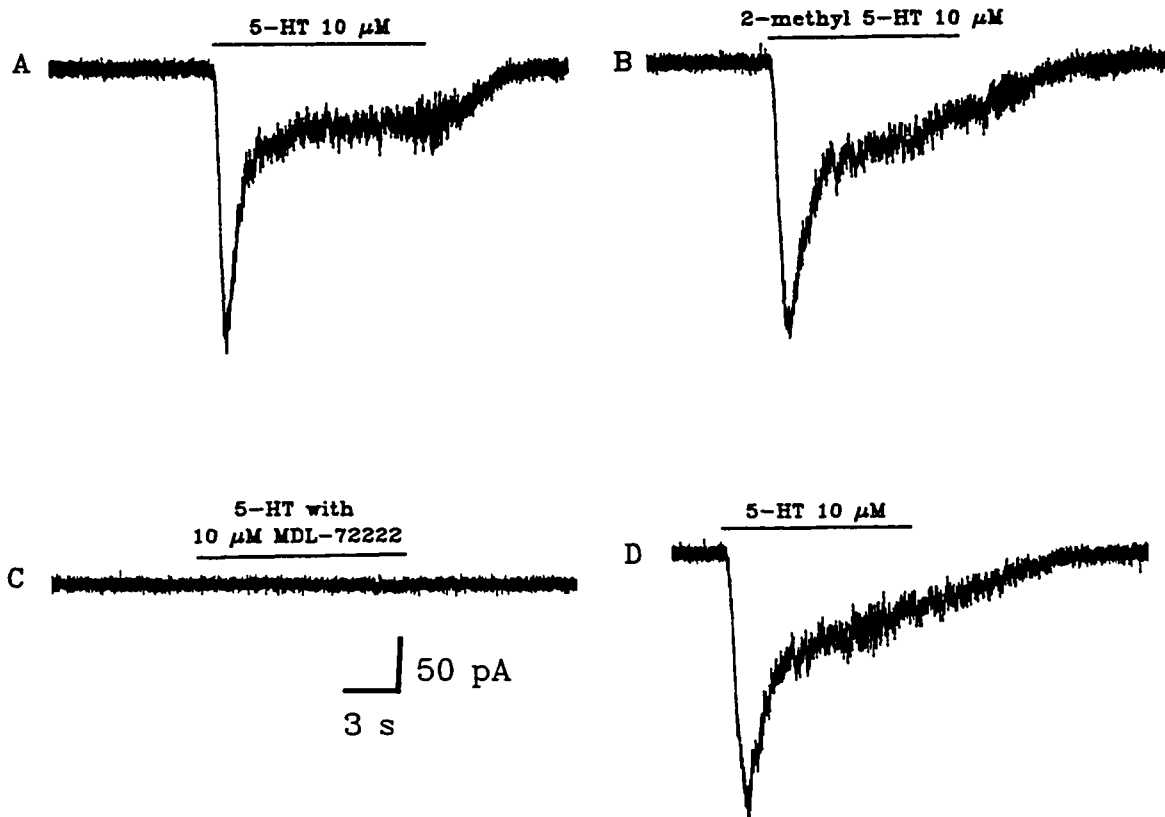


Figure 2. Evidence for 5-HT₃ receptor on petrosal neurons.

A. Under voltage-clamp at -60 mV, 5-HT (10 μ M) delivered by rapid perfusion (indicated by upper horizontal bar) induced a fast transient inward current which declined to a steady level. After 5-HT was removed the membrane current subsided to baseline level. B. The effect of 5-HT in A, was mimicked by the 5-HT₃ receptor-specific agonist (2-methyl-5-HT; 10 μ M). C. The effect of 5-HT was blocked by the 5-HT₃ receptor-specific antagonist, MDL-72222 (10 μ M), the original 5-HT response recovered after wash out of the antagonist (D).

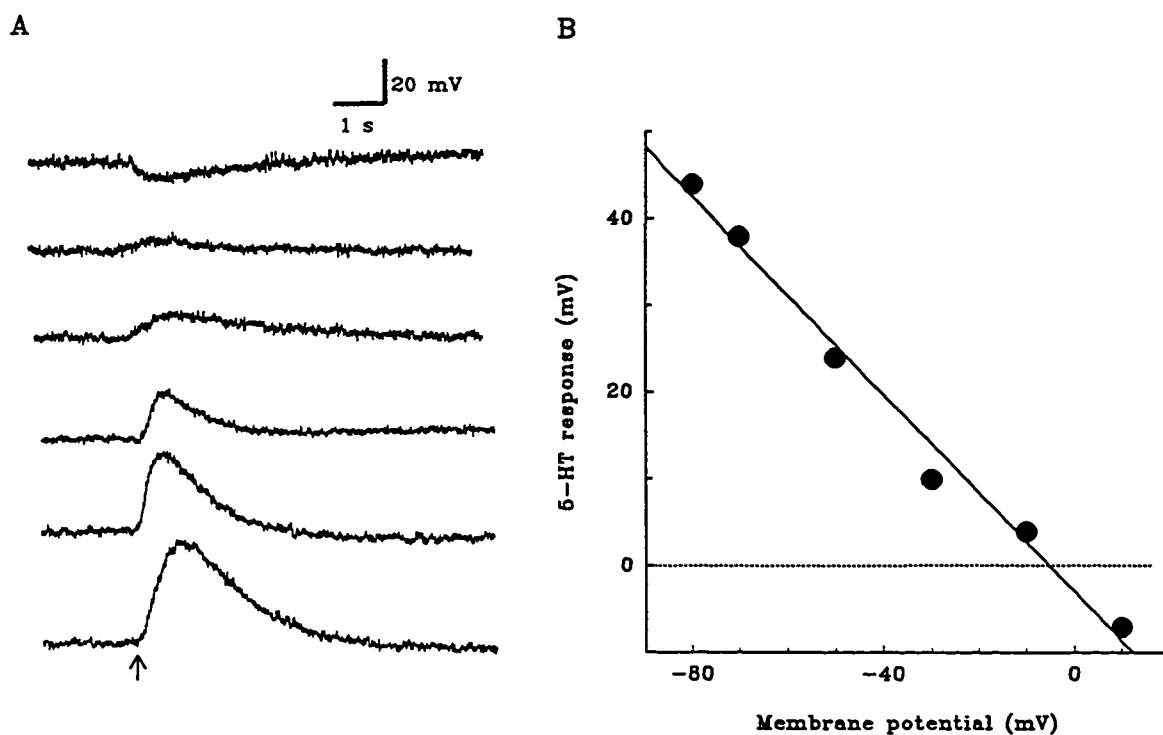


Figure 3. The reversal potential of 5-HT responses in petrosal neurons. A. An example of 5-HT evoked responses (mV) at different initial membrane potentials (-80, -70, -50, -30, -10, and +10 mV from bottom to top). 5-HT (0.1 mM) was applied by pressure ejection from a 'puffer' pipette at the time indicated by arrow. Note reversal of 5-HT response between +10 and -10 mV. B. The relationship of peak 5-HT responses vs initial membrane potential for cell in A was used to estimate the reversal potential of 5-HT induced depolarization. For this cell, the reversal potential was ~ -5 mV.

(Peters et al., 1993, $E_{5\text{-HT}} = -1.6 \pm 1.3$ mV; Fan and Weight, 1994, $E_{5\text{-HT}} = +4.1$ mV) and dorsal root (Robertson and Bevan, 1991, $E_{5\text{-HT}} = +6.9 \pm 1.7$ mV; Yakushiji and Akaike, 1992, $E_{5\text{-HT}} = -11$ mV) ganglia in different species. These data suggest that 5-HT₃ receptors on rat petrosal neurons are similar to those in other peripheral sensory neurons, and likely gate a mixed cationic current.

3.4. 5-HT dose-response relation

The dose-response relation for the 5-HT₃ receptors on petrosal neurons was studied under voltage clamp at -60 mV, during fast perfusion of various 5-HT concentrations over the range 0.1 to 100 μ M. As the concentration of 5-HT was increased the kinetics became more rapid, and the peak amplitude of $I_{5\text{-HT}}$ also increased, reaching a plateau at a concentration of ~ 20 μ M (Fig. 4A). The amplitude of the peak response ranged from 120 to 650 pA ($n = 12$) and the mean peak current density (+ S.E.M.) was $21.5 + 4.1$ pA/pF. To obtain the dose-response relation, the mean relative peak current (see Materials and methods) at each 5-HT concentration was fitted with the Hill equation:

$$I/I_{\max} = 1 / \{ 1 + (EC_{50}/[5\text{-HT}])^n \}$$

where I is the measured peak current for a given 5-HT concentration, I_{\max} is the maximal response, n is the Hill coefficient, and EC_{50} is the concentration of 5-HT required for half-maximal activation. As shown in Fig. 4B, the EC_{50} for receptor activation was ~ 3.4 μ M and the Hill coefficient was 1.6, suggesting two (or more) agonist binding sites are required for maximal activation of the receptor (Jackson and Yakel, 1995). Errors in these estimates may

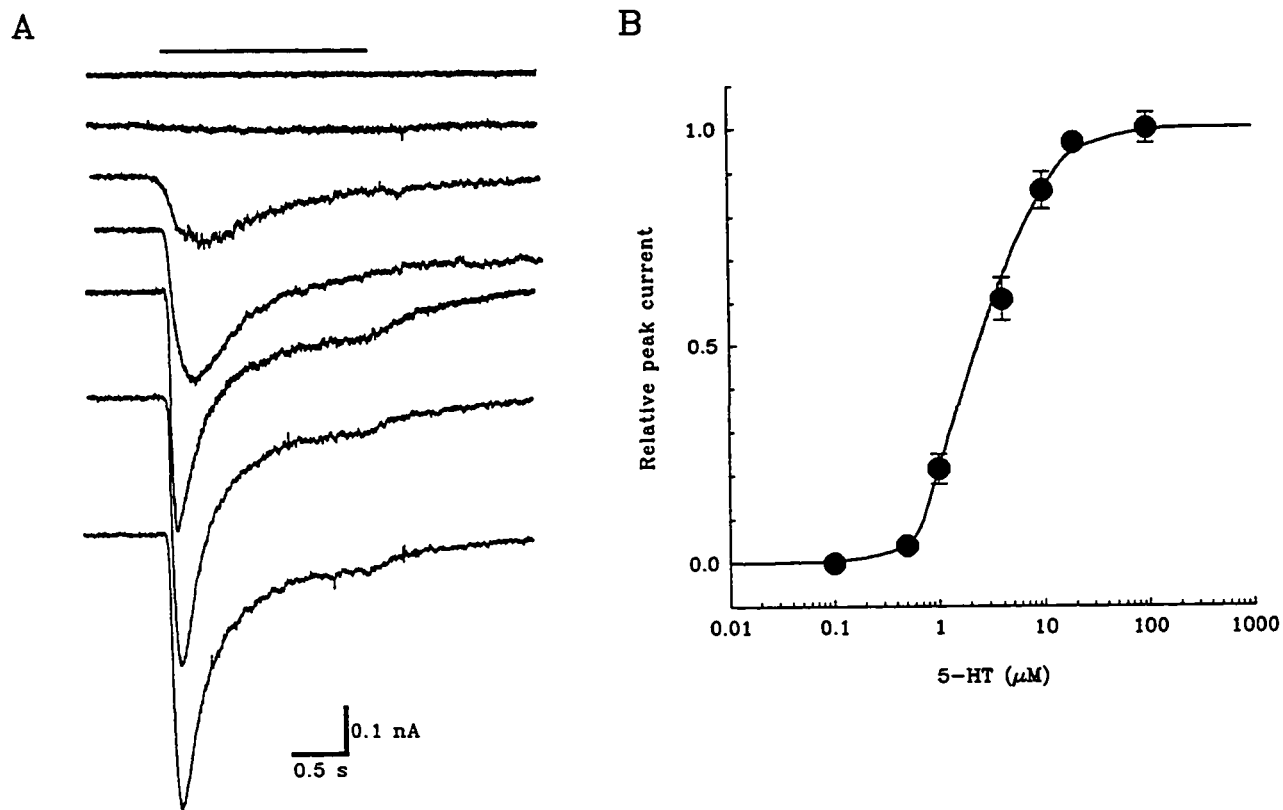


Figure 4. Dose-response curve of 5-HT effects on petrosal neurons. A. An example of whole-cell currents in response to application of 5-HT by fast perfusion (upper horizontal bar) at different concentrations (0.1, 0.5, 1, 4, 10, 20, 100 μM from top to bottom). The membrane potential of the cell was clamped at -60 mV. With increasing 5-HT concentrations the peak amplitude of $I_{5\text{HT}}$ increased and the kinetics became more rapid. B. The peak currents evoked by each concentration are expressed relative to the peak current evoked by 20 μM 5-HT and plotted against the log [5-HT]. Each point is the mean (\pm S.E.M.) response from 8 neurons; for some data points, the S.E.M. is smaller than the symbol size. The experimental data were fitted by a Hill equation with a Hill coefficient of 1.6, and $\text{EC}_{50} = 3.4$ μM .

arise from the method of 5-HT application and/or receptor desensitization (Higashi and Nishi, 1982; Jackson and Yakel, 1995), though the results are comparable to those in previous reports for 5-HT₃ receptors in other neurons (Fan and Weight, 1994: rat nodose EC₅₀=2.6, Hill coefficient =1.55; Yakel et al., 1991; clonal cells EC₅₀=3.3, Hill coefficient =1.8).

3.5. Kinetics of activation and desensitization of I_{5-HT}

As shown in Figure 4A, I_{5-HT} activated more rapidly at higher 5-HT concentrations. The kinetics of activation and desensitization of I_{5-HT} were studied during fast perfusion of 10 μM 5-HT onto petrosal neurons, voltage clamped at -60 mV (Fig. 5A). In Figs. 5B and 5C, the two regions of the current trace shown in Fig. 5A are displayed separately for clarity. The activation phase of I_{5-HT} was fitted by a single exponential of the form:

$$I_t = C + I_0 * \exp(-t/\tau)$$

where I_t is the current as a function of time; C is a constant; I₀ is the initial current; 't' is time in ms; τ is time constant of activation. The mean (± S.E.M.) time constant of activation (τ_a) was 45 ± 30 ms (n=6) which is comparable to that in a previous study on neuroblastoma cells (38 ms; Mienville, 1991). A common feature of 5-HT₃ receptors is their desensitization during continuous agonist application. At low concentrations (below 1 μM), 5-HT induced no obvious desensitization, but at higher concentrations the rate of desensitization was enhanced (Fig. 4A). Because of variability from cell to cell, we did not attempt to study this feature in detail. However, as shown in Figure 5C, the desensitization phase of I_{5-HT} was best fitted by a single exponential, with a mean (± S.E.M.) time constant τ_d = 660 ± 167 ms (n=6), a value

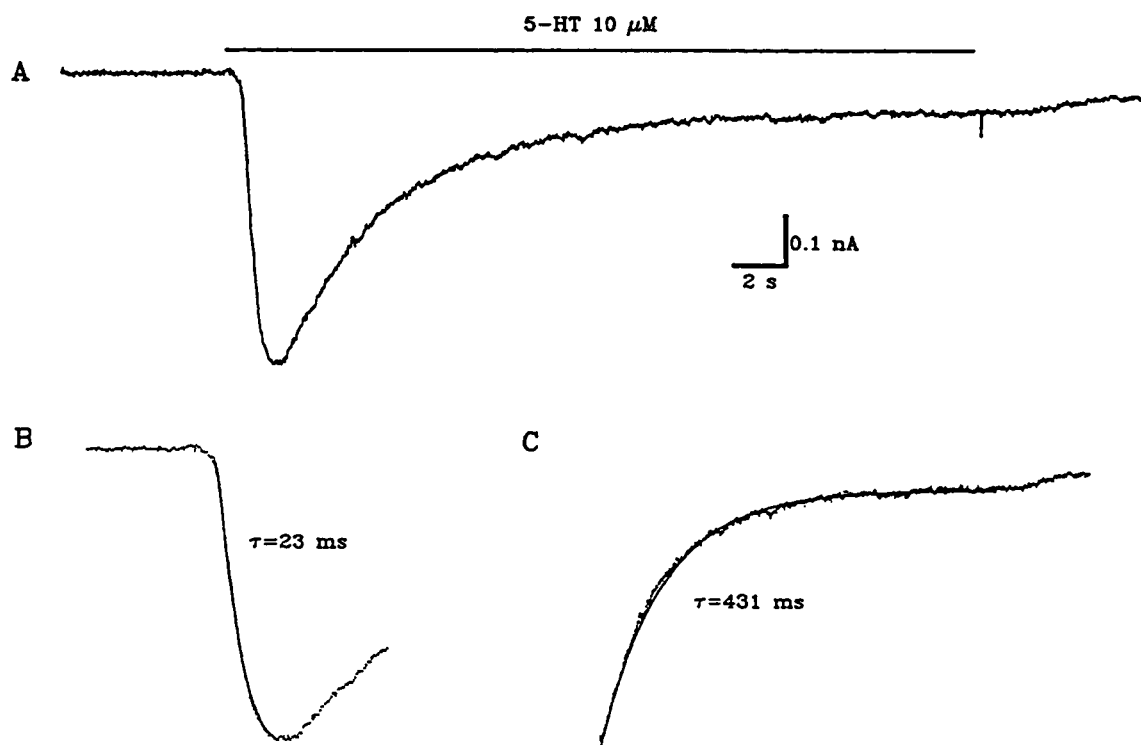


Figure 5. The activation and desensitization of $I_{5\text{-HT}}$. A. The trace shows the whole-cell current induced by prolonged application of 5-HT ($10\mu\text{M}$; at -60 mV) by fast perfusion. The top horizontal bar indicates the duration of 5-HT application. B. The onset of the $I_{5\text{-HT}}$ current from A is shown in more detail (dotted line). The activation of $I_{5\text{-HT}}$ was fitted by a single exponential (solid line) with an activation time constant $\tau_a = 23\text{ ms}$. C. The desensitization phase of $I_{5\text{-HT}}$ (dotted line) recorded during continued perfusion of 5-HT ($10\mu\text{M}$; at -60 mV) is fitted by a single exponential (solid line) with a time constant $\tau_s = 431\text{ ms}$.

comparable to that in frog DRG neurons ($\tau_d = 0.5-0.8$ s; Yakushiji and Akaike, 1992). However, in type 'C' neurons of rabbit nodose ganglion, 5-HT caused no desensitization (Higashi et al., 1982) while in other preparations bi-exponential kinetics were reported (Yakel et al., 1991; Yang et al., 1992; Furukawa et al., 1992).

3.6. Estimate of single channel conductance of 5-HT₃ receptors from fluctuation analysis

The single channel conductance of 5-HT₃ receptor channels was estimated using fluctuation analysis (Neher and Stevens, 1977). To obtain a steady, non-desensitizing current response suitable for noise analysis, a low concentration (0.5 μ M) of 5-HT was applied by bath perfusion onto petrosal neurons voltage clamped at -60 mV. A typical segment of a current record used for analysis is shown in Figure 6 (inset), where the rising phase of the I_{5-HT} response was accompanied by increased noise. The plot of the current variance versus mean current was linear (Fig. 6), and the average single channel conductance, γ , was estimated from the relationship:

$$\gamma = \delta^2 / \Delta I (V_h - V_{eq})$$

where δ^2 is the 5-HT-induced current variance, ΔI is the 5-HT-induced mean change in membrane current, V_h is the holding potential, and V_{eq} is the reversal or zero current potential of 5-HT responses, estimated as ~ -5 mV (see Fig. 3B). The mean single-channel conductance (\pm S.E.M.) obtained from the above relationship was 2.7 ± 1.5 pS at -60 mV ($n=5$), a value comparable to other studies (2.5 pS: rat SCG neurons, Yang et al., 1992; 4 pS:

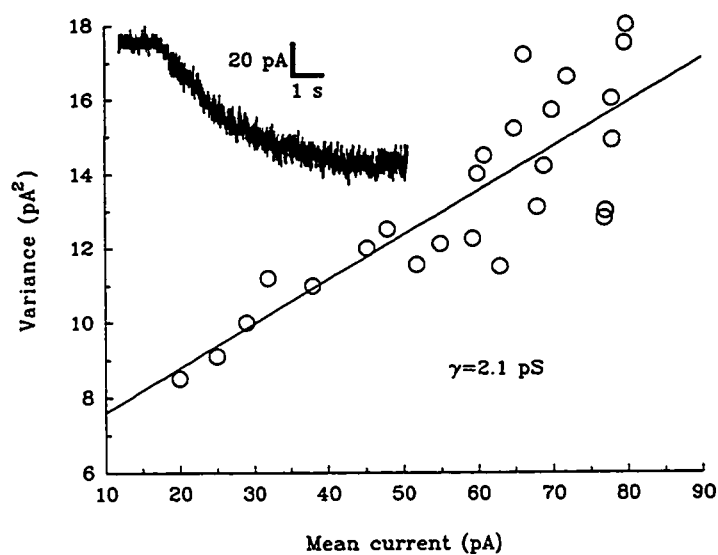


Figure 6. Estimation of the 5-HT₃ receptor single-channel conductance from fluctuation analysis of the 5-HT-induced whole-cell current in a petrosal neuron. The variance of current noise was plotted vs mean current and the single channel conductance, estimated from least-squares linear fit, was 2.1 pS. The inset shows a section of the record used for fluctuation analysis; inward current produced by perfusion of 0.5 μM 5-HT. Membrane noise was increased during the rising phase of the current evoked at a holding potential - 60 mV.

NG108-15 cells, Yakel et al., 1990). However, it was considerably higher than values from clonal cell lines (310 fs : Lambert et al., 1989; 593 fs: Yang, 1990), and lower than the value for rabbit nodose neurons (17 pS: Peter et al., 1993), and guinea-pig enteric neurons (15 and 9 pS: Derkach et al., 1989).

5-HT Sensitivity of Type 1 Cells

3.8 Effects of 5-HT on membrane potential of type 1 cells

In 14/20 type 1 cells investigated under current clamp, application of 5-HT (1 mM) from a 'puffer' pipette caused membrane depolarization associated with a conductance *decrease*, seen during injection of constant hyperpolarizing current pulses (Fig. 7A). In a few cases, the depolarization was sufficient to trigger (calcium) action potentials (Fig. 7B). The mean depolarization (\pm S.E.M.) obtained in this way from 6 cells was 14.3 ± 3.6 mV, and was mediated by 5-HT₂ receptors since it was completely and reversibly abolished by perfusion of the 5-HT₂ receptor specific antagonist, ketanserin (50 μ M), in each of 3 cases tested. The depolarization was unaffected by the 5-HT_{1A} receptor antagonist, spiperone (10⁻⁵M), and the 5-HT₃ receptor antagonist, MDL-72222 (not shown). One example of reversible block of the 5-HT response by ketanserin is shown in Fig. 7 B,C,D. The reversal potential of the 5-HT induced response was ~ -80 mV (mean \pm S.E.M. = -81.2 ± 3.1 ; n = 3), i.e. near the potassium equilibrium potential ($E_K = -83$ mV in this experiment). An example illustrating the 5-HT reversal potential in a type 1 cell is shown in Fig. 8 A,B. These results suggest that the membrane depolarization induced by 5-HT (see Fig. 7) is mediated by K⁺ channel closure at

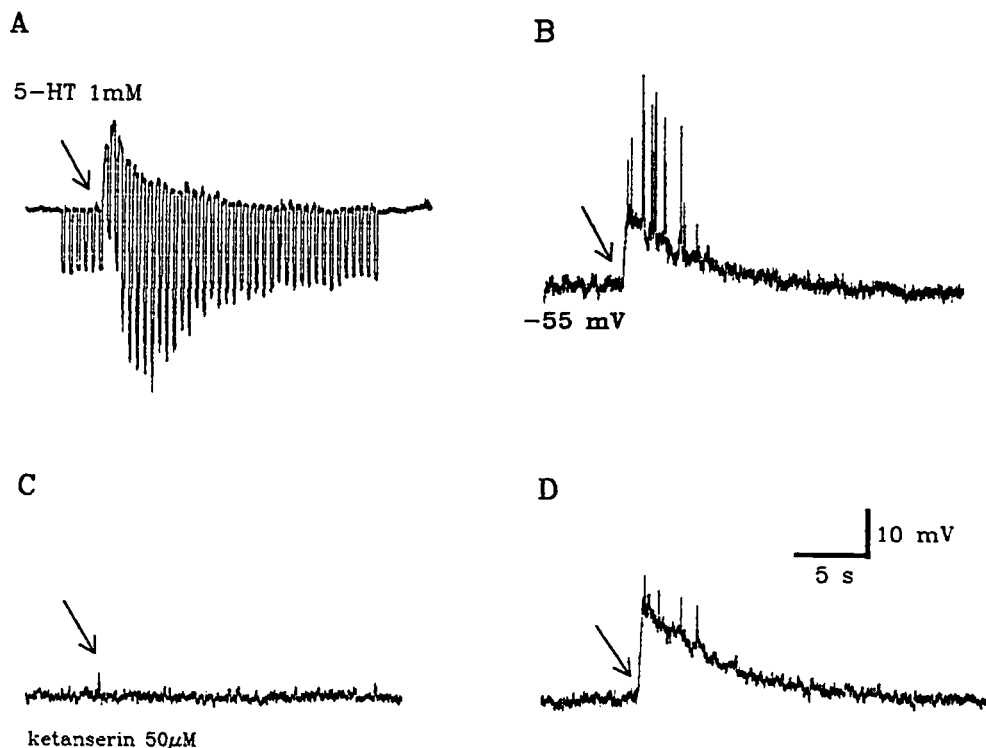


Figure 7. Effects of 5-HT on the membrane potential of cultured glomus cells. Application of 5-HT (1mM) by 'puffing' onto a glomus cell resulted in membrane depolarization with a conductance decrease as shown in A. In a few cases, the 5-HT-induced depolarization was accompanied by action potentials (e.g. Fig. B), and the response could be reversibly blocked by 5-HT₂ receptor antagonist, ketanserin (50 μ M; Fig. C, D). Note B, C, D are recordings from the same cell.

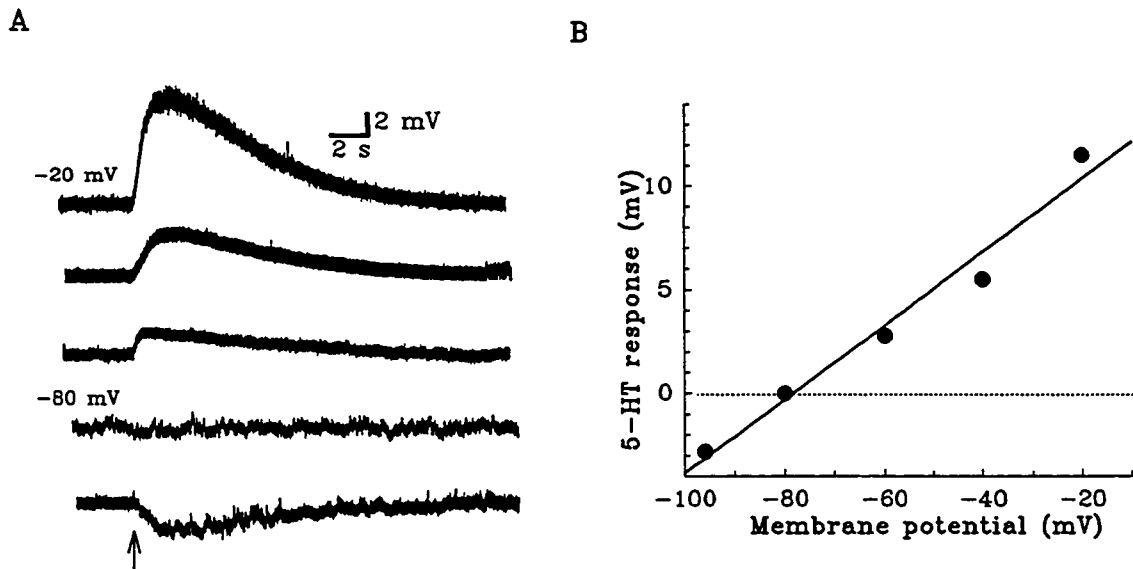


Figure 8. The reversal potential of 5-HT response in a glomus cell.

A. Application of 5-HT (1 mM; puffer pipette) at the time indicated by arrow to a glomus cell held at different initial membrane potentials (-98, -80, -60, -40, and -20 mV; from bottom to top trace) evoked responses under current-clamp. B. Peak amplitude of each response is plotted vs initial holding potential. The relationship of the amplitude of response (mV) vs membrane potential was used to estimate the reversal potential. For this cell, the reversal potential was ~ -80 mV, a value similar to the K^+ equilibrium potential ($E_K = -83$ mV).

the cell's resting potential.

3.9 5-HT suppresses outward K^+ current in type 1 cells

In the peripheral nervous system, 5-HT₂ receptors are usually coupled to K^+ channels via G-proteins and the phosphatidylinositol pathway (Hoyer et al., 1994). We tested whether 5-HT could regulate the outward K^+ current in type 1 cells under voltage clamp. This was the case as shown in Fig. 9 A-D, where bath perfusion of 0.1 mM 5-HT suppressed the outward K^+ current in type 1 cells. The mean suppression (\pm S.E.M.) evoked by this dose of 5-HT during a step from -60 to +40 mV was $23.5 \pm 5.4\%$ ($n = 6$). A current density plot of the I-V relation for a group of cells before, during, and after 5-HT is shown in Fig. 9C. To test whether the effects of 5-HT might involve activation of the protein kinase C (PKC) second messenger pathway (Hoyer et al., 1994), the PKC activator, 1-oleoyl-2-acetyl-glycerol (OAG), an analogue of diacylglycerol (DAG; Nishizuka, 1988), was applied to type 1 cells while K^+ current was monitored under voltage clamp. In 2 cells, 50 μ M OAG suppressed the outward K^+ current similar to 0.1 mM 5-HT, and this is consistent with 5-HT action via the PKC second messenger pathway.

Since in some neurons 5-HT increases electrical excitability by reducing the afterhyperpolarization, via suppression of a Ca^{2+} -dependent K^+ current (Wallen et al, 1989; Wikstrom et al., 1995), we tested whether the same occurs in type 1 cells. As shown in in Fig.9 A,B,D, 5-HT induced K^+ current suppression even in the presence of Ca^{2+} -free extracellular solution, suggesting it was not mediated by closure of Ca^{2+} -dependent K^+

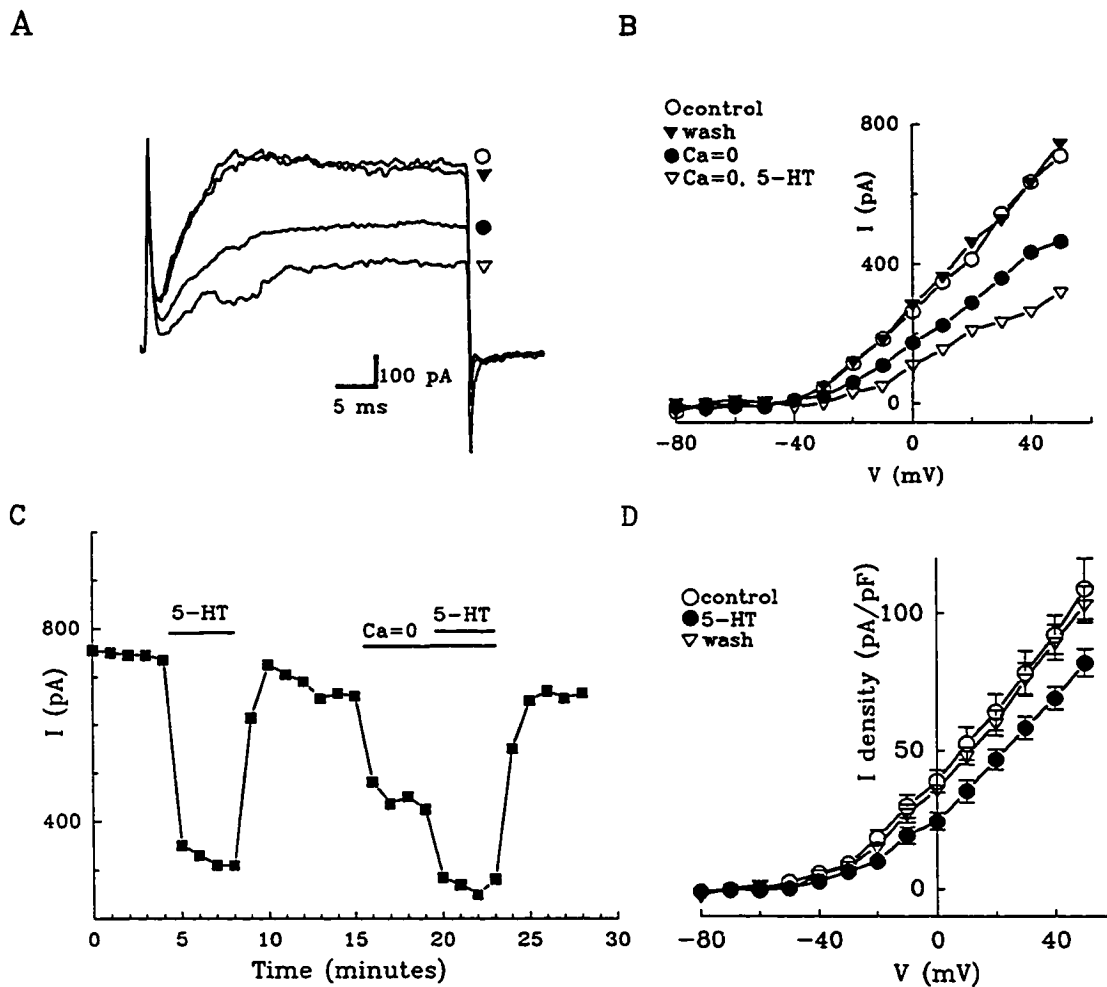
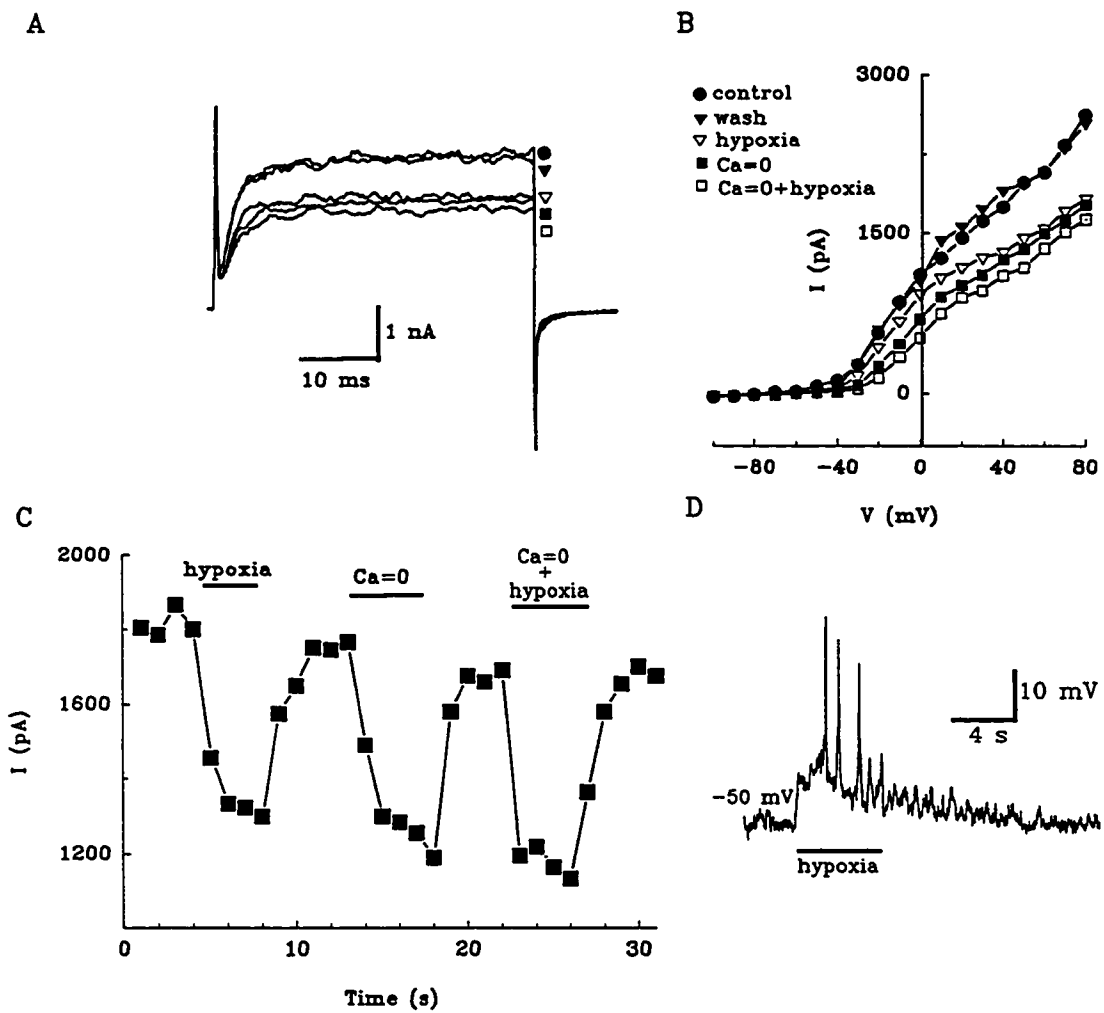


Figure 9. Effects of 5-HT on the membrane currents of cultured glomus cells. Bath perfusion of 5-HT (0.1 mM) reversibly suppressed peak K^+ current even in calcium-free medium (A). This suggests that the 5-HT-sensitive current is not an $I_{K(Ca)}$. B and C show the I-V relationship and the time course of 5-HT effects respectively, for the same cell. D. Effects of 5-HT on the current density of 4 cells; data points are mean (\pm S.E.M.) current density pA/pF, determined by dividing peak current at the indicated voltage, by the input capacitance.

Figure 10. Effects of hypoxia on whole-cell currents and membrane potential in cultured glomus cells . A. Voltage step from a holding potential of -60 to +50 mV elicits an outward K^+ current which is reversibly suppressed (~20%) on exposure to a hypoxic solution (P_{O_2} = ~20 mm Hg). In calcium-free solution, the outward K^+ current is suppressed by almost the same amount as hypoxia. B. I-V relationship of the same cell in A shows the effects of hypoxia (open triangles), calcium-free solution (filled square) and both together (open square) on the whole-cell currents. Control currents and recovery are represented by filled circle and filled triangles respectively. C. Time course of the effects of hypoxia and calcium-free solution on the same cell as in A and B. This result is consistent with hypoxia suppressing a Ca^{2+} -dependent K^+ current in rat glomus cells, as reported by Peers (1990). D. Hypoxia evoked membrane depolarization with superimposed (calcium) action potentials.



channels. Interestingly, in these chemoreceptor cells, closure of Ca^{2+} -dependent K^+ channels by low Po_2 is thought to be an important step during hypoxic chemotransduction (Peers, 1990), and this is illustrated for a cell in Fig. 10 A-D. Therefore, since hypoxia and 5-HT close different K^+ channel subtypes, these results allow for the possibility that during chemosensory stimulation (e.g. by hypoxia) release of 5-HT from type 1 cells could further enhance the cells' excitability by an autocrine or paracrine feedback loop via 5-HT₂ receptors

DISCUSSION

The present study demonstrates that ~43% (54/123) of petrosal neurons, isolated from neonatal rats are sensitive to 5-HT and that the responses are mediated principally by 5-HT₃ receptors. In a few cases, 8 out of 123 cells, the 5-HT response was mediated by 5-HT₂ receptors. The significance of this minority population is uncertain, but the ganglion contains neurons with different sensory phenotypes and peripheral projections. On the other hand, and as discussed later, 5-HT₂ receptors appear to be the main subtype located on type 1 cells, a major chemosensory target for these neurons.

In the majority of cases, application of 5-HT depolarized responsive petrosal neurons, often yielding a burst of action potentials. With TTX (1 μM) present, action potentials were abolished and 5-HT caused membrane depolarization accompanied by a conductance *increase*, and with a reversal potential near -5 mV. Under voltage clamp near the resting potential (-60 mV), 5-HT induced an inward current, $I_{5\text{-HT}}$, mimicked by 2-methyl-5-HT and inhibited by the 5-HT₃ receptor-specific antagonist MDL72222, suggesting it was mediated

by 5-HT₃ receptors. The concentration for half-activation of these channels was ~ 3.4 μ M, and at high concentrations the receptors showed rapid desensitization. Noise analysis revealed a mean single channel conductance of 2.7 pS, a value comparable to 5-HT₃ receptors in some preparations (Yakel and Jackson, 1988). The 5-HT response of petrosal neurons was detected as early as 4 hr after isolation and the frequency of responding cells remained relatively stable over 14 days in culture. Thus, although culture conditions are known to affect expression of 5-HT₃ receptors (e.g. PC 12 cells; Furukawa et al., 1992), their detection in the present study soon after isolation suggests the receptors were present on the neurons *in situ* prior to dissociation.

The prevalence of 5-HT₃ receptors on many petrosal neurons encountered in this study can explain several observations on chemosensory responses from the mammalian carotid body, if the afferent terminals express similar receptors to those on the cell body. For example, extracellular recording methods have demonstrated that application of exogenous 5-HT to the carotid body evoked repetitive firing in the carotid sinus nerve, by pathways presumed to involve activation of 5-HT₃ receptors on the sensory nerve endings (Nishi, 1975; Kirby and McQueen, 1984; Yoshioka, 1989). It is likely that our preparation includes carotid body chemoafferent neurons since we have recently demonstrated that at least a subpopulation of these neurons can form *de novo* functional (chemosensory) connections with type 1 cells in co-culture, where hypoxic signaling appears to be mediated in part by acetylcholine (ACh) release from type 1 cells onto petrosal neurons (Zhong et al., submitted). The present characterization of 5-HT receptors on petrosal neurons reveals properties expected of 5-HT₃

receptors described in other systems (Yakel and Jackson, 1988), including sensory (Higashi and Nishi, 1982; Robertson and Bevan, 1991; Fan and Weight, 1994) and sympathetic (Wallis and North, 1978; Yang, 1992) ganglia. It should be noted, however, that different subtypes of 5-HT₃ receptors exist (Jackson and Yakel, 1995).

Comparison with 5-HT receptors on type 1 cells

In contrast to petrosal neurons, the predominant 5-HT receptor found on type 1 cells was the 5-HT₂ subtype. Since type 1 cells constitute a major target group for petrosal chemoafferents, the presence of different receptor subtypes on pre- and post-synaptic elements attests to the difficulty of interpreting results based on 5-HT infusions into the carotid body *in situ* (Nishi, 1975; Kirby and McQueen, 1984; Yoshioko, 1989; McQueen and Evrard, 1990). In the present study, application of 5-HT to type 1 cells resulted in most cases in a transient membrane depolarization and occasional spike activity, and the effect was selectively blocked by the 5-HT₂ receptor blocker, ketanserin. This 5-HT response was associated with a conductance *decrease*, and was due to the closure of K⁺ channels since the response reversed direction near the potassium equilibrium potential (E_K). Under voltage clamp, 5-HT suppressed an outward K⁺ current even in the presence of Ca²⁺-free extracellular medium, suggesting that Ca²⁺-dependent K⁺ channels were not involved. This is in contrast to the effects of acute hypoxia, which closes Ca²⁺-dependent K⁺ channels in these cells as part of the transduction mechanism (Peers, 1990; Wyatt and Peers, 1995). The effects of 5-HT on the voltage dependent K⁺ current are likely mediated via the G-protein phosphoinositide

pathway, as is generally the case for 5-HT₂ receptors (Hoyer et al., 1994). Indeed, in the present study it was found that an activator of PKC (i.e. OAG, 50 μM) also suppressed outward K⁺ current in type 1 cells, similar to 5-HT.

Physiological significance of 5-HT in the carotid body

This study is the first attempt to characterize directly the 5-HT receptor subtypes present on the pre- and post-synaptic elements of the chemosensory carotid body. The chemoreceptors or type 1 cells are known to synthesize and release 5-HT (Gronblad et al., 1983; Fishman et al., 1985; Abramovici et al., 1991; Oomori et al., 1994), and results of extracellular recording from the CSN suggested the excitatory response of 5-HT is due to its direct action on sensory nerve endings (Kirby and McQueen, 1984). Since previous studies indicated that 5-HT₃ receptors expressed on the parent cell bodies of sensory afferent neurons are similar to receptors on their nerve terminals (Higashi and Nishi, 1982), it is likely the receptors we have characterized mediate the transient chemoexcitatory responses observed *in situ* during perfusion or infusion of 5-HT₃ agonists (Nishi, 1975; Sapru and Krieger, 1977; Kirby and McQueen, 1984). On the other hand, our observation that 5-HT₂ receptors are located predominantly on type 1 cells, provides a plausible explanation for the observed delayed chemoexcitation induced by 5-HT in the cat carotid body (Kirby and McQueen, 1984). Although the exact physiological role of 5-HT in synaptic transmission between type 1 cells and afferent nerve endings *in vivo* is unclear, the observed suppression of a Ca²⁺-*independent* outward K⁺ current in type 1 cells, due to 5-HT action on endogenous 5-HT₂

receptors, raises an interesting possibility in the rat carotid body. Conceivably, 5-HT released by hypoxia following closure of O₂-sensitive *Ca*²⁺-*dependent* K⁺ channels (Peers, 1990), could in turn facilitate secretion from type 1 cells by a positive feedback loop, where its action on 5-HT₂ autoreceptors might enhance membrane depolarization of type 1 cells.

CHAPTER 5

Characterization of GABA_A Receptors in Isolated

Rat Petrosal Sensory Neurons *in vitro*

Manuscript in preparation. Order of authors will be: H. Zhong, M. Zhang and

C. A. Nurse.

1. I maintained cell cultures; Cathy Vollmer prepared most (~95%) of the cultures.
2. For this study electrophysiological experiments and data collection were done jointly with Dr. M. Zhang. My contribution was ~ 50%.
3. I performed all data analysis and generated all figures in text.

ABSTRACT

1. Sensitivity to γ -aminobutyric acid (GABA) was examined in dissociated rat petrosal sensory neurons *in vitro*, using conventional whole-cell and perforated patch-clamp techniques. In response to GABA applied by fast perfusion or from a "puffer" pipette (50-1000 μ M), \sim 84% of petrosal sensory neurons (n=90) showed a rapid depolarization associated with an increase in membrane conductance.

2. The GABA-induced depolarization was mediated by GABA_A receptor since it was mimicked by GABA_A receptor agonist (muscimol, 50 μ M) and blocked by the specific GABA_A receptor antagonist (bicuculline; 100 μ M). Further, it was unaffected by the GABA_B receptor antagonist (phaclofen; 100 μ M), and there was no response to application of the GABA_B receptor agonist (baclofen; 1mM).

3. The mean (\pm S.E.M.) reversal potential of the GABA response (E_{GABA}) was -30.4 ± 3.5 mV (n=8) and was dependent on extracellular Cl⁻ ($[\text{Cl}^-]_o$) but not the extracellular Na⁺ ($[\text{Na}^+]_o$). The intracellular Cl⁻ ($[\text{Cl}^-]_i$), estimated from the Nernst equation, was 36.2 ± 4.3 mM assuming that the GABA responses were mediated purely by Cl⁻ channels (GABA_A receptors).

4. Application of GABA (10^{-7} to 10^{-3}) to the cell body produced a dose-dependent response; the amplitude of the response versus GABA concentration was fitted by the Hill equation with

$EC_{50}=11.5\mu\text{M}$ and Hill coefficient=1.1 (n=6).

5. Fluctuation analysis of GABA-induced current under voltage-clamp yielded an apparent single-channel conductance of 11.7 ± 3.4 pS at -70 mV (n=5). Spectral analysis of current response to GABA showed that power spectra could be fitted by a single Lorentzian curve and the mean open time constant of the GABA_A receptor channel was 16.1 ± 3.4 ms (n=3).
6. In the majority (95%) of cells (n=66), the GABA-induced depolarization did not trigger action potentials. However, GABA inhibited spike activity evoked by depolarizing current pulses in 8 out of 10 neurons tested. Thus, in petrosal neurons GABA inhibition may result in suppression of excitatory inputs by a shunting mechanism.

INTRODUCTION

GABA is a well known inhibitory neurotransmitter in both the central and peripheral nervous system (Hille, 1992), though recent reports indicate that at early developmental stages it may be excitatory (Serafini et al., 1995; Chen et al., 1996). In a number of studies, GABA-induced depolarizing potentials have been observed in both immature (Obata, 1974; Serafini et al., 1995) and adult (Deschenes et al., 1976; Taube, 1993) neurons. In primary afferent neurons, a GABA-induced depolarization has been reported and the effect is blocked by the GABA_A receptor antagonist, bicuculline, and is accompanied by an increase in membrane conductance (Obata, 1974; Gallagher et al., 1978). The depolarization induced by GABA is known to be Cl⁻ dependent and mediated by GABA_A receptors (Gallagher et al., 1978; MacDonald and Olsen, 1994), though it is unclear whether the effect is inhibitory or

excitatory in sensory neurons.

Immunohistochemical evidence suggests GABA is colocalized with catecholamines and serotonin in almost all chemoreceptor (glomus) cells of the mouse carotid body (Oomori et al., 1994), a major target for visceral sensory neurons of the petrosal ganglia. GABA sensitivity has been noted in neurons of other sensory ganglia, including dorsal root ganglia (DRG; Obata, 1974; Gallagher et al., 1978), and nodose ganglia (Wallis et al., 1982; Ashworth-Preece et al., 1997). Since, the petrosal ganglion derives from a similar embryonic region, i.e. the ectodermal placode, as the nodose ganglion and innervates a group of chemosensory target cells that contain GABA, it is possible that GABA released during chemosensory stimulation could influence firing of these afferent neurons. Since the discharge of petrosal (carotid body) afferents in turn influences respiratory drive, whether the effect of GABA are excitatory or inhibitory have important physiological consequences. Therefore, in the present study we examined the effects of GABA on isolated rat petrosal neurons *in vitro*, using whole cell recording. We avoided conventional whole cell methods since a serious complication can arise due to alteration of the intracellular chloride concentration ($[Cl^-]_i$) by chloride diffusion from and into the electrode, given that the polarity of the response to GABA is determined by $[Cl^-]_i$ (see above). To resolve this problem, we used gramicidin-perforated patch recordings because the permeability of chloride through the gramicidin-formed pores is negligible (Myers and Haydon, 1972; Ebihara et al., 1995). This method gives a relatively accurate measurement of the intact GABA-gated chloride reversal potential and an estimate of the intracellular chloride concentration. We found that GABA_A receptors were

present on the majority of rat petrosal neurons, and their effects were largely inhibitory.

METHODS

Cell culture

Dissociated cells from petrosal ganglia were obtained from 2-14-day-old rat pups (Wistar, Charles River, Quebec) as previously described (Stea and Nurse, 1992). Briefly, petrosal ganglia were enzymatically and mechanically dissociated to yield a cell suspension, and plated onto a thin layer of Matrigel (Collaborative Research, Bedford, MA) that was previously applied to the central wells of 35-mm tissue-culture dishes. Cultures were grown at 37° C in a humidified atmosphere of 95% air-5% CO₂ for 4 hr to 14 days before they were used in the perforated-patch-clamp/whole-cell experiments. The growth medium was changed every 4-6 days.

Solutions and drugs

Most experiments were performed using extracellular fluid (ECF) of the following composition (mM): Na gluconate, 24; NaCl, 111; KCl, 5; CaCl₂, 2; MgCl₂, 1; glucose, 10; N-2-hydroxyethylpiperazine-N'-2-ethane sulphonic acid (HEPES), 10 at pH 7.4 ; in some cases, NaCl, 111; KCl, 5; CaCl₂, 2; MgCl₂, 1; glucose, 10; NaHCO₃, 24, bubbled with 5% CO₂ at pH 7.4 was used. In some experiments NaCl was substituted by TrisCl, CholineCl or Na Gluconate. The stock pipette solution or intracellular fluid (ICF) for perforated-patch recordings contained (mM): K gluconate, 105; KCl, 35; CaCl₂, 1; HEPES, 10 and gramicidin (or nystatin; 30 or 300 µg/ml), at pH 7.2. The pore-forming antibiotics (gramicidin or

nystatin) were dissolved in dimethylsulfoxide (DMSO 30 mg/ml), vortexed for ~30 s, sonicated for 5 min and kept as a stock solution at -20°C for one week. For each experiment, the antibiotic-DMSO solution was added to the electrode solution (ICF) to give a final concentration of 30 or 300 $\mu\text{g/ml}$ for gramicidin and nystatin respectively. Before filling with antibiotic solution, the tip of the electrode was always loaded with a small volume of antibiotic-free ICF in order to avoid interference of the antibiotic with seal formation (Myers and Haydon, 1972; Ebihara et al., 1995).

Drugs or reagents

Bicuculline, muscimol, baclofen, and phaclofen were obtained from Research Biochemicals Inc. (RBI; Natick, MA). Tetrodotoxin (TTX), tetraethylammonium (TEA), gramicidin, and nystatin were obtained from Sigma Chemical Co. (St. Louis, MO).

Application of GABA and antagonists

GABA was freshly prepared in a 10 mM stock solution in ECF and then diluted to its final concentration in appropriate solutions just before application. GABA or agonists were applied to petrosal cell bodies in one of three ways. In most experiments GABA (0.1-1 mM) was delivered by pressure ejection from a pipette diameter $\sim 30\ \mu\text{m}$, positioned 20-40 μm from the neuronal surface. This procedure permitted fast application of the agonist at a low pressure (4-8 psi; 50-200 ms). In experiments designed to vary GABA concentrations and maximize speed of application, double-barreled pipettes were used. One of the pipettes contained a variable concentration of GABA and the other contained ECF. Fast exchange

between the pipettes, aided by an electromechanical switch, allowed the dose-response relation to be studied. The peak response amplitude elicited by the test concentration was compared with that elicited by 100 μM GABA, and the ratio plotted versus the test concentration. With this method, all dose-responses were normalized to 100 μM GABA, a concentration that elicited the maximum response. To study the elementary event using fluctuation analysis, a low concentration of GABA (2 μM) was applied by conventional bath perfusion to permit slow activation of the receptors with minimal desensitization. Antagonists were also applied by conventional bath perfusion under gravity.

Whole-cell recording

Procedures for whole-cell recording were similar to those described in detail elsewhere (Stea and Nurse, 1991a, 1992;). Patch pipettes were fabricated from Corning 7052 glass (1.5 mm O.D.) pulled in a Flaming/Brown horizontal puller (Sutter Instrument Co., Novato, CA). The pipettes were fire-polished and their resistance varied between 2-10 $\text{M}\Omega$. In some experiments, gramicidin perforated-patch recording was used as described elsewhere (Ebihara et al., 1995). Junction potentials were cancelled at the beginning of the experiment and series resistance (typically 10-20 $\text{M}\Omega$) was compensated (~ 80%) in most experiments. The temperature of the recording solutions was $\sim 34 \pm 2^\circ\text{C}$. Whole-cell currents or membrane potentials were recorded with an Axopatch 1D patch clamp amplifier and a Digitata 1200 A-D converter (Axon Instruments Inc., Foster City, CA), and stored on a 486 personal computer. Current and voltage clamp protocols, data acquisition and analysis were performed

using pCLAMP software (version 5.5., and 6.0.2, Axon Instruments Inc.).

Current fluctuations induced by GABA under whole-cell voltage clamp were analyzed as described elsewhere (Ishida and Cohen, 1988). GABA-induced currents were sampled at 0.5~1 kHz and stored in a computer before analysis.

Data analysis

Sigma Plot was used to fit the dose response to the Hill equation. The Hill slope (n) and half-maximal activation (EC_{50}) were adjusted for best fit of the curve to the observed data, and the least-squares differential was used to obtain the best fit. The apparent single-channel conductance was estimated from the relation of the current noise and mean current (Neher and Stevens, 1977). A fast Fourier transform routine which yields a spectral function, $S(f)$, was used to estimate spectral densities for GABA-induced fluctuation. An averaged control spectrum of background noise taken immediately before application of GABA was subtracted to remove background contributions from non-receptor membrane currents and electronic noise (Ishida and Cohen, 1988; Serafini et al., 1995). A single Lorentzian curve was used to fit the spectrum and the cut-off frequency and single channel open time constant were calculated (Anderson and Stevens, 1973; Ishida and Cohen, 1988). Most of the results are represented in the text as mean \pm standard error of the mean (S.E.M.).

RESULTS

1. GABA responses in petrosal neurons

In response to GABA applied from a "puff" pipette or by fast perfusion (50 μ M), ~84% of petrosal neurons (n=90) showed a rapid depolarization from a resting membrane potential of ~ -60 mV. The depolarization was associated with increase in membrane conductance, as indicated by application of brief hyperpolarizing current pulses (Fig. 1A), and was observed under both recording conditions, i.e. gramicidin/nystatin perforated-patch and conventional whole-cell recording. Since conventional whole-cell and nystatin-perforated patch recordings perturb intracellular chloride (see Introduction), most experiments were performed using the gramicidin perforated-patch method, where the access resistance displays negligible chloride permeability (Hladky and Haydon, 1984). With the gramicidin method the series resistance decreased to ~20 M Ω over 20-35 min, compared to 10-25min for nystatin. Under voltage clamp at -70 mV, GABA induced an inward current in petrosal neurons as shown in Figure 1B.

2. GABA responses exhibit GABA_A receptor pharmacology

The GABA-induced depolarization was reversibly blocked by the GABA_A receptor antagonist (bicuculline). In figure 2A, application of GABA from a "puff" pipette (0.1 mM at arrow), elicited membrane depolarization (upper trace), that was blocked by the GABA_A receptor antagonist (bicuculline; 0.1 mM) in the bath (middle trace) and the effect was reversible (lower trace). The GABA response could be also mimicked by the GABA_A receptor

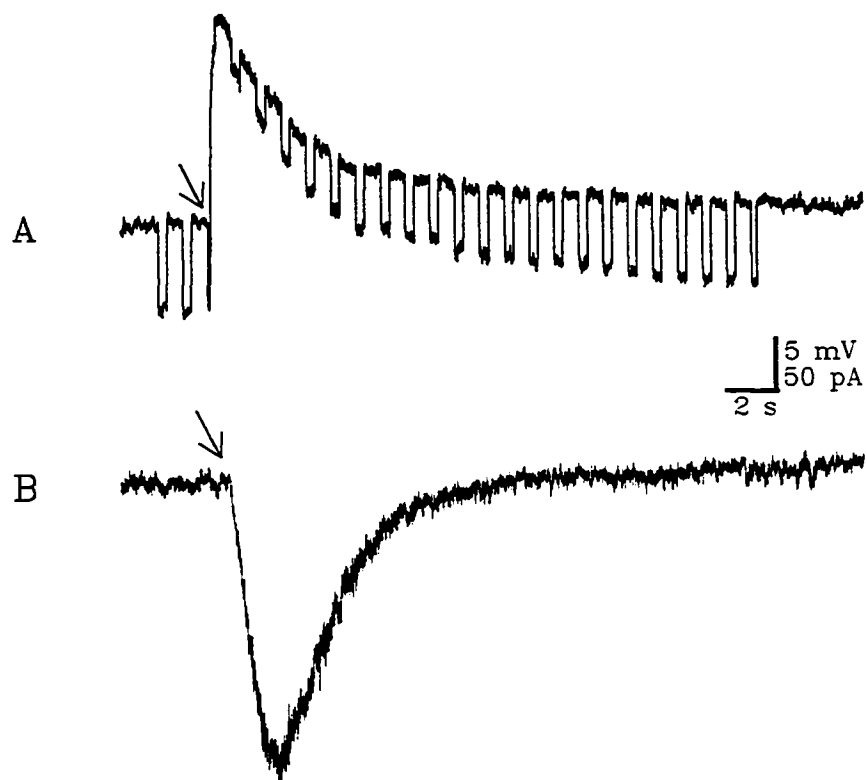


Figure 1. Effects of GABA on petrosal sensory neurons *in vitro*.

A. Under current-clamp a 'puff' of GABA (1 mM applied at the arrow) delivered by pressure ejection from a 'puffer' pipette, evoked membrane depolarization with a conductance increase, indicated by passing constant hyperpolarizing current pulses (downward deflections). Resting potential was -70 mV. B. Under voltage-clamp (-70 mV), a 'puff' of GABA (1mM, at arrow) induced a rapid inward current in this petrosal neuron. Vertical calibration bar represents 5 mV for A and 50 pA for B respectively.

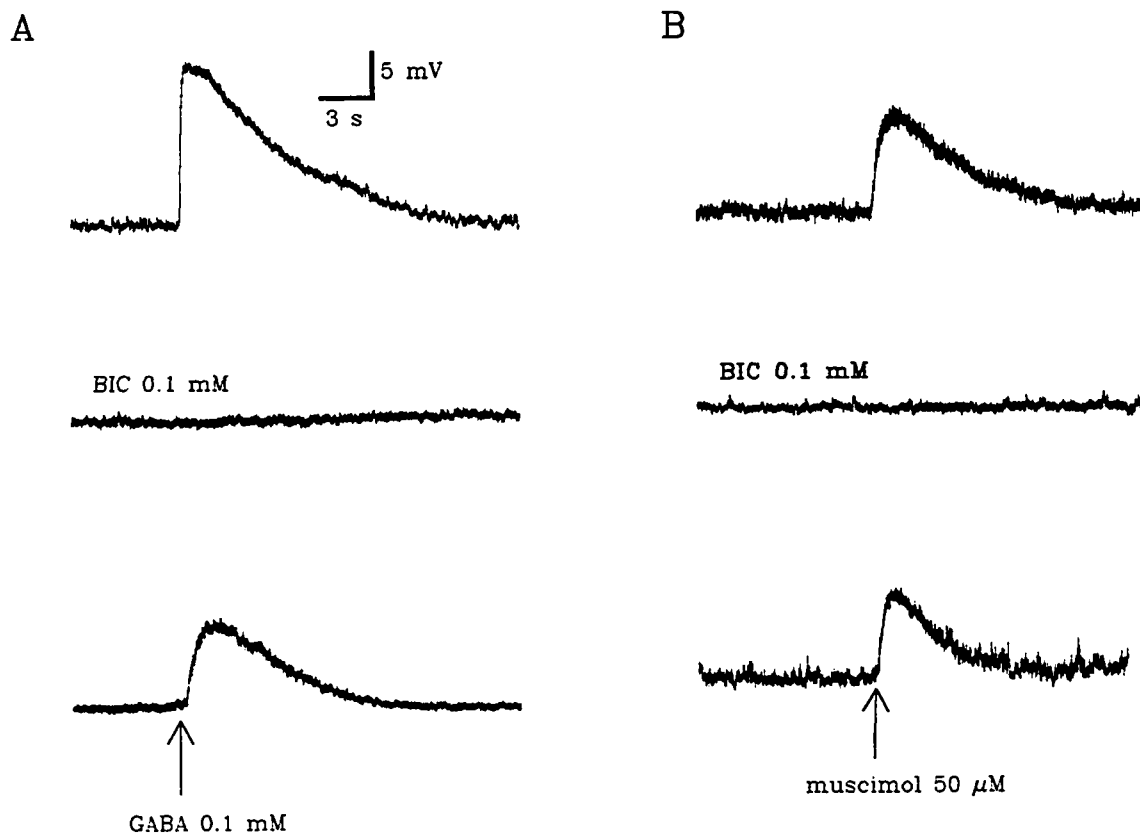


Figure 2. GABA_A receptors mediate depolarization in cultured petrosal neurons. **A.** Application of a 'puff' of GABA (0.1 mM applied at arrow) elicited membrane depolarization (upper trace) from resting potential of ~ 70mV. With GABA_A receptor antagonist (bicuculline; 0.1mM) in the bath, the effect of GABA was blocked (middle trace). After washing out the drug, the cell was once again responsive to GABA (lower trace). **B.** Using same procedure as in A, application of a 'puff' of GABA_A receptor agonist (muscimol; 50 μM at arrow) mimicked the response of GABA (upper trace), and again the response was reversibly blocked by bicuculline (lower two traces).

agonist (muscimol; 50 μM) and again, the effect was reversibly blocked by bicuculline (Fig. 2B). Baclofen, a GABA_B receptor agonist (1mM, a "puff" pipette), had no detectable effect on petrosal neurons, and phaclofen, a GABA_B receptor antagonist (0.1 mM), had no effect on the GABA-induced response (not shown). These results indicate that the GABA-induced depolarization was mediated by GABA_A receptors, which are known to regulate a chloride selective ion channel (MacDonald and Olsen, 1994).

3. The reversal potential of GABA-induced response

The reversal potential of GABA (E_{GABA}) was estimated from the relationship between amplitude of GABA-induced response and the membrane potential, using gramicidin perforated-patch recording. To minimize the activation of voltage-gated conductances by depolarization, Na⁺ and K⁺ -channels were blocked by the addition of TTX and TEA respectively to the ECF. It was found that the amplitude of the GABA-induced responses increased on hyperpolarization, but decreased and then reversed on depolarization. The results from one of the experiments is shown in Fig. 3A. B., where the GABA response reversed direction at ~ -30 mV. The apparent E_{GABA} was $\sim -30.4 \pm 3.5$ mV (n=8) and this value is similar to that for other systems (Obata, 1974).

Altering the Na⁺ concentration in ECF by substitution of Na⁺ with choline or Tris did not alter the GABA response amplitude or shift E_{GABA} , suggesting a Na⁺ conductance was not involved (n=3, not shown). Decreasing extracellular Cl⁻ from 112 to 60 mM, by substituting Cl⁻ with gluconate in the ECF, caused an increase in the amplitude of the GABA-induced

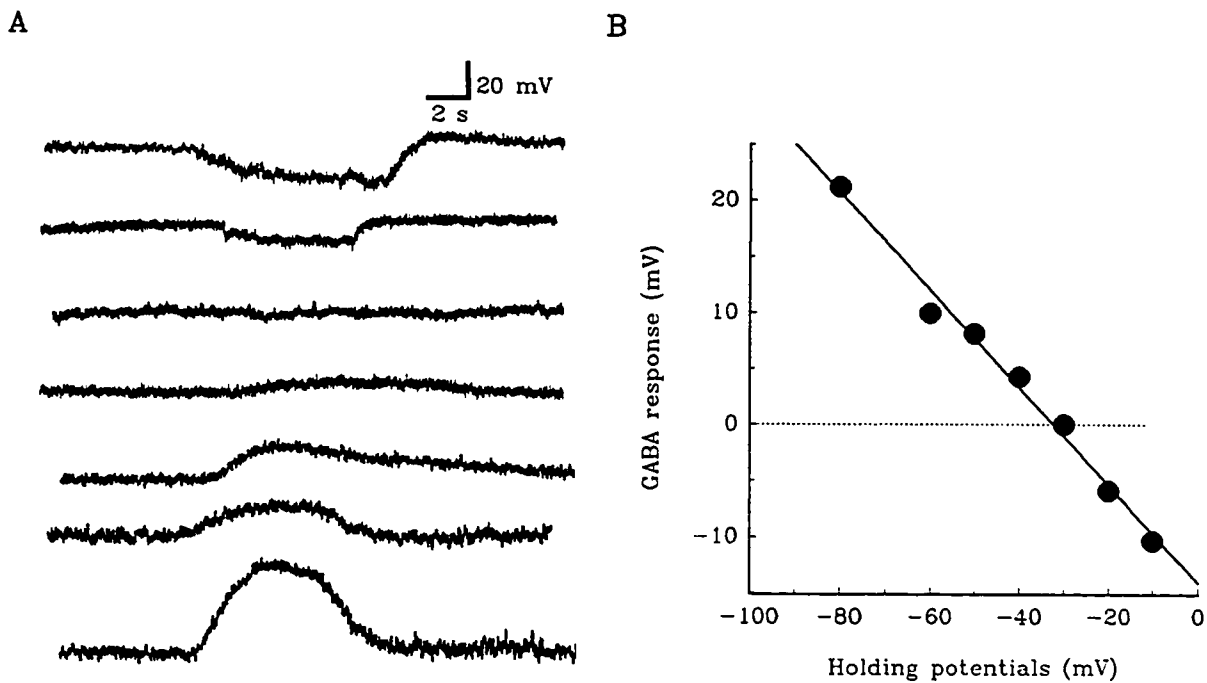


Figure 3. The reversal potential of GABA_A receptor channels in a petrosal neuron.

A. Application of GABA (0.1 mM, by fast perfusion) to a petrosal neuron held at different initial membrane potentials (-80, -60, -50, -40, -30, -20, and -10 mV; from bottom to top trace) evoked (voltage) responses under current-clamp. **B.** Peak amplitude of each response is plotted vs initial holding potential for this cell. The relationship of the amplitude of response vs membrane potential was used to estimate the reversal potential of the GABA_A receptor-channel. For this cell, the reversal potential was ~ -30 mV.

depolarization ($n=3$, not shown) that is in agreement with the prediction of the Nernst equation assuming Cl^- selectivity. Substitution of HEPES-buffered ECF with $\text{HCO}_3^-/\text{CO}_2$ -buffered ECF did not alter the GABA response amplitude suggesting HCO_3^- movement did not contribute more to the response as described in rat spinal motoneurons (Gao and Ziskind-Conhaim, 1995; see however, Kaila and Voipio, 1987).

Based on previous studies (Hille, 1992; MacDonald and Olsen, 1994), GABA_A receptor is almost a pure Cl^- permeable channel though HCO_3^- permeability has been reported (Kaila and Voipio, 1987). If so, in bicarbonate-free solutions E_{GABA} should be identical to the Cl^- equilibrium potential (E_{Cl^-}), providing that the intracellular Cl^- concentration ($[\text{Cl}^-]_i$) is not altered during gramicidin-perforated patch recording. The value of $[\text{Cl}^-]_i$ can then be estimated from the following Nernst equation :

$$E_{\text{Cl}^-} = (RT/ZF) * \ln\{[\text{Cl}^-]_o/[\text{Cl}^-]_i\}$$

where R is the gas constant, T is the absolute temperature, Z is the valence of the ion (-1 for Cl^-), and F is Faraday's constant (Hill, 1992). The apparent $[\text{Cl}^-]_i$ estimated from the equation is 36.2 ± 4.3 mM which is comparable with that observed in other neurons (Reichling et al., 1994; Rohrbough and Spitzer, 1996).

4. Dose-response relation

GABA-induced responses increased in a sigmoidal manner with GABA concentration over the range 0.1 to 1000 μM . The response evoked by 1000 μM GABA activated faster than that by lower GABA concentrations. To obtain the dose-response curve, the peak

response at each GABA concentration was normalized to the response elicited by 100 μM . The pooled results were plotted as a function of [GABA] and the complete dose-response curve was described by the Hill equation :

$$P/P_{\max} = 1/(1+(EC_{50}/[GABA])^n)$$

where P is the measured peak response , P_{\max} is the response elicited by 100 μM GABA, n is the Hill slope, and EC_{50} is the concentration of GABA required for half-maximal activation. The EC_{50} for GABA_A receptor activation in petrosal neurons was 11.5 μM and the Hill slope was 1.1 (n=6); these values are similar to previous reports in other systems (EC_{50} =9.9, n= 1.6, Liu et al., 1996 in hippocampal neurons; EC_{50} =27, n=1.7, Feigenspan and Bormann, 1994 on rat retinal bipolar cells; EC_{50} =4, n=1.5, Bormann and Feigenspan, 1995). In Fig. 4, the closed circles represent data from 6 different cells and the solid curve was obtained from the Hill equation. The slope factor, n, for the steepness of the rise of the Hill curve is greater than unity, suggesting two or more agonist binding sites are required to activate each GABA receptor (see Gallagher et al., 1978).

5. Fluctuation analysis of the GABA_A receptor channel

5.1 Noise variance and single channel conductance

The apparent single-channel conductance of the GABA_A receptor channel was estimated using fluctuation analysis; this assumes that whole-cell currents arise from identical and independent channels (Ishida and Cohen, 1988; Zhou and Fain, 1995). To obtain a steady, nondesensitizing response suitable for noise analysis, a low concentration (2 μM) of GABA

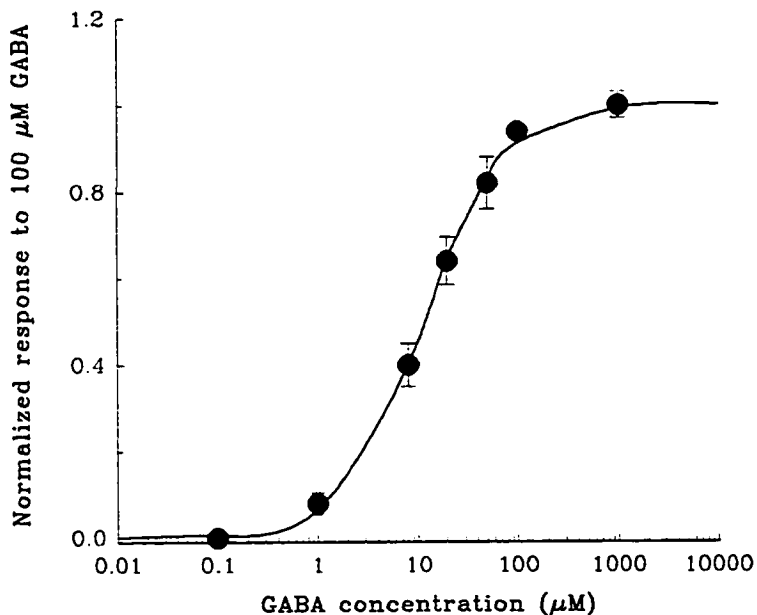


Figure 4. Dose-response relationship of GABA-evoked responses in petrosal neurons. Peak GABA-induced responses at different concentrations (0.1, 1, 10, 20, 40, 100, and 1000 μM) were normalized to the peak response amplitude elicited by applying 100 μM GABA in each cell (see text). Each data point is the mean (\pm S.E.M.) response from 6 different cells. The solid line is a fit of the normalized data to the Hill equation; with $EC_{50}=11$ μM and Hill coefficient = 1.1.

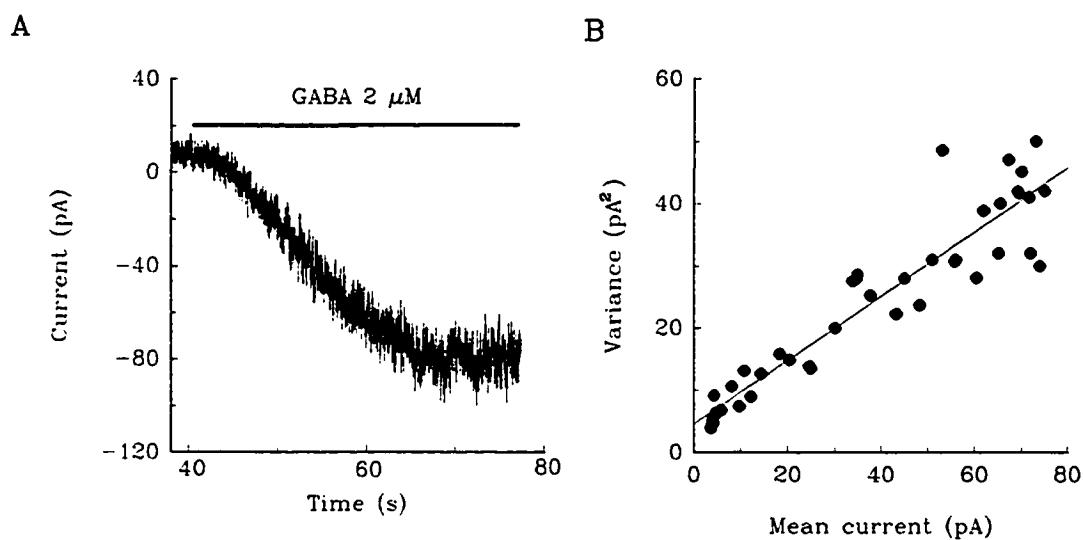


Figure 5. Estimation of the GABA_A receptor single-channel conductance from fluctuation analysis of the GABA-induced whole-cell current in a petrosal neuron. **A.** A typical section of a current trace used for fluctuation analysis; note increase in average whole-cell current response to bath application of GABA (horizontal bar, 2 μM), at a holding potential = -70 mV. An increase in current noise accompanies the increase in mean current during the response. **B.** The variance of current noise is plotted vs the mean current. The single channel conductance, estimated from the slope of the least-squares line fit, was ~11.2 pS for this cell.

was applied by bath perfusion. A typical response used for noise analysis is shown in Fig. 5A, where the rising phase of the response was accompanied by an increase in current noise. The variance of the current fluctuation increased linearly with the mean current and a plot of current variance versus mean current (Fig. 5B) was used to estimate the average single channel conductance, γ , according to the relationship:

$$\gamma = \delta^2 / \Delta I (V_h - V_{eq})$$

where the δ^2 is the GABA-induced variance, ΔI is the GABA-induced mean membrane current change, V_h is the holding potential, and V_{eq} is the reversal potential of GABA response, estimated as -30 mV (see Fig. 3). The mean (\pm S.E.M.) single-channel conductance obtained from the relationship was 11.7 ± 3.4 pS ($n=5$), a value comparable to other reports (McBurney and Barker, 1978; Hill, 1992).

5.2 Spectral analysis of GABA_A receptor channel open time constant

Noise analysis was carried out on records of I_{GABA} to obtain further information on channel characteristics. In the present study it appeared that GABA_A receptors in petrosal neurons desensitize though this property was not investigated. To minimize desensitization and maintain a steady membrane current for noise analysis we used moderate doses of GABA (2 μ M) and analyzed small membrane currents taken before significant desensitization had occurred. The properties of GABA-induced fluctuation in current noise were characterized by spectral densities. An example of I_{GABA} spectra analysis is illustrated in Fig. 6, where τ_{noise} of GABA_A receptor was 16.6 ms. A typical response used for noise analysis is shown in Fig.

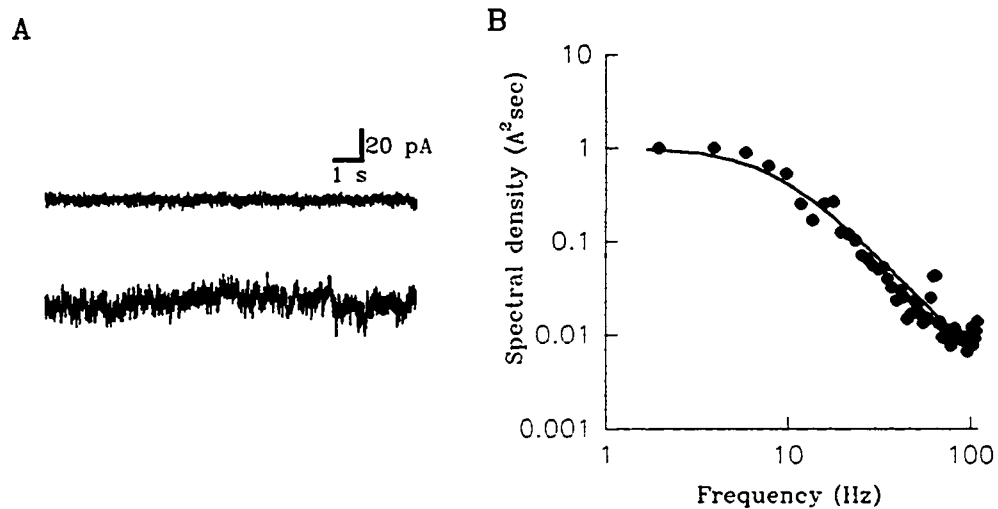


Figure 6. Power spectral density analysis of GABA-induced current noise in a petrosal neuron. **A.** The top trace shows an example of whole-cell current fluctuations recorded before the application of GABA. The lower trace shows an example of current fluctuations induced by the application of GABA ($2 \mu\text{M}$; at -70 mV) from the same cell; this response was used for power spectrum analysis in **B.** **B.** Spectral density was plotted against frequency on a double logarithmic scale. The points represent the difference between the control and GABA spectra in **A.** The line is a single Lorentzian component fitted by least squares to points with a cut-off frequency of 9.54 Hz . The estimated mean open time constant (τ_{noise}) was $\sim 16.6 \text{ ms}$.

6A. The spectra can be approximated by a Lorentzian function (Fig. 6B):

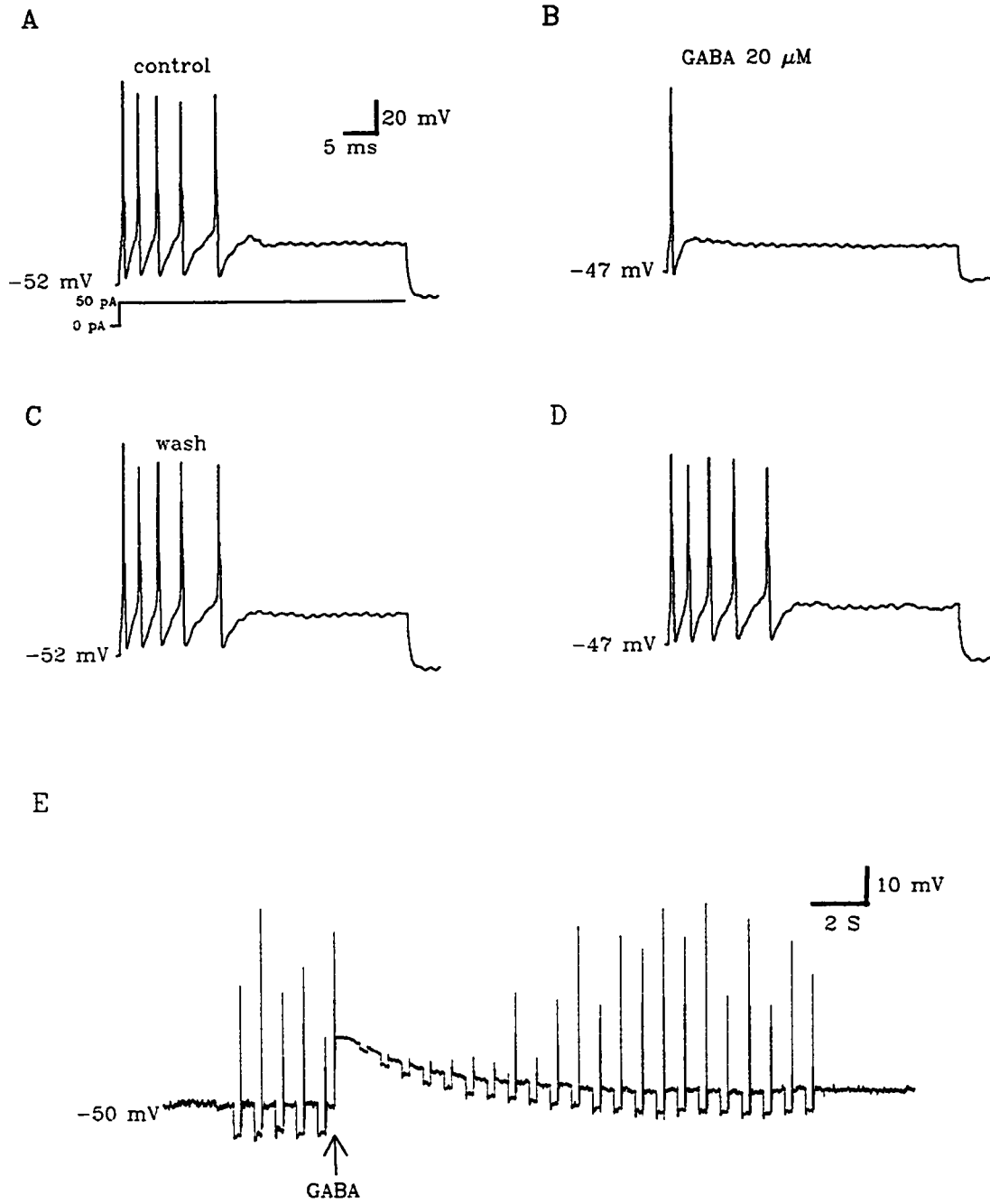
$$S(f) = S(0)/[1+(f/f_c)^2]$$

where $S(f)$ and $S(0)$ are power densities at the frequencies f and 0 Hz, respectively, and f_c is the cut-off frequency that corresponds to $S(f)=S(0)/2$ (Anderson and Stevens, 1973; Ishida and Cohen, 1988). Under specific assumptions for the operation of fast ligand gated channels, e.g. a simple model of channel operation details of which have been considered elsewhere (Kate and Miledi, 1971; Neher and Stevens, 1977), the open-state time constant of the channel, τ_{noise} , can be obtained from the cut-off frequency (f_c) of the spectra according to : $\tau_{\text{noise}}=1/(2\pi f_c)$. The mean open-state time constant of the GABA_A channel in petrosal neurons, τ_{noise} , obtained from spectral analysis, was 16.1 ± 3.4 ms ($n=3$), which is similar to reports in other systems (Feignspan et al., 1993; Ishida and Cohen, 1988, 30 ms; McBurney and Barker, 1978, 20 ms).

6. GABA-mediated inhibition

To test whether GABA could affect the excitability of petrosal neurons, a depolarizing current pulse was used to trigger action potentials before, during, and after perfusing GABA on to the neuron. As shown in figure 7A, a depolarizing current pulse (50 pA) triggered multiple spikes in an isolated petrosal neuron. With GABA (20 μ M) in the bath, the membrane potential depolarized by ~ 5 mV and only a single spike could be triggered by the same depolarizing stimulus (Fig.7B). The effects of GABA on spike activity was reversible (Fig.7C). To rule out the depolarization effect on the membrane excitability, we continuously

Figure 7. GABA reduces excitability of petrosal neurons. **A.** Under current-clamp, a long depolarizing current pulse (50 pA; 50 ms) triggered multiple action potentials. **B.** GABA (20 μ M) in the bath depolarized the membrane potential by \sim 5 mV and only single action potential could be triggered by the same depolarizing current pulse as in A. **C.** On washing out GABA, the control response recovered. **D.** The GABA-induced membrane depolarization was mimicked by artificially injecting a continuous current to depolarize the cell by \sim 5 mV. However, this artificial depolarization did not mimic the inhibitory effect of GABA, as the depolarizing current pulse still triggered multiple action potentials similar to A. **E.** Action potentials triggered by anode break excitation (after a hyperpolarizing current pulse; 20 pA, 30 ms) were suppressed by GABA-induced depolarization; as before this GABA-induced depolarization was accompanied by a conductance increase indicated by the downward deflections during the hyperpolarizing current pulses.



injected current to depolarize the cell by 5 mV, and then gave same depolarizing stimulus as before. This artificial depolarization did not mimic the inhibitory effect of GABA (Fig. 7D). Similar results were observed in 8 out of 10 petrosal neurons which favour the notion that GABA is inhibitory and the mechanisms underlying this inhibition may be due to the shunting of excitatory input (see Staley and Mody, 1992). To test whether GABA indeed inhibits the excitability of petrosal neurons, we triggered the anode break induced spikes after a long hyperpolarizing current pulse (20 pA, 30 ms). These spikes were also reversibly suppressed by GABA-induced depolarization (n=6; Fig. 7E).

DISCUSSION

These experiments demonstrate that rat petrosal neurons in culture depolarize during application of the inhibitory neurotransmitter GABA and this is due to opening of Cl⁻ selective GABA_A receptor channels. The depolarization responses to GABA are not unique to rat petrosal neurons. For example, a similar response occurs in CNS (Taube, 1993; Chen et al., 1996; Ashworth-Preece et al., 1997) and other sensory neurons (Obata, 1974; Gallagher et al., 1978). The ionic fluxes responsible for these depolarizing responses are not fully understood, though in many instances, it has been suggested that Cl⁻ is responsible for carrying the depolarizing GABA current (Misgeld et al., 1986). One hypothesis is that a concentration of ionic pumps results in a local reversal of the chloride gradient and so when GABA activates the receptor, chloride ions flow out of the cell resulting in a depolarization (Rohrbough and Spitzer, 1996).

Gramicidin perforated patch recording

The antibiotic perforated-patch recording technique has been used in a variety of cells since its introduction by Horn and Marty (1988). The pores formed by nystatin are permeable only to small monovalent cations and anions. Gramicidin shares some of these properties, but is distinguished by its lack of chloride permeability (Myers and Haydon, 1972). With gramicidin however, it took longer (relative to nystatin) to achieve perforation and this is probably related to the fact that two gramicidin molecules, forming a head-to-head dimer, are required for formation of a functional channel (Hladky and Haydon, 1984). Nystatin, on the other hand, is able to form cation-selective channels in its monomeric form, thus achieving faster perforation (Kleinberg and Finkelstein, 1984). Since gramicidin-formed pores lack significant chloride permeability an estimate of $[Cl^-]_i$, ~ 36 mM, was obtained for petrosal neurons in this study, assuming a Cl^- selective channel, for which the reversal potential is identical to E_{Cl^-} .

Depolarization-induced inhibition

A mechanism suggested by the present results may serve as the basis of GABA inhibition in these neurons. First, the depolarization response produced by GABA could inactivate voltage-dependent Na^+ channels and decrease excitability. Second, because the reversal potential of the GABA response is relatively near the resting potential, it could shunt part of the excitatory input. Finally, the depolarization produced by GABA may be sufficient

to activate the slowly and noninactivating potassium current that is present in chemosensory petrosal neurons (Stea and Nurse, 1992). These currents are activated by depolarization and result in an additional decrease in input resistance. As a consequence any subsequent EPSPs are less effective. Interestingly, an inhibitory effect of endogenous GABA on baroreceptor function appears to be mediated by the GABA_A receptor (Jordan et al., 1988).

Other possible functions

In addition to a possible role in synaptic inhibition in the carotid body, where it is colocalized to chemoreceptor cells (Gaiarsa et al., 1995). GABA could have a trophic function as well. Cherubini et al. (1991) have suggested that GABA-induced depolarization early in life is the primary source of *excitation* (see introduction) and could serve a trophic role by triggering a cascade of events leading to a rise in intracellular Ca²⁺. In addition, studies have shown that the survival and phenotype of petrosal neurons in early development are dependent on afferent activity (Katz and Black, 1986). At present, the precise neurochemical signals involved in the trophic support of these neurons are not completely understood. There is evidence that neurotrophic factors (NGF, BDNF) can regulate such processes (Conover et al., 1995), but it is possible that GABA_A receptors could still play a primary or supportive role.

CHAPTER 6

Synapse Formation and Hypoxic Signaling in Co-cultures of Rat Petrosal Neurons and Carotid Body Type 1 Cells

Submitted to *Journal of Physiology (London)*

Manuscript has been submitted for publication. Order of authors is:
H. Zhong, M. Zhang and C. A. Nurse.

1. I maintained cell cultures and prepared about 5 % of co-cultures; Cathy Vollmer prepared about 95% of co-cultures and carried out double-label immunofluorescence in Figure 1.
2. I performed about 90% of the electrophysiological experiments. The main observations that *de novo* chemical synapses form between petrosal neurons and glomus cells in co-culture and that acetylcholine mediates hypoxic signaling were made by me (see Zhong and Nurse, 1994). Dr. M. Zhang assisted in the design of the fast perfusion system for applying hypoxic solutions. He collaborated in the later stages, particularly in data collection that validated my initial observation that ACh was secreted in co-culture.
3. I performed all data analysis and generated all figures in text except figure 1.

ABSTRACT

1. To investigate synaptic mechanisms mediating chemosensory signaling in the carotid body, we developed co-cultures of chemoreceptor type 1 cell clusters and dissociated petrosal neurons (PN) from 7-14 day-old rat pups and tested for functional connectivity in $\text{CO}_2\text{-HCO}_3^-$ - or HEPES-buffered medium at $\sim 35^\circ\text{C}$.
2. When cultured without type 1 cells, PN were almost always quiescent ($n=104$) and unresponsive to hypoxia ($\text{Po}_2 \sim 25$ mm Hg) during perforated-patch, whole-cell recordings of membrane potential or voltage-activated currents; in contrast, many PN (77/170) that were juxtaposed to type 1 cell clusters in co-culture displayed spontaneous activity, comprising spikes and subthreshold potentials (SSP) that resembled synaptic potentials.
3. Additional tests suggested that *de novo* chemical synapses developed between PN and type 1 cell clusters *in vitro*; for example, (i) the spontaneous activity was reversibly suppressed by substituting low calcium/ high magnesium in the bath; (ii) SSP had variable amplitudes, and persisted following action potential blockade with tetrodotoxin (TTX; $1\ \mu\text{M}$); (iii) the interval distribution between successive spontaneous events appeared random; and (iv) the frequency of spontaneous potentials was diminished (reversibly) by the nicotinic antagonist, hexamethonium ($100\ \mu\text{M}$), suggesting contributions from the spontaneous release of acetylcholine (ACh).

4. Many complexes of 'juxtaposed' PN and type 1 clusters were physiologically functional, since exposure to hypoxia caused a reversible depolarization and/or increased spike discharge in ~30% of such neurons (n= 140). The hypoxia-induced spike discharge persisted in presence of dopamine D₂-receptor blocker, spiperone (10-50 μM; n = 5); however, this discharge was reversibly inhibited by 100 -200 μM hexamethonium, suggesting it was mediated, at least in part, by ACh acting through nicotinic receptors.

5. The hypoxia-induced spike discharge and frequency of spontaneous potentials in co-cultured PN were reversibly suppressed when the buffer was switched from CO₂-HCO₃⁻ to HEPES (10 mM) at pH 7.4; further, 'functional' PN that displayed spontaneous activity and/or hypoxia-induced responses in co-culture were encountered more frequently in CO₂-HCO₃⁻ (≥40%) than in HEPES (≤26%) buffer.

6. We conclude that functional chemical synapses can develop *de novo* in cultures of carotid body type 1 cells and petrosal neurons and that ACh is likely an important excitatory neurotransmitter secreted from type 1 cells during hypoxic chemotransduction in the rat carotid body.

INTRODUCTION

The mammalian carotid body (CB) is a peripheral chemosensory organ which senses arterial

P_{O_2} , P_{CO_2} and pH, and signals, via the respiratory control center, reflex responses appropriate for the maintenance of blood homeostasis (Eyzaguirre & Zapata, 1984; Gonzalez, Almaraz, Obeso & Rigual, 1994). Thus, whole animal exposure to acute hypoxia results in a compensatory reflex hyperventilation, originating at O_2 -chemoreceptors in the CB and mediated via an increased afferent discharge in the carotid sinus nerve. Though the details of the transductive events remain controversial (Biscoe & Duchon, 1990; Lahiri, 1994; Gonzalez *et al.*, 1994; Montoro, Urena, Fernandez-Chacon, Alvarez de Toledo & Lopez-Barneo, 1996; Buckler, 1997), it is widely accepted that CB type 1 cells are the actual O_2 transducers. For instance, these cells depolarize and /or increase firing frequency during acute hypoxia (Lopez-Barneo, Lopez-Lopez, Urena & Gonzalez, 1988; Delpiano & Hescheler, 1989; Buckler & Vaughan-Jones, 1994), leading to the entry of extracellular calcium and enhanced catecholamine release (Buckler & Vaughan-Jones, 1994; Montoro *et al.*, 1996). These responses appear to be initiated or facilitated by the closure of various K^+ channels during hypoxia, a property observed in type 1 cells from different species (Lopez-Barneo *et al.* 1988; Delpiano & Hescheler, 1989; Peers, 1990; Stea & Nurse, 1991a; Buckler, 1997). Since type 1 cells form reciprocal chemical synapses with afferent terminals of second-order petrosal neurons (McDonald & Mitchell, 1975), relay of chemosensory information is presumed to occur via hypoxia-induced release of neurotransmitter(s) from type 1 cells onto petrosal terminals (Gonzalez *et al.* 1994).

Despite the attractive features of the above scheme, the neurotransmitter mechanisms that

operate during chemosensory signaling are poorly understood. Doubtless, the presence of multiple neurotransmitters or neuromodulators in type 1 cells, including biogenic amines, acetylcholine and neuropeptides, contribute to the complexity (Fidone, Gonzalez, Dinger & Hanson, 1988; Gonzalez *et al.*, 1994). Perhaps more significantly, it has proved difficult to obtain stable recordings from petrosal terminals *in situ* due to, their small size, poor visibility, and restricted access encountered during microelectrode recordings from intact CB (Hayashida, Koyano & Eyzaguirre, 1980). As a result, most studies of chemosensory transmission in the CB have relied on monitoring of afferent spike discharge in the carotid sinus nerve, at locations far away from the transductive and synaptic sites (see Eyzaguirre & Zapata, 1984; Gonzalez *et al.*, 1994); this necessarily limits understanding of the mechanisms underlying synaptic events (Katz, 1969).

In the present study we developed and tested a preparation aimed at understanding the synaptic mechanisms at CB chemoreceptor complexes, while circumventing some of the difficulties described above. Particularly, dissociated rat petrosal neurons and clusters of carotid body type 1 cells were allowed to grow in co-culture, with the expectation that *de novo* functional connections would develop between appropriate 'chemosensory' neurons and type 1 cell clusters. To circumvent difficulties associated with nerve terminal recordings and facilitate monitoring of subthreshold events, we used the perforated-patch, whole-cell technique to record mainly from neuronal cell bodies that were adjacent or juxtaposed to type 1 cell clusters. Interestingly, we obtained evidence that *de novo* chemical synapses developed

between some petrosal neurons (PN) and type 1 clusters; moreover, many chemosensory complexes were able to transduce a hypoxic stimulus and translate it into an increased action potential frequency in the apposed neuron. We also found that $\text{CO}_2\text{-HCO}_3^-$ was a more effective buffer than HEPES for the successful recording of these events.

METHODS

Cell culture

Dissociated cells were obtained from carotid bodies or petrosal ganglia of 7-14 day-old rat pups (Wistar, Charles River, Quebec) as previously described (Stea & Nurse, 1991a, 1992). The carotid bifurcation, with attached nodose/petrosal complex, was excised after pups were first rendered unconscious by a blow to the head, and killed immediately by decapitation. Since in the rat, chemoafferent neurons are located in the distal one-third to one-half of the petrosal ganglion (Katz & Black, 1986; Finley, Polak & Katz, 1992), we attempted to enrich for these during isolation by pulling on the glossopharyngeal (IXth) nerve, which joins the ganglion at the distal end. Following separation from the IXth nerve, the excised ganglia were exposed to a 0.1% trypsin/ 0.1% collagenase enzymatic solution for 1 hr at 37° C, and then mechanically dissociated with forceps. The dispersed cell suspension was collected and triturated in growth medium containing: F-12 nutrient medium (Gibco, Grand Island, NY) supplemented with 10% fetal bovine serum (Gibco), 80 U/l insulin (Sigma Chemical Co., St. Louis, MO), 0.6% glucose, 2 mM glutamine and 1% penicillin-streptomycin (Gibco). For petrosal (alone) cultures, this cell suspension was plated onto a thin layer of Matrigel

(Collaborative Research, Bedford, MA) that was previously applied to the central wells of modified tissue-culture dishes. For co-cultures, petrosal neurons were grown together with a major target, i.e. type 1 cells of the carotid body (CB). These co-cultures were obtained by first preparing cultures of dissociated rat CB as previously described (Nurse, 1987; 1990; Stea & Nurse, 1991a), and then adding an overlay of dissociated petrosal neurons 3-5 days later. All cultures were grown at 37°C in a humidified atmosphere of 95% air: 5% CO₂.

Electrophysiological recording and data analysis

Typically, patch clamp experiments were carried out on co-cultures 3-6 days after plating the neurons. Some experiments were performed using extracellular fluid (ECF) of the following composition (mM): NaCl, 115; NaHCO₃, 24; KCl, 5; CaCl₂, 2; MgCl₂, 1; glucose, 10; sucrose, 12 at pH 7.4, maintained by bubbling 5% CO₂, 95% air. In other experiments a HEPES-buffered ECF was used and contained (in mM): NaCl, 135; KCl, 5; CaCl₂, 2; MgCl₂, 1; glucose, 10; HEPES, 10 at pH 7.4. For perforated-patch recording, the pipette solution contained (mM): potassium gluconate, 105; KCl, 35; CaCl₂, 1; HEPES, 10 and nystatin 300 µg/ml at pH 7.2. All solutions were filtered through a 0.45 µm millipore filter before use. Unless indicated otherwise, drugs and reagents used in this study were obtained from Sigma.

To simulate hypoxia the CO₂-HCO₃⁻-buffered perfusion fluid was bubbled continuously with a gas mixture consisting of 95% N₂, 5% CO₂; for HEPES-buffered fluid the gas mixture contained 100% N₂. All solutions were added to the recording chamber by perfusion under gravity (~1 ml / min) and withdrawn by vacuum suction. Initially, the hypoxic ECF was

applied by conventional bath perfusion resulting in a relatively slow change in P_{O_2} of the bath. In later experiments, to maximize the speed of stimulus application a 'fast-perfusion' method, utilizing double-barreled pipettes (diameter $\sim 600 \mu\text{m}$ each) positioned within $300 \mu\text{m}$ of a type 1 cell cluster, was used. One barrel delivered hypoxic ECF ($P_{O_2} \sim 25 \text{ mm Hg}$), and the other normoxic ECF ($P_{O_2} \sim 160 \text{ mm Hg}$), at a flow rate of $\sim 1 \text{ ml / min}$, while the patch pipette monitored membrane potential in a 'juxtaposed' petrosal neuron. A piezo-electromechanical switch permitted a rapid change of the perfusate from one barrel to the other, resulting in a fast, local application of the hypoxic stimulus directly over the chemoreceptor cell cluster. All recordings were performed at $\sim 35^\circ\text{C}$. Drugs were applied by conventional gravity perfusion.

Procedures for perforated-patch, whole-cell recording were similar to those described in detail elsewhere (Stea & Nurse, 1991a,b; 1992). Patch pipettes were fabricated from Corning 7052 glass (1.5 mm O.D.) pulled with a Flaming/Brown horizontal puller (Sutter Instrument Co., Novato, CA). The pipettes were fire-polished and had resistances of 2-10 $\text{M}\Omega$. Approximately 75% of the series resistance, typically in the range 10-20 $\text{M}\Omega$, was compensated in voltage clamp experiments. The seal resistance between pipette and cell varied between 2 and 10 $\text{G}\Omega$. Junction potentials, in the range 2-10 mV, were canceled at the beginning of the experiment. Whole-cell currents or membrane potentials were recorded with an Axopatch 1D patch clamp amplifier, a Digidata 2000 A-D converter (Axon Instruments Inc., Foster City, CA), and stored on a 486 personal computer. Current and voltage clamp protocols, data acquisition and analysis were performed using pCLAMP software (version 5.7., and 6.0.2, Axon Instruments Inc.).

Fluorescence immunocytochemistry

Some co-cultures, and cultures of petrosal neurons alone, were processed for tyrosine hydroxylase or TH-immunoreactivity, a biochemical marker for both petrosal CB-chemoafferent neurons in the rat (Katz & Black, 1986; Finley *et al.*, 1992), and type 1 cells (see Nurse, 1990). This procedure provided a rough estimate of the frequency of 'appropriate' chemosensory neurons surviving in culture, and allowed a test in a few cases of whether a chemosensory neuron, identified electrophysiologically in co-culture by a positive response to hypoxia, also had the expected biochemical phenotype (i.e. TH-immunoreactivity). The procedures used for processing the cultures for TH-immunofluorescence were similar to those described previously (Nurse, 1990); the primary TH-antibody (rabbit; Chemicon, El Segundo, CA) was visualized with a fluorescein-conjugated goat anti-rabbit IgG (Cappel, Malvern, PA). To visualize processes (and cell bodies) of petrosal neurons, cultures were immunostained for neurofilament (NF 68 kD) protein, as described previously (Jackson & Nurse, 1995); the primary NF- antibody (mouse monoclonal; Boehringer Mannheim, Montreal, Quebec) was visualized with a Texas red-conjugated goat anti-mouse IgG (Jackson Immunoresearch Lab, Westgrove, PA). Thus, dual staining of a co-culture for both TH and NF 68kD allowed the relationship between type 1 cell clusters and petrosal processes to be visualized using two fluorochromes, fluorescein and Texas red respectively

RESULTS

Appearance of Co-cultures

The procedures used in this laboratory for the dissociation and culture of carotid body cells result in the long-term survival of small islands or clusters of 3-30 type 1 cells, surrounded by fibroblasts and sustentacular cells (Nurse, 1990; Stea & Nurse, 1991a; Jackson & Nurse, 1995). These clusters are easily identified in living cultures and confirmation that they consist mainly of type 1 cells has been routinely carried out using immunofluorescent staining for tyrosine hydroxylase (TH; Nurse, 1990; Jackson & Nurse, 1995). Addition of dissociated petrosal ganglia in co-culture produces oval, phase -bright, isolated neurons, the majority of which are found interspersed between type 1 clusters, though their processes tended to be obscured by the presence of proliferating background cells. These processes could be revealed by immunofluorescent staining (Texas red label) for neurofilament protein (NF 68kD) and, as shown in Fig. 1, when the procedure was combined with TH-immunofluorescence (fluorescein label), the processes appeared to form an intimate association with type 1 cell clusters. In these co-cultures, many petrosal neurons (PN) display a pseudo-unipolar morphology, illustrated by the NF-positive neuron in Fig. 1. Typically, a single process emanates from the cell body and after growing a short distance, it appears to bifurcate into two main branches before ramifying over the monolayer of carotid body cells. Interestingly, similar to type 1 cells, the PN in Fig. 1 was also positive for TH, i.e. an established phenotypic marker for rat carotid body chemoafferent neurons (Katz & Black, 1986; Finley *et al.*, 1992); coincidence of the red and green fluorescence accounts for the orange appearance of

Figure 1. Immunofluorescent staining of a co-culture of dissociated rat petrosal neurons and carotid body type 1 cells.

Culture was immunostained with tyrosine hydroxylase (TH) and neurofilament (NF 68 kD) antibodies and visualized with a fluorescein- and Texas red-conjugated secondary antibody respectively. The two type 1 cell clusters are TH- positive (cytoplasmic green fluorescence), and are intimately associated with NF- positive petrosal processes (red fluorescence); nuclei of type 1 cells in the clusters appear dark. The single petrosal cell body is both TH- and NF- positive, accounting for the yellow-orange fluorescence; note a NF-positive pseudounipolar process leaves the petrosal cell body and appears to bifurcate into two main branches, each which projects to a type 1 cell cluster. The petrosal neuron and type 1 cells were together for 8 days *in vitro*; scale bar represents 10 μm .



the PN cell body in Fig.1. In these co-cultures, some 60-65% of the neurons are TH-positive (Nurse, Vollmer & Zhong; unpublished observations), suggesting that our isolation procedures yield a favourable proportion of chemosensory neurons.

Effects of hypoxia on type 1 cells and petrosal neurons cultured separately

As expected, in several tests exposure of type 1 cells to acute hypoxia ($P_{O_2} = \sim 25$ mmHg) caused a reversible suppression in outward K^+ current under voltage clamp (e.g. Fig. 2A), and ~ 10 mV depolarization under current clamp (e.g. Fig. 2B). Application of brief hyperpolarizing current pulses before, during, and after the hypoxic stimulus in Fig. 2B, reveals that the depolarization is accompanied by a conductance *decrease* (by $\sim 10\%$) consistent with hypoxia closing a subset of ion channels that are open at the resting potential of ~ -50 mV (see Buckler, 1997). Though the actual mechanisms remain controversial, these results support the generally-accepted notion that type 1 cells are the actual O_2 -sensors in the carotid body (Gonzalez *et al.*, 1994). We therefore anticipated that isolated petrosal neurons (PN), cultured alone, would be unresponsive to hypoxia. This was generally the case for $>95\%$ PN ($n=104$) exposed to acute hypoxia. In a typical example, Fig. 2C, hypoxia ($P_{O_2} = \sim 25$ mm Hg) was without effect on voltage-activated outward (K^+) or inward (Na^+) currents in voltage clamp experiments (see also, Stea & Nurse, 1992); in addition, hypoxia also failed to affect the resting membrane potential or input conductance in almost all PN during current clamp recordings (e.g. Fig. 2D). Taken together, these results support the model where chemosensory signaling in the carotid body involves a transduction step in type 1 cells,

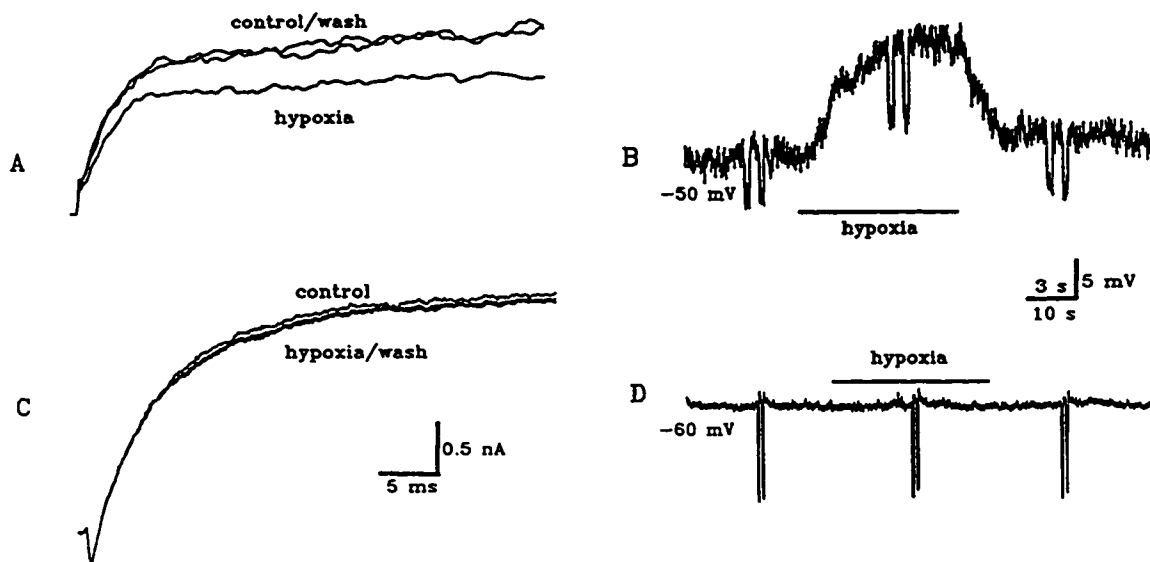


Figure 2. Comparison of the effects of hypoxia on carotid body type 1 cells and petrosal neurons cultured separately.

A. Under voltage clamp, hypoxia ($P_{O_2} \approx 25$ mm Hg) causes suppression of voltage-dependent outward K^+ current in a type 1 cell; voltage step (not shown) from -60 mV to $+50$ mV. B. Under current clamp, hypoxia depolarizes type 1 cell from a resting membrane potential of -50 mV; this depolarization is associated with a conductance *decrease* (by $\sim 10\%$), indicated by passing constant hyperpolarizing current pulses (downward deflections). Unlike type 1 cells, a similar hypoxic exposure had no effect on the outward K^+ current (Fig. C; voltage step from -60 mV to $+50$ mV) or membrane potential (Fig. D) recorded in a typical petrosal neuron (PN); input conductance in petrosal neurons was also unaffected by hypoxia (Fig. D; downward deflections).

followed by information transfer (presumably via chemical synapses) from type 1 cells to PN terminals. We next explored this possibility using co-cultures of PN and type 1 cells.

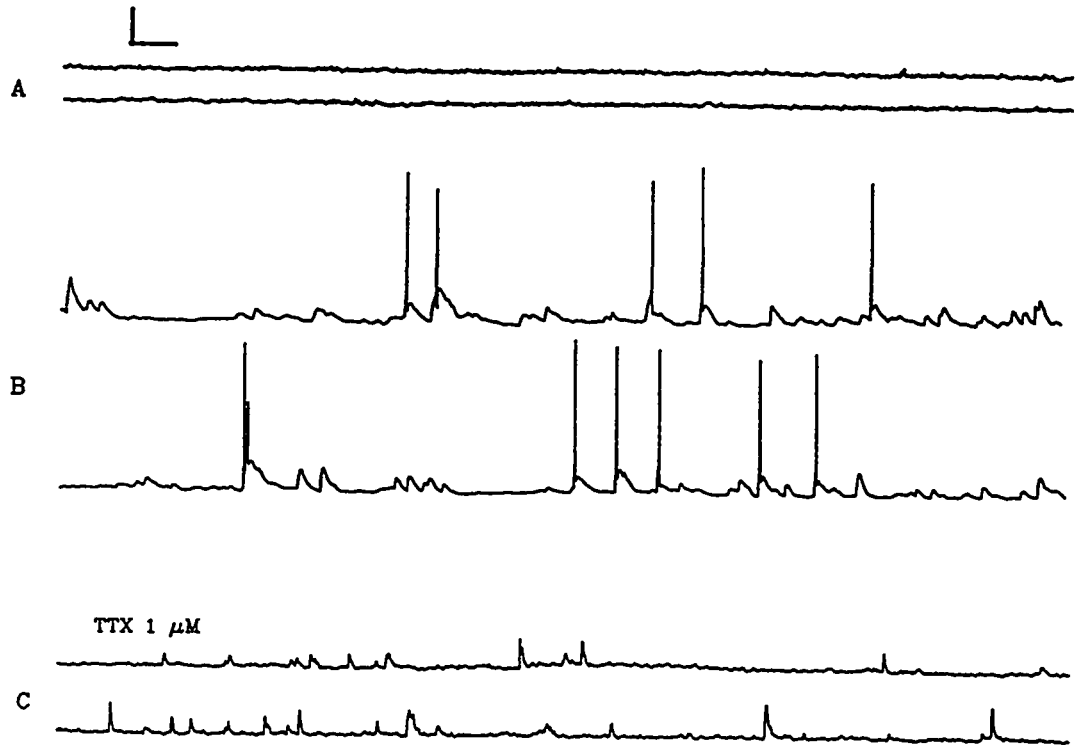
Evidence for *de novo* chemical synapses between type 1 cells and petrosal neurons in co-culture

Nystatin whole-cell recordings of membrane potential revealed that PN, cultured *without* type 1 cells, were largely quiescent (n= 104). An example is shown in the current clamp recording of Fig. 3A, where the membrane potential tended to remain steady over time and spontaneous activity was rare or absent. In contrast, similar recordings from PN in *co-culture* resulted in the frequent appearance (107 cases out of 269) of spontaneous potentials, comprising spikes and subthreshold potentials (e.g. Fig. 3B) that resembled spontaneous excitatory post synaptic potentials or e.p.s.p.'s seen at conventional chemical synapses (Katz, 1969). To facilitate recording of subthreshold potentials, and therefore obtain a better understanding of synaptic mechanisms, we selected for investigation neurons that were juxtaposed (within a few microns) to type 1 cell clusters. These were primarily neurons that fortuitously settled at the edge, or on top of a type 1 cell cluster after plating.

As shown in Fig. 3B, the spontaneous subthreshold potentials (SSP) in the PN had several expected features of e.p.s.p.'s including, the characteristic rapid rise-time followed by a slower decay, the ability to summate with another SSP occurring at roughly the same time, and the variability in peak amplitude sometimes being large enough to elicit action potentials. The duration of individual SSP varied from 30 to 260 ms, with a mean \pm SEM of 108.6 ± 29.2

Figure 3. Effects of co-culture on spontaneous membrane activity recorded with the perforated-patch technique from petrosal neurons.

A. Typical recording illustrating lack of spontaneous activity in a petrosal neuron (PN) cultured *without* type 1 cells; membrane potential, indicated by the two displaced continuous traces remained relatively steady over time. Note in Figs. A,B,C the right end of the top trace is continuous with the beginning (left end) of the lower trace. B. In *co-culture*, a typical PN that was juxtaposed to a type 1 cell cluster, showed spontaneous spikes and subthreshold potentials (two displaced traces), resembling e.p.s.p.'s seen at chemical synapses. C. Perfusion of tetrodotoxin (TTX; 1 μ M) to block action potentials, did not eliminate subthreshold spontaneous potentials (SSP) recorded in a different PN, juxtaposed to a type 1 cluster. Vertical scale bar (top left) represents 20 mV; horizontal bar represents 1 s in A, B and 1.5 s in C. The resting membrane potential was -65 mV in A, -60 mV in B, -70 mV in C.



ms (n = 245) ; the time-to-peak ranged from 12 to 88 ms, with a mean \pm SEM of 31.9 ± 1.2 ms (n= 245). As occurs at conventional chemical synapses (Katz, 1969), application of the sodium channel blocker, tetrodotoxin or TTX ($1 \mu\text{M}$; n= 4), eliminated spike activity, but SSP could still be detected (Fig. 3C).

In all cases tested (n=3), the spontaneous potentials seen in co-cultures were sensitive to manipulation of the extracellular divalent cation concentration. An example is shown in Fig. 4 A-C, where removal of extracellular calcium, combined with elevation of extracellular magnesium (10 mM), resulted in a reversible suppression of spontaneous activity. This suggests that the spontaneous activity originated at chemical synapses between type 1 cells and PN. Since the PN were added to a pre-existing monolayer containing type 1 cell clusters, such putative synapses could only have formed in culture *de novo*.

Sampling of a few neurons situated further away ($>100 \mu\text{m}$) from the nearest type 1 cell cluster revealed that spontaneous activity was sometimes seen, but this consisted only of propagating spikes (not shown; n =5), without the accompanying subthreshold events seen in Fig. 3B. We presume in these cases that any subthreshold potentials would have decayed electrotonically before reaching the recording electrode.

Amplitude and interval distribution of spontaneous subthreshold potentials

In a classical preparation, the skeletal neuromuscular junction, transmitter release is quantal and occurs in multiples of the basic unitary event or quantum (Katz, 1969). At central neuron-to- neuron synapses (see Stevens, 1993), and in the present study, the situation appears more

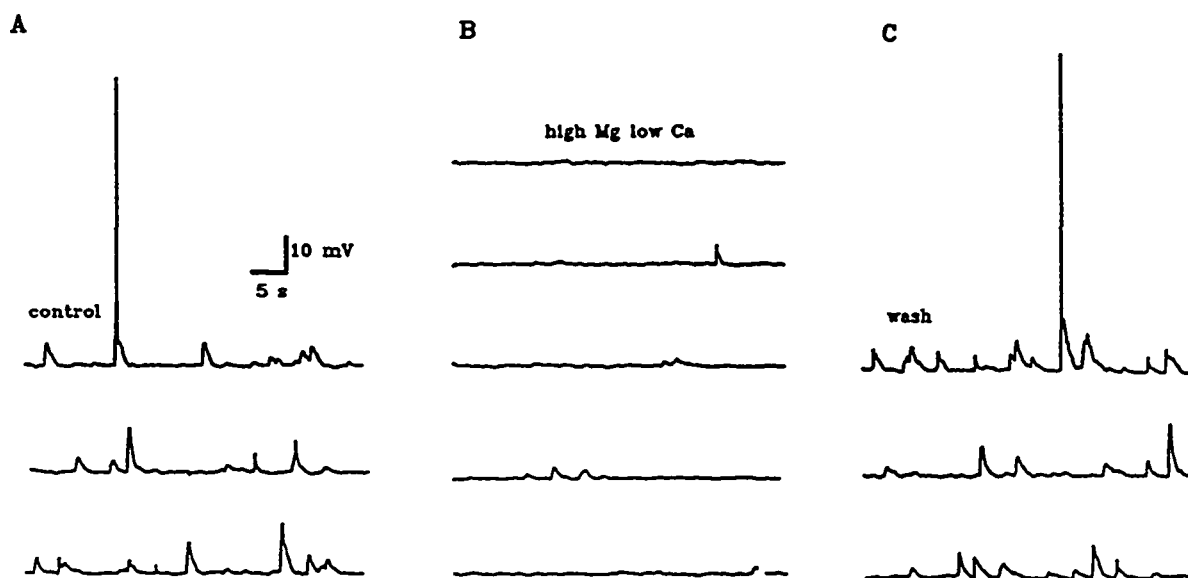


Figure 4. Effect of low calcium/ high magnesium on the spontaneous activity recorded in a co-cultured petrosal neuron.

Spontaneous activity recorded from a petrosal neuron (PN), juxtaposed to a type 1 cell cluster, in control extracellular solution containing 2 mM Ca^{2+} / 1mM Mg^{2+} (A; left), nominally 0 mM Ca^{2+} / 10 mM Mg^{2+} (B; middle), and following wash in control solution (C; right); note marked suppression of spontaneous activity in low Ca^{2+} , high Mg^{2+} . Vertical bar (top left) represents 10 mV; horizontal bar represents 5 sec in A-C. The resting membrane potential was -55 mV.

complicated because of the opportunity for a single neuronal process to branch and form synapses at spatially separate sites (see Fig. 1). This, together with the presence of multiple potential neurotransmitters in type 1 cells (Fidone *et al.* 1988; Gonzalez *et al.* 1994), prevented a rigorous analysis of spontaneous release. Nevertheless, it was of interest to compare the distribution of SSP in these cultures with that at known chemical synapses. Figure 5A shows an example of the amplitude distribution of SSP recorded in a PN (juxtaposed to a type 1 cell cluster) under control (normoxic) conditions; in this case there were few spontaneous action potentials. Unlike the classical neuromuscular junction where the spontaneous miniature potentials are normally distributed (Katz, 1969), the distribution in Fig. 5A is skewed to the right. Many of the SSP were clustered around a peak amplitude of 2-3 mV, both in the absence (Fig. 5A) and presence of TTX (not shown; see Fig. 3C).

We also tested whether the occurrence of the SSP was random, as in the case of the skeletal neuromuscular junction (Katz, 1969). Consistent with this interpretation, we found in a few cases (n=3) that the intervals between successive spontaneous events were well described by the exponential function:

$$n = N_T \Delta t / T_m \exp (-t / T_m),$$

where n = number of events separated by time interval t , N_T = total number of events, Δt = class interval, and T_m = mean time interval (Katz, 1969). An example based on the analysis of a segment from a continuous recording of spontaneous potentials in a PN (juxtaposed to a type 1 cell cluster) is shown in Fig. 5B.

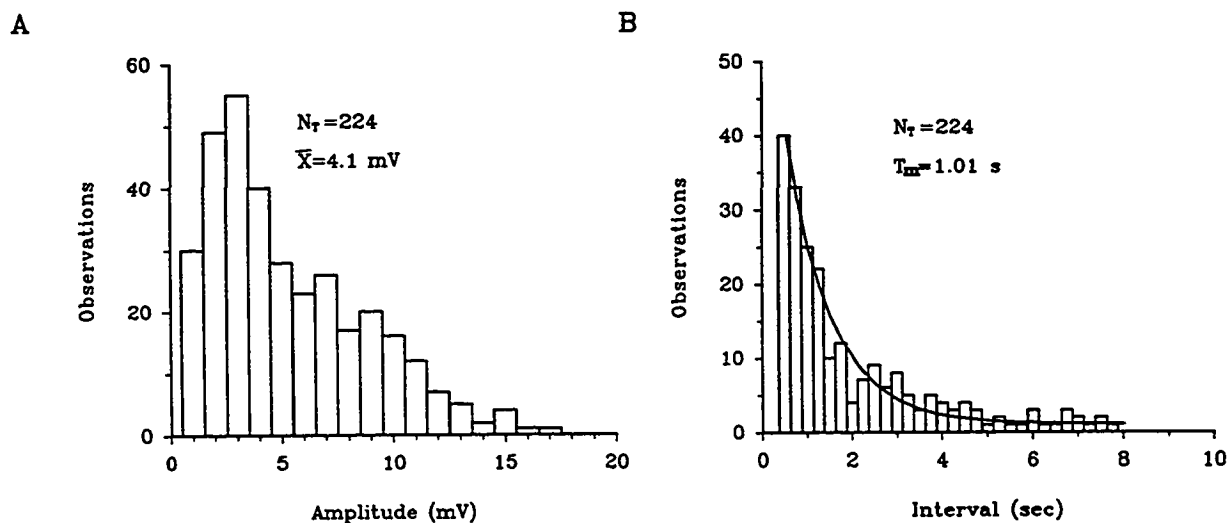


Figure 5. Amplitude and interval distribution of spontaneous subthreshold potentials (SSP) in a co-cultured petrosal neuron.

A. Histogram shows the amplitude distribution of 224 SSP obtained during continuous whole-cell recording from a PN juxtaposed to a type 1 cell cluster. The distribution is skewed to the right, and the majority of spontaneous events had amplitudes in the range 2-3 mV. B. Histogram shows the interval distribution of 224 successive SSP from the same co-cultured PN in A. The mean time interval was 1.01 sec. Smooth curve was drawn according to the theoretical relation expected for a random process: $n = N_T \Delta t / T_m \exp(-t / T_m)$, where n = number of events with time interval, t ; N_T = total number of events; Δt = class interval; and T_m = mean time interval.

Hypoxic chemotransduction and afferent signaling in co-cultures

The evidence presented above suggests that in co-cultures at least some PN form *de novo* chemical synapses with type 1 cells. To test whether these putative synapses are physiologically functional, we investigated whether application of a hypoxic stimulus can result in afferent signaling. In perforated-patch recordings from 140 PN that were juxtaposed to type 1 cell clusters, 45 of them (i.e. ~30%) responded with a depolarization and/or increased spike discharge during application of a hypoxic stimulus ($P_{O_2} = \sim 25$ mm Hg). Three successful examples of functional transmission in co-culture are illustrated in Fig. 6. Application of a hypoxic stimulus, by a rapid-perfusion technique (Fig. 6A), resulted in a strong excitatory response in the PN shown in Fig. 6B. During hypoxia, this neuron responded with a burst of action potentials that lasted for most of the duration of the stimulus (~15 sec); the action potential frequency was ~ 0.11 Hz before, 1.83 Hz during, and 0.04 Hz after stimulus application, indicating that hypoxia caused a >10 fold increase in spike frequency. Data from other examples where the hypoxia-induced PN spike discharge exceeded 1 hz are summarized in Fig. 7A.

In Fig. 6C hypoxia, delivered by slow perfusion (see METHODS), caused a less intense response in another PN, resulting in a burst of action potentials near the beginning of the stimulus and this was superimposed on a slow depolarization that reached a peak value of ~ 10 mV. In Fig. 6D, hypoxia was applied in the presence of TTX (1 μ M) to block spike propagation, and in this case a slow depolarization with superimposed SSP (upward deflections) was seen during hypoxia. In all cases tested (n=5), the hypoxia-evoked

depolarization in 'functional' PN was accompanied by a conductance *increase*, as measured by the application of brief hyperpolarizing current pulses (downward deflections in Fig. 6D). This contrasts with the direct effect of hypoxia on type 1 cells, i.e. the O₂-sensors, where the depolarization was accompanied by a conductance *decrease* (presumably caused by K⁺ channel closure) as illustrated in Fig. 2B.

In many examples, including Figs. 6B-D, there was a noticeable increase in the frequency of SSP during stimulus application; this was most evident during the interspike intervals (e.g. Fig. 6B), and is consistent with enhanced neurotransmitter release during hypoxia. The frequency of 'postsynaptic potentials' (PSP), including both SSP and spikes, before, during, and after hypoxia, is shown for a group (n=14) of 'functional' PN that were juxtaposed to type 1 clusters (Fig. 7B). As was the case for spike discharge (Fig. 7A), there was a significant increase in PSP frequency in the neurons during hypoxia.

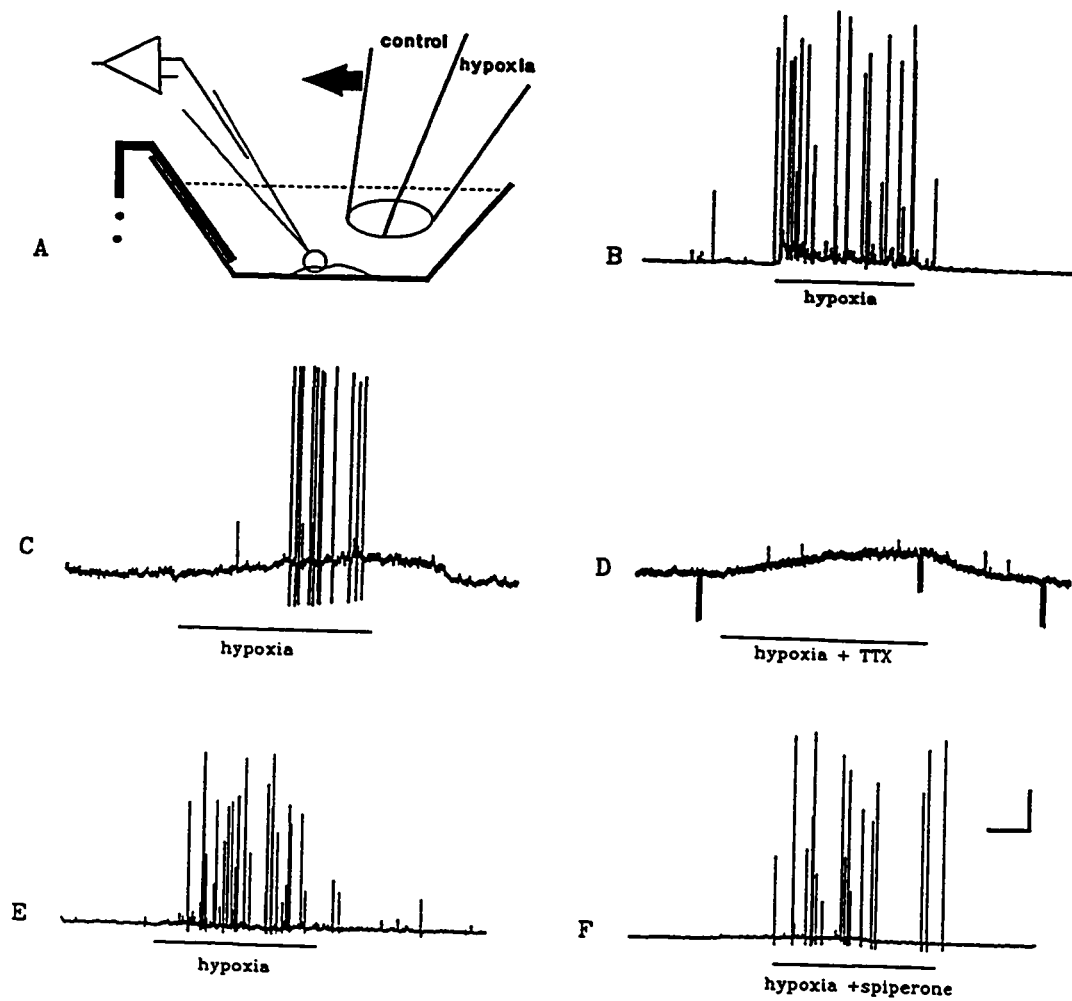
In a few cases (n=3), we confirmed that 'functional' neurons capable of signaling a hypoxic stimulus in co-culture also stained positively for TH- immunoreactivity (not shown), a biochemical marker for carotid body chemoafferent neurons in the rat (Katz & Black, 1986; Finley *et al.*, 1992). A more detailed analysis than the one undertaken here is required to address whether all functional PN in culture express this phenotype.

Does dopamine and/or acetylcholine mediate hypoxic signaling in co-culture?

The excitatory neurotransmitter that mediates afferent discharge in the carotid body during hypoxia remains controversial (Gonzalez *et al.* 1994; Fitzgerald & Shirahata, 1994; Donnelly,

Figure 6. Chemotransduction and afferent signaling of a hypoxic stimulus in co-culture.

A. Schematic diagram of the fast perfusion system used for rapid delivery of the hypoxic stimulus. One bore of a double-barreled pipette delivered 'normoxic' ECF (under gravity flow) over the type 1 cell cluster, while the patch pipette monitored membrane potential in a 'juxtaposed' PN; the other bore of the pipette delivered 'hypoxic' ECF. A piezo-electromechanical switch permitted a rapid change of the perfusate from one pipette to the other. B. A hypoxic stimulus ($P_{O_2} \approx 25$ mm Hg), delivered by fast perfusion (see A) during the period indicated by the lower horizontal bar, elicited a rapid depolarization and increased spike frequency in a 'juxtaposed' PN; note increase in frequency of SSP's during the interspike intervals. C. Slower depolarization and action potentials induced in another 'juxtaposed' PN, during bath application of a hypoxic solution by 'slow' perfusion (see METHODS). D. Perfusion of the hypoxic solution in presence of tetrodotoxin (TTX; $1 \mu\text{M}$) induced depolarization *without* spike discharge in another functional PN, juxtaposed to a type 1 cell cluster; this depolarization, however, in contrast to that induced by hypoxia in type 1 cells (see Fig. 2B), was accompanied by a conductance *increase*, indicated by passing brief constant hyperpolarizing current pulses (downward deflections) before, during, and after the stimulus. Note the presence of SSP during hypoxia and TTX. Another 'functional' PN shows hypoxia-induced increase in spike discharge in both the absence (E), and presence (F), of the dopamine D_2 -receptor blocker, spiperone ($20 \mu\text{M}$); note the spike discharge was still prominent with the blocker present, suggesting that dopamine is not the main excitatory neurotransmitter that mediates hypoxic signaling. Vertical calibration bar (lower right) represents 20 mV; horizontal bar represents 5 s in B, E, F and 10 s in C, D.



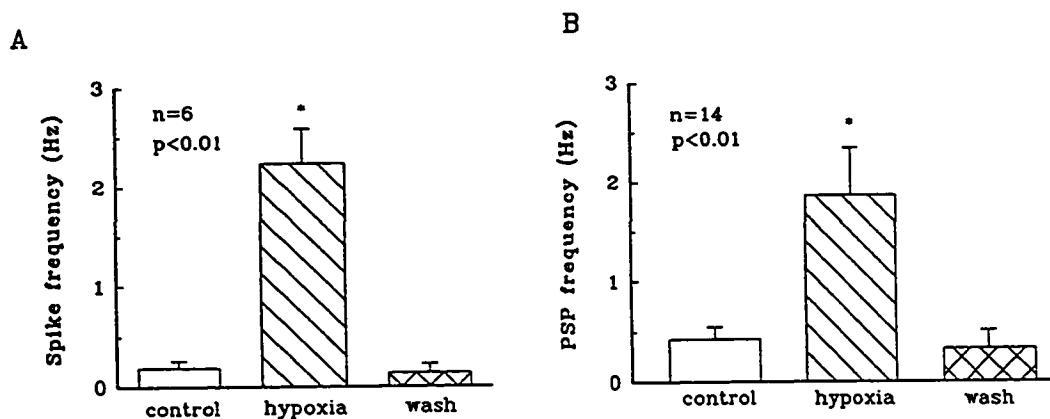


Figure 7. Effect of hypoxia on frequency of action potentials and postsynaptic potentials (PSP) in co-cultured PN. **A.** Histogram shows the action potential or spike frequency plotted for a group of PN ($n=6$) before (control), during (hypoxia), and after (wash) exposure of the culture to a low P_{O_2} (~ 25 mm Hg) perfusate; for this group the hypoxia-induced spike frequency exceeded 1 hz, and was significantly greater ($\sim 10\times$; $p < 0.01$, Student's paired t test) than the control frequency in normoxia ($P_{O_2} \sim 160$ mm Hg). **B.** Similar plot as A, except that the ordinate represents the frequency of 'postsynaptic potentials' or PSP, including both action potentials and subthreshold potentials (SSP), from a larger population of co-cultured PN ($n=14$); the PSP frequency was also significantly greater ($\sim 5\times$; $p < 0.01$) during hypoxia.

1995). Since dopamine is the best studied neurotransmitter in the carotid body, and its release from type 1 cells is well correlated with hypoxic stimulation (Gonzalez *et al.* 1994), we tested whether perfusion of the D₂-receptor blocker, spiperone (10-50 μ M), significantly affected the hypoxia-induced chemosensory discharge in co-culture. In 5 cases, one of which is illustrated in Fig. 6E,F, spiperone did not prevent the hypoxia-induced increase in spike discharge in a 'functional' PN in co-culture. However, a more detailed analysis than the one undertaken here would be required to determine if subtle changes in the discharge occurred in the presence of spiperone. We have preliminary evidence that in these cultures many (>60%) PN appear to express the D₂ receptor, based on binding of a fluorescent D₂ receptor ligand, N-(*p*-aminophenethyl) spiperone, or bodipy-NAPS (C. Nurse, C. Vollmer & H. Zhong, unpublished observations).

We next investigated whether nicotinic cholinergic antagonists can affect hypoxic signaling in co-culture, since acetylcholine (ACh) has long been considered an important excitatory neurotransmitter in CB chemoreception (Hollinshead & Sawyer, 1945; Eyzaguirre & Zapata, 1984; Fitzgerald & Shirahata, 1994). Interestingly, we found that application of the nicotinic blocker, hexamethonium (100 - 200 μ M), abolished the hypoxia-induced spike discharge in many cases (n= 12). An example is illustrated in Fig. 8, where application of the drug reversibly inhibited the spike discharge during hypoxia, as well as the frequency of spontaneous subthreshold potentials (SSP). The effects of hypoxia and hexamethonium, alone and in combination, on the frequency of postsynaptic potentials (SSP and spikes) in a functional PN is shown in Fig. 9; the depression in frequency by hexamethonium during

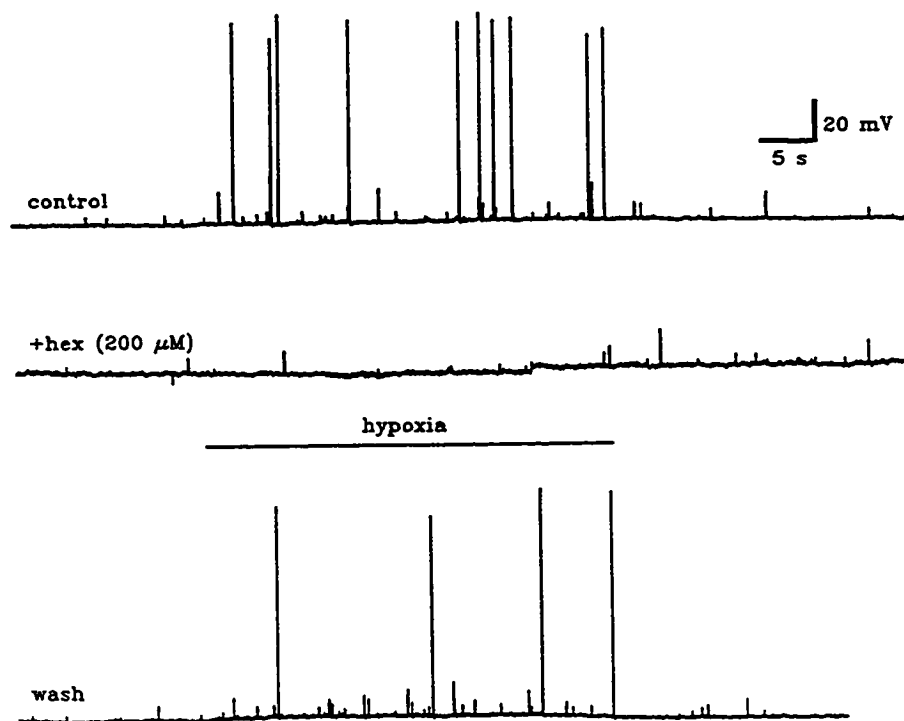


Figure 8. Evidence for involvement of nicotinic acetylcholine receptors (nAChR) in hypoxic signaling in co-culture. One of 12 examples indicating that perfusion of the nAChR blocker, hexamethonium (200 μM), inhibits reversibly the hypoxia-induced increase in firing and SSP frequency in a PN, juxtaposed to a type 1 cell cluster. Upper trace shows that hypoxia ($\text{Po}_2 \sim 25 \text{ mm Hg}$), applied during the period indicated by horizontal bar (below middle trace), increases the frequency of action potentials and subthreshold events. This effect of hypoxia is largely abolished in presence of 200 μM hexamethonium (middle trace); on washing out the drug the response to hypoxia recovers (lower trace). Resting potential = -60 mV. In general, this dose of hexamethonium had no obvious effect on action potential threshold, as measured during injection of depolarizing current pulses ($n=12$; not shown).

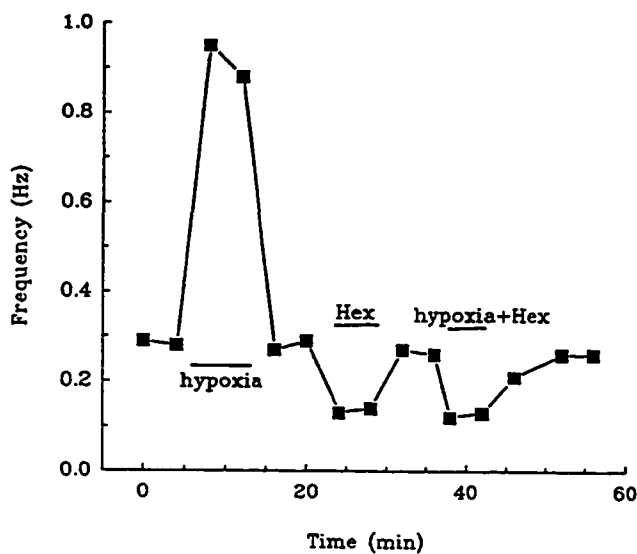


Figure 9. Effect of hypoxia and hexamethonium on frequency of postsynaptic potentials in a co-cultured PN.

The PSP (spikes and SSP) frequency obtained from a single PN in co-culture is plotted vs time after the indicated treatments that lasted for ~1 hr. Each point represents the PSP frequency determined over ~ 1 min of recording time. Note that hypoxia alone caused ~3 fold increase in PSP frequency, that was inhibited in the presence of 200 μ M hexamethonium (hypoxia + hex); the drug also suppressed PSP frequency in normoxic conditions (hex), suggesting that ACh is released spontaneously under normal recording conditions.

normoxia and hypoxia is consistent with an on-going release of ACh over a broad range of P_{O_2} (160 to 25 mmHg).

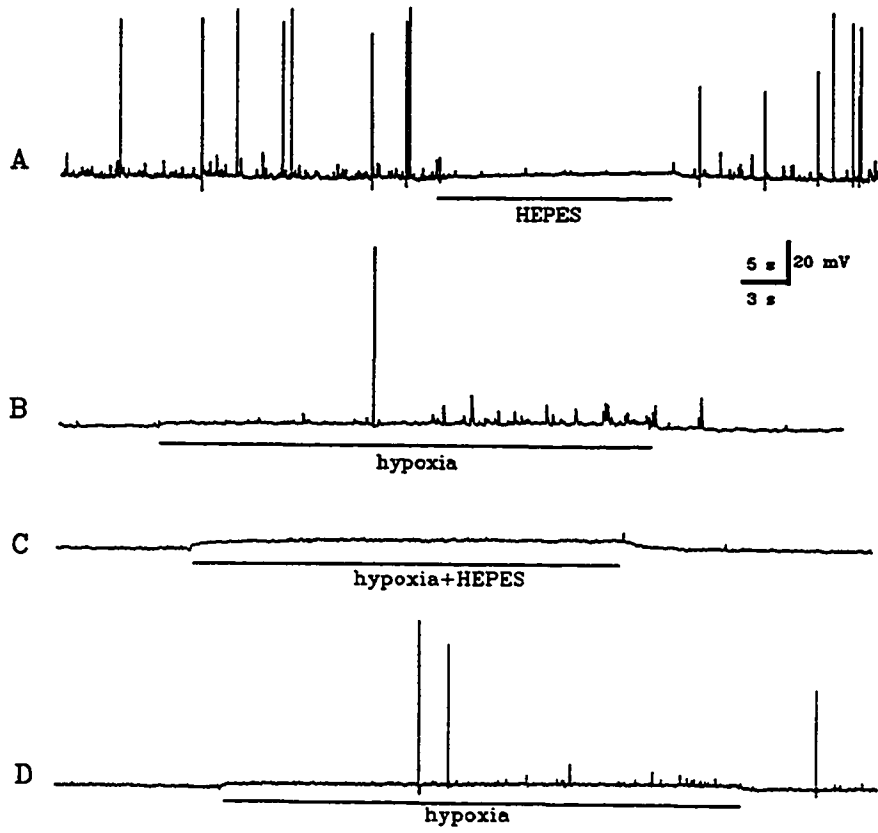
The abolition of hypoxia-induced spiking in the presence of hexamethonium did not appear to be due to a non-specific blockade of the action potential mechanism, since with the drug present, injection of depolarizing current pulses readily elicited spikes in 'functional' PN without obvious changes in firing threshold ($n=12$; not shown). Taken together, these data argue that ACh, rather than dopamine, is likely a major excitatory neurotransmitter during hypoxic signaling in the rat carotid body (see also; Donnelly, 1995). However, in a few experiments ($n=4$) high concentrations of hexamethonium (200 μ M) were insufficient to block completely the hypoxia-induced depolarization, though action potentials were abolished. These findings raise the possibility that in such cases ACh release was too intense for blockade by these doses of hexamethonium (see, Furshpan, MacLeish, O'Lague & Potter, 1976), or that other excitatory neurotransmitters may contribute to the hypoxic response.

Effects of HEPES vs CO_2 - HCO_3^- buffer on hypoxic signaling and spontaneous activity in co-culture

The physiology of type 1 cells (Buckler, Vaughan-Jones, Peers & Nye, 1991; Stea & Nurse, 1991b) as well as carotid body chemosensory discharge in response to hypoxia (Shirahata & Fitzgerald, 1991; Iturriaga & Lahiri, 1991) are reported to be influenced by the extracellular buffer. In the present study we found that switching the buffer from CO_2 - HCO_3^- to HEPES at constant pH (7.4) markedly inhibited the spontaneous discharge in co-cultured PN ($n=6$);

Figure 10. Contrasting effects of $\text{CO}_2\text{-HCO}_3^-$ vs HEPES- buffered media on spontaneous activity and hypoxic signaling in co-cultured PN.

A. One of 6 examples which illustrate that switching the buffering in the perfusate from $\text{CO}_2\text{-HCO}_3^-$ to HEPES, during the period indicated by the horizontal bar below the trace, reversibly abolishes spike activity and suppresses the frequency of SSP in a PN juxtaposed to a type 1 cell cluster. In B-D, another PN was exposed to hypoxia ($\text{Po}_2 \sim 25 \text{ mm Hg}$) in presence of $\text{CO}_2\text{-HCO}_3^-$ before (B), and after (D), switching the buffering to HEPES (C). The hypoxic stimulus (and HEPES buffer in C) was applied during the period indicated by lower horizontal bar. Note the marked suppression in spike activity and frequency of SSP during hypoxia when HEPES was the buffer present; however, the hypoxia-induced depolarization was still persisted in HEPES buffer. Resting potential was $\sim -60 \text{ mV}$ in A, and B-D.



an example is shown in Fig. 10A, where the frequency of both spontaneous spikes and subthreshold events were reversibly suppressed during rapid switch to HEPES buffer at normoxic P_{O_2} (~160 mm Hg). Moreover, the frequency of hypoxia-induced spike(s) and subthreshold potentials was reversibly abolished or suppressed on switching to HEPES buffer (Fig. 10B-D). Interestingly, the hypoxia-induced depolarization was still present in HEPES buffer (Fig. 10C). Thus a major effect of this buffer was to suppress spontaneous activity at both low and high P_{O_2} . A comparison of the effects of the two buffers on spontaneous activity and the hypoxic response in co-cultured PN is shown in Table 1. It is evident that the ability to detect spontaneous activity and 'functional' neurons in co-culture is greatly enhanced in CO_2 - HCO_3^- buffer.

Table 1. Frequency of responding petrosal neurons in co-cultures
exposed to HEPES vs CO₂-HCO₃⁻-buffered media *

Response	HEPES buffer	CO ₂ -HCO ₃ ⁻ buffer
Spontaneous activity	39/150 (26%)	68/125 (54%)
Hypoxia-induced depolarization and/or action potentials	22/120 (18%)	50/123 (40%)

* In some experiments the same neuron was tested in both buffers.

Values in table are expressed as the percentage of responding PN relative to total number of neurons sampled. Data include neurons that were juxtaposed and non-juxtaposed to type 1 cell clusters

DISCUSSION

In this study we introduce and test a novel preparation, based on co-culture of arterial chemoreceptor cell clusters and petrosal neurons (PN), which appears attractive for studying mechanisms of chemosensory signaling in the rat carotid body. *In vivo*, these chemoreceptors or type 1 cells are the primary O₂-sensors, which form morphological reciprocal (chemical) synapses with petrosal terminals (McDonald & Mitchell, 1975), and signal reflex hyperventilation as a compensatory response to a fall in blood Po₂ or hypoxia (Eyzaguirre & Zapata, 1984; Biscoe & Duchon, 1990; Gonzalez *et al.*, 1994). We show that in co-culture, at least some PN (~30% for all recording conditions) form *de novo* functional connections with neighboring type 1 cell clusters. Though we have no direct evidence, it is plausible that at least some of the neurons that failed to make functional connections include those that would normally subserve other sensory modalities, but were unavoidably carried into culture. Our ability to record synaptic-like activity was undoubtedly aided by the selection for study those neurons that were fortuitously 'juxtaposed' to type 1 cell clusters in co-culture. This strategy appeared advantageous for two reasons: (i) since cell body recordings were employed throughout, the electrode was more likely to be at a favourable distance from the synaptic contacts, and thereby facilitate monitoring of subthreshold events before substantial electrotonic decay; and (ii) since there was a requirement that *de novo* chemical synapses develop between type 1 cells and PN, the chances of forming successful contacts were

occurrence in PN of spontaneous potentials with several properties expected of post synaptic potentials seen at conventional chemical synapses (Katz, 1969). Among the noteworthy features, these spontaneous subthreshold potentials or SSP: (i) showed a rapid rise time followed by a slower decay; (ii) had variable amplitudes (1-15 mV) that were often large enough to trigger action potentials; (iii) persisted even after action potential blockade with the Na⁺-channel blocker, tetrodotoxin; (iv) showed marked reduction in frequency of occurrence when extracellular the calcium to magnesium ratio was reduced, and when the cholinergic antagonist, hexamethonium (100-200 μM) was present; (v) showed an interval distribution expected for a random process; and (vi) were notably absent in PN cultured without type 1 cells. Interestingly, the SSP observed in this study (e.g. Fig. 3) resemble the spontaneous depolarizing potentials or SDPs recorded when intracellular microelectrodes successfully impaled petrosal nerve terminals in the isolated, but intact, cat carotid body *in vitro* (Hayashida *et al.*, 1980). Thus, it would appear that our recordings in culture from 'juxtaposed' PN cell bodies, located within only a few microns from a type 1 cell cluster, reflected spontaneous activity with origins close to the afferent terminations. The amplitude of spontaneous subthreshold events had a skewed distribution and this prevented a rigorous test of 'quantal' release. Assuming a synaptic origin, many factors may have contributed to this skewed distribution including: (i) variability in quantal unit size, and number of quanta released from type 1 cells; (ii) multiple release sites using the same transmitter but located at different distances from the recording electrode (perhaps occurring at different type 1 cells within the cluster); (iii) release of multiple transmitters from type 1 cells; and (iv)

combinations of these.

Hypoxic chemotransduction and afferent signaling in co-culture

Perhaps the most noteworthy feature of the preparation was that in many cases, especially in $\text{CO}_2\text{-HCO}_3^-$ buffer, a physiological stimulus, hypoxia ($\text{P}_{\text{O}_2} = \sim 25$ mm Hg), was transduced and relayed to a second-order afferent neuron in the form of a depolarization and superimposed spike activity. In a previous study, co-cultures of dissociated rat carotid body and nodose (sensory) neurons were used as a model for investigating chemosensory mechanisms *in vitro* (Alcayaga & Eyzaguirre, 1990). These authors found that whereas spontaneous action potentials in nodose neurons occurred more frequently when type 1 cells were present, and acid-induced responses could be detected in co-culture, there was *no* evidence for hypoxic signaling. Perhaps in the latter study, use of the 'foreign' nodose ganglion resulted in a low frequency of 'appropriate' chemosensory neurons and a relative paucity of successful contacts. In the co-cultures investigated in the present study, the hypoxia-induced depolarization in the neuron was accompanied by a conductance *increase*, implying its origin was due to a different mechanism from the one seen in type 1 receptor cells. As expected, the latter cells depolarized during hypoxia, but with a *decrease* in membrane conductance (see Fig. 2), due likely to the closing of K^+ channels that were open at the resting potential (Delpiano & Hescheler, 1989; Buckler & Vaughan-Jones, 1994; Wyatt, Wright, Bee & Peers, 1995; Buckler, 1997). Therefore, since hypoxia is known to stimulate neurotransmitter transmitter release from type 1 cells (Fidone *et al.*, 1988; Gonzalez *et al.*, 1994; Montoro *et al.*, 1996), the excitatory

neurotransmitter(s) that mediate hypoxic signaling might be expected to open ion channels in petrosal terminals. The available evidence, however, suggests that the best studied neurotransmitter in type 1 cells, i.e. dopamine, is not the principal mediator of the hypoxia-induced excitation seen in co-culture. In a few experiments, the dopamine D₂-receptor blocker, spiperone (10 -50 μM) had no appreciable effect on the hypoxic discharge in functional co-cultured PN. The role of dopamine in carotid body chemotransmission remains controversial (see, Gonzalez *et al.*, 1994), though other recent studies suggest it is unlikely to be the mediator of hypoxic signaling in the mammalian carotid body (Donnelly, 1995; Iturriaga, Alcayaga & Zapata, 1996).

We also found that optimal mediation of the hypoxic response in co-cultured PN required the presence of CO₂-HCO₃⁻-buffered medium. Both spontaneous and hypoxia-induced synaptic activity were inhibited following a switch to HEPES-buffered medium. These results are in general agreement with several studies based on the intact CB-sinus nerve preparation *in vitro*, where hypoxic signaling was augmented in CO₂-HCO₃⁻-buffered solutions (Shirahata & Fitzgerald, 1991; Iturriaga & Lahiri, 1991), and where the sensitivity of the Po₂ response was increased via interaction with Pco₂ (Pepper, Landauer & Kumar, 1995). Doubtless, the importance of buffering in the CB hypoxic response relates to previous findings indicating that the physiology of chemoreceptor type 1 cells is altered on switching from HEPES to bicarbonate buffer (Buckler *et al.*, 1991; Stea & Nurse, 1991b).

Evidence for ACh involvement in hypoxic signaling in co-culture

A significant finding was that in several cases the hypoxia-induced increase in afferent firing in co-cultured PN was markedly suppressed by the nicotinic cholinergic antagonist, hexamethonium (100-200 μM), suggesting ACh was a mediator. The idea of ACh as the main excitatory neurotransmitter in CB chemosensory signaling during hypoxia has had a long and controversial history (Hollingshead & Sawyer, 1945; Eyzaguirre & Zapata, 1984; Nurse, 1987; Fitzgerald & Shirahata, 1994). Though we cannot formally exclude the possibility that ACh synthesis by type 1 cells could have been induced by the culture conditions (see Furshpan *et al.*, 1976), there is evidence *in vivo* that type 1 cells have the ability to synthesize and degrade ACh (for references, see Gonzalez *et al.*, 1994). Blockade of the hypoxia-induced spike discharge required high doses (100- 200 μM) of the ganglionic blocker, hexamethonium, but this did not appear to be due to a non-specific blockade of the action potential mechanism. Moreover, even higher concentrations (150 - 1000 μM) of hexamethonium were required to block nicotinic cholinergic transmission at sympathetic neuronal synapses in cultures where ACh secretion was intense (Furshpan *et al.*, 1976). The fact that hypoxia elicited a small depolarization in some co-cultured PN even in the presence of high doses of hexamethonium suggests either that the drug concentration was still not high enough for complete blockade, or that other co-released CB excitatory transmitters (e.g. substance P, purines, etc) participated in the response. These latter possibilities remain to be tested.

Interestingly, the frequency of spontaneous subthreshold events was also suppressed by

100 - 200 μM hexamethonium, suggesting that ACh also contributes to the neurotransmitter pool that is released spontaneously from type 1 cells, even at the relatively high (normoxic) Po_2 of ~ 160 mm Hg. Since in these cultures $>60\%$ PN express hexamethonium-sensitive nicotinic AChR (Zhong & Nurse, 1996; 1997), the simplest explanation of our results is that hypoxia stimulates release of ACh from type 1 cells, and this in turn acts on nicotinic receptors located on petrosal terminals that formed *de novo* synapses in culture. However, the presence of nicotinic receptors on rat type 1 cells (Wyatt & Peers, 1993; our unpublished observations) makes tenable the possibility that ACh, released by hypoxia, might act *indirectly*, via these receptors in an autocrine or paracrine fashion to release an as yet unidentified excitatory transmitter from type 1 cells.

Additional studies are required to confirm the validity of this co-culture preparation as a general model for studying carotid body function. For example, do other established chemoexcitants including, acidosis, hypercapnia and cyanide produce the expected increase in discharge in co-cultured neurons? Nevertheless, the ability of these co-cultures to transduce and relay information about an important physiological stimulus (hypoxia) to a second-order neuron suggests that the preparation is an attractive one for studying mechanisms of carotid body chemotransmission.

CHAPTER 7

Discussion of the Mechanisms of Chemotransduction and Chemotransmission in the Carotid Body

In this chapter I will attempt to discuss the physiological relevance of my studies to the mechanisms of chemoreception in the carotid body (CB). The significance of the electrophysiological properties and neurotransmitter sensitivities of petrosal neurons will be described in detail. To aid integration of the ideas, chemotransduction mechanisms in glomus cells will first be mentioned though they were not the main focus of the thesis. There will be some emphasis on the mechanisms of chemotransmission between the chemosensor and afferent sensory neurons, as well as on the modulation of this process by putative carotid body neurotransmitters.

1. Mechanisms of hypoxic transduction

1.1 Roles of ionic channels and intracellular Ca^{2+} in hypoxic chemotransduction

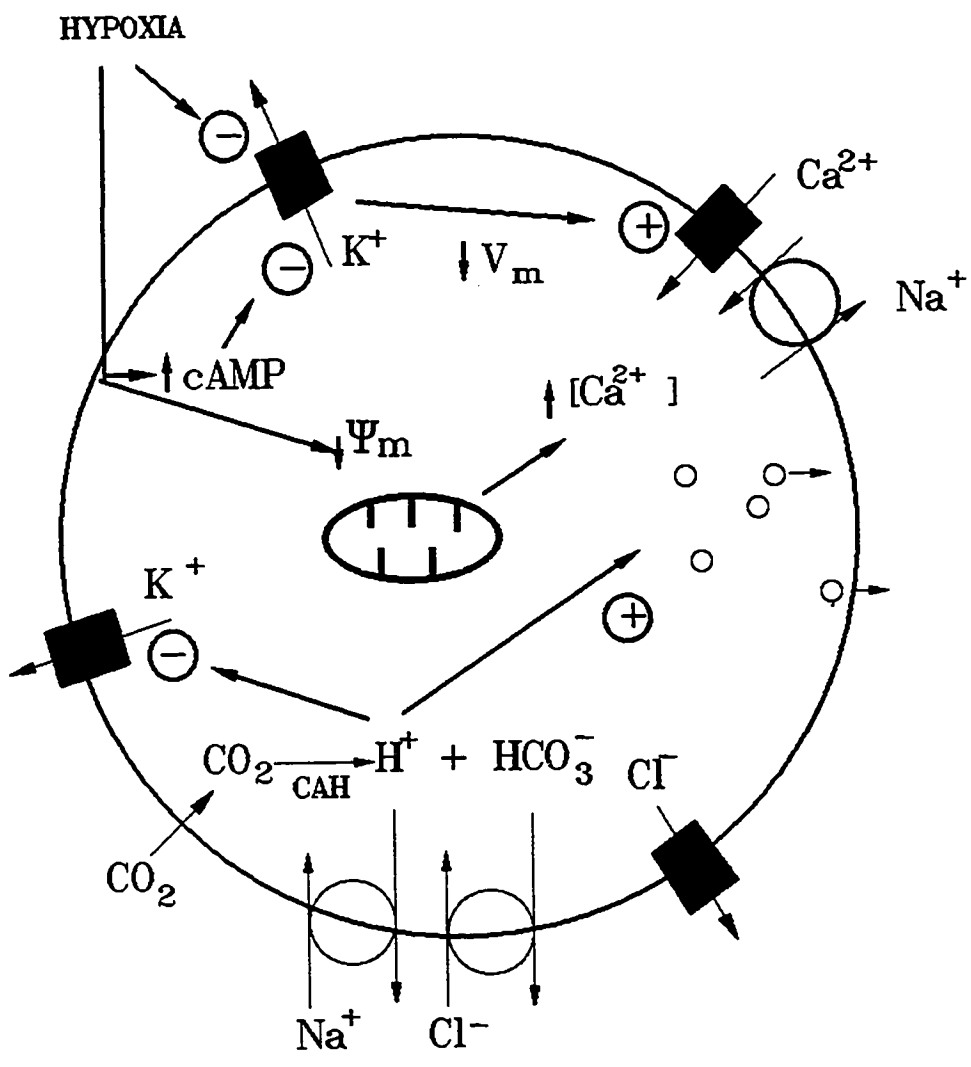
The carotid body is a complex sensory organ in which the sensory nerve fibers are connected to specialized receptor cells (glomus or type I cells). Previous experimental data, including the results of Chapter 6, suggest that glomus cells play a principal role in transduction of chemosensory stimuli in the CB. In response to acute hypoxia, rat glomus cells show a depolarization of membrane potential (receptor potential) with a conductance decrease as seen in Chapter 6. These results agree with previous findings in rat (Buckler and

Vaughan-Jones, 1994) and rabbit (Lopez-Lopez et al., 1989; Lopez-Barneo, 1996), where acute hypoxia has been shown to depolarize and increase action potential frequency in glomus cells. In whole-cell voltage clamp experiments it was found that acute hypoxia inhibited a voltage-dependent, Ca^{2+} -insensitive K^+ current in rabbit glomus cells (Lopez-Barneo et al., 1988; Hescheler et al., 1989; Delpiano and Hescheler, 1989; Ganfornina and Lopez-Barneo, 1991), in contrast to rat, where acute hypoxia inhibited a Ca^{2+} -dependent K^+ current (Peers, 1990; Wyatt and Peers, 1995; this thesis Chapter 4). In more recent studies, Buckler (1997) revealed a novel O_2 -sensitive leak K^+ channel in rat glomus cells that showed little voltage sensitivity. This channel was proposed to be the main cause of the receptor potential in these cells since it was opened at resting membrane potential, and therefore could be closed by hypoxia. It is curious that O_2 -sensitive K^+ channels are so variable between species (Lopez-Barneo, 1994) and it appears, at least in the rat, that different K^+ channels in the same cell may be used to sense oxygen. Exactly how these O_2 -sensitive K^+ channels are regulated by Po_2 remains to be clarified, though some ideas will be discussed in the following paragraphs.

The inhibition of the K^+ channel by hypoxia can occur directly (Ganfornina and Lopez-Barneo, 1991), but may also involve cyclic AMP which is elevated during hypoxia, and can itself inhibit the K^+ channel in rabbit glomus cells (Lopez-Lopez et al., 1993; see however Hatton and Peers, 1996b). As mentioned in the Introduction, K^+ channel activity is an important determinant of the glomus cell resting membrane potential and closure of K^+ channels by hypoxia would cause cell depolarization. The hypoxia-induced depolarization would in turn lead to the opening of voltage-gated Ca^{2+} channels, entry of extracellular Ca^{2+}

Figure 7.1 Possible mechanisms for hypoxic chemotransduction in glomus cells. Hypoxia inhibits K^+ channel activity directly, but may also cause increased cyclic AMP which can itself inhibit K^+ channels. Closure of K^+ channels causes cell membrane depolarization (decrease V_m) which in turn leads to the opening of voltage-activated Ca^{2+} channels and Ca^{2+} influx into the cell. Alternatively, hypoxia can reduce the mitochondrial membrane potential (Ψ_m) which may lead to the release of Ca^{2+} from mitochondria. A rise in intracellular Ca^{2+} levels promotes neurotransmitter(s) release. There are many regulating mechanisms by which the response of glomus cell to chemical stimuli may be modulated. For example, the Na^+/H^+ antiporter can extrude H^+ ions and increase intracellular Na^+ which in turn may reverse the Na^+-Ca^{2+} exchanger and lead to a rise in intracellular Ca^{2+} . The Cl^-/HCO_3^- exchanger, which promotes HCO_3^- efflux, can regulate the glomus cell intracellular pH and function. The Cl^- channel, which is also permeable to HCO_3^- , has been proposed to contribute to resting membrane potential of glomus cells. Increasing CO_2 can decrease intracellular pH due to the hydration of the CO_2 to HCO_3^- and H^+ , catalyzed by intracellular carbonic anhydrase. The elevated intracellular H^+ can inhibit the activity of K^+ channels and increase intracellular Ca^{2+} . It is also possible that acidification directly stimulates transmitter release as described in other cells (Drapeau and Nachshen, 1988) [this figure is adapted from Peers, 1994].

Glomus Cell



and neurotransmitter release. The results of Chapter 6 provide evidence that hypoxia-induced afferent discharges in petrosal neurons are mediated by chemical synapses with chemosensory (glomus) cells. Hence, the release of transmitter(s) from these chemosensors is critical for translating the effects of chemostimuli into afferent nerve impulses. A schematic diagram summarizing the possible physiological roles of the K^+ channel and cytosolic Ca^{2+} in a glomus cell is shown in Figure 7.1. This model is based on results from several studies including this thesis.

Figure 7.1 also illustrates an alternative mechanism by which hypoxia might elevate $[Ca^{2+}]_i$ of the glomus cell. Previous reports by Duchen and Biscoe (1992) have provided evidence that a specialized mitochondrial electron transport accounts for glomus cell chemosensitivity. These authors found that hypoxia can elevate $[Ca^{2+}]_i$, not by stimulating influx across the plasma membrane, but by causing its release primarily from mitochondrial stores (Duchen and Biscoe, 1992). These results are markedly different from those of Buckler and Vaughan-Jones (1994), in which the removal of extracellular Ca^{2+} ($[Ca^{2+}]_o$) abolished the hypoxia-induced rise of $[Ca^{2+}]_i$, indicating a fundamental role for Ca^{2+} influx. Although current views favour the notion that the source of the hypoxia-induced rise of $[Ca^{2+}]_i$ is extracellular Ca^{2+} , recent studies (Dasso et al., 1997) on isolated rat glomus cells revealed that the full response to muscarinic agents involved Ca^{2+} release from intracellular stores. This suggests that ACh released during hypoxia could activate calcium release from intracellular stores.

1.2 Effects of $\text{HCO}_3^-/\text{CO}_2$ buffered media and pH_i on hypoxic chemotransduction

As demonstrated in Chapter 6, substitution of $\text{HCO}_3^-/\text{CO}_2$ buffered media (BBM) for HEPES-buffered media (HBM) significantly increases hypoxia-induced responses in co-cultures during recordings from 'juxtaposed' petrosal neurons. Since no obvious differences between HBM and BBM were seen when the sensitivity of petrosal neurons to putative carotid body neurotransmitters (e.g. ACh, 5-HT, GABA) was tested, it was inferred that the effect of the buffer was mainly on the chemoreceptors. Indeed, previous work in our laboratory using patch-clamp recording has demonstrated a major increase in leak conductance of the glomus cell and a decrease in voltage-activated outward K^+ current in bicarbonate/ CO_2 (Stea and Nurse, 1991a). This complemented earlier work showing that glomus cells have a large-conductance anion channel which is permeable to both Cl^- and HCO_3^- and sensitive to the anion channel blocker, 9-AC (Stea and Nurse, 1989). Hypercapnic suppression of a voltage-activated outward K^+ current is shown in appendix 1 C, D,. These results suggest that bicarbonate and/or pH_i modulate ion channel activity and membrane permeability of glomus cells. Later, Carpenter and Peers (1996) confirmed the existence of Cl^- channels whose activity was regulated by pH and cyclic AMP. Several other observations also suggest that anions play an essential role in carotid body function. In particular, Shirahata and Fitzgerald (1991) observed that HCO_3^- -free perfusates virtually eliminated the nerve response to hypoxia, although in another study, HEPES buffer only reduced the speed of response to hypoxia without reducing its magnitude (Iturriaga and Lahiri, 1991).

Recently, Panisello and Donnelly (1996) observed the enhancement effect of HCO_3^-

/CO₂ on CB catecholamine secretion during hypoxia, whereas 9-AC significantly reduced the magnitude of hypoxia-induced catecholamine secretion in the presence of HCO₃⁻/CO₂. The regulation of intracellular pH was likely to be physiologically important in the chemosensory response of glomus cells, since the sensitivity of isolated rabbit glomus cells to hypoxia was reported to be increased by acidity (Biscoe and Duchon, 1990). Furthermore, glomus cells are known to contain intracellular carbonic anhydrase (Rigual et al, 1985; Nurse, 1990; Gonzalez et al., 1994), and perfusion with BBM (and 5% CO₂, see Chapter 6) was expected to cause cytoplasmic acidification (Buckler et al., 1991) and a concomitant inhibition of K⁺ channel (Peers and Green, 1991; Stea and Nurse, 1991a; Stea et al., 1991). As shown in Appendix 1 C, D, hypercapnia reversibly inhibited an outward K⁺ current due possibly to cytoplasmic acidification, catalyzed by carbonic anhydrase in glomus cells. This observation agrees with previous reports (Stea and Nurse, 1991b; Stea et al., 1991; Buckler and Vaughan-Jones, 1994). An alternative explanation of the enhanced chemosensory response in BBM is that BBM-induced intracellular acidification directly stimulates neurotransmitter(s) release from glomus cells as described in other cells (Drapeau and Nachshen, 1988).

Based on results from this thesis and several other studies, the following model for the modulation of chemosensory response by HCO₃⁻/CO₂ is proposed: the hypoxia-induced increase in [Ca²⁺]_i via Ca²⁺ influx and/or release from stores may be directly affected by changes in pH_i. Perfusing with BBM (and 5% CO₂) results in CO₂ diffusion into the cell and a rapid decrease in pH_i in the presence of carbonic anhydrase. This cytoplasmic acidification may be enhanced by the loss of HCO₃⁻ possibly via the large conductance anion channel (Stea

and Nurse, 1989) and/or a $\text{Cl}^-/\text{HCO}_3^-$ exchanger and may be modulated by Na^+/H^+ antiports. Changes in pH_i may stimulate transmitter release either by regulating $[\text{Ca}^{2+}]_i$ levels via modulation of ion channels or a direct Ca^{2+} -independent mechanism (Drapeau and Nachshen, 1988). This model allows for the effects of hypoxia and other chemosensory stimuli to be mediated through intracellular $[\text{Ca}^{2+}]_i$. It suggests possible mechanisms for $\text{HCO}_3^-/\text{CO}_2$ enhancing the chemosensory sensitivity in co-cultures (Fig. 7.1).

1.3 Model of oxygen-sensing mechanisms

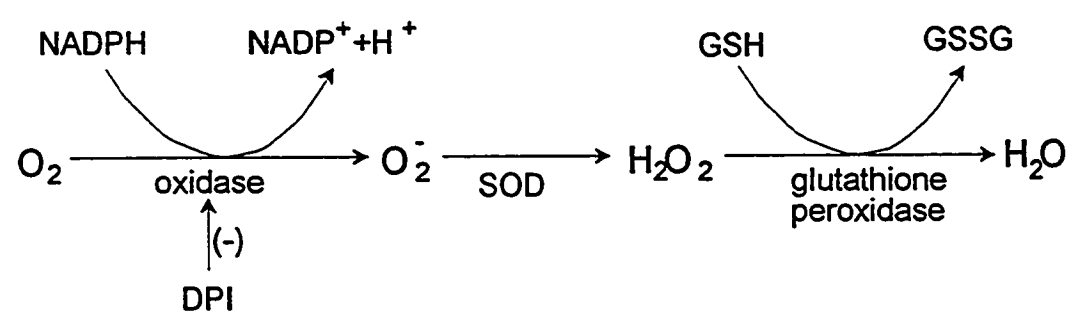
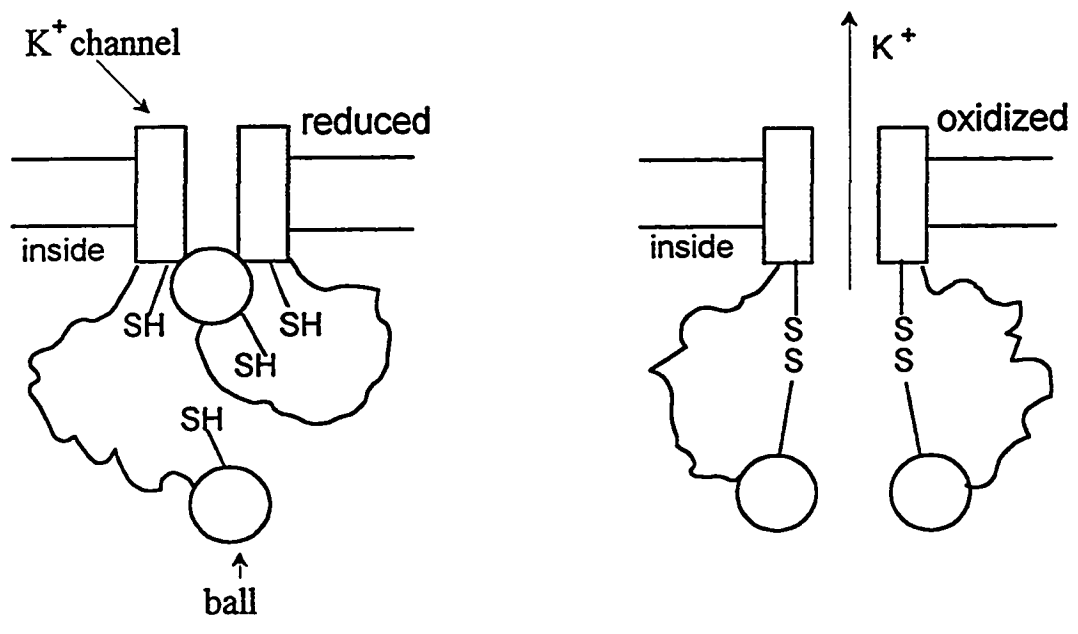
There are various mechanisms proposed to explain how O_2 tension influences ion-channel activity. One possibility is that O_2 interacts directly with a special region of the four α subunits that form the basic structure of the K^+ channel (Hille, 1992; Lopez-Barneo, 1994). It is possible that O_2 could bind reversibly to molecules with metal-protein sites (Karlin, 1993; Lopez-Barneo, 1994); however, whether the K^+ channel has such structural motifs to allow O_2 binding is unknown. An alternative idea is that O_2 interacts with a sensor protein which might be either independent (requiring a mediator) or closely associated with the K^+ channel. Indeed findings to date are incomplete and there is no consensus as to whether this effect is membrane delimited or requires cytosolic mediators (Lopez-Lopez et al., 1989; Hatton and Peers, 1996a). It has also been proposed that the O_2 sensor in glomus cells is an intrinsic heme-linked membrane protein (Acker et al., 1992), for example, a membrane-bound NADPH oxidase containing a b-type cytochrome, similar to the one that generates the respiratory burst in neutrophils (Cross et al., 1990). This oxidase, composed of five subunits, is thought to

synthesize superoxide (O_2^-) under normoxic conditions. The superoxide will be dismutated to hydrogen peroxide (H_2O_2) which can be scavenged by catalase and/or glutathione oxidase. Consequently, the ratio of 2GSH/GSSG will vary and the higher level of GSH under reduced conditions (e.g. hypoxia) would lead to closing of GSH-sensitive K^+ channels (see Ruppertsberg et al., 1991; Yuan et al., 1995). On the other hand, the higher level of GSSG under normoxia would lead to opening of GSH-sensitive K^+ channels and keep the cell membrane potential near the resting level (Peers and Buckler, 1995). One of the observations in Appendix 1 A, B, shows that H_2O_2 can modulate K^+ channel activity in rat glomus cells. Similar results have been reported for other chemosensory cells e.g. the rabbit neuroepithelial body (NEB) cells (Wang et al., 1996) and H_2O_2 has also been found to modulate certain cloned K^+ channels expressed in frog oocytes (Vega-Saenz de Miera and Rudy, 1992). Furthermore, diphenylene iodonium (DPI; a NADPH oxidase inhibitor) blocks chemoreceptor discharges triggered by low Po_2 (Cross et al., 1990) and inhibits voltage-dependent K^+ current in rabbit NEB cells (Youngson et al., 1993). Experimental evidence for this theory is not complete and many unanswered questions remain. A schematic representation summarizing a possible O_2 detecting mechanism in glomus cells is shown in Figure 7.2 (adapted from Ruppertsberg et al., 1991; Acker, 1994). This model will need revision as more information becomes available.

The hypoxia response seen in petrosal neurons in co-culture is almost always absent in petrosal neurons cultured alone. The simplest explanation is that the glomus cells sense hypoxia and release excitatory neurotransmitters onto the apposed sensory nerve endings. An

Figure 7.2 Mechanism of detection of the hypoxic stimulus.

This model proposes that the formation of disulphide bridges between the ball domain and the channel portion of the protein might modulate K^+ channel activity. It is assumed that both the ball and the K^+ channel have cysteine-containing regions which are prone to oxidation. In the reduced state (hypoxia) the ball can move freely and block the K^+ channel. If this channel contributes to the resting membrane potential, its closure will lead to membrane depolarization. In the oxidized state the ball domains are immobilized by the disulphide bridges so that the ball cannot block the K^+ channel. K^+ crosses the cell membrane through the channel and maintains the membrane potential hyperpolarized. In the lower part, molecular oxygen can easily pass through the plasma membrane into the glomus cell. Under normoxic conditions the NADPH-oxidase can synthesize superoxide (O_2^-) which is then converted to H_2O_2 by superoxide dismutase (SOD). The H_2O_2 is further reduced to H_2O by glutathione peroxidase with the consequent oxidation of glutathione. The oxidized form of glutathione (GSSG) can keep the K^+ channel open as mentioned above. Under hypoxic conditions the production of H_2O_2 decreases, raising the ratio of reduced glutathione relative the oxidized form. The reduced form of glutathione (GSH) can inhibit K^+ channel via the ball and chain model (adapted from Acker, 1994; Ruppertsberg et al., 1991; see also Peers and Buckler, 1995).



alternative interpretation is that hypoxic transduction occurs in sensory nerve endings only if they are "conditioned" by intimate contact with glomus cells. However, there is no direct experimental evidence to support this idea (see however, Sun and Reis, 1994). The evidence provided in Chapter 6 of this thesis strongly favours the idea that neurotransmitter release is intimately involved in hypoxic signaling in the carotid body.

2. I_h and the electrophysiology of afferent petrosal sensory neurons

Petrosal sensory neurons are endowed with Na^+ , K^+ , and Ca^{2+} channels which are important for encoding and relaying chemosensory signals (Gallego, 1983; Stea and Nurse, 1992). In addition to these conventional channel types, a novel type of channel was revealed in this study. As described in Chapter 2, the majority of petrosal neurons (~ 78%) have a hyperpolarization-activated inward current (I_h) which is also a time- and voltage-dependent, non-inactivating, cation current. Immunofluorescence experiments reveal that more than 65% of our cultured petrosal neurons are TH-positive (C. Vollmer; unpublished observations), and it is likely that at least some of these are carotid body chemoafferent neurons, based on studies on distribution of the TH-phenotype in the rat petrosal ganglion *in vivo* (Finley et al., 1992).

In Chapter 2, it was found that some neurons exhibiting I_h were also TH-positive, suggesting that I_h may be present in carotid body chemoafferent neurons. In this study we found that I_h was blocked by cesium, had a reversal potential of ~ -33 mV, and was activated at potentials negative to -60 mV. I_h is known to regulate pacemaker currents and hence

interspike intervals in cardiac muscle cells (Irisawa et al., 1993). *In vivo*, petrosal neurons discharge spontaneously and display sharp changes in spike frequency in response to chemostimuli (Gonzalez et al., 1994). It is possible that I_h regulates spike frequency during chemosensory transmission by a similar mechanism to cardiac muscle cells. When I_h is activated at negative potentials, it could oppose strong hyperpolarization and initiate a depolarization since its reversal potential is ~ -33 mV (Hille, 1992). In this way I_h could contribute to the shortening of the interspike interval in petrosal neurons. This idea is consistent with a recent study using an *in vitro* sinus nerve-carotid body preparation from the rat (Doyle and Donnelly, 1994). In the latter study extracellular cesium (a blocker of I_h) markedly inhibited the hypoxia-induced increase in discharge, suggesting I_h may play an important physiological role during chemosensory signaling.

The I_h described in Chapter 2 is different from the previously-reported inward rectification in cat petrosal neurons, where rectification appears to result from a TTX-sensitive delayed increase in Na^+ conductance (Gallego, 1983). The inward rectification, spike activity (multiple vs single), and the shape of action potential (with or without a hump) have been used to classify petrosal neurons in cat (Belmonte and Gallego, 1983). Although some of these electrophysiological features were observed in the present study, I_h was present in neurons which showed very different spiking behaviours. Therefore, chemosensory neurons in cat and rat may not have identical electrophysiological properties, and the results from the two species may not be easily compared. In previous electrophysiological studies on rat petrosal neurons, however, I_h was not observed (Stea and Nurse, 1992). Perhaps, the

command voltage pulses were not long enough (in most cases 50 ms) in the latter study to reveal the presence of I_h .

3. Chemosensory transmission between CB chemoreceptors and afferent nerve endings

3.1 The coding of sensory information and hypoxia threshold

How is sensory information passed from the receptors of the carotid body to the respiratory center in the central nervous system? To address this question Biscoe and colleagues (1970) recorded from sensory fibers of the cat CSN, while the CB was exposed to hypoxia. They found that the frequency of impulse discharge in the CSN increased exponentially with increasing intensities of hypoxia. Therefore, it appears that information about the intensity of the sensory stimulus is carried as a frequency code (Gonzalez et al., 1994). The P_{O_2} gradient in the carotid body tissue during resting conditions is controversial (see Gonzalez et al., 1994). Forster (1968) proposed that the P_{O_2} drop from carotid body capillaries to the center of glomus cell clusters is in the range 10-20 mm Hg; Whalen and Nair (1983) found values for carotid body P_{O_2} of ~ 70 mm Hg in normoxic conditions. During hypoxia, a threshold carotid body tissue P_{O_2} for increase of the CSN discharge was ~ 50 mm Hg and a P_{50} for the hypoxia response was 32 mm Hg (Whalen and Nair, 1983; Buerk et al., 1989). These values correlate well with similar measurements in arterial blood, where the threshold P_{O_2} for the CSN response is 70-75 mm Hg and the P_{50} is around 40 mm Hg (Lahiri, 1977).

3.2 Receptor potential and generator potential

In Chapter 6, hypoxia induced depolarization in glomus cells but *not* in petrosal neurons cultured alone. This membrane depolarization in glomus cells is considered a *receptor potential*, defined as a potential change in the receptor cell (or in the sensory nerve terminal) induced by the action of the stimulus. In the case of baroreceptors of the rat carotid sinus, the receptor potential is the same as the generator potential, since the stimulus produces a potential change which in turn generates discharges (action potentials) in the endings of the same afferent nerve. However, when the receptor cell is separate, any ensuing receptor potential must be converted to a generator potential in the apposed nerve terminal. Thus hypoxia caused depolarization of the resting glomus cell or a "receptor potential" in this and other studies (Buckler and Vaughan-Jones, 1994; Wyatt et al., 1995; Buckler, 1997). On the other hand, the depolarizing potentials recorded from co-cultured petrosal neurons in this study or from afferent sensory terminals in the intact CB *in situ* (Hayashida et al., 1980; Eyzaguirre and Zapata, 1984) could be considered as "generator potentials".

There is abundant evidence indicating the existence of synaptic connections between glomus cells and petrosal neurons *in situ* (McDonald, 1981; Eyzaguirre and Zapata, 1984; Gonzalez et al., 1994). Chemical transmission at synapses involves the release of transmitters from the presynaptic cell and subsequent binding to postsynaptic receptors. Thus, a local depolarization of postsynaptic membrane or generator potential will be evoked, as seen in a wide variety of sensory nerve endings (Aidley, 1989), including afferent terminals (Hayashida et al., 1980). If generator potentials are produced by chemical transmission, then they should

be inhibited by lowering $[Ca^{2+}]_o$ or blocked by specific antagonists. It is known that the resting discharge and response of superfused carotid bodies to hypoxia *in vitro* are strongly dependent on $[Ca^{2+}]_o$ (Zapata, 1982; Eyzaguirre and Zapata, 1984). Such observations favour the idea of a chemical synapse between glomus cells and sensory nerve endings. The results from co-cultured PN in Chapter 6 of this thesis, suggest that nerve impulses are generated by intermittent depolarizations occurring at petrosal endings, probably due to quantal release of excitatory transmitter(s) from glomus cells.

3.3 The initiation of sensory nerve impulses

The mass response and spike discharge of the carotid body afferent sensory nerve can be studied by extracellular recording from the CSN (Eyzaguirre and Nishi, 1976), but the generator potentials which initiate the discharges at the nerve terminals were difficult to record (Hayashida et al., 1980; Eyzaguirre et al., 1983). Co-cultures, discussed in Chapter 6, provided a novel and attractive preparation for studying mechanisms of chemosensory signaling, including generator potentials. It was found that approximately a quarter of the petrosal neurons formed *de novo* functional connections with neighbouring glomus cell clusters in co-culture based on electrophysiological evidence. The newly-formed junctions between the chemosensors and petrosal neurons (PN) seemed to transmit chemically. Spontaneous potentials were frequently seen in co-cultured PN and had several properties of postsynaptic potentials (PSP) that occur at conventional chemical synapses (Katz, 1969). For example, the PSP persisted even after the action potentials were blocked with tetrodotoxin,

and showed a marked reduction in frequency of occurrence when extracellular calcium was reduced and magnesium elevated. A striking feature of the PSP observed in Chapter 6 was that they resembled the spontaneous depolarizing potentials or SDPs recorded in a few successful cases from petrosal nerve terminals *in situ* (Hayashida et al., 1980). The intervals between successive spontaneous events were well described by an exponential function as expected for a random process. Therefore, the PSP may represent postsynaptic potentials elicited by intermittent release of neurotransmitters from glomus cells.

Petrosal neurons had a resting membrane potential of about -60 mV. Depolarization of the membrane by 10 mV or more results in the production of action potentials which propagate along the axon. We found that the depolarizing potentials, referred to as postsynaptic potentials (PSP) or generator potentials, were often of sufficient size to elicit action potentials in petrosal neurons juxtaposed to glomus cell clusters. There is evidence that generator potentials at many sensory receptors are produced, in part, by an increase in sodium conductance of the membrane (Diamond et al., 1958; Aidley, 1989).

In Chapter 6, the results indicated that nicotinic acetylcholine receptors (nAChR) mediated, at least part of, the spontaneous subthreshold potentials (SSP) and hypoxia-induced PSP. The nicotinic AChR are cation permeable ligand-gated channels (Sargent, 1993; McGehee and Role, 1995), and their opening results in an inward current and local depolarization, which can in turn activate voltage-gated sodium channels and trigger action potentials. In Chapter 3, we showed directly, by fast perfusion or "puffing" of ACh, that nAChR mediate excitatory effects (depolarization and/or action potentials) in rat petrosal

neurons. The intensity of the response is related to the concentration of ACh over the range 5 to 1000 μM . This result is consistent with previous *in vivo* or *in vitro* electrophysiological and biochemical studies in the carotid body. These studies showed that the frequency of action potentials is related to the intensity of the stimulus, which is proportional to glomus cell secretion as measured by catecholamine release (Gonzalez et al., 1994). Therefore, our results favour the notion that the hypoxic sensory information is converted into a frequency code of action potentials in the nerve fibers via transmitter release from chemoreceptors onto apposed petrosal nerve endings. The excitatory transmitter, however, did not appear to be the well-studied dopamine, since the D_2 -receptor blocker, spiperone, did not markedly affect the postsynaptic response to hypoxia.

In this thesis, the experimental data cannot rule out the possibility of electrical coupling between chemoreceptors and petrosal neurons. As shown in Chapter 6, the hypoxia-induced activity in the neuron could be substantially blocked by a specific cholinergic antagonist (hexamethonium), and there was other circumstantial evidence indicating chemical synapses played an important role in chemotransmission. We infer that electrical coupling, if present, may not play a critical role in hypoxic signaling. It was recently suggested that gap junctions (which mediate electrical coupling) are present between glomus cells and petrosal nerve endings in the rat carotid body *in situ* (Kondo and Iwasa, 1996).

4. Acetylcholine (ACh) and its receptors

As discussed in Chapter 6, an interesting feature of the co-cultures was that in many

cases a physiological stimulus, hypoxia, was transduced and relayed to an afferent neuron in the form of depolarization and superimposed spike activity. Neurotransmitters are expected to be involved in this process. When considering a substance as a transmitter, the following criteria should be satisfied: (i) the presynaptic cell should store and synthesize it; (ii) the substance should be released in amounts sufficient to exert its supposed action on stimulation; (iii) application of the substance exogenously to the postsynaptic cell should mimick the effects of normal transmission; and (iv) the action of the substance on the postsynaptic cells should be affected by competitive antagonists blockers in the same way as synaptic transmission (Aidley, 1989). It was difficult during this thesis to demonstrate experimentally all of these features at the newly-formed synapses in culture. However, these criteria will be considered in the following paragraphs where putative carotid body transmitters are discussed.

4.1 Excitatory effects of ACh in the carotid body

Experimental data have demonstrated that the glomus cells of the carotid body contain choline acetyltransferase, the ACh biosynthetic enzyme, as well as ACh (Eyzaguirre et al., 1965; Fidone et al., 1977). The latter can be released on stimulation and exerts chemosensory excitation when applied exogenously (Eyzaguirre and Zapata, 1984). Hence, it was hypothesized that the neurotransmitter ACh released from glomus cells contributes significantly to petrosal neuron depolarization and excitation during hypoxia. The idea has been addressed recently by Fitzgerald and Shirahata (1994) who reported that hypoxia-

induced ACh release from glomus cells of cat, and hypoxic signaling in the carotid body are inhibited by cholinergic blockers. In Chapter 3 we demonstrated that ACh depolarizes and excites > 60% of petrosal neurons and that the effect is mediated via hexamethonium-sensitive, nicotinic ACh receptors (nAChR).

4.2 Involvement of nAChR in hypoxic chemosensory transmission

In co-cultures, ACh contributes, at least in part, to the spontaneous PSP or generator potential, since hexamethonium suppressed the spontaneous activity and the hypoxia-evoked response recorded from postsynaptic petrosal neurons (see Chapter 6). These results strongly suggest that ACh released from glomus cell contributes significantly to chemosensory signaling. However, ~ 32% of all petrosal neurons tested (n=109) failed to respond to ACh applied to their cell bodies. This suggests that cholinergic-insensitive neurons in the cultures were viable but probably did not take part in functional associations with glomus cells. Whether these represent petrosal neurons that would have normally innervated other targets *in vivo*, but were carried into culture is presently unknown. A most recent electrophysiological study from our laboratory showed evidence that suramin-sensitive P_{2X} -like receptors, which are ligand-gated cation channels regulated by extracellular ATP, were present in all PN tested (n=41, unpublished observation). As mentioned in Chapter 6, hexamethonium, a nAChR antagonist, could only partially block hypoxia-induced responses in many co-cultures even at high concentrations. However, in our most recent experiments, hexamethonium combined with suramin completely blocked the hypoxia-induced responses

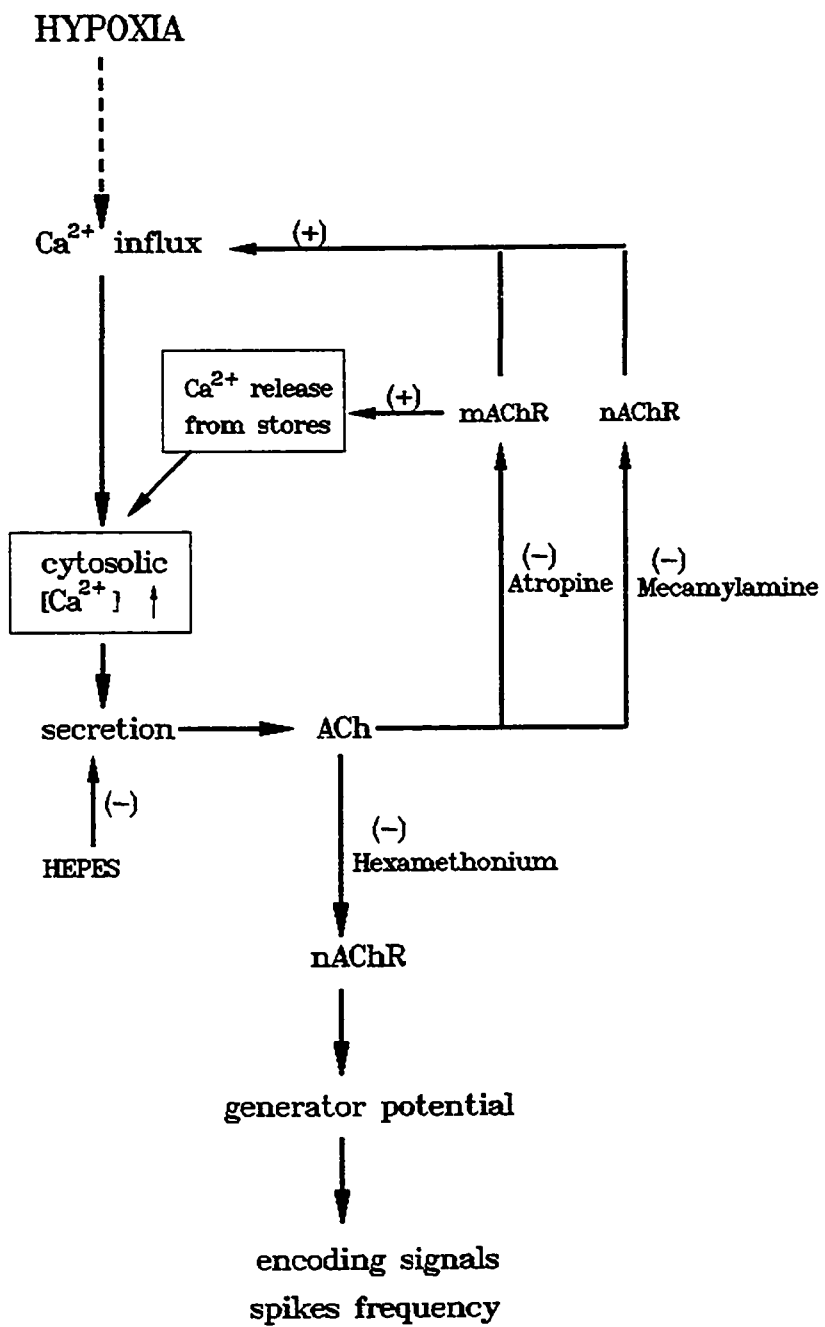
(n=5, unpublished observation) in petrosal neurons, suggesting ATP and ACh are cotransmitters involved in hypoxic signaling in co-culture.

4.3 Are AChRs on glomus cells mediators of positive feedback?

In addition to the evidence for ACh as an excitatory transmitter released from glomus cells onto petrosal nerve endings, there is growing evidence that ACh may act directly on autoreceptors on glomus cells. Both nicotinic and muscarinic acetylcholine receptors have been found in glomus cells of rabbit (Dinger et al., 1985; Dinger et al., 1986). Moreover, we recently confirmed the previous report by Wyatt and Peers (1993) that nicotinic agonists evoke an inward current and cause depolarization in isolated rat glomus cells (Zhong and Zhang; unpublished observations; see also Dasso et al., 1997). An important feature of neuronal nicotinic ACh receptors (nAChR) is their permeability to calcium, which is more pronounced for some nAChR than for others (McGehee and Role, 1995). With regards to the carotid body, there is evidence that cholinergic agonists evoke Ca^{2+} influx in glomus cells and raise $[\text{Ca}^{2+}]_i$ (Pietruschka, 1985; Peers and Buckler, 1995). The mechanisms responsible for this increase of $[\text{Ca}^{2+}]_i$ appear to involve both nicotinic and muscarinic receptors during application of ACh (Dasso et al., 1997). The chemotransduction of physiological stimuli in glomus cells is considered to involve a rapid increase in $[\text{Ca}^{2+}]_i$ (Buckler and Vaughan-Jones, 1994; Gonzalez et al., 1994; Lopez-Barneo, 1996), which promotes neurosecretion and excitation of afferent nerve endings. In this respect, the activation of nicotinic and muscarinic receptors increases $[\text{Ca}^{2+}]_i$ that coupled at least partially to glomus cell secretion. Therefore

Figure 7.3 Schematic diagram of proposed hypoxia transduction, neurosecretion and ACh function.

Hypoxia induces a rise of $[Ca^{2+}]_i$ in the glomus cell via Ca^{2+} influx from the external medium (top dotted arrow) and release from intracellular stores. Consequently neurosecretion is enhanced, but HEPES buffer can inhibit secretion (see Chapter 6). The ACh released from the chemoreceptors will cross the synaptic cleft, bind to nAChRs on petrosal terminals and cause membrane depolarization with increased spike activity. This postsynaptic response can be suppressed by hexamethonium. The released ACh may act directly upon the nAChR on the same or neighbouring glomus cells and lead to an increase in $[Ca^{2+}]_i$ via Ca^{2+} influx from the external medium or from internal stores. Thus, autoreceptors for ACh could mediate a positive feedback excitation of glomus cells during hypoxic chemoreception.



it is speculated that ACh may also act in an autocrine or paracrine manner as an excitatory transmitter within clusters of glomus cells. Chemical synapses between neighbouring glomus cells have been observed in the electron microscope (McDonald and Mitchell, 1975; McDonald, 1981). The possible mechanisms by which ACh affects carotid body chemoreceptors are presented in Figure 7.3.

5. Putative excitatory neurotransmitters/neuromodulators

5.1 The effects of 5-HT in the carotid body

5-HT has been known as an excitatory neurotransmitter in the carotid body *in situ* (Nishi, 1975), and its effects appeared to be mediated by the 5-HT₃ receptor (Kirby and McQueen, 1984). Chapter 4 of this thesis demonstrated that 5-HT₃ receptors are present on approximately 46 % of petrosal neurons tested. 5-HT₃ receptors are known to be ligand-gated cation-selective channels and mediate a rapid depolarization in this and other preparations (Jackson and Yakel, 1995). In petrosal neurons the 5-HT-induced depolarization was often accompanied by spike activity, suggesting 5-HT could act as an excitatory neurotransmitter, if it was released from glomus cells during stimulus application. However, in a preliminary study MDL-72222, a specific 5-HT₃ receptor blocker, did not block the hypoxia-induced responses in co-culture (see Appendix 2). These results, though preliminary, suggest that 5-HT is less likely to be a dominant mediator of hypoxic excitation, but probably a regulator of the function of other neurotransmitters, e.g. ACh (see Chapter 6), as described in other systems (Garcia-Colunga and Miledi, 1995; Schrattenholz et al., 1996). Another possibility

is that *in vivo* the 5-HT₃ receptors are located outside of the petrosal neuron-glomus cell synapses, e.g. the axon or cell body, and thus regulated by 5-HT from sources other than glomus cells, such as mast cells or serum.

It should be noted, however, that glomus cells also responded to 5-HT as shown in Chapter 4 of this thesis. Among 20 glomus cells tested, 14 cells responded to exogenous 5-HT with a rapid membrane depolarization; in a few cases (n=4), action potentials were superimposed and probably arose from Ca²⁺ spikes, since Na⁺ spikes are rare in these cells (Stea and Nurse, 1991a). The 5-HT-induced depolarization of glomus cells was associated with a conductance *decrease*, which is opposite from the 5-HT response in petrosal neurons. The depolarization and spike activity may result in enhanced secretion due to a rise of [Ca²⁺]_i following entry via voltage-gated Ca²⁺ channels. In light of this, the 5-HT induced response in glomus cells appears excitatory, and is mediated via 5-HT₂ receptors since ketanserin, a 5-HT₂ receptor-specific antagonist, blocked the 5-HT induced response in all cases tested (n=3). Under voltage-clamp, 5-HT suppressed an outward K⁺ current even in calcium-free medium, suggesting that the 5-HT sensitive current is not a calcium-dependent K⁺ current, a known component of the O₂-sensitive K⁺ current in these cells (Chapter 4 of this thesis; Peers, 1990; Wyatt and Peers, 1995). This could amplify overall K⁺ suppression, membrane depolarization and neurosecretion, if 5-HT, released by hypoxia after closure of Ca²⁺-dependent K⁺ channels, acted *in situ* in an autocrine or paracrine manner. The mechanisms linking 5-HT₂ receptor to K⁺ channel closure are not clear. Results obtained in this thesis are consistent with PKC involvement since in two cases, PKC agonist (1-oleoyl-2-acetyl-glycerol

or OAG) mimicked the effects of 5-HT on glomus cells. Previous reports have demonstrated that 5-HT could inhibit different kinds of K^+ channels e.g. calcium-dependent K^+ channel (Walsh and Byrne, 1989; Wikstrom et al., 1995), S-type K^+ channel (Ks) (Siegelbaum et al 1982; Hille, 1992) and hyperpolarization-activated inward rectifier (I_h) (Boker and William, 1989; Takahashi and Berger, 1990). It was shown that the 5-HT₂ receptors were coupled to G_q protein and then activated the phospholipase C (PLC), diacylglycerol (DAG), protein kinase C (PKC) pathway (Nicoll et al., 1990; Hille, 1992) which may lead to phosphorylation and closure of K^+ channels (Stevens et al., 1992; Bobker, 1994). In addition, recent experimental data show that G proteins are present in carotid body chemoreceptor tissue, and they seem to be coupled to transduction and/or transmission of the hypoxic stimulus (Prabhakar et al., 1995). Therefore, it is hypothesized that during chemostimulation 5-HT excites the carotid body through at least two pathways. The first involves ligand-gated channels, i.e. 5-HT₃ receptors, located on the postsynaptic membrane of petrosal afferent terminals. The second pathway requires activation of 5-HT₂ autoreceptors, which consequently suppress an outward K^+ current, which is distinct from the one (i.e. Ca^{2+} -dependent K^+ current) suppressed by hypoxia.

5.2 Substance P and NK-1 receptors

During the course of this thesis, a fast transient K^+ current (I_A) was identified in approximately one-half (n= 66) of petrosal neurons tested (Appendix 4B). However, in previous electrophysiological studies, I_A was not observed in rat petrosal neurons (Stea and

Nurse, 1992). The reasons for missing I_A may be partially due to: (i) the use of younger animals, (ii) recording techniques, for example the holding potentials were not hyperpolarized enough (in most cases at -60 mV), and/or (iii) the command voltage pulses were too short (in most cases 50 ms). Interestingly, substance P (SP) was found to suppress the outward K^+ current (mainly I_A) and increase excitability of co-cultured rat petrosal neurons (see Appendix 3, 4). In a few cases ($n=4$), SP shifted the activation curve of I_A to more depolarized potentials (Appendix 4C). Whereas SP suppression of several K^+ currents has been demonstrated in many neurons (Nicoll et al., 1990), there have been no previous reports of SP affecting the fast transient K^+ current (I_A). Notably, SP had no obvious effects on the resting membrane potential of petrosal neurons ($n=18$) or glomus cells ($n=4$) cultured alone. Only in co-culture, where petrosal neurons are near a major target, i.e. glomus cells, can SP increase the spontaneous activity (21/36 cases tested), indicating the excitatory effects of SP require the existence of presynaptic chemoreceptors. Previous studies using mRNA *in situ* hybridization in rat carotid body have shown that SP mRNA and SP receptor mRNA were abundant in petrosal neurons, but not detectable in glomus cells (Gauda and Gerfen, 1996). These data suggest that SP effects were likely to be postsynaptic. It is proposed here that SP enhances the excitability of co-cultured petrosal neurons mainly via a postsynaptic mechanism, i. e. suppression of an A-type K^+ current, I_A , that activates at more depolarized potentials. In co-culture, the glomus cells spontaneously release neurotransmitters onto the apposed petrosal neurons causing spontaneous postsynaptic potentials (SPP) as described in Chapter 6 of this thesis. Following SP suppression of I_A , SPP can more easily reach the action

potential threshold due to reduced K^+ efflux. The preliminary data from these experiments suggest that SP might be an excitatory neuromodulator rather than a main transmitter during chemosensory signaling. An alternative explanation for the excitatory effects of SP on the carotid body is that SP may act on unknown SP receptors on glomus cells and cause release of neurotransmitters which modulate firing of petrosal neurons (see below).

In certain sensory systems, SP has been considered as a putative neurotransmitter released from primary afferents and appears to depolarize neurons by decreasing K^+ currents (Nicoll et al., 1990). Studies on the carotid body demonstrate that SP is present in glomus tissue of rat (Pouncet et al., 1996), cat (Prabhakar et al., 1989), and rabbit (Hanson et al., 1986). Glomus cells of the cat can synthesize SP and the enzyme responsible for its hydrolysis (neutral endopeptidase) is also present in the tissue (Prabhakar et al., 1989; Kumar et al., 1990). Exogenous application of SP stimulates carotid body activity in cat (McQueen, 1980; Prabhakar et al., 1993), rat (Cragg et al., 1994) and rabbit (Gallagher et al., 1985) and the excitatory responses seem to be mediated by NK-1 receptors, since the effects can be prevented by the SP receptor (NK-1) antagonist, spantide (Prabhakar, 1994). Thus, the effects of SP in the carotid body appear excitatory, and consistent across species, based on studies described thus far (Prabhakar, 1994; see however Bisgard et al., 1994). Using more specific pharmacological reagents, the role of SP in the carotid body response to chemical stimuli is being re-investigated. Administration of peptidyl SP antagonists (for NK-1 receptor, spantide and DPDT-SP), at doses that blocked the excitatory effects of exogenous SP, markedly attenuated the chemosensory response to hypoxia in the cat and rat (Prabhakar,

1994). However, SP antagonist had no effect on the carotid body response to hypercapnia or other excitatory stimuli (Prabhakar et al., 1993; Cragg et al., 1994). These studies provide evidence that endogenous SP is coupled to hypoxic excitation of the carotid body via NK-1 receptors, but not hypercapnic excitation. The location of NK-1 receptors and the underlying mechanisms which couple the receptors to chemosensory function have not been established. Previous reports suggest that SP may act directly on glomus cells. For instance, Prabhakar (1994) found exogenous SP increases intracellular Ca^{2+} of glomus cells isolated from the rat carotid body. Eyzaguirre and colleagues (1990) observed a SP-induced depolarization in 69% of cat glomus cells. It appears that SP may act on the glomus cell itself and play a positive feedback role via an autocrine or paracrine pathway. In other preparations, SP has been shown to modulate the electrophysiology of post-synaptic neurons via a second messenger pathway (Nicoll et al., 1990). An effect of SP on post-synaptic petrosal neurons was also observed in the present preliminary study, but the second messengers involved are still unknown. Thus the effects of SP in the carotid body seem to be complex and further studies are required.

6. Putative inhibitory neurotransmitters/neuromodulators

6.1 GABA_A receptors on petrosal neurons

GABA is another putative inhibitory neurotransmitter and has been shown to exist in glomus cells of the mouse carotid body based on immunocytochemical staining (Oomori et al., 1994). In Chapter 5 of this thesis, ~ 84% of rat petrosal sensory neurons (n = 90) had

bicuculline-sensitive GABA_A receptors. Application of GABA or GABA_A agonist (muscimol) caused a rapid depolarization of petrosal neurons associated with an increase in membrane conductance. Under voltage-clamp, GABA induced an inward current at a holding potential of -60 mV. During perfusion, GABA inhibited the spike discharge induced by depolarizing stimuli, suggesting an inhibitory effect on the sensory neuron, possibly via a shunting mechanism (see Chapter 5). The GABA_A receptor has been characterized as a Cl⁻-selective anion channel (MacDonald and Olsen, 1994), with reversal potential equal to Cl⁻ equilibrium potential (E_{Cl}). Therefore, its physiological function also depends on the concentration gradient of Cl⁻ across the cell membrane. Depending on the type of neurons and developing stage, GABA_A receptors could mediate hyperpolarization or depolarization according to location of E_{Cl} relative to the resting potential. In adult neurons, GABA_A receptors play an inhibitory role through hyperpolarizing the membrane potential (Aidley, 1989; MacDonald and Olsen, 1994; Rohrbough and Spitzer, 1996), or depolarizing the membrane while shunting the excitatory input (Staley and Mody, 1992). However, recent studies show that GABA_A receptors could mediate excitation in rat hippocampal (Gaiarsa et al., 1995) and hypothalamamic neurons (Chen et al., 1996) at early development stages. This excitatory response becomes inhibitory in adult because the intracellular level of Cl⁻ varies during development (Rohrbough and Spitzer, 1996). In the present study (Chapter 5), 1-2 week-old pups were used and > 95% of cells showed inhibitory responses to GABA. In the adult rat, probably all petrosal neurons will show inhibitory responses to GABA assuming adult levels of intracellular Cl⁻ (Rohrbough and Spitzer, 1996). The physiological significance of GABA

in carotid body chemosensory function has not yet been established and further studies are required.

6.2 Dopamine and D₂ receptors

There is little doubt that dopamine is the most abundant and also the most extensively studied neurotransmitter in the carotid body. More than 90% of glomus cells contain dopamine and its rate-limiting synthetic enzyme, tyrosine hydroxylase. Additionally, dopamine is released from carotid body during hypoxia in a calcium-dependent manner, and release is well correlated with hypoxic stimulation (Gonzalez et al., 1994). But its physiological significance in chemotransmission is still debatable. Because of its abundance and its release by hypoxia, it has been proposed that dopamine may mediate chemosensory excitation. However, many of the pharmacological studies suggest that dopamine is in fact an inhibitory transmitter in the carotid body (Fidone and Gonzalez, 1986; Prabhakar, 1994). Exogenous administration of dopamine was mostly inhibitory to carotid body sensory discharge in cats, dogs, and rabbits (Fidone and Gonzalez, 1986). On the other hand, using *in vitro* preparations Monti-Bloch and Eyzaguirre (1980) found that dopamine augmented the chemosensory discharge in rabbits. Recently Buerk and Lahiri (1993), working with cat carotid bodies, found that dopamine release coincided with the neural response to hypoxia. However, Donnelly (1996) observed no apparent relation between dopamine release and chemosensory discharges by hypoxia in the rat. Similarly, Iturriaga et al. (1996) measured the chemosensory discharges and dopamine release during hypoxia and found that dopamine release was not

essential for hypoxia-induced chemosensory excitation in the cat carotid body. Accordingly, dopamine may act as a "modulator" of the chemosensory response, and its presence in the carotid body may be required for maintaining proper chemosensitivity. This might be achieved through modulation of ionic permeability or receptor expression in the sensory terminals, and this could regulate the sensitivity to released transmitters. Alternatively, dopamine might act on the chemoreceptor glomus cell itself, as discussed later.

In Chapter 6, our results did not favour the idea that dopamine mediates hypoxic chemoexcitation since D₂ receptor blockade did not block the hypoxic response in co-culture. However, D₂ receptors are present on petrosal neurons in culture since many (> 60%; 261/413) of them express the D₂ receptor, based on the binding of a fluorescent D₂ receptor ligand, N-(p-aminophenethyl) spiperone, or bodipy-NAPS (unpublished observations by Zhong and Vollmer). In a preliminary study we found that approximately 30% of petrosal neurons (21/69) responded to perfusion of dopamine with slight depolarization, and in most cases there was no obvious change in membrane conductance. In a few cases (n= 6), the depolarization was accompanied by a conductance decrease (see Appendix 5D), but no action potentials were seen. However, we did find that dopamine suppressed the spike activity triggered by depolarizing stimuli (n=4; Appendix 5 A-C). Also, dopamine had no detectable effect on I_h (n=4; not shown), a current known to regulate spike frequency in many excitable cells and characterized in detail (for petrosal neurons) in Chapter 2 of this thesis. These preliminary data favour the idea that dopamine may play an inhibitory role in the carotid body. Furthermore, blockade of dopaminergic receptors by haloperidol or domperidone increases

the baseline activity and potentiates the sensory response to hypoxia in cat carotid body (Lahiri et al., 1980; Tomares et al., 1994), suggesting endogenous dopamine release *in situ* may play an inhibitory role. Several other studies suggest that dopamine may have a dual action on the carotid body, namely, an initial inhibition and a subsequent excitation (Prabhakar, 1994).

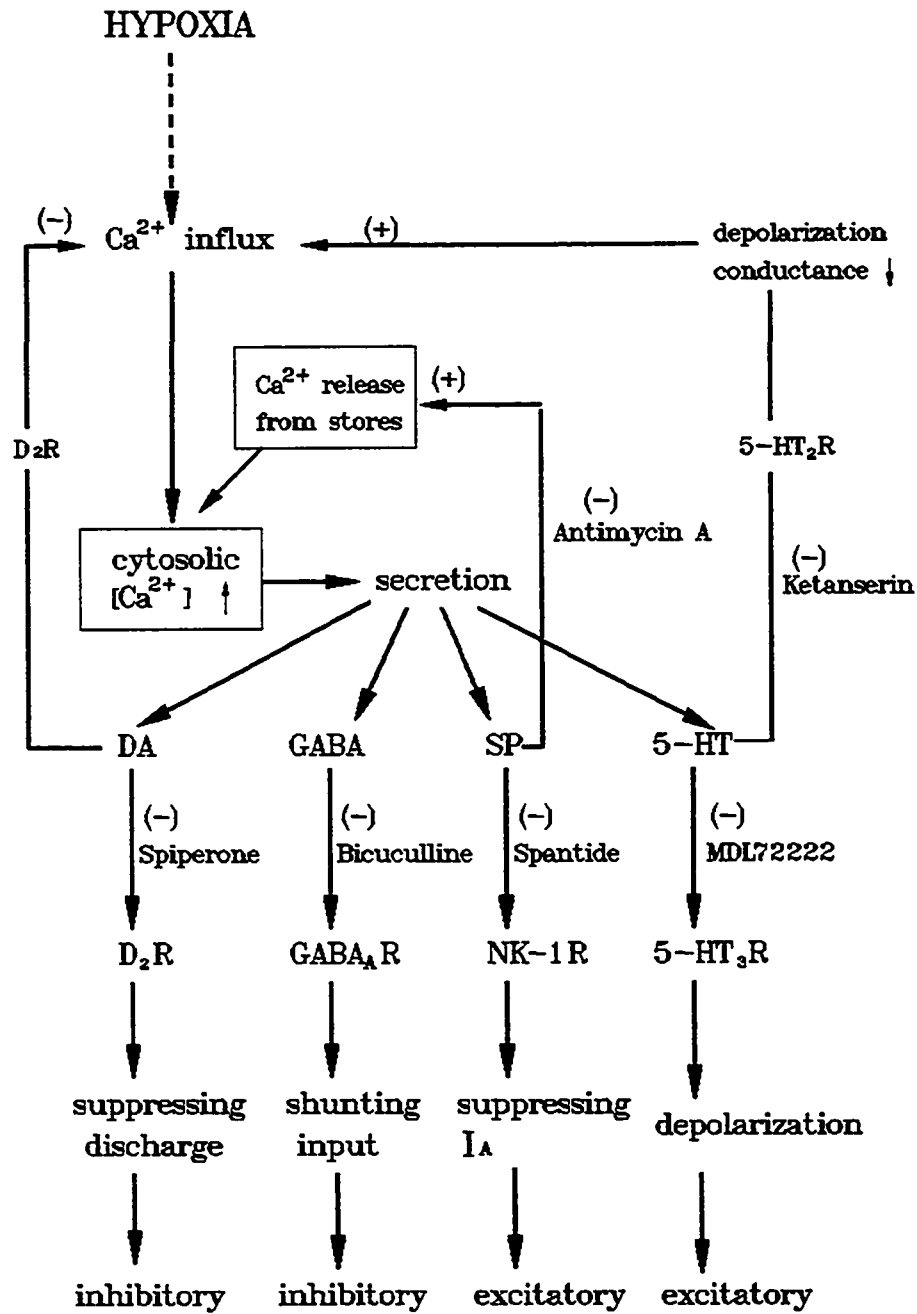
Taken together, these data indicate that the effects of dopamine on the carotid body are complex. This complexity could be due to its action on multiple dopaminergic receptors and/or their locations. With regards to the carotid body, D₂ receptors have been demonstrated both on glomus cells (presynaptic) and afferent sensory neurons (postsynaptic) by binding, *in situ* hybridization and functional studies (Dinger et al., 1981; Mir et al., 1984; Schamel and Verna, 1993). It is known that glomus cells have autoreceptors for catecholamines (Dinger et al., 1981), and their physiological role appears inhibitory since exogenous dopamine attenuated CSN activity (Fidone and Gonzalez, 1986). Further, the calcium current in rabbit glomus cells was inhibited by dopamine in voltage-clamp studies (Benot and Lopez-Barneo, 1990). These findings suggest that dopamine, secreted in response to carotid body chemostimuli, regulates Ca²⁺ influx and depresses further transmitter release. In this way, the chemoresponse of the glomus cells could be down-regulated by feedback action of their own secretory products. The modulation of Ca²⁺ channels by dopamine may have special physiological significance in situations of intense stimulation, when released dopamine may limit the amount of Ca²⁺ entry and thus prevent calcium overload or toxicity of the chemoreceptors. Thus far, the physiological significance of D₂ receptors on petrosal neurons

or glomus cells in chemotransduction is still unclear, and *in vivo* other subtypes of dopaminergic receptors (e.g. D₁ receptors on blood vessels) may contribute to the overall response of the organ to blood-borne stimuli (Gonzalez et al., 1994). A flow diagram in Figure 7.4 summarizes the effects of various carotid body neurotransmitters.

In summary, it is concluded that petrosal neurons possess ion channels that mediate I_h and I_A, in addition to I_{Na+}, various I_{K+} and I_{Ca2+}. The I_h may be related to the regulation of spike frequency during a hypoxic stimulus. Nicotinic AChR and 5-HT₃ receptors reside on a subpopulation of petrosal neurons and both mediate excitatory responses. Acute hypoxia inhibits a leak K⁺ current and I_{K(Ca)} and depolarizes chemoreceptor glomus cells of rat carotid body, though the majority of petrosal neurons do not appear to be affected directly by hypoxia. In co-culture, hypoxia induces glomus cells to release neurotransmitters onto 'juxtaposed' petrosal neurons. Consequently, the neuron is excited and in this way a hypoxic stimulus is transduced and coded as a change in spike frequency. Hexamethonium suppresses the hypoxia-induced responses suggesting ACh is a transmitter involved in chemosensory transmission. As nAChR, dopamine D₂ receptors, and 5-HT receptors also reside in a subpopulation of glomus cells, it is possible that the CB chemosensory responses are regulated via autocrine and/or paracrine mechanisms. SP can excite petrosal neurons, probably via inhibition of I_A, while GABA inhibits petrosal neurons by shunting the excitatory input. Dopamine appears inhibitory, though the underlying mechanisms require clarification.

Figure 7.4 Flow diagram summarizing the effects of some carotid body transmitters.

Hypoxia induces a rise of $[Ca^{2+}]_i$ triggering neurosecretion. Dopamine released from the glomus cell can bind to D_2 receptors of the sensory nerve endings and inhibit the spike activity. Alternatively, dopamine may bind to the D_2 receptors of the glomus cell and inhibit the neurosecretion by closing voltage-gated Ca^{2+} channels. If the glomus cell also releases GABA during stimulation, the GABA may bind to the $GABA_A$ receptors located on the sensory neuron and inhibit spike activity. Glomus cell secretes SP which can bind with NK-1 receptors on the petrosal neuron and increase its excitability via inhibition of an I_A current. Alternatively, SP may act on the glomus cell and increase $[Ca^{2+}]_i$. Glomus cells release 5-HT which can bind to $5-HT_3$ receptors on the sensory neuron or bind to $5-HT_2$ receptors on the glomus cell itself. The effects of 5-HT are proposed to be excitatory based on results in Chapter 4.



7. Future directions

The present data and other studies suggest that P_{O_2} can influence the gating properties of K^+ channels in carotid body chemoreceptor cells. A membrane-bound NADPH-oxidase has been proposed as a putative O_2 sensor (Acker et al., 1992). It would be of interest in the future to examine the details of the transduction step. A plausible approach to this study could involve patch-clamp analysis of glomus cells during chemosensory stimulation with/without the subunits of NADPH-oxidase or its inhibitors. There is evidence that NADPH-oxidase is involved in hypoxia sensing in other chemosensory cells. For instance, a NADPH-oxidase inhibitor, diphenylene iodonium (DPI) has been shown to suppress an oxygen-sensitive K^+ current (Youngson et al., 1993) and H_2O_2 , a product of the NADPH-oxidase reaction, enhances a K^+ current in neuroepithelial body (NEB) cells (Wang et al., 1996). This information together with studies on gene knock-out mouse models of NADPH-oxidase subunits may provide a useful approach for the study of the role of this oxidase.

Another direction for future studies could involve a further extension of the use of co-cultures of sensory petrosal neurons and glomus cells. We have already shown that a hypoxic stimulus can be transduced and the electrical events relayed to the opposed neuron via chemical transmission in co-culture (this thesis Chapter 6). ACh has been shown to be an important transmitter for hypoxic signaling. The fact that hypoxia elicited a small depolarization in some co-cultured petrosal neurons, even in the presence of high doses of hexamethonium, suggested other co-released CB excitatory transmitters (e.g. substance P, purines, 5-HT) may participate in the response. This possibility is currently being tested, and

indeed, in preliminary studies ATP also appears to contribute to the hypoxic response (unpublished observation). It has also been proposed that the hypoxic chemosensory mechanism is different from that of hypercapnia and acidity (Gonzalez et al., 1992; Peers and Buckler, 1995). It would be of interest to know whether other established chemoexcitants including, hypercapnia and acidosis, produce the expected increase in discharge in co-cultured neurons as occurs *in vivo*. If this is true, the preparation would be attractive for studying the neurotransmitter(s) involved. These co-cultures could also be used for testing, with pharmacological tools, whether the release of other transmitters such as dopamine, 5-HT, ATP/adenosine, and/or substance P accompany hypoxic signaling.

We have characterized a cation non-selective, hyperpolarization-activated inward current (I_h) in most of the petrosal neurons (Chapter 2). The I_h is thought to regulate action potential firing patterns in other cells. It is likely that this current may control the chemosensory discharge in the carotid body, especially since in a recent study, Doyle and Donnelly (1994) observed that cesium, an I_h blocker, markedly suppressed the afferent nerve discharge due to acute hypoxia. Both current- and voltage-clamp recordings can be used to test whether the inward rectification or I_h in petrosal neurons is affected by exogenously applied neurotransmitters. Some neurotransmitters, including ACh, 5-HT, dopamine, and noradrenaline, have been found to modulate I_h in other cells (McCormick and Pape, 1990b; Harris-Warrick et al., 1995); several of these are known to be present in glomus cells in a variety of species (Gonzalez et al., 1994). In order to avoid intracellular dialysis of second messengers, nystatin perforated patch recording is recommended for these studies since there

is evidence that some of these neurotransmitters act on I_h via intracellular second messengers (McCormick and Pape, 1990b).

References

- Abramovici, A., Pallot, D.J. and Polak, J.M. (1991). Immunohistochemical approach to the study of the cat carotid body. *Acta Anat.* 140:70-74.
- Acker, H., Bolling, B., Delpiano, M.A., Dufau, E., Gorch, A. and Holtermann, G. (1992). The meaning of H₂O₂ generation in carotid body cells for PO₂ chemoreception. *J. Auton. Nerv. Syst.* 41:41-52.
- Acker, H. (1994). Mechanisms and meaning of cellular oxygen sensing in the organism. *Resp. Physiol.* 95:1-10.
- Aidley, D.J. (1989). *The physiology of excitable cells*. Cambridge Univ. Press, New York.
- Alcayaga, J. and Eyzagurre, C. (1990). Electrophysiological evidence for the reconstitution of chemosensory units in co-cultures of carotid body and nodose ganglion neurons. *Brain Res.* 534:324-328.
- Anderson, C.R. and Stevens, C.F. (1973). Voltage clamp analysis of acetylcholine produced end-plate current fluctuation at frog neuromuscular junction. *J. Physiol.* 235:655-691.
- Andreev, A.A., Vepintsev, B.N. and Vulfius, C.A. (1984). Two-component desensitization of nicotinic receptors induced by acetylcholine agonists in *Lymnaea stagnalis* neurons. *J. Physiol.* 353:375-391.
- Archer, S.L. Huang, J.M.C., Reeve, H.L. Hampl, V., Tolarova, S., Michelakis, E. and Weir, E. K. (1996). Differential distribution of electrophysiologically distinct myocytes in conduit and resistance arteries determines their response to nitric oxide and hypoxia. *Circulation Res.* 78:431-442.
- Ashworth-Peece, M., Krstew, E., Jarroitt, B., and Lawrence, A. J. (1997). Functional GABA_A receptors on the rat vagal afferent neurones. *Br. J. Pharmacol.* 120:469-475.
- Baxter, G., Kennett, G., Blaney, F. and Blackburn, T. (1995). 5-HT₂ receptor subtypes: a family re-united? *TIPS* 16:105-110.
- Bayliss, D.A., Viana, F., Bellingham, M.C. and Berger, A.J. (1994). Characteristics and postnatal development of a hyperpolarization-activated inward current in rat hypoglossal motoneurons in vitro. *J. Neurophysiol.* 71:119-128.

- Belmonte, C. and Gallego, R. (1983). Membrane properties of cat sensory neurons with chemoreceptor and baroreceptor endings. *J. Physiol.* 342:603-614.
- Benham, C.D., Bolton, T.B., Denbigh, J.S. and Lang, R.J. (1987). Inward rectification in freshly isolated single smooth muscle cells of the rabbit jejunum. *J. Physiol. Lond.* 383:461-476.
- Benot, A.R. and Lopez-Barneo, J. (1990). Feedback inhibition of Ca²⁺ currents by dopamine in glomus cells of the carotid body. *Eur. J. Neurosci.* 2:809-812.
- Biscoe, T.J., Purves, M.J. and Sampson, S.R. (1970). The frequency of nerve impulses in single carotid body chemoreceptor afferent fibres recorded in vivo with intact circulation. *J. Physiol.* 208:121-131.
- Biscoe, T.J. (1971). Carotid body: structure and function. *Physiol. Rev.* 51:437-491.
- Biscoe, T.J. and Duchen, M.R. (1990). Cellular basis of transduction in carotid chemoreceptors. *Am. J. Physiol.* 258:L271-L278.
- Bisgard, G.E., Mitchell, R.A. and Herbert, D.A. (1979). Effects of dopamine, norepinephrine and 5-hydroxytryptamine on the carotid body of the dog. *Resp. Physiol.* 37:61-80.
- Bisgard, G.E., Pizarro, J., Ryan, M. and Hedrink, M. (1994). Substance P inhibits ventilation in the goat. *Adv. Exp. Med. Biol.* 360:277-281.
- Blanchi, A.L., Denavit-Saubie, M. and Champagnat, J. (1995). Central control of breathing in mammals: Neuronal circuitry, membrane properties, and neurotransmitters. *Physiol. Rev.* 75:1-45.
- Bock, P. (1980). Adenine nucleotides in the carotid body. *Cell Tissue Res.* 206:279-290.
- Bocker, D. H. (1994). A slow excitatory postsynaptic potential mediated by 5-HT₂ receptors in nucleus prepositus hypoglossi. *J. Neurosci.* 14:2428-2434.
- Boker, D.H. and Williams, J.T. (1989). Serotonin augments the cationic current I_h in central neurons. *Neuron* 2:1535-1540.
- Borday, A., Feltz, P. and Trouslard, J. (1996). Patch-clamp characterization of nicotinic receptors in subpopulation of lamina X neurons in rat spinal cord slices. *J. Physiol.* 490:673-678.

- Bormann, J. and Feigenspan, A. (1995). GABA_C receptors. *Trends Neurosci.* 18:515-519.
- Bowman, W.C. and Rand, M.J. (1980). *Text Book of Pharmacology*, 2nd edn, Blackwell Scientific Publications, Oxford, .
- Boyd, J.D. (1937). The development of the human carotid body. *Contrib. Embryol.* 152:1-31.
- Brown, H. and DiFrancesco, D. (1980). Voltage-clamp investigations of membrane currents underlying pacemaker activity in rabbit sino-atrial node. *J. Physiol. Lond.* 308:331-351.
- Buckler, K.J., Vaughan-Jones, R.D., Peers, C., Lagadic-Gossman, D. and Nye, P.C.G. (1991). Effects of extracellular pH, Pco₂ and HCO₃⁻ on intracellular pH in isolated type-I cells of the neonatal rat carotid body. *J. Physiol.* 444:703-721.
- Buckler, K.J. and Vaughan-Jones, R.D. (1994). Effects of hypercapnia on membrane potential and intracellular calcium in rat carotid body type I cells. *J. Physiol.* 478:157-171.
- Buckler, K.J. (1997). A novel oxygen-sensitive potassium current in rat carotid body type I cells. *J. Physiol.* 493:649-662.
- Buerk, D.G., Nair, P.K. and Whalen, W.J. (1989). Evidence for second metabolic pathway for O₂ from PO₂ measurements in denervated cat carotid body. *J. Appl. Physiol.* 67:1578-1584.
- Buerk, D.G. and Lahiri, S. (1993). Detecting dopamine release in cat carotid body in response to hypoxia using nafion, thin-film coated recessed microelectrodes. *FASEB J.* 7:3661.
- Burnstock, G. (1990). Co-transmission. *Arch. Int. Pharmacodyn Ther.* 304:7-33.
- Cardenas, H. and Zapata, P. (1981). Dopamine-induced ventilatory depression in the rat mediated by carotid nerve afferents. *Neurosci. lett.* 24:29-33.
- Carpenter, E. and Peers, C. (1996). Swelling-, cAMP- and acidosis-induced chloride currents recorded from isolated rat carotid body type I cells. *International meetings on biology.* Madrid, Spain.
- Chen, G., Trombley, P. Q. and van den Pol, A. N. (1996). Excitatory actions of GABA in developing rat hypothalamic neurones. *J. Physiol.* 494:451-464.

Cherubini, E., Gaiarsa, J.L. and Ben-Ari, Y. (1991). GABA: an excitatory transmitter in early postnatal life. *Trends Neurosci.* 14:515-519.

Colquhoun, D. and Ogden, C.D. (1988). Activation of ion channels in the frog end-plate by high concentration of acetylcholine. *J. Physiol.* 395:131-159.

Conover, J.C., Erickson, J.T., Katz, D.M., Bianchi, L.M., Poueymirou, W.T., McClain, J., Pan, L., Helgren, M., Ip, N.Y., Boland, P., Friedman, B., Wiegand, S., Vejsada, R., Kato, A.C., DeChiara, T.M. and Yancopoulos, G.D. (1995). Neuronal deficits, not involving motor neurons, in mice lacking BDNF and/or NT4. *Nature* 375:235-240.

Constanti, A. and Galvan, M. (1983). Fast inward-rectifying current accounts for anomalous rectification in olfactory cortex neurons. *J. Physiol. Lond.* 335:153-178.

Cooper, E., Couturier, S. and Ballivet, M. (1991). Pentameric structure and subunit stoichiometry of a neuronal acetylcholine receptor. *Nature* 350:235-238.

Cooper, E. and Lau, M. (1986). Factors affecting the expression of acetylcholine receptors on rat sensory neurons in culture. *J. Physiol.* 377:409-420.

Cragg, P.A., Runold, M., Kou, Y.R. and Prabhakar, N.R. (1994). Tachykinin antagonists in carotid body responses to hypoxia and substance P in the rat. *Resp. Physiol.* 95:295-310.

Crepel, F. and Penit-Soria, J. (1986). Inward rectification and low threshold calcium conductance in rat cerebellar Purkinje cells. *J. Physiol. Lond.* 372:1-23.

Cross, A.R., Henderson, L., Jones, O.T., Delpiano, M.A., Hentschel, J. and Acker, H. (1990). Involvement of a NADPH oxidase as a PO₂ sensor protein in the rat carotid body. *Biochem. J.* 272:743-747.

Dasso, L.L.T., Buckler, K.J. and Vaughan-Jones, R.D. (1997). Muscarinic and nicotinic receptors raise intracellular Ca²⁺ levels in rat carotid body type I cells. *J. Physiol.* 498:327-338.

De Castro, F. (1928). Nuevas observaciones sobre la inervación de la región carotídea. Los quimioy prosorreceptores. *Trab. Lab. Invest. Biol. Univ. Madrid* 32: 297-384.

De Castro, F. and Rubio, M. (1968). The anatomy and innervation of the blood vessels of the carotid body and the role of chemoreceptive reactions in the autoregulation of the blood flow. In: *Arterial Chemoreceptors*. Edited by R.W. Torrance. Oxford, England, Blackwell Sci. Publns. pp 267-277.

- Delpiano, M.A. and Hescheler, J. (1989). Evidence for a Po_2 -sensitive K^+ channel in the type I cell of the rabbit carotid body. *FEBS Lett.* 249: 195-198.
- Demsey, J.A. and Forster, H.V. (1982). Mediation of ventilation adaptations. *Physiol. Rev.* 62:262-364.
- Derkach, V., Surorenant, A. and North, R.A. (1989). 5HT_3 receptors are membrane ion channels. *Nature* 339:707-709.
- Deschenes, M., Feltz, P. and Lamour, Y. (1976). A model for an estimate in vivo of the ionic basis of presynaptic inhibition: an intracellular analysis of the GABA-induced depolarization in rat dorsal root ganglia. *Brain Res.* 118:486-493.
- Diamond, J. (1955). Observations on the excitation by acetylcholine and by pressure of sensory neurons in the cat carotid sinus. *J. Physiol.* 130:513-532.
- Diamond, J., Gray, J.A.B. and Inman, D.R. (1958). The relation between receptor potentials and the concentration of sodium ions. *J. Physiol.* 142:382-394.
- DiFrancesco, D., Ferroni, A., Mazzanti, M. and Tromba, C. (1986). Properties of the hyperpolarizing-activated current (i_f) in cells isolated from the rabbit sino-atrial node. *J. Physiol. Lond.* 377:61-88.
- DiFrancesco, D. (1981). A new interpretation of the pace-maker current in calf Purkinje fibers. *J. Physiol. Lond.* 314:359-376.
- DiFrancesco, D. and Tromba, C. (1988). Inhibition of the hyperpolarization-activated current (i_f) induced by acetylcholine in rabbit sino-atrial node myocytes. *J. Physiol. Lond.* 405:477-491.
- Dilger, J.P. and Lui, Y. (1992). Desensitization of acetylcholine receptors in BC3-H1 cells. *Pflügers Arch.* 420:479-485.
- Dinger, B., Gonzalez, C., Yoshizaki, K. and Fidone, S. (1981). $[3\text{-H}]\text{-spiroperidol}$ binding in normal and denervated carotid bodies. *Neurosci. Lett.* 21:51-55.
- Dinger, B., Gonzalez, C., Yoshizaki, K. and Fidone, S. (1985). Localization and function of cat carotid body nicotinic receptors. *Brain Res.* 339:295-304.
- Dinger, B., Hirano, G.T. and Fidone, S. (1986). Autoradiographic localization of muscarine receptors in rabbit carotid body. *Brain Res.* 367:328-331.

- Dinger, B., Almaraz, L., Hirano, T., Yoshizaki, K., Gonzalez, C, Gomez-Nino, A. and Fidone, S.J. (1991). Muscarinic receptor localization and function in rabbit carotid body. *Brain Res.* 562:190-198.
- Docherty, R.J. and McQueen, D.S. (1978). Inhibitory action of dopamine on cat carotid chemoreceptors. *J. Physiol.* 279:425-436.
- Donnelly, D.F. (1993). Electrochemical detection of catecholamine release from rat carotid body in vitro. *J. Appl. Physiol.* 74:2330-2337.
- Donnelly, D.F. (1995). Does catecholamine secretion mediate the hypoxia-induced increase in nerve activity? *Biol. Signals* 4:304-309.
- Donnelly, D.F. (1996). Chemoreceptor nerve excitation may not be proportional to catecholamine secretion. *Am. J. Physiol.* 81: 657-664.
- Doyle, T.P. and Donnelly, D.F. (1994). Effect of Na⁺ and K⁺ channel blockade on baseline and anoxia-induced catecholamine release from rat carotid body. *J. Appl. Physiol.* 77:2606-2611.
- Drapeau, P. and Nachshen, D.A. (1988). Effects of lowering extracellular and cytosolic pH on calcium fluxes, cytosolic calcium levels, and transmitter release in presynaptic nerve terminals isolated from rat brain. *J. Gen. Physiol.* 91:305-315.
- Duchen, M.R. and Biscoe, T.J. (1992). Relative mitochondrial membrane potential and [Ca²⁺]_i in type I cells isolated from the rabbit carotid body. *J. Physiol.* 450:33-61.
- Ebihara, S., Shirato, K., Harata, N. and Akaike, N. (1995). Gramicidin-perforated patch recording: GABA response in mammalian neurons with intact intracellular chloride. *J. Physiol.* 482:77-86.
- Edmonds, B., Gibb, A.J. and Colquhoun, D. (1995). Mechanisms of activation of muscle nicotinic acetylcholine receptors and the time course of endplate current. *Ann. Rev. Physiol.* 57:469-93.
- Eyzaguirre, C. and Koyano, H. (1965a). Effects of hypoxia, hypercapnia, and pH on the chemoreceptor activity of the carotid body in vitro. *J. Physiol.* 178:385-409.
- Eyzaguirre, C. and Koyano, H. (1965b). Effects of some pharmacological agents on chemoreceptor discharges. *J. Physiol.* 178: 410-437.
- Eyzaguirre, C., Koyano, H. and Taylor, J.R. (1965). Presence of acetylcholine and

transmitter release from carotid body chemoreceptors. *J. Physiol.* 178:463-476.

Eyzaguirre, C. and Zapata, P. (1968). The release of acetylcholine from carotid body tissues. Further study on the effects of acetylcholine and cholinergic blocking agents on the chemosensory discharge. *J. Physiol.* 195:589-607.

Eyzaguirre, C. and Nishi, K. (1976). Effects of different ions in resting polarization and on the mass receptor potential of carotid body chemosensors. *J. neurobiol.* 7:417-434.

Eyzaguirre, C., Monti-Bloch, L., Hayashida, Y. and Baron, M. (1983). Biophysics of the carotid body receptor complex. In: *Physiology of the peripheral arterial chemoreceptors*. Edited by H. Acker and R.G. O'Regan. Elsevier Science Publishers B.V. pp 59-87.

Eyzaguirre, C. and Zapata, P. (1984). Perspectives in carotid body research. *J. Appl. Physiol.; Resp. Environ. Exerc. Physiol.* 57:931-957.

Eyzaguirre, C., Monti-Bloch, L., Baron, M., Hayashida, Y. and Woodbury, J.W. (1989). Changes in glomus cell membrane properties in response to stimulants and depressants of carotid nerve discharge. *Brain Res.* 477:265-279.

Eyzaguirre, C., Monti-Bloch, L. and Woodbury, J.W. (1990). Effects of putative neurotransmitters of the carotid body on its own glomus cells. *Eur. J. Neurosci.* 2:77-88.

Eyzaguirre, C. (1993). Those strange glomus cells. *Adv. Exp. Med. Biol.* 337:123-131.

Fain, G.L. and Lisman, J.E. (1981). Membrane conductances of photoreceptors. *Prog. Biophys. Mol. Biol.* 37:91-147.

Fan, P. and Weight, F.F. (1994). The effect of atropine on the activation of 5-hydroxytryptamine₂ channels in rat nodose ganglion neurons. *Neurosci.* 62:1287-1292.

Feigenspan, A., Wassle, H. and Bormann, J. (1993). Pharmacology of GABA receptor Cl⁻ channels in rat retinal bipolar cells. *Nature* 361:159-162.

Feigenspan, A. and Bormann, J. (1994). Differential pharmacology of GABA_A and GABA_C receptors on rat retinal bipolar cells. *Euro. J. Pharmacol.* 188:97-104.

Fidone, S.J. and Sato, A. (1969). A study of chemoreceptor and baroreceptor A and C-fibres in the cat carotid nerve. *J. Physiol.* 205:527-548.

Fidone, S.J., Weintraub, S., Stavinoha, W.B., Stirling, C. and Jones, L. (1977). Endogenous acetylcholine levels in cat carotid body and the autoradiographic localization

of a high affinity component of choline uptake. In: *Chemoreception in the Carotid Body*. Edited by H. Acker, S. Fidone, D. Pallot, C. Eyzaguirre, D.W. Lubbers, and R.W. Torrance. Berlin Springer Verlag. pp 106-113.

Fidone, S.J., Gonzalez, C. and Yoshizaki, K. (1982). Effects of low oxygen on the release of dopamine from the rabbit carotid body in vitro. *J. Physiol.* 333:93-110.

Fidone, S.J. and Gonzalez, C. (1986). Initiation and control of chemoreceptor activity in the carotid body. In: *Handbook of Physiology-Section 3: The Respiratory System*. Edited by N.S. Cherniack and J.G. Widdicombe. Am. Physiol. Soc., Bethesda, MD.

Fidone, S.J., Gonzalez, C., Dinger, B. and hanson, G.R. (1988). Mechanisms of chemotransmission in the mammalian carotid body. *Prog. Brain Res.* 74:169-179.

Fidone, S.J., Gonzalez, C., Obeso, A., Gomez-Nino, A. and Dinger, B. (1990). Biogenic amine and neuropeptide transmitters in carotid body chemotransmission. In: *Hypoxia. The Adaptations*, Philadelphia, PA.

Finley, J.C.W., Polak, J. and Katz, D.M. (1992). Transmitter diversity in carotid body afferent neurons: dopaminergic and peptidergic phenotypes. *Neuroscience* 51:973-987.

Fishman, M.C., Green, L.W. and Platika, D. (1985). Oxygen chemoreception by carotid body cells in culture. *Proc. Natl. Acad. Sci. USA* 82:1448-1450.

Fitzgerald, R.S., Garger, P., Hauer, M.C., Raff, H. and Fechter, L. (1983). Effect of hypoxia and hypercapnia on catecholamine content in cat carotid body. *J. Appl. Physiol.* 54:1408-1413.

Fitzgerald, R.S. and Shirahata, M. (1994). Acetylcholine and carotid body excitation during hypoxia in the cat. *J. Appl. Physiol.* 76:1566-1574.

Fitzgerald, R.S. and Shirahata, M. (1996). Release of acetylcholine from the in vitro cat carotid body. *Adv. Exp. Med. Biol.* 410:227-232.

Foster, R.E. (1968). The diffusion of gases in the carotid body. In: *Arterial chemoreceptors*. Edited by R.W. Torrance. Oxford, Blackwell scientific. pp 115-132.

Furshpan, E.J., MacLeish, P.R., O'Lague, P.H. and Potter, D.D. (1976). Chemical transmission between rat sympathetic neurons and cardiac myocytes developing in microcultures: Evidence for cholinergic, adrenergic, and dual-function neurons. *Proc. Natl. Acad. Sci. USA* 73:4225-4229.

- Furukawa, K., Akaike, N., Onodera, H. and Kogure, K. (1992). Expression of 5-HT₃ receptors in PC12 cells treated with NGF and 8-Br-cAMP. *J. Neurophysiol.* 67:812-819.
- Gaiarsa, J.-L., McLean, H., Congar, P., Leinekugel, X., Khazipov, R., Tseeb, V. and Ben-Ari, Y. (1995). Postnatal maturation of gamma-aminobutyric acid_{A and B}-mediated inhibition in the CA3 hippocampal region of the rat. *J. Neurobiol.* 26:339-349.
- Gallagher, J.P., Higashi, H. and Nishi, S. (1978). Characterization and ionic basis of GABA-induced depolarizations recorded in vitro from cat primary afferent neurons. *J. physiol.* 275:263-282.
- Gallagher, P.J., Paxinos, G. and White, S.W. (1985). The role of substance P in arterial chemoreflex control of ventilation. *J. Auton. Nerv. System.* 12:195-210.
- Gallego, R. and Eyzaguirre, C. (1978). Membrane and action potential characteristics of A and C nodose ganglion cells studied in whole ganglia and in tissue slices. *J. Neurophysiol.* 41:1217-1232.
- Gallego, R. (1983). The ionic basis of action potentials in petrosal ganglion cells of the cat. *J. Physiol.* 342:591-602.
- Ganfomina, M.D. and Lopez-Barneo, J. (1991). Single K⁺ channels in membrane patches of arterial chemoreceptor cells are modulated by O₂ tension. *Proc. Natl. Acad. Sci. USA* 88: 2927-2930.
- Gao, B. and Ziskind-Conhaim, L. (1995). Development of glycine- and GABA-gated currents in rat spinal motoneurons. *J. Neurophysiol.* 74:113-121.
- Garcia-Colunga, J., and Miledi, R. (1995). Effects of serotonergic agents on neuronal nicotinic acetylcholine receptors. *Proc. Natl. Acad. Sci. USA* 92:2919-2923.
- Gauda, E.B. and Gerfen, C.R. (1996). Expression and localization of enkephalin, substance P, and substance P receptor genes in the rat carotid body. *Adv. Exp. Med. Biol.* 410:313-319.
- Gay, L. and Stanfield, P.R. (1977). Cs⁺ causes a voltage dependent block of inward K⁺ currents in resting skeletal muscle fibers. *Nature* 267:169-170.
- Goldberg, M.A., Dunning, S.P. and Bunn, H.F. (1988). Regulation of the erythropoietin gene: evidence that the oxygen sensor is a heme protein. *Science* 242:1412-1415.
- Gonzalez, C., Almarez, L., Obeso, A. and Rigual, R. (1992). Oxygen and acid

chemoreception in the carotid body chemoreceptors. *Trends Neurosci.* 15:146-153.

Gonzalez, C., Almaraz, L., Obeso, A. and Rigual, R. (1994). Carotid body chemoreceptors: from natural stimuli to sensory discharges. *Physiol. Rev.* 74:829-898.

Gonzalez-Guerrero, P.R., Rigual, R. and Gonzalez, C. (1993). Co-utilization and interactions of catecholamine and opioid peptides in the carotid body chemoreceptors. *J. Neurochem.* 60:1762-1768.

Gronblad, M., Liesi, P. and Rechartd, L. (1983). Serotonin-like immunoreactivity in rat carotid body. *Brain Res.* 276:348-350.

Hagiwara, S. and Takahashi, K. (1974). The anomalous rectification and cation selectivity of the membrane of a starfish egg cell. *J. Membrane Biol.* 18:61-80.

Halliwell, J.V. and Adams, P.R. (1982). Voltage-clamp analysis of muscarinic excitation in hippocampal neurons. *Brain Res.* 250:71-92.

Hamill, O.P., Marty, A., Neher, E., Sackmann, B. and Sigworth, F.J. (1981). Improved patch-clamp techniques for high-resolution current recordings from cells and cell-free membrane patches. *Pfluegers Arch.* 391: 85-100.

Hanbauer, I. and Hellstrom, S. (1978). The regulation of dopamine and noradrenaline in the rat carotid body and its modification by denervation and by hypoxia. *J. Physiol.* 282:21-34.

Hanson, G., Jones, L. and Fidone, S. (1986). Physiological chemoreceptor stimulation decreases enkephalin and substance P in the carotid body. *Peptides* 7:767-769.

Harris-Warrick, R.M., Coniglio, L.M., Levini, R.M., Gueron, S. and Guckenheimer, J. (1995). Dopamine modulation of two subthreshold current produces phase shifts in activity of an identified motoneuron. *J. Neurophysiol.* 74:1404-1420.

Hatton, C.J. and Peers, C. (1996a). Effects of cytochrome P-450 inhibitors on ionic currents in isolated rat type I carotid body cells. *Am. J. Physiol.* 271:C85-92.

Hatton, C.J. and Peers, C. (1996b). Hypoxic inhibition of K⁺ currents in isolated rat type I carotid body cells: evidence against the involvement of cyclin nucleotides. *Pflügers Arch* 433:129-135.

Hayashida, Y., Koyano, H. and Eyzaguirre, C. (1980). An intracellular study of chemosensory fibers and endings. *J. Neurophysiol.* 44:1077-1088.

Hellstrom, S. and Koslow, S. H. (1975). Biogenic amines in carotid body of adult and infant rats: A gas chromatographic-mass spectrometric assay. *Acta Physiol. Scand.* 93: 540-547.

Hescheler, J., Delpiano, M.A., Acker, H. and Pietruschka, F. (1989). Ionic currents on type-I cells of the rabbit carotid body measured by voltage-clamp experiments and the effect of hypoxia. *Brain Res.* 486:79-88.

Higashi, H. and Nishi, S. (1982). 5-hydroxytryptamine receptors of visceral primary afferent neurons on rabbit nodose ganglia. *J. Physiol.* 323:543-567.

Higashi, H., Ueda, N., Nishi, S., Gallagher, J.P. and Shinnick-Gallagher, P. (1982). Chemoreceptors for serotonin (5-HT), acetylcholine (ACh), bradykinin (BK), histamine (H) and gamma-aminobutyric acid (GABA) on rabbit visceral afferent neurons. *Brain Research Bulletin* 8:23-32.

Hille, B. (1992). *Ionic channels of excitable membrane*. Sinauer Associates Inc., Sunderland, Mass, USA.

Hirano, T., Dinger, B., Yoshizaki, K., Gonzalez, C. and Fidone, S. (1992). Nicotinic versus muscarinic binding sites in cat and rabbit carotid bodies. *Biol. Signals* 1:143-149.

Hladky, S.B. and Haydon, D.A. (1984). Ion movements in gramicidin channels. *Curr. Topics Membr. Transport* 21:327-372.

Hodgkin, A.L. and Huxley, A.F. (1952). A quantitative description of membrane current and its application to conduction and excitation in nerve. *J. Physiol.* 117:500-544.

Hollinshead, W.H. and Sawyer, C.H. (1945). Mechanisms of carotid body excitation. *Am. J. Physiol.* 144:79-86.

Horn, R. and Marty, A. (1988). Muscarinic activation of ionic currents measured by a new whole-cell recording method. *J. Gen. Physiol.* 92:145-159.

Hoyer, D., Clarke, D.E., Fozard, J.R., Hartig, P.R., Martin, G.R., Mylecharane, E.J., Saxena, P.R. and Humphrey, P.A. (1994). VII. International union of pharmacology classification of receptors for 5-hydroxytryptamine (serotonin). *Pharmacol. Rev.* 46:157-203.

Ichikawa, H., Rabchevsky, A. and Helke, C. (1993). Presence and coexistence of putative neurotransmitters in carotid sinus baro- and chemoreceptor afferent neurons. *Brain Res.* 611: 67-74.

- Ingram, S.L. and Williams, J.T. (1994) Opioid inhibition of I_h via adenylyl cyclase. *Neuron* 13:179-186.
- Irisawa, H., Brown, H. F. and Giles, W. (1993). Cardiac pacemaking in the sinoatrial node. *Physiol. Rev.* 73:197-227.
- Ishida, A.T. and Cohen, B.N. (1988). GABA-activated whole-cell currents in isolated retinal ganglion cells. *J. Neurophysiol.* 60:381-396.
- Iturriaga, R. and Lahiri, S. (1991). Carotid body chemoreception in the absence and presence of $\text{CO}_2\text{-HCO}_3^-$. *Brain Res.* 568:253-260.
- Iturriaga, R., Alcayaga, J. and Zapata, P. (1996). Dissociation of hypoxia-induced chemosensory responses and catecholamine efflux in cat carotid body superfused in vitro. *J. Physiol.* 497:551-564.
- Jackson, M.B. and Yakel, J.L. (1995). The 5HT_3 receptor channel. *Ann. Rev. Physiol.* 57:447-468.
- Jackson, A. and Nurse, C. (1995). Plasticity in cultured carotid body chemoreceptors: environmental modulation of GAP-43 and neurofilament. *J. Neurobiol.* 26:485-496.
- Jackson, A. and Nurse, C.A. (1997). Catecholaminergic Properties in Cultured Rat Carotid Body Chemoreceptors Grown in Normoxic and Hypoxic Environments. submitted to *J. Neurochemistry*
- Jacob, M.H. and Berg, D.K. (1987). Effects of preganglionic denervation and postganglionic axotomy on acetylcholine receptors in the chick ciliary ganglion. *J. Cell Biol.* 105:1847-1854.
- Jones, J.V. (1975). Localization and quantitation of carotid body enzymes: their relevance to the cholinergic transmitter hypothesis. In: *The Peripheral Arterial Chemoreceptors*. Edited by M.J. Purves. London: Cambridge Univ. press. pp.143-162.
- Jones, S.W. (1990). Whole-cell and microelectrode voltage clamp. Neuromethods. In: *Neurophysiological Techniques: Basic Methods and Concepts* Vol.14. Edited by A.A. Boulton, G.B. Baker and C.H. Vanderwolf. The Humana Press, Clifton, N.J., pp 143-192.
- Jordan, D. Mifflin, S.W. and Spyer, K.M. (1988). Hypothalamic inhibition of neurones in the nucleus tractus solitarius of the cat is GABA mediated. *J. Physiol.* 399:389-404.

- Kaila, K. and Voipio, J. (1987). Postsynaptic fall in intracellular pH induced by GABA-activated bicarbonate conductance. *Nature* 330:163-165.
- Kamondi, A. and Reiner, P.B. (1991). Hyperpolarization-activated inward current in histaminergic tuberomammillary neurons of the rat hypothalamus. *J. Neurophysiol.* 66:1902-1911.
- Karlin, K.D. (1993). Metalloenzymes, structural motifs, and inorganic models. *Science* 261:701-708.
- Katz, B. (1949). Les constantes electriques de la membrane du muscle. *Arch. Sci. Physiol.* 3:285-299.
- Katz, B. (1969). *The release of neural transmitter substances* (Charles C Thomas, Springfield, III.)
- Katz, B. and Miledi, R. (1971). Further observations on acetylcholine noise. *Nature* 232:124-126.
- Katz, D.M. and Black, I.B. (1986). Expression and regulation of catecholaminergic traits in primary sensory neurons: relationship to target innervation *in vivo*. *J. Neurosci.* 6:983-989.
- Khakh, B. S., Humphrey P. P. A. and Surprenant A. (1995). Electrophysiological properties of P2X-purinoreceptors in rat superior cervical, nodose and guinea-pig coeliac neurones. *J. Physiol.* 484: 385-395.
- Kholwadwala, D. and Donnelly, D.F. (1992). Maturation of carotid chemoreceptor sensitivity to hypoxia: In vitro studies in the newborn rat. *J. Physiol.* 453:461-473.
- Kiehn, O. and Harris-Warrick, R.M. (1992). 5-HT modulation of hyperpolarization-activated inward current and calcium-dependent outward current in a crustacean motor neuron. *J. Neurophysiol.* 68:496-508.
- Kirby, G.C. and McQueen, D.S. (1984). Effects of the antagonists MDL 72222 and ketanserin on response of cat carotid body chemoreceptors to 5-hydroxytryptamine. *Br. J. Pharmacol.* 83:259-269.
- Kleinberg, M.E. and Finkelstein, A. (1984). Single-length and double length channels formed by nystatin in lipid bilayer membranes. *J. Membr. Biol.* 80:257-269.
- Kobayashi, S. (1971). Comparative cytological studies of the carotid body I.

- Demonstration of monoamine-storing cells by correlated chromaffin reaction and fluorescence histochemistry. *Arch. Histol. Japan* 33: 319-339.
- Kondo, H. (1975). A light and electron microscope study of the embryonic development of the rat carotid body. *Am. J. Anat.* 144: 275-294.
- Kondo, H. and Iwasa, H. (1996). Re-examination of the carotid body ultrastructure with special attention to intercellular membrane appositions. *Adv. Exp. Med. Biol.* 410:45-51.
- Kumar, G.K., Runold, M., Ghai, R.D., Cherniack, N.S. and Probhakar, N.R. (1990). Occurrence of neutral endopeptidase activity in the cat carotid body and its significance in chemoreception. *Brain Res.* 517:341-343.
- Kuo, S. S., Saad, A. H., Kong, A. C., Hahn, G. M. and Giaccia, A. J. (1993). Potassium-channel activation in response to low doses of γ -irradiation involves reactive oxygen intermediates in nonexcitatory cells. *Proc. Natl. Acad. Sci. USA* 90:908-912.
- Lahiri, S. (1977). Introductory remarks: oxygen linked response of carotid chemoreceptors *Adv. Exp. Med. Biol.* 78:185-202.
- Lahiri, S., Nishino, T., Mokashi, A. and Mulligan, E. (1980). Interaction of dopamine and haloperidol with O_2 and CO_2 chemoreception in carotid body. *J. Appl. Physiol.* 49:45-51.
- Lahiri, S., Iturriaga, R., Mokashi, A., Ray, D.K. and Chugh, D. (1993). CO reveals dual mechanisms of O_2 chemoreception in the cat carotid body. *Resp. Physiol.* 94:227-240.
- Lahiri, S. (1994). Chromophores on O_2 chemoreception: the carotid body model. *News Physiol. Sci.* 9:161-165.
- Lambert, J.J., Peters, J.A., Hales, T.G. and Dempster, J. (1989). The properties of $5HT_3$ receptors in clonal cell lines studied by patch-clamp techniques. *Br. J. Pharmacol.* 97:27-40.
- LeDouarin, N.M., Smith, J. and LeLievre, C.S. (1981). From the neural crest to the ganglia of the peripheral nervous system. *Annu. Rev. physiol.* 43:653-671.
- Lester, R.A.J. and Dani, J.A. (1995). Acetylcholine receptor desensitization induced by nicotine in rat medial habenula neurons. *J. Neurophysiol.* 74:195-206.
- Lever, J.D. and Boyd, J.D. (1957). Osmiophile granules in glomus cells of the rabbit carotid body. *Nature* 179:1082-1083.

- Li, S.-J., Wang, Y., Strahlendorf, H K. and Strahlendorf, J.C. (1993). Serotonin alters an inwardly rectifying current (I_h) in rat cerebellar Purkinje cells under voltage clamp. *Brain Res.* 617:87-95.
- Liu, Q.Y., Schaffner, A.E., Li, Y.X., Dunlap, V., and Barker, J.L. (1996). Upregulation of GABA_A current by astrocytes in cultured embryonic rat hippocampal neurons. *J Neurosci.* 16:2912-2923.
- Lopez-Barneo, J., Lopez-Lopez, J.R., Urena, J. and Gonzalez, C. (1988). Chemotransduction in the carotid body: K⁺ current modulated by Po₂ in type I chemoreceptor cells. *Science* 241: 580-582.
- Lopez-Barneo, J. (1994). Oxygen-sensitive ion channels: how ubiquitous are they? *TINS* 17:133-135.
- Lopez-Barneo, J. (1996). Oxygen-sensing by ion channels and the regulation of cellular functions. *Trends Neurosci.* 19:435-440.
- Lopez-Lopez, J., Gonzalez, C., Urena, J. and Lopez-Barneo, J. (1989). Low PO₂ selectively inhibits K channel activity in chemoreceptor cells of the mammalian carotid body. *J. Gen. Physiol.* 93:1001-1015.
- Lopez-Lopez, J.R., Deluis, D.A. and Gonzalez, C. (1993). Properties of a transient K⁺ current in chemoreceptor cells of rabbit carotid body. *J. Physiol.* 460:15-32.
- Lorenzon, N.M. and Foehring, R.C. (1992). Relationship between repetitive firing and afterhyperpolarizations in human neocortical neurons. *J. Neurophysiol.* 67:350-363.
- MacDonald, R.L. and Olsen, R. W. (1994). GABA_A receptor channels. *Ann. Rev. Neurosci.* 17:569-602.
- Mandelzys, A. and Cooper, E. (1992). Effects of ganglionic satellite cells and NGF on the expression of nicotinic acetylcholine current by rat sensory neurons. *J. Neurophysiol.* 67:1213-1221.
- Mathie, A., Colquhoun, D. and Cull-Candy, S.G. (1990). Rectification of current activated by nicotinic acetylcholine receptors in rat sympathetic ganglion neurons. *J. Physiol.* 427:625-655.
- Mayer, M.L. and Westbrook, G.L. (1983). A voltage-clamp analysis of inward (anomalous) rectification in mouse spinal sensory ganglion neurons. *J. Physiol. Lond.* 340:19-45.

- McBurney, R.N. and Barker, J.L. (1978). GABA-induced conductance fluctuations in cultured spinal neurons. *Nature* 274:596-597.
- McCormick, D.A. and Pape, H.-C. (1990a). Properties of a hyperpolarization-activated cation current and its role in rhythmic oscillation in thalamic relay neurons. *J. Physiol. Lond.* 431:291-318.
- McCormick, D.A. and Pape, H.-C. (1990b). Noradrenergic and serotonergic modulation of a hyperpolarization-activated cation current in thalamic relay neurons. *J. Physiol. Lond.* 431:319-342.
- McDonald, D.M. (1981). Peripheral chemoreceptors. In: *Regulation of Breathing*. Part 1. Edited by T.F. Hornbein. Marcel Dekker, Inc. New York, pp 105-319.
- McDonald, D.M. (1983). Morphology of the rat carotid sinus nerve. I. Course, connections, dimensions and ultrastructure. *J. Neurocytol.* 12:345-372.
- McDonald, D.M. and Mitchell, R.A. (1975). The innervation of glomus cells, ganglion cells and blood vessels in the rat carotid body: a quantitative ultrastructural analysis. *J. Neurocyt.* 4:177-230.
- McGehee, D.S. and Role, L.W. (1995). Physiological diversity of nicotinic acetylcholine receptors expressed by vertebrate neurons. *Ann. Rev. Physiol.* 57:521-546.
- McQueen, D.S. (1980). Effects of substance P on carotid chemoreceptor activity in cats. *J. Physiol.* 302:31-47.
- McQueen, D.S. and Evrard, Y. (1990). Use of selective antagonists for studying the role of putative transmitters in chemoreception. In: *Arterial Chemoreception*. edited by C. Eyzaguirre, S.J. Fidone, R.S. Fitzgerald, S. Lahiri, and D.M. McDonald. New York: Springer-Verlag, pp168-173.
- McQueen, D.S. and Ribeiro, J.A. (1983). On the specificity and type of receptor involved in carotid body chemoreceptor activation by adenosine in the cat. *Br. J. Pharmacol.* 80:347-354.
- Metz, B. (1969). Release of acetylcholine from the carotid body by hypoxia and hypoxia plus hypercapnia. *Resp. Physiol.* 6:386-394.
- Mienville, J. M. (1991). Comparison of fast responses to serotonin and 2-methyl-serotonin in voltage-clamped N1E-115 neuroblastoma cells. *Neurosci. Lett.* 133:41-44.

- Mir, A.K., McQueen, D.S., Pallot, D.J. and Nahorski, S.R. (1984). Direct biochemical and neuropharmacological identification of dopamine D-2 receptors in the rabbit carotid body. *Brain Res.* 291:273-283.
- Misgeld, U., Deisz, R.A., Dodt, H.U. and Lux, H.D. (1986). The role of chloride transport in postsynaptic inhibition of hippocampal neurons. *Science* 232:1413-1415.
- Monti-Bloch, L. and Eyzaguirre, C. (1980). A comparative physiological and pharmacological study of cat and rabbit carotid body chemoreceptors. *Brain Res.* 193:449-470.
- Monti-Bloch, L. and Eyzaguirre, C. (1990). Effects of different stimuli and transmitters on glomus cell membranes and intercellular communications. In: *Arterial Chemoreception*. Edited by C. Eyzaguirre, S.J. Fidone, R.S. Fitzgerald, S. Lahiri, D.M. McDonald. Springer Verlag, New York. pp 157-167.
- Monti-Bloch, L., Stensaas, L.J. and Eyzaguirre, C. (1983). Carotid body grafts induce chemosensitivity in muscle nerve fibers of the cat. *Brain Res.* 270:77-92.
- Montoro, P.J., Urena, J., Fernandez-Chacon, R., Alvarez de Toledo, G. and Lopez-Barneo, J. (1996). Oxygen sensing by ion channels and chemotransduction in single glomus cells. *J. Gen. Physiol.* 107:133-143.
- Myers, V.B. and Haydon, D.A. (1972). Ion transfer across lipid membranes in the presence of gramicidin A. II. The ion selectivity. *Biochimica et Biophysica Acta* 274:313-322.
- Nakazawa K. (1994). ATP-activated current and its interaction with acetylcholine-activated current in rat sympathetic neurons. *J. Neurosci.* 14:740-750.
- Neher, E. and Sakmann, B. (1976). Single-channel currents recorded from membrane of denervated frog muscle fibers. *Nature* 260:779-802.
- Neher, E. and Stevens, J.H. (1977). Conductance fluctuations and ionic pores in membrane. *Annu. Rev. Biophys. Bioeng.* 6:345-381.
- Nicoll, R.A., Malenka, R.C. and Kauer, J.A. (1990). Functional comparison of neurotransmitter receptor subtypes in mammalian central nervous system. *Physiol. Rev.* 70:514-547.
- Nishi, K. (1975). The action of 5-hydroxytryptamine on chemoreceptor discharges of the

cat's carotid body. *Br. J. pharmacol.* 55:27-40.

Nishizuka, Y. (1988). The molecular heterogeneity of protein kinase C and its implications for cellular regulation. *Nature* 334:739-767.

Nurse, C.A. (1987). Localization of acetylcholinesterase in dissociated cell cultures of the carotid body of the rat. *Cell Tiss. Res.* 250:21-27.

Nurse, C.A. (1990). Carbonic anhydrase and neuronal enzymes in cultured glomus cells of the carotid body of the rat. *Cell Tiss. Res.* 261:65-71.

Nusser, Z., Roberts, J. D. B., Baude, A., Richards, J. G. and Somogy, P. (1995). Relative densities of synaptic and extrasynaptic GABAA receptors on cerebellar granule cells as determined by a quantitative immunogold method. *J. Neurosci.* 15:2948-2960.

Obata, K. (1974). Transmitter sensitivities of some nerve and muscle cells in culture. *Brain Res.* 73:71-88.

Okajima, Y. and Nishi, K. (1981). Analysis of inhibitory and excitatory actions of dopamine on chemoreceptor discharges of carotid body of cat in vivo. *Jpn. J. Physiol.* 31:695-704.

Oomori, Y., Nakaya, K., Tanaka, H., Iuchi, H., Ishikawa, K., Satoh, Y. and Ono, K. (1994). Immunohistochemical and histochemical evidence for the presence of noradrenaline, serotonin and gamma-aminobutyric acid in the chief cells of the mouse carotid body. *Cell Tissue Res.* 278:249-254.

Panisello, J.M. and Donnelly, D.F. (1996). Catecholamine secretion from glomus cells is dependent on extracellular bicarbonate. *Adv. Exp. Med. Biol.* 410:267-275.

Park, M.K., Lee, S.H., Ho, W. and Earm, Y.E. (1995). Redox agents as a link between hypoxia and the responses of ionic channels in rabbit pulmonary vascular smooth muscle. *Exp. Physiol.* 80:835-842.

Pearse, A.G.E., Polak, J.M., Rost, F.W.D., Fontaine, J., Le Lievre, C. and Le Douarin, N. (1973). Demonstration of the neural crest origin of type I (APUD) cells in avian carotid body, using a cytochemical marker system. *Histochemie* 34:191-203.

Peers, C. (1990). Hypoxic suppression of K⁺ currents in type I carotid body cells: selective effect on the Ca²⁺-activated K⁺ current. *Neurosci. Lett.* 119:253-256.

Peers, C. and Green, F.K. (1991). Inhibition of Ca²⁺-activated K⁺ currents by

- intracellular acidosis in isolated type I cells of the neonatal rat carotid body. *J. Physiol.* 437:589-602.
- Peers, C. and Buckler, K.J. (1995). Transduction of chemostimuli by the type I carotid body cell. *J. Membrane Biol.* 144:1-9.
- Pepper, D.R., Landauer, R.C. and Kumar, P. (1995). Postnatal development of CO₂-O₂ interaction in the rat carotid body in vitro. *J. Physiol.* 485:531-541.
- Perrin, D.G., Chan, W., Cutz, E., Madapallimattam, A. and Sole, M.J. (1986). Serotonin in the human infant carotid body. *Experientia Basel* 42:562-564.
- Peters, J.A., Malone H.M. and Lambert, J.J. (1993). An electrophysiological investigation of the properties of 5-HT₃ receptors of rabbit nodose ganglion neurons in culture. *Br. J. pharmacol.* 110:665-676.
- Pietruschka, F. (1985). Calcium influx in cultured carotid body cells is stimulated by acetylcholine and hypoxia. *Brain Res.* 347:140-143.
- Poncet, L., Denoroy, L., Dalmaz, Y., Pequignot, J.M. and Jouvet, M. (1996). Alteration in central and peripheral substance P- and neuropeptide Y-like immunoreactivity after chronic hypoxia in the rat. *Brain Res.* 733:64-72.
- Prabhakar, N.R., Cao, H., Lowe, J.A. III and Snider, R.M. (1993). Selective inhibition of the carotid body sensory response to hypoxia by the substance P receptor antagonist CP-96,345. *Proc. Natl. Acad. Sci. USA* 90:10041-10045.
- Prabhakar, N.R., Kou, Y.R. and Kumar, G.K. (1995). G proteins in carotid body chemoreception. *Biol. Signals* 4:271-277.
- Prabhakar, N.R., Landis, S.C., Kumar, G.K., Mullikin-Kilpatrick, D., Cherniack, N.S. and Leeman, S. (1989). Substance P and neurokinin A in the cat carotid body: localization, exogenous effects and changes in content in response to arterial PO₂. *Brain Res.* 481:205-214.
- Prabhakar, N.R. (1994). Neurotransmitters in the carotid body. *Adv. Exp. Med. Biol.* 360:57-71.
- Reichling, D.B., Kyrozis, A., Wang, J. and MacDermott, A.B. (1994). Mechanisms of GABA and glycine depolarization-induced calcium transients in rat dorsal horn neurons. *J. Physiol.* 476:411-421

- Reyes, A.D., Rubel, E.W. and Spain, W.J. (1994). Membrane properties underlying the firing of neurons in the avian cochlear nucleus. *J. Neurosci.* 14:5352-6364.
- Rhoads, R. and Pflanzner, R. (1992). The control of breathing. In: *Human Physiology*. 2nd Ed. Saunder College Publishing, Florida, USA.
- Rigual, R., Lopez-Lopez, J.R. and Gonzalez, C. (1991). Release of dopamine and chemoreceptor discharge induced by low pH and high Pco₂. Stimulation of the cat carotid body. *J. Physiol.* 433:519-531.
- Rigual, R., Iniguez, C., Carreres, C. and Gonzalez, C. (1985). Localization of carbonic anhydrase in the cat carotid body. *Histochemistry* 82:577-580.
- Robertson, B. and Bevan, S. (1991). Properties of 5-hydroxytryptamine₃ receptor-gated currents in adult rat dorsal root ganglion neurons. *Br. J. Pharmacol.* 102:272-276.
- Rohrbough, J. and Spitzer, N.C. (1996). Regulation of intracellular Cl⁻ levels by Na⁺-dependent Cl⁻ cotransport distinguishes depolarizing from hyperpolarizing GABA_A receptor-mediated responses in spinal neurons. *J. Neurosci.* 16:82-91.
- Rudy, B. (1988). Diversity and ubiquity of K channels. *Neurosci.* 25:729-749.
- Runold, M., Prabhakar, N.R. and Cherniack, N.S. (1990). Effect of adenosine on chemosensory activity of the cat carotid body. *Resp. Physiol.* 80:299-306.
- Ruppersberg, J.P., Stocker, M., Pongs, O., Heinemann, S.H., Frank, R. and Koenen, M. (1991). Regulation of fast inactivation of cloned mammalian I_K(A) channels by cysteine oxidation. *Nature* 352:711-714.
- Sakmann, B. and Neher, E. (1983). *Single channel recording*. Plenum, New York.
- Sapru, H.N. and Krieger, A.J. (1977). Effect of 5-hydroxytryptamine on the peripheral chemoreceptors in the rat. *Res. Commun. Chem. Pathol. Pharmacol.* 16:245-250.
- Sargent, P.B. (1993). The diversity of neuronal nicotinic acetylcholine receptors. *Annu. Rev. Neurosci.* 16:403-443.
- Schamel, A. and Verna, A. (1993). Localization of dopamine D₂ receptor mRNA in the rabbit carotid body and petrosal ganglion by *in situ* hybridization. *Adv. Exp. Med. Biol.* 337:85-92.
- Schrattenholz, A., Pereira, E.F.R., Roth, U., Weber, K.H., Albuquerque, E.X. and Maelicke, A. (1996). Agonist responses of neuronal nicotinic acetylcholine receptors are potentiated by

- a novel class of allosterically acting ligands. *Mol. Pharmacol.* 49:1-6.
- Schweitzer, A. and Wright, S. (1938). Action of prostigmine and acetylcholine on respiration. *Q. J. Exp. Physiol.* 28:33-47.
- Schwindt, P.C., Spain, W.J. and Crill, W.E. (1988). Influence of anomalous rectifier activation on afterhyperpolarizations of neurons from cat sensorimotor cortex in vitro. *J. Neurophysiol.* 59:468-481.
- Scroggs, R.S., Todorovic, S.M., Anderson, E.G. and Fox, A.P. (1994). Variation in I_{H} , I_{IR} and I_{LEAK} between acutely isolated adult rat dorsal root ganglion neurons of different size. *J. Neurophysiol.* 71:271-280.
- Sebastiao, A.M. and Ribeiro, J.A. (1996). Adenosine A₂ receptor-mediated excitatory actions on the nervous system. *Prog. Neurobiol.* 48:167-189.
- Serafini, R., Valeyev, A.Y., Barker, J.L. and Poulter, M.O. (1995). Depolarizing GABA-activated Cl⁻ channels in embryonic rat spinal and olfactory bulb cells. *J. Physiol.* 488:371-386.
- Shirahata, M. (1989). Effects of substance P on the carotid chemoreceptor responses to natural stimuli. In: *Chemoreceptors and Reflexes in breathing*. edited by S. Lahiri, R.E. Forster, R.O. Davies and A.I. pack. New York: oxford Univ. press. pp139-145.
- Shirahata, M., and Fitzgerald, R.S. (1991). The presence of CO₂/HCO₃⁻ is essential for hypoxic chemotransduction in vivo perfused carotid body. *Brain Res.* 545:297-300.
- Siegelbaum, S.A., Camardo, J.S. and Kandel, E.R. (1982). Serotonin and cyclic AMP close single K_v channels in Aplysia sensory neurons. *Nature* 299:413-417.
- Smith, P., Gosney, J., Heath, D. and Burnett, H. (1990). The occurrence and distribution of certain polypeptides within the human carotid body. *Cell Tissue Res.* 261:565-571.
- Spain, W.J., Schwindt, P.C. and Crill, W.E. (1987). Anomalous rectification in neurons from cat sensorimotor cortex in vitro. *J. Neurophysiol.* 57:1555-1576.
- Spergel, D. and Lahiri, S. (1993). Differential modulation by extracellular ATP of carotid chemosensory responses. *J. Appl. Physiol.* 74:3052-3056.
- Staley, K.J. and Mody, I. (1992). Shunting of excitatory input to dentate gyrus granule cells by a depolarizing GABA_A receptor-mediated postsynaptic conductance. *J. Neurophysiol.*

- Stea, A. and Nurse, C. A. (1992). Whole-cell currents in two subpopulations of cultured rat petrosal neurons with different tetrodotoxin sensitivities. *Neuroscience* 47:727-736.
- Stea, A., Alexander, S.A. and Nurse, C.A. (1991) Effect of pH_i and pH_e on membrane currents recorded with the perforated-patch method from cultured chemoreceptors of the rat carotid body. *Brain Res.* 567:83-90.
- Stea, A. and Nurse, C.A. (1989). Chloride channels in cultured glomus cells of the rat carotid body. *Am. J. Physiol.* 257:C174-C181.
- Stea, A. and Nurse, C.A. (1991a). Whole-cell and perforated-patch recordings from O_2 - sensitive rat carotid body cells grown in short- and long-term cultures. *Pflügers Archiv* 418: 93-101.
- Stea, A. and Nurse, C. A. (1991b). Contrasting effects of HEPES vs HCO_3^- -buffered media on whole-cell currents in cultured chemoreceptors of the rat carotid body. *Neurosci. Lett.* 132:239-242.
- Stea, A. and Nurse, C. A. (1992). Whole-cell currents in two subpopulations of cultured rat petrosal neurons with different tetrodotoxin sensitivities. *Neuroscience* 47:727-736.
- Steele, R. H. and Hinterberger, H. (1972). Catecholamines and 5-hydroxytryptamine in the carotid body in vascular, respiratory and other diseases. *J. Lab. Clin. Med.* 80:63-70.
- Stevens, C. F. (1993). Quantal release of neurotransmitter and long-term potentiation. *Cell* 72:55-75.
- Stevens, D. R., McCarley, R. W. and Greene, R. W. (1992) Serotonin₁ and serotonin₂ receptors hyperpolarize and depolarize separate populations of medial pontine reticular formation neurons in vitro. *Neurosci.* 47:545-553.
- Sun, M.K. and Reis, D.J. (1994). Dopamine or transmitter release from rat carotid body may not be essential to hypoxic chemoreception. *Am. J. Physiol.* 267:R1632-R1639.
- Swanson, L.W., Simmons, D.M., Whiting, P.J. and Lindstrom, J. (1987). Immunohistochemical localization of neuronal nicotinic receptors in the rodent central nervous system. *J. Neurosci.* 7: 3334-3342.
- Takahashi, T. and Berger, A. J. (1990). Direct excitation of rat spinal motoneurons by serotonin. *J. Physiol.* 423:63-76.
- Taube, J. S. (1993). Electrophysiological properties of neurones in the rat subiculum in

vitro. *Exp. Brain Res.* 96:304-318.

Tokimasa, T. and Akasu, T. (1990). Cyclic AMP regulates an inward rectifying sodium-potassium current in dissociated bull-frog sympathetic neurons. *J. Physiol. Lond.* 420:409-429.

Tomares, S.M., Bamford, O.S., Sterni, L.M., Fitzgerald, R.S. and Carroll, J.L. (1994). Effects of domperidone on neonatal and adult carotid chemoreceptors in the cat. *J. Appl. Physiol.* 77:1274-1280.

Travagli, R.A. and Gillis, R.A. (1994). Hyperpolarization-activated currents, I_H and I_{KIR} , in rat dorsal motor nucleus in vitro. *J. Neurophysiol.* 71:1308-1317.

Trzebski, A., Sato, Y., Suzuki, A. and Sato, A. (1995). Inhibition of nitric oxide synthesis potentiates the responsiveness of carotid chemoreceptors to systemic hypoxia in the rat. *Neurosci. Lett.* 190:29-32.

Urena, J., Lopez-lopez, J., Gonzalez, C. and Lopez-Barneo, J. (1989). Ionic currents in dispersed chemoreceptor cells of the mammalian carotid body. *J. Gen. Physiol.* 93: 979-999.

Vega-Saenz de Miera, E. and Rudy, B. (1992). Modulation of K^+ channels by hydrogen peroxide. *Biochem. Biophys. Res. Com.* 186:1681-1687.

Wallen, P., Buchanan, J. T., Grillner, S., Hill, R. H., Christenson, J. and Hokfelt, T. (1989). Effect of 5-hydroxytryptamine on the afterhyperpolarization, spike frequency regulation, and oscillatory membrane properties in lamprey spinal cord neurons. *J. Neurophysiol.* 61:759-768.

Wallis, D. I., Stansfeld, C. E. and Nash, H. L. (1982). Depolarizing responses recorded from nodose ganglion cells of the rabbit evoked by 5-hydroxytryptamine and other substances. *Neuropharmacol.* 21:31-40.

Wallis, D.I. and North, R.A. (1978). The action of 5-hydroxytryptamine on single neuron of the rabbit superior cervical ganglion. *Neuropharmacol.* 17:1023-1028.

Walsh, J.P. and Byrne, J.H. (1989). Modulation of a steady-state Ca^{2+} -activated, K^+ current in tail sensory neurons of aplysia: role of serotonin and cAMP. *J. Neurophysiol.* 61:32-44.

Wang, W.-J., Cheng, G.-F., Yoshizaki, K., Dinger, B. and Fidone, S.J. (1991). The role of cyclic AMP in chemoreception in the rabbit carotid body. *Brain Res.* 540:96-104.

- Wang, W.-J., He, L., Chen, J., Dinger, B. and Fidone, S. (1993). Mechanisms underlying chemoreceptor inhibition induced by atrial natriuretic peptide in rabbit carotid body. *J. Physiol.* 460:427-441.
- Wang, Z.-Z., Stensaas, L.J., Dinger, B.G. and Fidone, S.J. (1995). Nitric oxide mediates chemoreceptor inhibition in the cat carotid body. *Neuroscience* 65:217-229.
- Wang, Z.-Z., He, L., Stensaas, L.J., Dinger, B.G. and Fidone, S.J. (1991). Localization and in vitro actions of atrial natriuretic peptide in the cat carotid body. *J. Appl. Physiol.* 70: 942-946.
- Wang, D., Youngson, C., Wong, V., Yeager, H., Dinauer, M.C., Vega-Saenz de Miera, E., Rudy, B. and Cuts, E. (1996). NADPH-oxidase and a hydrogen peroxide-sensitive K⁺ channel may function as an oxygen sensor complex in airway chemoreceptors and small cell lung carcinoma cell lines. *Proc. Natl. Acad. Sci. USA* 93:13182-13187.
- Weaver, D.R. (1993). A_{2a} adenosine receptor gene expression in developing rat brain. *Mol. Brain Res.* 20:313-327.
- Welsh, M.J., Heistad, D.D. and Abboud, F.M. (1978). Depression of ventilation by dopamine in man. Evidence for an effect on the chemoreceptor reflex. *J. Clin. Invest.* 61:708-713.
- Whalen, W.J. and Nair, P. (1983). Oxidative metabolism and tissue PO₂ of the carotid body. In: *Physiology of the peripheral arterial chemoreceptors*. Edited by H. Acker and R.G. O'Regan. Amsterdam, Elsevier. pp 117-132.
- Wikstrom, M., Hill, R., Hellgren, J. and Grillner, S. (1995). The action of 5-HT on calcium-dependent potassium channels and on the spinal locomotor network in lamprey is mediated by 5-HT_{1A}-like receptors. *Brain Res.* 678:191-199.
- Wollmuth, L.P. and Hille, B. (1992). Ionic selectivity of I_k channels of rod photoreceptors in tiger salamanders. *J. Gen. Physiol.* 100:749-765.
- Wyatt, C.N. and Peers, C. (1993). Nicotinic acetylcholine receptors in isolated type I cells of the neonatal rat carotid body. *Neuroscience* 54:275-281.
- Wyatt, C.N. and Peers, C. (1995). Ca²⁺-activated K⁺ channels in isolated type I cells of the neonatal rat carotid body. *J. Physiol.* 483:559-565.
- Wyatt, C. N., Wright, C., Bee, D. and Peers, C. (1995). O₂-sensitive K⁺ currents in carotid body chemoreceptor cells from normoxic and chronically hypoxic rats and their

roles in hypoxic chemotransduction. *Proc. Natl. Acad. Sci. USA* 92:295-299.

Yakel, J.L., Shao, X.M. and Jackson, M.B. (1991). Activation and desensitization of the 5-HT₃ receptor in a rat glioma x mouse neuroblastoma hybrid cell. *J. Physiol.* 436:293-308.

Yakel, J.L. and Jackson, M.B. (1988). 5HT₃ receptors mediate rapid responses in cultured hippocampus and a clonal cell line. *Neuron* 1:615-621.

Yakel, J.L., Shao, X.M. and Jackson, M.B. (1990). The selectivity of channel coupled to the 5-HT₃ receptor. *Brain Res.* 533:46-52.

Yakushiji, T. and Akaike, N. (1992). Blokade of 5-HT₃ recertor-mediated currents in dissociated frog sensory neurons by benzoxazine derivative, Y-25130. *Br. J. Pharmacol.* 107:853-857.

Yanagihara, K. and Irisawa, H. (1980). Inward current activated during hyperpolarization in the rabbit sinoatrial node cell. *Pflügers Arch.* 385:11-19.

Yang, J. (1990). Ion permeation through 5-hydroxytryptamine-gated channels in neuroblastoma N18 cells. *J. Gen. Physiol.* 96:1177-1198.

Yang, J., Mathie, A. and Hille, B. (1992). 5-HT₃ receptor channels in dissociated rat superior cervical ganglion neurons. *J. Physiol.* 448:237-256.

Yoshioka, M. (1989). Effect of a novel 5-hydroxytryptamine-3-antagonist, GR38032F, on the 5-hydroxytryptamine-induced increase in carotid sinus nerve activity in rats. *J. Pharmacol. Exp. Ther.* 250:637-641.

Youngson, C., Nurse, C. Yeger, H. and Cutz, E. (1993). Oxygen sensing in airway chemoreceptors. *Nature* 365:153-155.

Yuan, X.-J., Goldman, W.F., Tod, M.L., Rubin, L.J. and Blaustein, M.P. (1993). Hypoxia reduces potassium currents in cultured rat pulmonary but not mesenteric arterial myocytes. *Am. J. Physiol.* 264:L116-123.

Yuan, X.-J., Tod, M.L., Rubin, L.J. and Blaustein, M.P. (1995). Hypoxic and metabolic regulation of voltage-gated K⁺ channels in rat pulmonary artery smooth muscle cells. *Exp. Physiol.* 80:803-813.

Zapata, P. (1982). Arterial Chemoreceptors: searching for transmitter and modulator substances. In: *Trends in autonomic pharmacology*. Edited by S. Kalsner, M.D.

Baltimore. Urban and Schwarzenberg. pp 343-361.

Zapata, P., Hess, A. and Eyzaguirre, C. (1969). Reinnervation of carotid body and sinus with superior laryngeal nerve fibers. *J. Neurophysiol.* 32:215-228.

Zhong, H. and Nurse, C.A. (1994). Interactions between sensory petrosal neurons and carotid body chemoreceptors in co-culture. *Soc. Neurosci. Abstr.* 402:10.

Zhong, H. and Nurse, C.A. (1995). Basic fibroblast growth factor regulates ionic currents and excitability of fetal rat carotid body chemoreceptors. *Neurosci. Lett.* 202:41-44.

Zhong, H. and Nurse, C.A. (1996). Co-cultures of rat petrosal neurons and carotid body type 1 cells: A model for studying chemosensory mechanisms. *Adv. Exp. Med. Biol.* 410:189-193.

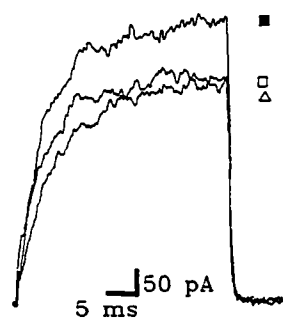
Zhong, H. and Nurse, C.A. (1997). Nicotinic acetylcholine sensitivity of rat petrosal sensory neurons in dissociated cell culture. *Brain Res.* in press.

Zhou, Z.J. and Fain, G.L. (1995). Neurotransmitter receptors of starburst amacrine cells in rabbit retinal slices. *J. Neurosci.* 15:5334-5345.

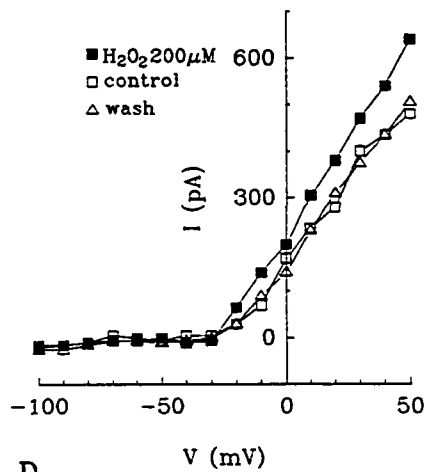
APPENDICES

Appendix 1. Effects of hydrogen peroxide and hypercapnia on whole-cell currents from cultured glomus cells. Exposure of 14 cells to hydrogen peroxide (200 μM , H_2O_2) during perforated patch, whole-cell recording resulted in an increase in the peak outward current in 5 cells. H_2O_2 reversibly increased ($\sim 20\%$) the current evoked during a voltage step from -60 mV to $+50$ mV. One of these examples is shown in the figure. **A.** Increase of K^+ current in response to bath application of hydrogen peroxide (200 μM , H_2O_2). **B.** I-V curve from the same cell of steady state outward K^+ current before, during, and after addition of H_2O_2 . Exposure of 16 cultured glomus cells to increased Pco_2 from 5% to 10%, resulted in a suppression of the outward K^+ current in 7 cells. **C.** Reduction of K^+ current on exposure to a hypercapnic ($\text{Pco}_2 \sim 10\%$, pH 7.4) solution. **D.** Peak K^+ current-voltage relation of the same cell shows the effect of hypercapnia.

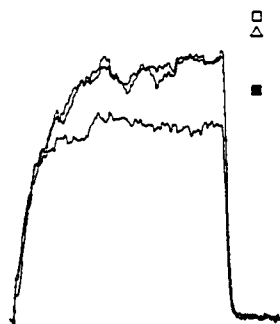
A



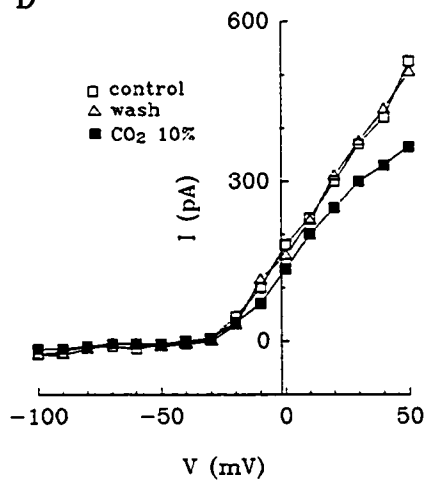
B

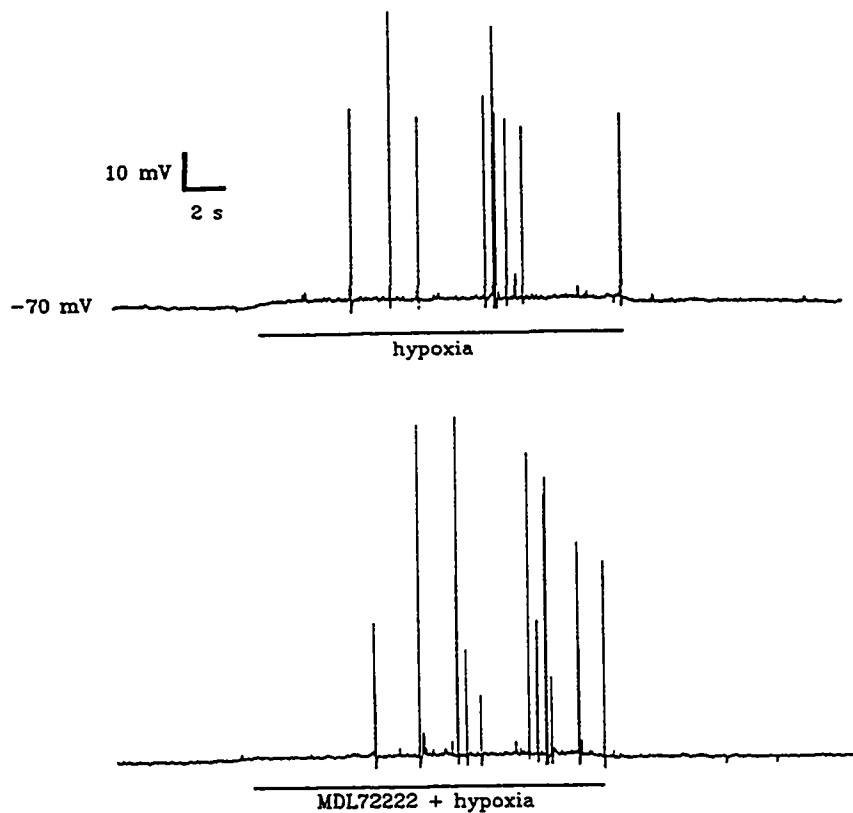


C

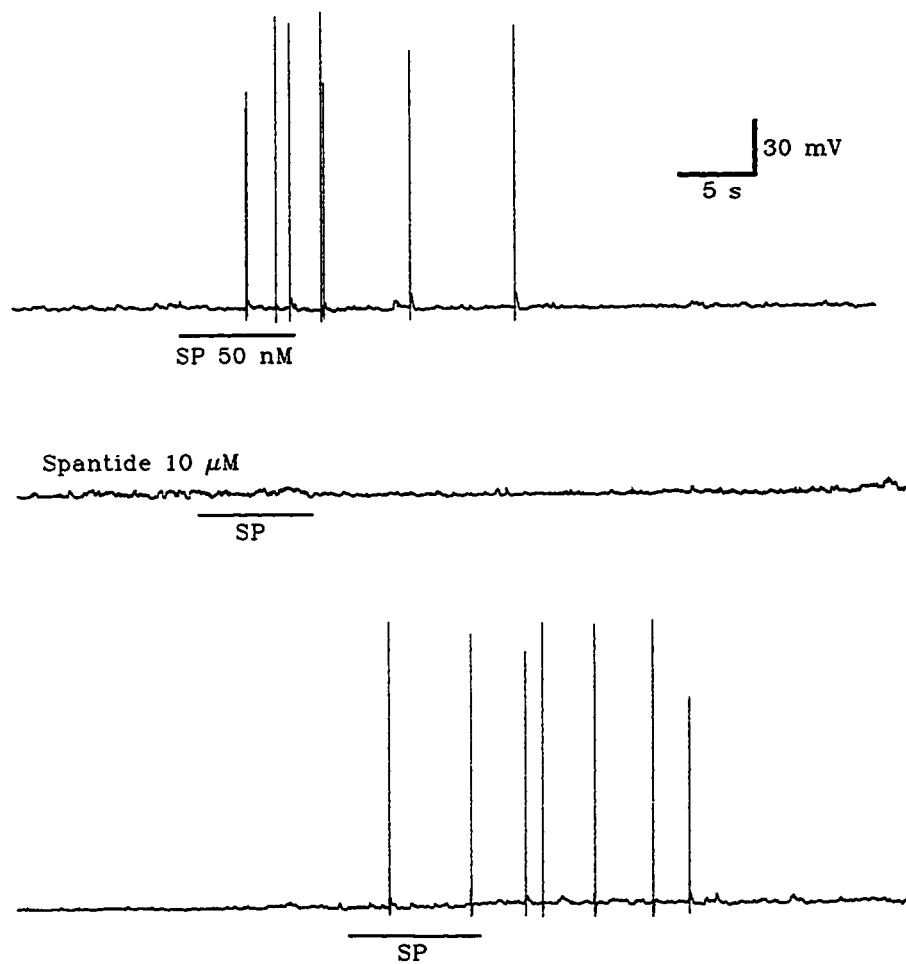


D





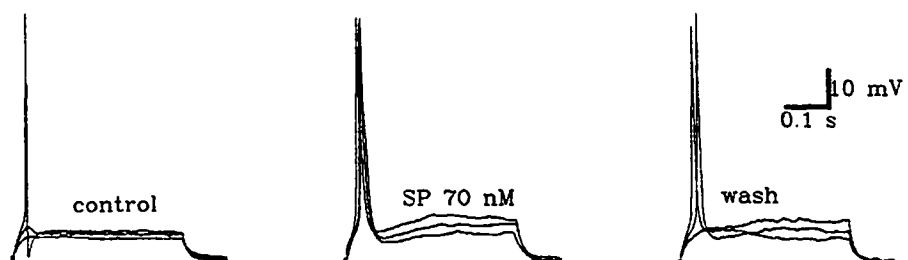
Appendix 2. Effect of 5-HT₃ receptor antagonist on chemosensory signaling in co-culture. Top trace shows a current-clamp recording from a 'functional' petrosal neuron juxtaposed to a glomus cell cluster. Hypoxia ($P_{O_2} \sim 25$ mm Hg) induced an increase in discharge and the effect was reversible. The 5-HT₃ receptor-specific antagonist (MDL72222, 10 μ M) did not block the hypoxia-induced discharge (lower trace).



Appendix 3. Effects of substance P (SP) on the membrane activity of co-cultured petrosal neurons. Bath perfusion of SP, 14-140 nM, to 36 co-cultured petrosal neurons resulted in increased spike activity in 21 cells. The figure shows an example where SP effects were reversibly blocked by SP NK-1 receptor-specific blocker (spantide; 10 μM).

Appendix 4. Effects of SP on spike activity and membrane currents of dissociated petrosal neurons. **A.** Increasing depolarizing stimuli (+20, +30, +40 pA) resulted in a single action potential only when the longest stimulus was applied (left; control). Bath perfusion of substance P (SP, 70 nM) increased excitability of the neuron since the same 3 similar stimuli triggered an action potential in each case (middle). After washing out SP, excitability declined (right). In other cases, repetitive firing was triggered by a depolarizing stimulus and bath perfusion of SP (70 nM) reversibly increased the spike frequency (not shown, n=4). Resting membrane potential of the cell was - 65 mV. **B.** Under voltage-clamp, steps from a holding potential (V_h) of - 90 mV to more depolarized potentials (from - 60 to + 60 mV; 10 mV increments) elicited outward current, including a transient I_A current (left). Bath perfusion of SP (70 nM) reversibly suppressed the outward current, especially the transient component (right). **C.** I_A is isolated by subtracting the currents evoked by depolarizing voltage steps from a V_h of - 20 mV from the currents evoked from a V_h of - 90 mV. The two panels in C are the subtracted traces before (left) and after (right) SP (70 nM). **D.** The peak currents from C are plotted against the voltage steps; (○) and (●) represent control and SP-treated responses respectively (left). In the right panel, the activation of I_A (G/G_{max}) is fitted by Boltzmann distribution (solid line) with coefficient for activation $k = 13.8$ and 16 , and half-activation voltage ($V_{1/2}$) = 1.18 mV and 12.4 for control and SP treated respectively. The Boltzmann equation is as follows: $G/G_{max} = 1/\{1+\exp[(V_{1/2} - V_m)/k]\}$. Where $G=I/(V_m - E_K)$ is the conductance at membrane potential V_m ; E_K is the K^+ equilibrium potential; G_{max} is the maximum conductance; $V_{1/2}$ is the voltage at half-maximal conductance; $k =$ Boltzmann coefficient. Note SP shifted the activation curve of I_A to the right, i.e. to more depolarized potentials.

A



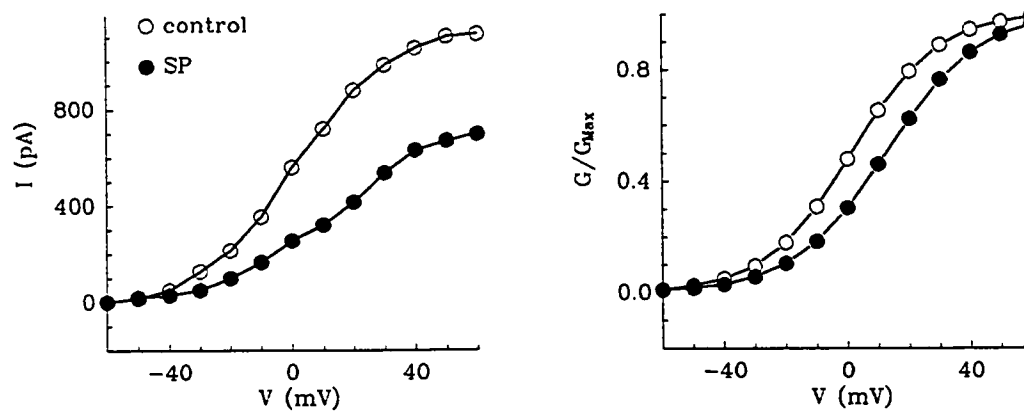
B

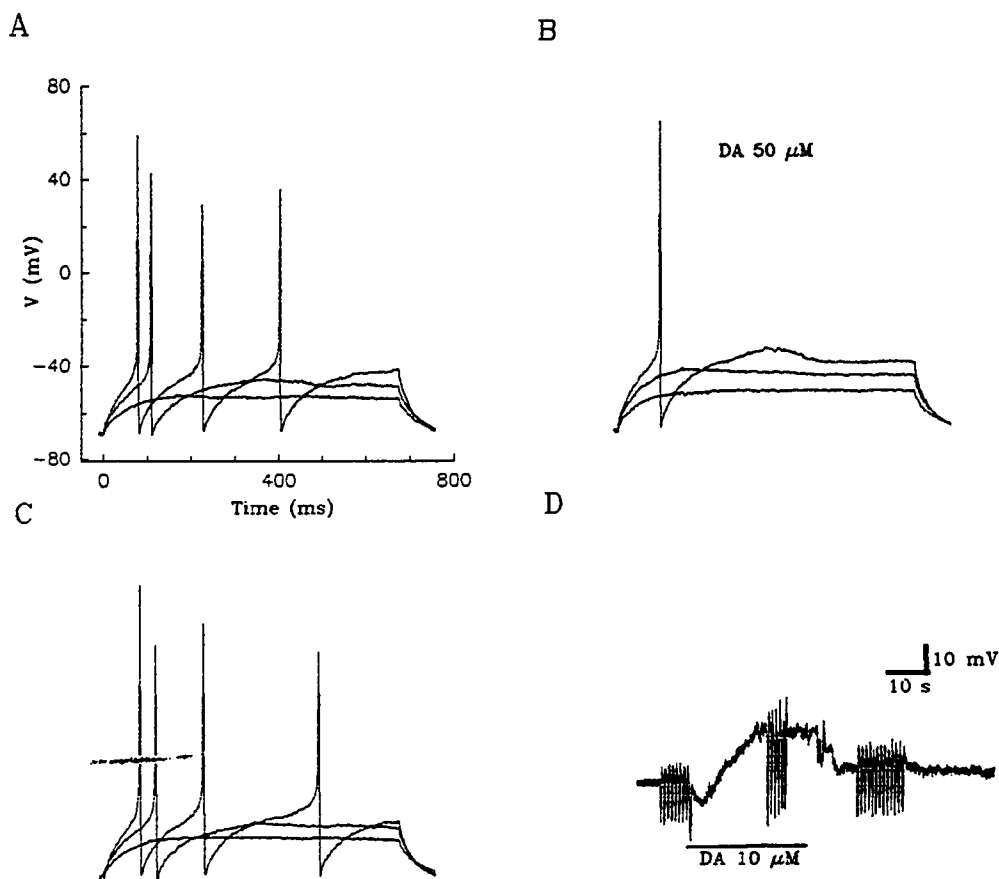


C



D





Appendix 5. Effects of dopamine on spike activity and membrane potential of dissociated petrosal neurons. Among 69 petrosal neurons exposed to dopamine 10-50 μM , 21 cells responded with membrane depolarization. In few cases ($n=4$) dopamine decreased spike activity. **A. B. C.** are current clamp recordings from a petrosal neuron and spike activity was triggered by depolarizing stimuli. Dopamine (DA) raised the threshold for spike activity and decreased the spike frequency (B), compared to control responses (A), and the effect was reversible after wash out of DA (C). **D.** Dopamine depolarized the membrane potential of a petrosal neuron with a conductance decrease.